

Algal Biofuels Production using Hydrothermal Liqufaction of Microalgae and Hydrotreating of Biocrude Oil over Algal Hydrochar-Based Catalysts

A Thesis Submitted to the College of
Graduate and Postdoctoral Studies
in Partial Fulfilment of the Requirements for
the Degree of Doctor of Philosophy in the
Department of Chemical and Biological Engineering
University of Saskatchewan
Saskatoon, Saskatchewan

By

Shima Masoumi

Permission to Use

In presenting this thesis in partial fulfillment of the requirements for a Doctor of Philosophy Degree from the University of Saskatchewan, I agree that the libraries of this University may make this thesis freely available for inspection. I further agree that permission for copying of this thesis in any manner, in whole or in part, for scholarly purpose may be granted by Professor Ajay Kumar Dalai who supervised my thesis work or, in their absence, by the Head of the Department or the Dean of the College of Graduate Research and Studies in which the thesis work was complete. It is understood that any copying or publication or use of this thesis or parts thereof for financial gain shall not be allowed without my written permission. It is also understood that due recognition shall be given to me and to the University of Saskatchewan in any scholarly use which may be made of any material in my thesis.

Requests for permission to copy or to make other use of material in this thesis in whole or parts shall be addressed to:

Head

Department of Chemical and Biological Engineering
University of Saskatchewan
Saskatoon, Saskatchewan
S7N 5A9, Canada

or

Dean

College of Graduate and Postdoctoral Studies
University of Saskatchewan
116 Thorvaldson Building, 110 Science Place
Saskatoon, Saskatchewan
S7N 5C9, Canada

Abstract

Due to the environmental concerns related to CO₂ emissions and the finite supply of energy from non-renewable fossil fuels, more attention has been paid to renewable energy. Of the candidate biomass (as sustainable energy source), microalgae has been considered one of the most promising alternatives for biofuel production, due to its high growth rate and the high CO₂ capture ability compared to other biomasses. Eco-friendly transportation fuel such as biofuel produced from algal biocrude oil upgradation is considered a promising alternative due to its environmentally favorable and superior properties such as low sulfur content, non-toxicity and better lubricating efficiency. The overall objective of this research was to aid the development of commercially feasible technology for the production of sustainable fuels from microalgae. The study plan for this research was divided into four sub-objectives or phases.

In first phase, production and characterization of biocrude oil and hydrochar obtained from hydrothermal liquefaction of microalgae using methanol-water in a batch reactor system was investigated. The effects of methanol to water mass ratios at critical conditions were investigated to determine the maximum biocrude oil production. The comparatively higher yield of biocrude oil (47 wt.%) obtained at a methanol-water mass ratio of 0.75:0.25 also contained a higher amount of ester components resulting in higher biocrude oil quality. Response surface methodology was applied to study the effects of temperature (222-322°C), and reaction time (10-60min) at a constant pressure of 11.5MPa for methanol-water and biomass-solvent ratios of 0.75:0.25 and 1:5, respectively. The optimum yield of biocrude oil (57.8 wt.%) and the highest energy recovery (85.3%) was obtained at 272°C and a reaction time of 35 min. Subcritical conditions (temperature of 222°C, pressure of 11.5MPa) resulted in the highest hydrochar yield (19.5 wt.%).

Suitable utilization of the hydrochar obtained from the hydrothermal liquefaction (HTL) process could improve the overall economics of algal biofuel production. As hydrochar shows a low porosity, chemical activation becomes necessary to improve its physico-chemical properties. Hence, in second phase, a systematic approach was employed to study the effects of different activation factors such as temperature (T), impregnation ratio (mass ratios of KOH and hydrochar) (R), nitrogen flow rate (F), and different chemical activators during the chemical activation process on the characteristics of activated carbon obtained from hydrothermal algal-derived hydrochar.

Based on the optimum condition of $T=675\text{ }^{\circ}\text{C}$, $R=1.5$ and $F=267\text{ cm}^3/\text{min}$ and using potassium carbonate as a chemical agent, the highest BET surface area of $2638\text{ m}^2/\text{g}$ was obtained, which also revealed micropore and mesopore volumes of 0.68 and $1.02\text{ cm}^3/\text{g}$, respectively, with $79\text{ wt.}\%$ of carbon content and a yield of $63.1\text{ wt.}\%$.

Since algal biocrude oil obtained from HTL process explained in the first phase had a high amount of oxygenated compounds ($14.5\text{ wt.}\%$), it cannot be used directly as a transportation fuel and requires further processing to remove heteroatoms. Therefore, in third phase, hydrodeoxygenation (HDO) was used to upgrade the HTL biocrude oil. The most significant challenge for HDO of biocrude oil is developing a cost effective catalyst with high activity. Hence, in the third phase, a novel heterogeneous catalyst using activated algal-derived hydrochar as a support was developed. In this regard, for the first time different impregnation (incipient or co-impregnation) and reduction methods were used to synthesize the carbide phase of activated algal-derived hydrochar-supported NiMo to study their effects on catalyst characteristics, as well as their application for hydrodeoxygenation of algal biocrude oil to produce value added hydrocarbons. The NiMo carbide synthesized through co-impregnation and carbothermal reduction processes showed high activity for oxygen removal due to its higher acidity and active phase (Mo_2C) as well as providing active hydrogen for HDO reactions. At reaction conditions of $T=400\text{ }^{\circ}\text{C}$, $t=2.75\text{ h}$ and $10\text{ wt.}\%$ catalyst loading, a minimum oxygen content of $0.9\text{ wt.}\%$ due to removal of $94\text{ wt.}\%$ oxygen from algal biocrude oil using NiMoC catalysts was achieved.

In fourth phase, techno-economic analysis (TEA) and life cycle analysis (LCA) of algal biofuels production in a two-stage process were investigated. Aspen plus simulation and SimaPro software were used to analyze process economics and greenhouse gas (GHG) emissions. The minimum fuel selling price (MFSP) for two stages of algal biofuels production was $\$8.8/\text{gal}$ to balance total production cost. For this study, the discounted cash flow rate of return (DCFROR) was 23% , greater than the internal discount rate, which means the project was profitable. Thus, the proposed two-stage HTL and catalytic HDO provides a feasible and profitable technology for the production of high quality algal biofuels. The effects of process conditions for biofuels production on the GHG emissions performance were estimated at $-1.13\text{ g CO}_2\text{-eq}/\text{MJ}$, which is much lower than petroleum-based fuels GHG emissions of $91\text{ g CO}_2\text{-eq}/\text{MJ}$.

Acknowledgements

I would like to express my sincere appreciation and gratitude to my supervisor, Dr. Ajay Kumar Dalai for his patience, guidance, significant support and encouragement during my doctoral study. His deep understanding of catalytic science are greatly valued and highly appreciated. Financial supports through CGPS Dean's scholarship, NSERC Discovery grant and Canada Research Chair Program awarded to Professor Dalai are highly appreciated.

I would like to express my deepest appreciation to the members of my advisory committee: Dr. Hui Wang, Dr. Lifeng Zhang (Department of Chemical and Biological Engineering), Dr. Yongfeng Hu (Canadian Light Source, Inc.), Dr. Robert T. Tyler (College of Agriculture and Bioresources), and Dr. Rick Green (Director, Manufacturing Process Development at KeyLeaf company) for their constructive comments and suggestions they have given me throughout my doctorate program. Their valuable advice and suggestions helped me to improve the quality of my work.

I would like to extend my thanks to Mr. RLee Prokopishyn, Ms. Rosa Do Phuong, Ms. Heli Eunike, Mr. Richard Blondin, and Mrs. Jayasinghe Dushmanthi for their technical assistance in the laboratory. Special thanks to Mr. Majak Mapiour for his insightful comments and discussions. I am also grateful to Dr. Jianfeng Zhu (Saskatchewan Structural Sciences Centre) for helping with the NMR and XRD analyses and Mrs. Danielle Covelli, Mr. Ketan Sandhi (Saskatchewan Structural Sciences Centre) for helping me with XPS analysis. I am also thankful to Dr. Thushan S. Withana-Gamage (KeyLeaf Company) and Yuguang Ying (Department of Animal and Poultry Science) for Lipid and protein analyses. Funding from Natural Sciences and Research Council of Canada (NSERC), university of Saskatchewan in form of Dean's scholarship and the Canada Research Chair (CRC) Program is widely acknowledged.

My sincere thanks go to the other members of Dr. Dalai's research group especially Mr. Girish Kamath, Dr. Philip. E. Boahene, Dr. Sundar Vedachalam, Dr. Venu Borugadda, Dr. Sonil Nanda and Dr. Ankeeta Kurhade for their assistant and valuable advice at every stage of this work.

My special thanks also go to my lovely, very kind and supportive friends including Marge, Somayeh, Mohsen and Abbas who supported me with endless love and words of encouragements during the adversity period of my life.

I derived joy from the most especial people in my life; my family. My beloved father, mother, brothers and sister. Thank you all for your support and love.

Dedication

To My Dad, Hossein, who I loved and cherished more than life itself (Rest in Peace Dad), I know you still pray for me from Heaven.

To My Mom, Zahra, for being a great source of love, motivation, inspiration and patience, I am sure that without your prayers I would not be able to be where I am now.

To My brothers, Mahdi and Hadi, who are the best brothers in the world, the men I can truly trust.

And to My Sweet Sister, Bitra, who is such a soft hearted girl, I know how proud you are of my achievements although you feel alone in my absence.

Table of Contents

Permission to Use	i
Abstract	ii
Acknowledgements	iv
Dedication	vi
Table of Contents.....	vii
List of Tables	xii
List of Figures	xiv
Nomenclature	xvii
Glossary of Terms.....	xix
Chapter 1: Introduction and Thesis Outline.....	1
1.1 Introduction.....	1
1.2 Knowledge gaps	2
1.3 Hypotheses.....	3
1.4 Research Objectives	3
1.5 Organization of the thesis.....	4
Chapter 2: Literature Review.....	7
2.1 Abstract	7
2.1 Introduction.....	8
2.2 Limitations of first and second generation biofuels	9
2.3 Biomass conversion technologies	11
2.3.1 Hydrothermal liquefaction of microalgae	12
2.3.1.1 Hydrochar vs Biochar	14
2.4 Effects of hydrothermal liquefaction process parameters on biocrude oil yield.....	15

2.4.1 Effect of reaction temperature-----	15
2.4.2 Effect of reaction time-----	16
2.4.3 Effects of solvent-----	16
2.4.4 Effects of algal composition and loading -----	17
2.4.5 Effects of Catalysts -----	17
2.5 Algal biocrude oil upgradation techniques for liquid transportation fuels production-----	18
2.5.1 Hydrodeoxygenation, Hydrotreating and Hydrocracking -----	18
2.5.2 Catalytic hydrotreating -----	20
2.6 Technoeconomic analysis (TEA)-----	21
2.7 Life Cycle Assessment (LCA) -----	22
2.8 Conclusions-----	22
Chapter 3: Experimental Section -----	24
3.1 Materials section -----	24
3.2 Characterization methods-----	24
3.3 Hydrothermal liquefaction process (HTL) -----	29
3.4 Activated carbon production -----	30
3.5 Methylene blue adsorption test -----	32
3.6 Catalyst synthesis procedure -----	32
3.7 Hydrodeoxygenation (HDO) process -----	33
Chapter 4: Biocrude oil and hydrochar production and characterization obtained from hydrothermal liquefaction of microalgae in methanol-water system-----	34
4.1 Abstract -----	35
4.2 Introduction-----	35
4.3 Materials and methods -----	37
4.4 Results and discussion -----	37
4.4.1 Effects of different mass ratios of methanol/water in critical reaction condition -----	38

4.4.1.1 The effects of methanol/water mass ratios on product distributions -----	38
4.4.1.2 The effects of methanol/water ratios on elemental composition of biocrude oil -----	40
4.4.1.3 The effects of methanol/water ratios on boiling point distribution of biocrude oils ---	41
4.4.1.4 The effects of methanol/water ratios on chemical compositions of biocrude oils -----	42
4.4.1.5 NMR spectroscopy for biocrude oils -----	45
4.4.2 Effects of operating condition on HTL of microalgae using methanol-water system----	47
4.4.3 Hydrochar characterization -----	54
4.4.3.1 Elemental analysis and surface properties of hydrochars -----	54
4.4.3.2 FT-IR of hydrochars-----	55
4.4.3.3 Thermal stability of hydrochars-----	57
4.5 Conclusions-----	58
Chapter 5: Optimized production and characterization of highly porous	
activated carbon from algal-derived hydrochar -----	59
5.1 Abstract -----	59
5.2 Introduction-----	60
5.3 Materials and methodology -----	62
5.4 Results and discussion -----	62
5.4.1 Physiochemical properties of algae biomass and algal hydrochar -----	62
5.4.2 Effects of different process variables on porous structure and yield -----	64
5.4.3 Effects of different chemical agents on properties of activated carbons -----	70
5.4.3.1 Yield and porous characteristics of prepared activated carbons -----	70
5.4.3.2 Elemental and proximate analysis of AC-----	74
5.4.3.3 Surface morphology and particle size distributions of AC -----	76
5.4.3.4 XRD analysis -----	79
5.4.3.5 Chemical composition of AC (XPS) -----	80
5.4.3.6 FT-IR analysis-----	81
5.4.4 Methylene blue adsorption-----	81
5.5 Conclusions-----	83

Chapter 6: NiMo carbide supported on algal derived activated carbon for hydrodeoxygenation of algal biocrude oil	84
6.1 Abstract	84
6.2 Introduction	85
6.3 Materials and methods	87
6.4 Results and discussion	87
6.4.1 Physical and chemical characterizations of synthesized carbide catalysts	87
6.4.2 Effects of catalysts on product distributions and algal biofuels characteristics	93
6.4.3 Effects of operating conditions of HDO to oxygen removal from algal biocrude oil	99
6.5 Conclusions	105
Chapter 7: Techno-economic and life cycle analysis of algal biofuel production via hydrothermal liquefaction of microalgae in methanol-water system and catalytic hydrotreatment using hydrochar as a catalyst support	106
7.1 Abstract	106
7.2 Introduction	107
7.3 Materials and Methods	109
7.3.1 Algal feedstock	110
7.3.2 Process overview	111
7.3.3 Hydrothermal liquefaction process	112
7.3.4 Utilization of hydrochar	113
7.3.5 Hydrotreating process description	115
7.3.6 Economic evaluation	116
7.3.7 Life cycle assessment (LCA)	116
7.4 Results and discussion	118
7.4.1 Techno-economic analysis of algal biocrude oil production	118
7.4.1.1 Utilization of hydrochar as a by-product of HTL	120
7.4.2 Techno-economic evaluation of algal biofuel production	123
7.4.3 Discounted cash flow analysis	126

7.4.4 Sensitivity analysis-----	126
7.4.5 Life cycle assessment for hydrochar utilization using two different methods -----	128
7.5 Conclusions-----	130
Chapter 8: Conclusions and Recommendations -----	131
8.1 Summary -----	131
8.2 Conclusions-----	131
8.3 Recommendations -----	133
Reference-----	135
Appendix A: Analytical data for microalgae-----	151
Appendix B: Process outline for HTL, and synthesis of the catalysts and HDO process -----	152
Appendix C: Temperature profile of furnace -----	153
Appendix D: GC-MS results for biocrude oil, and upgraded biocrude oil -----	155
Appendix E: Calibration curve for NH ₃ -TPD analysis -----	171
Appendix F: XPS results from Casa-XPS software-----	172
Appendix G: Calibration results for GC -----	173
Appendix H: ASPEN Plus results -----	174
Appendix I: Permission to use -----	179

List of Tables

Table 2.1: Oil contents of different feedstocks for biofuels production (Baskar and Aiswarya, 2016)	10
Table 2.2: List of representative companies working to develop algal fuels (Saber et al., 2016) 11	
Table 4.1: Biochemical properties, elemental analysis and HHV of microalgae	37
Table 4.2: Biocrude oil yield and product compositions	38
Table 4.3: Elemental composition and HHV of biocrude oils	41
Table 4.4: Elemental analysis and HHV of biocrude oils obtained from different reaction conditions	48
Table 4.5: Variables and their examined levels used in experimental design	49
Table 4.6: Analysis of variance (ANOVA) for biocrude oil yield (wt.%)	52
Table 4.7: Analysis of variance (ANOVA) for C content (%) presents in biocrude oils	53
Table 4.8: Elemental analysis and surface properties of hydrochars from different reaction conditions	54
Table 5.1: Physico-chemical properties of microalgae and algal hydrochar	63
Table 5.2: Independent process variables and their examined levels used in experimental design	64
Table 5.3: Porous characteristic of chemically activated carbons using different process parameters	66
Table 5.4: Analysis of variance (ANOVA) for BET surface area of chemically activated carbon	68
Table 5.5: Analysis of variance (ANOVA) for chemically activated carbons yield	69
Table 5.6: Porous characteristics of activated carbons prepared by different chemical agents....	74
Table 5.7: Elemental analysis, proximate contents and HHV of activated carbons	75
Table 5.8: Particle size distributions of thermally and chemically activated carbons	76
Table 6.1: Porous characteristics of synthesized catalysts.....	90
Table 6.2: XPS data of synthesized catalysts.....	91
Table 6.3: Product distribution and elemental analysis of upgraded oil over synthesized catalysts	95
Table 6.4: ¹ H NMR and ¹³ C NMR analysis results for algal biocrude oil and upgraded oil	98

Table 6.5: Independent process variables and their examined levels used in experimental design	100
Table 6.6: Elemental analysis results of upgraded biocrude oil in different process conditions	101
Table 6.7: ANOVA table obtained from response surface methodology	102
Table 7.1: Proximate and ultimate analyses of microalgae	111
Table 7.2: HTL process conditions and products yield	113
Table 7.3: Major inputs and products for HDO system.....	116
Table 7.4: Cost parameters and assumptions for economic analysis of algal biofuels production	117
Table 7.5: Main components used to represent biocrude oil	120
Table 7.6: Hydrodeoxygenation reactions based on model compounds.....	123
Table 7.7: Comparison of total production costs for algal biofuel production	125
Table A.1: Analytic data for microalgae.....	151
Table D.1: Algal biocrude oil compounds.....	155
Table D.2: Upgraded biocrude oil compounds.....	158
Table D.3: Water soluble compounds.....	166
Table F.1: XPS results for NiMoC/AC obtained from Casa-XPS software.....	172
Table G.1: Calibration results for GC.....	173
Table H.1: Aspen Plus results for HDO process.....	174
Table H.2: Aspen plus results for HTL +method#1.....	175
Table H.3: Aspen plus results for HTL + method#2.....	177

List of Figures

Figure 1.1: Flow diagram of this Ph.D. research program.....	6
Figure 2.1: Procedures for extraction of hydrothermal liquefaction products.....	13
Figure 2.2: Phase diagram of water (Tran et al., 2017)	17
Figure 3.1: Schematic diagram of HTL process	30
Figure 3.2: Schematic diagram of setup for activated carbon production	31
Figure 4.1: Effect of methanol/water ratio on liquefaction product distribution (Numbers 1,2,3,4 and 5 indicate the biocrude oil obtained by pure water, 25 wt.% of methanol, 50 wt.% of methanol, 75 wt.% of methanol and pure methanol as solvent at constant reaction time of 60 min).....	39
Figure 4.2: Sim-Dist boiling point fractions of HTL biocrude oils (Numbers 1,2,3,4 and 5 indicate the biocrude oil obtained by pure water, 25 wt.% of methanol, 50 wt.% of methanol, 75 wt.% of methanol and pure methanol as solvent at constant reaction time of 60 min).....	42
Figure 4.3: GC-MS analysis of biocrude oils obtained from different mass ratios of methanol and water.....	43
Figure 4.4: Potential reaction pathways for hydrothermal liquefaction of microalgae in methanol-water system.....	44
Figure 4.5: ¹ H NMR distribution of functional groups present in biocrude oils (Numbers 1,2,3,4 and 5 indicate the biocrude oil obtained by pure water, 25 wt.% of methanol, 50 wt.% of methanol, 75 wt.% of methanol and pure methanol as solvent at constant reaction time of 60 min)	46
Figure 4.6: ¹³ C NMR distribution of functional groups present in biocrude oils ((Numbers 1,2,3,4 and 5 indicate the biocrude oil obtained by pure water, 25 wt.% of methanol, 50 wt.% of methanol, 75 wt.% of methanol and pure methanol as solvent at reaction time of 60 min)	47
Figure 4.7: Biocrude oil yields obtained from different reaction conditions at constant pressure of 11.5 MPa	49
Figure 4.8: The response surface for biocrude oil yield (wt.%) and carbon content (wt.%) as a function of temperature and time at constant pressure of 11.5 MPa.....	51

Figure 4.9: Effects of reaction time and temperature on hydrochar yield at constant pressure of 11.5 MPa	55
Figure 4.10: FT-IR spectra of hydrochar obtained from HTL of microalgae.....	56
Figure 4.11: Thermogravimetric analysis of hydrochars obtained from HTL.....	57
Figure 4.12: Differential thermogravimetric analysis of hydrochars obtained from HTL	58
Figure 5.1: Typical isotherm of chemically activated carbons produced from algal hydrochar .	67
Figure 5.2: Three-dimensional plot of BET surface area model of activated carbons prepared by chemical activation of algal hydrochar	71
Figure 5.3: Three-dimensional plot of product yield model of activated carbons prepared by chemical activation of algal hydrochar	73
Figure 5.4: Thermal behaviors of microalgae, algal hydrochar and chemically activated ((a) indicates thermogravimetric analysis and (b) indicates differential thermogravimetric analysis)	77
Figure 5.5: SEM images of microalgae, algal hydrochar and prepared activated carbons.....	78
Figure 5.6: Particle size distribution of algal hydrochar and chemically prepared activated carbon	79
Figure 5.7: X-ray diffraction pattern of microalgae, algal hydrochar and prepared activated carbon	80
Figure 5.8: C 1s XPS spectra of the chemically prepared activated carbon	81
Figure 5.9: FT-IR spectra of AC, hydrochar and microalgae	82
Figure 5.10: Methylene blue adsorption profiles for CAC and AC.....	82
Figure 6.1: XRD pattern of AC and synthesized catalysts (♦ indicating Mo ₂ C and ■ indicating NiC).....	89
Figure 6.2: XPS patterns of synthesized catalysts	92
Figure 6.3: TPD-NH ₃ results for MoC and NiMoC	93
Figure 6.4: Boiling point distribution of upgraded oil obtained from HDO over a) MoC b) NiMoC catalysts.....	96
Figure 6.5: GC-MS pattern of biocrude oil and upgraded oil and WSC	97
Figure 6.6: FTIR analysis results of algal biocrude oil and upgraded oil	98
Figure 6.7: The response surface for oxygen content (wt.%)	104
Figure 7.1: Process flow diagram of algal biofuels production	112

Figure 7.2: Schematic block diagram for LCA of algal biofuels.....	118
Figure 7.3: Hydrothermal liquefaction of microalgae in methanol-water system.....	119
Figure 7.4: HTL process and utilization of hydrochar through combustion.....	121
Figure 7.5: HTL process and utilization of hydrochar through chemical activation	122
Figure 7.6: HDO process simulation with Aspen plus	124
Figure 7.7: Cash flow diagram for algal biofuels production plant.....	126
Figure 7.8: Effect of algae feedstock cost on total production cost and MFSP	128
Figure 7.9: GHG emissions from method #1 and method #2	130
Figure B.1: Process outline for the production of algal biofuels.....	152
Figure C.1: Schematic diagram of the furnace and thermocouple.....	153
Figure C.2: Calibration curve for furnace temperature.....	154
Figure E.1: Calibration curve for NH ₃ -TPD analysis.....	171

Nomenclature

AC	Activated carbon
ASTM	American society for testing and materials
BET	Brunauer-Emmett-Teller
CHR	Carbothermal hydrogen reduction
CR	Carbothermal reduction
CRC	Canada Research Chair Program
DBEP	Discounted break-even point
DCFROR	Discounted cash flow rate of return
ER	Energy Recovery
FCI	Fixed Capital Investment
gal	Gallon
GHG	Greenhouse gas
HDO	Hydrodeoxygenation
HHV	Higher Heating Value
HTL	Hydrothermal liquefaction
IPCC	Intergovernmental panel on climate change
LCA	Life cycle analysis
LED	Light-emitting diode
MBSP	Minimum biomass selling price
MeOH	Methanol
MFSP	Minimum fuel selling price
NMR	Nuclear Magnetic Resonance
NPV	Net present value

NSERC	Natural Sciences and Engineering Research Council of Canada
OPR	Open raceway ponds
PBP	Payback period
PBR	Photobioreactor
SEM	Scanning Electron Microscope
Sim-Dist	Simulated Distillation
TCI	Total Capital Investment
TEA	Techno-economic analysis
TPD	Temperature Programmed Desorption
TPR	Temperature-programmed reaction
XPS	X-ray Photoelectron Spectroscopy

Glossary of Terms

- **Higher Heating Value (HHV) and Lower Heating Value (LHV)**

There are two kinds of combustion heat, which are called higher heating value (HHV) (gross calorific value) and lower heating value (LHV) (net calorific value). HHV and LHV are measured with a bomb calorimeter, and are defined as the amount of heat released by combusting a specified quantity of the fuel sample (initially at 25°C) once it is combusted and returning back to the temperature of 25 °C (using secondary condenser) and 150 °C, respectively. The combustion of fuels results in releasing water which is evaporated while combusting in the chamber. In the case of HHV, the latent heat of vaporization of water is counted, while in the case of LHV, the amount of heat related to water vaporization is not recovered.

- **Net present value (NPV)**

The final cumulative discounted cash flow value at project conclusion, is called net present value.

- **Fixed Capital Investment (FCI) and Total Capital Investment (TCI)**

Fixed capital Investment (FCI) is defined as the money spent on the required process equipment. FCI cannot be recovered easily as it is considered financially immobile. Working capital is the required money that is spent to bring the plant to a productive state. Working capital may not be lost and is partly returned back to the investors at the end of the plant's life. Total capital investment (TCI) is calculated as the sum of FCI and working capital. TCI is considered to be the total amount of money that is spent by investors to build and operate a plant.

- **Payback period (PBP)**

Payback period (PBP) is the point after startup (construction time should not be counted) where undiscounted cash flow reaches the level of negative working capital.

- **Discounted break-even point (DBEP)**

Discounted break-even point (DBEP) is the time period from the time that investors make a decision to build and run a plant (construction time should be counted), until discounted cumulative cash flow becomes positive.

- **Discounted cash flow rate of return (DCFROR)**

Discounted cash flow rate of return (DCFROR) is defined as the discount rate, which brings the net present value to zero.

Chapter 1: Introduction and Thesis Outline

1.1 Introduction

Under the Paris agreement, Canada is committed to reduce its greenhouse gas emissions by 30% below the 2005 level, which was about 730 Megatonnes of carbon dioxide equivalent, by 2030 (<https://www.canada.ca/content/dam/eccc/documents/pdf/cesindicators/progress-towards-canada-greenhouse-gas-reduction-target/2020/progress-ghg-emissions-reduction-target.pdf>).

Due to the environmental concerns related to CO₂ emissions and the finite energy supply from non-renewable fossil fuels, more attention has been paid to the renewable energies which are considered sustainable and secure resources, such as hydrocarbon liquid products obtained from biomass feedstocks through thermochemical and biochemical technologies (Zhu et al., 2018).

Conventional first and second generation biomass sources such as woody biomass or agricultural crops require large land areas, which also results in competition with food crops. As a result, microalgae as a third generation feedstock has attracted much attention. Higher photosynthetic efficiency, effective CO₂ sequestration, and the ability to grow in saline wastewater are some of the advantages of using microalgae as a biomass source (Galadima and Muraza, 2018). Hydrothermal liquefaction (HTL) of microalgae as a thermochemical conversion method is considered a promising technology for production of algal biocrude oil. Algal biocrude oil obtained from HTL contains large amounts of heteroatoms such as N, O and various organics (Y. Guo et al., 2015). In order to be suitable for use as transportation fuels, subsequent upgrading techniques are required. Catalytic hydrodeoxygenation (HDO) has been considered the most promising technology to upgrade algal biocrude oil due to its higher selectivity toward hydrocarbons, and also this method requires milder conditions (Wu et al., 2018).

The most significant challenges for HDO of biocrude oil is the development of a cost effective catalyst with high activity, stability and a long lifetime, due to its crucial impact on the yield of products. Compared to homogenous catalysts, heterogeneous catalysts have attracted much attention due to their separation and reusability. The catalysts that have been used for biocrude oil upgrading techniques include transition metals or noble metals supported on different

supports such as alumina, zeolites or activated carbon. Carbon-based catalysts showed higher catalytic activity during reactions (Yang et al., 2018; Zou et al., 2017).

As the suitable utilization of by-products results in improving the overall economics of the process, algal hydrochar as a by-product of HTL can be utilized to produce renewable adsorbents or catalysts/catalyst supports (Safari et al., 2018). As hydrochars show low surface area ($\sim 4 \text{ m}^2/\text{g}$) and porosity ($\sim 0.02 \text{ cm}^3/\text{g}$), physical or chemical activation methods are required to improve the physio-chemical properties of hydrochars such as their porous structure characteristics (Tan et al., 2017).

Transition metal carbides have gained much attention due to their higher catalytic activity during HDO reactions to produce valuable products from algal biocrude oil, which contains a lot of oxygenated compounds. Compared to noble metals, transition metal carbides are less expensive and they have demonstrated very high thermal stability. It also has been found that among traditional metals (NiMo and CoMo) used for HDO, NiMo showed better catalytic performance during HDO reactions such as decarboxylation and deoxygenation (C-O bond cleavage) (Zhou and Lawal, 2016).

One of the main challenges regarding the commercialization of algal biofuels production is economics. Techno-economic analysis (TEA) is considered the most useful and fundamental tool to determine the feasibility of a new process. Algal biofuel can be employed as one of the alternatives to reduce climate change, however, it has environmental impacts as well. Life cycle assessment (LCA) is the most useful and accepted method to determine and quantify these impacts. Many researchers have focused on economic analysis reporting selling costs and life cycle assessments for algal biofuels ranging between \$1.64-30.00/gal and -75-534 $\text{gCO}_2\text{-eq MJ}^{-1}$, respectively (Quinn and Davis, 2015). The variable results are due to various systems used for the cultivation of algae and different reaction pathways, product distribution and handling, and co-product utilization.

1.2 Knowledge gaps

According to the literature review (Chapter 2) carried out for algal biofuels production using hydrotreating of HTL biocrude oil, the knowledge gaps were extracted as below:

- There are limited studies available that evaluate the impact of methanol/water mass ratio in subcritical and supercritical conditions on biocrude oil and hydrochar yield and their characterization in HTL of microalgae using a co-solvent.

- There are limited reports available on the synthesis and characterization of highly porous activated carbon using different process parameters and chemical agents through chemical activation of algal-derived hydrochar.
- There are limited studies available that studied the synthesis and characterization of algal hydrochar-based catalysts impregnated with Mo and NiMo through different impregnation and reduction methods, and their application for hydrodeoxygenation of algal biocrude oil.
- There are limited reported studies on Technoeconomic analysis (TEA) and Life cycle assessment (LCA) of HTL of microalgae to produce biocrude oil and subsequent upgradation of biocrude oil to produce high quality biofuels using heterogeneous catalysts.

1.3 Hypotheses

Based on the above knowledge gaps, the hypotheses are stated below:

- Use of methanol/water co-solvent in HTL process leads to maximum biocrude oil yield at relatively lower pressure and temperature.
- Use of algal derived hydrochar as a raw material can produce high quality activated carbon in terms of surface area and functional groups through a chemical activation process.
- Impregnating Mo and NiMo on highly porous algal derived activated carbon can make it useful as an environmentally friendly catalyst, which can be used to upgrade algal biocrude oil by a hydrodeoxygenation process to reduce the amount of heteroatoms present in biocrude oil.
- GHG emissions involved in the HTL of microalgae to produce biocrude oil and its subsequent upgradation can be less than from conventional fuels production.

1.4 Research Objectives

The overall aim of this research was to aid the development of commercially feasible technology for the production of sustainable fuels from microalgae. The project focused on three areas: the hydrothermal liquefaction of microalgae to produce biocrude oil, upgradation of biocrude oil using novel heterogeneous catalysts through a hydrodeoxygenation process, and Technoeconomic and life cycle analysis of algal biofuel production. In order to achieve these objectives, the following sub-objectives were considered:

- **Sub-objective 1:** Production of high quality biocrude oil and hydrochar through HTL in sub- and supercritical conditions using a methanol-water co-solvent system

- **Sub-objective 2:** Synthesis and characterization of activated carbons through activation of algal hydrochar as a by-product of HTL
- **Sub-objective 3:** Synthesis and characterization of hydrochar-based catalysts impregnated with Mo and NiMo through different impregnation and reduction methods and subsequent hydrodeoxygenation of algal biocrude oil over synthesized catalysts
- **Sub-objective 4:** Technoeconomic analysis (TEA) and Life Cycle Analysis (LCA) of algal biofuels production

1.5 Organization of the thesis

The flow diagram of this Ph.D. research program is shown in Figure 1.1. This PhD thesis organized in eight chapters. It is structured according to the manuscript-style thesis guidelines of the College of Graduate and Postdoctoral studies. Chapter 2 has been published as a book chapter. The manuscripts described in Chapters 4 was published in journal of Energy, Chapter 5 in journal of Cleaner Production, and Chapter 6 in journal of Energy Conversion and Management. The manuscript described in Chapter 7 has been submitted to the journal of Biomass & Bioenergy.

An introduction to the subject matter is given in Chapter 1. Chapter 2 presents relevant literature reviews of algal biocrude oil production and its upgradation methods, and of different types of catalysts used for upgradation techniques. In Chapter 3 the experimental procedures are discussed, including all the materials, processes (HTL, HDO and chemical activation procedure), and techniques used to characterize biomass, hydrochar, catalysts and oil samples used in this study. Following that, based on the research objectives and sub-objectives of the thesis, subsequent chapters are briefly highlighted.

Chapter 4 describes production and characterization of biocrude oil and hydrochar obtained from hydrothermal liquefaction of microalgae in a methanol-water system. The effects of methanol-water mass ratio, reaction temperature, time and their interactions on biocrude oil and hydrochar yield and their characterization in a methanol-water system were investigated. The chemical compositions (CHNSO) of the biocrude oil and its physical properties (boiling point distributions, higher heating values, etc.) were analyzed. The solid by-product (algal hydrochar) obtained from the HTL process was thoroughly analyzed by characterization techniques such as CHNSO, BET, FTIR and TGA to investigate the effects of methanol/water mass ratio, time and temperature on its physico-chemical properties.

Utilization of the hydrochar obtained from the HTL process for the production of algal biofuels is described in Chapter 5. For the first time, a systematic approach was employed to study the effects of different activation factors such as temperature, impregnation ratio (mass ratios of KOH and hydrochar), nitrogen flow rate, and different chemical activators on the characteristics of prepared activated carbon obtained from hydrothermal algal-derived hydrochar.

Since algal biocrude oil obtained from the HTL process contained a high level of oxygenated compounds, it could not be used directly as a transportation fuel and required further processing to remove heteroatoms. Hydrodeoxygenation (HDO) was used to upgrade the HTL biocrude oil. In Chapter 6, development of a heterogeneous catalyst using activated algal-derived hydrochar as a support is described. For the first time, different impregnation (incipient or co-impregnation) and reduction methods were used to synthesize the carbide phase of activated algal-derived hydrochar-supported NiMo, to study their effects on catalyst characteristics as well as their application for hydrodeoxygenation of algal biocrude oil to produce value-added hydrocarbons.

The main challenge regarding the commercialization of algal biofuels production is economics. Techno-economic analysis (TEA) is considered the most useful and fundamental tool to determine the feasibility of a new process. Algal biofuels can be employed as one of the alternatives to reduce climate change. Life cycle assessment (LCA) is the most useful and accepted method to determine and quantify these impacts. Therefore, in Chapter 7, techno-economic analysis (TEA) and life cycle analysis (LCA) of algal biofuels production in a two stage process are presented. Aspen plus simulation and SimaPro software were used to analyze process economics and greenhouse gas (GHG) emissions.

Chapter 8 provides the overall conclusions and recommendations from this research study. The references for all the chapters are collected in the References section, and appropriate additional information is provided in the Appendices.

Phase 4: TEA and LCA of two stage algal biofuels production

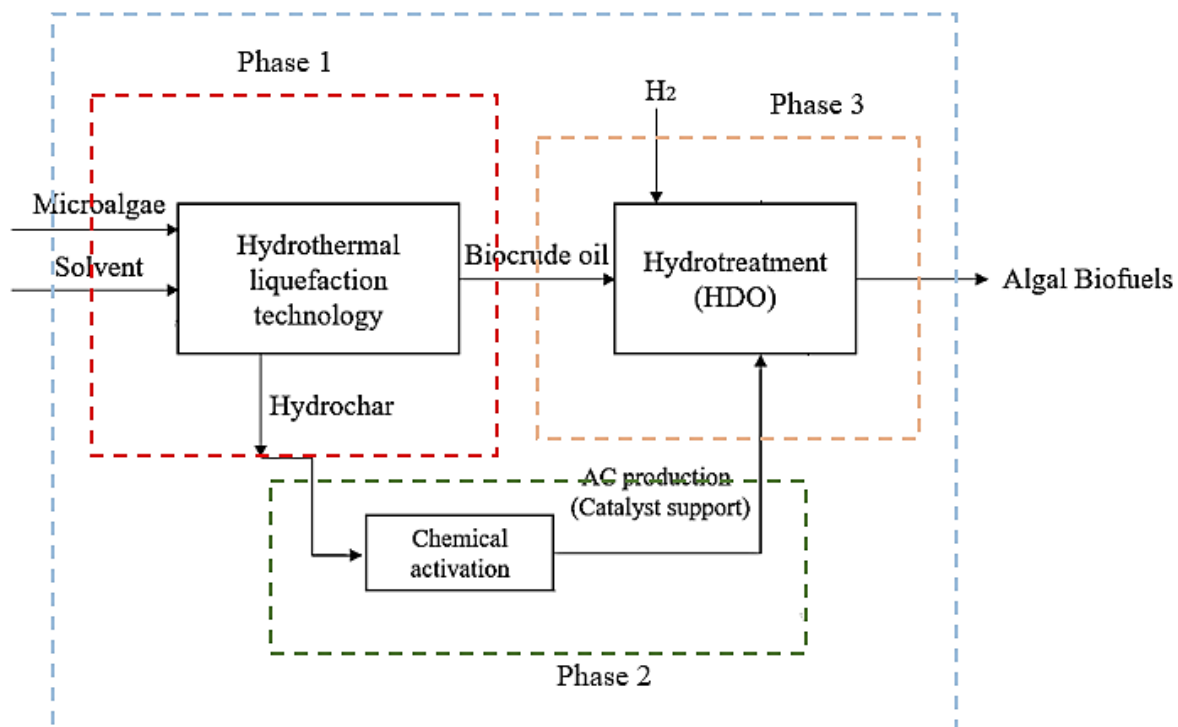


Figure 1.1: Flow diagram of this Ph.D. research program

Chapter 2: Literature Review

Biocrude Oil Production via Hydrothermal Liquefaction of Algae and Upgradation Techniques to Liquid Transportation Fuels

Apart of the content of this chapter has been published as a book chapter cited below:

Masoumi, S., Borugadda, V.B., Dalai, A.K., 2020. Biocrude Oil Production via Hydrothermal Liquefaction of Algae and Upgradation Techniques to Liquid Transportation Fuels, in: Biorefinery of Alternative Resources: Targeting Green Fuels and Platform Chemicals. Springer, Singapore, 249-270.

Contribution of the Ph.D. Candidate

The manuscript was drafted by Shima Masoumi with guidance and suggestions provided by Dr. Venu Borugadda and Dr. Ajay K. Dalai.

Contribution of this Chapter to Overall Ph.D. Research

This chapter gives an overview of biofuels production using different feedstocks, followed by focusing on microalgae, techniques used to produce biocrude oil from microalgae, hydrochar vs biochar, upgradation techniques used for upgradation of biocrude oil and catalysts used for upgradation method. This chapter led to define knowledge gaps, hypothesis, and subsequently objectives and sub-objectives of the research carried out in this thesis.

2.1 Abstract

Hydrothermal liquefaction of algae is regarded as a favorable thermochemical process to produce biocrude oil from biomass with potential to complement conventional crude oil. This chapter discusses the production of biocrude oil via hydrothermal liquefaction of microalgae. Due to the presence of high protein content in algal species, the catalytic removal of heteroatoms is required to make liquid transportation fuels from algal biocrude oil. Therefore, different

upgradation techniques are explored to remove the heteroatoms using various heterogeneous acid catalysts. Special focus is given to the effects of process parameters on hydrothermal liquefaction and upgradation techniques to escalate biocrude oil yield and liquid transportation fuels.

2.1 Introduction

For the last few decades, due to incremental human population, industrialization and energy consumption, there is a rapid increase in carbon dioxide (CO₂) emission to the environment. Further, a drastic increase in energy consumption and the lack of sustainable resources have concerned scientists for alternative sources of energy. Therefore, many researchers have focused on finding an alternative fuel source for commercialization. Biomass is regarded as inexhaustible and sustainable future energy source. This includes biomass sources such as wood wastes, agricultural products and residues, and animal wastes. Of the candidate biomass feedstocks for biofuel production, much attention has been paid to microalgae due to faster growth and higher yield, higher ability for CO₂ sequestration as compared to other biomasses (Duan and Savage, 2011a). Algal biofuels, the third generation of biofuels, can be obtained from thermochemical conversion processes. HTL of algae is considered as a well-known technique to transform the algae feedstocks into biocrude oil in water/solvent medium under high pressure and moderate temperature. Although high biocrude oil yield can be obtained through this process, large amounts of nitrogen, sulfur, and oxygen can still be present in the biocrude oil (Y. Guo et al., 2015).

This leads to instability of biocrude oil that creates many difficulties for its applications. So, subsequent upgrading and improving the stability of biocrude oil makes it more suitable for producing liquid transportation fuels. Environmentally friendly transportation fuels such as upgraded algal biocrude oil is a promising alternative due to its advantages such as higher flash point, low sulfur content and it also can be considered as a better lubricant. The lubricity or wear resistance reduction of bio oil is higher than of conventional fuel due to the presence of the oxygenated compounds, although these compounds accelerate the corrosion (Xu et al., 2010). Research has been focused on heterogeneous catalysts, due to their separation and reusability over the homogeneous catalysts. An option that has a great possibility, but has not been fully explored, is the preparation of catalysts from sustainable renewable sources. Functionalized biochar based catalysts are considered desirable because of their favorable properties such as

low material cost, high surface area and thermal stability (Manayil et al., 2016). Thus, production of biocrude oil from algae via liquefaction and upgradation routes are discussed with focusing on the effect of process parameters on biocrude oil yield and liquid transpiration fuel production technologies.

2.2 Limitations of first and second generation biofuels

Based on the nature of the feedstock used to produce biofuels, they are divided into three generations. The first-generation biofuels are obtained from food crops like corn, wheat, and soybean, which can also be consumed as human food. Their use leads to an increase in food prices, and utilization of first-generation biofuels creates social, economic and environmental challenges. Following are the most common first-generation biofuels: Biodiesel - extraction of vegetable oils (seeds of plants), Bio-ethanol - fermentation of sugars such as sugar crops, and Biogas - anaerobic fermentation of organic waste. Non- edible oils, which are made from non-food crops such as grass, wood and agricultural wastes are considered as the feedstocks to produce second-generation biofuels, it is more difficult to extract oil from these feedstocks. Second-generation biofuels are known as “advanced biofuels” because advanced technologies are required to extract the biocrude oil. The need for a large area of land with moist soil is one of the disadvantages of second-generation biofuels (Azad et al., 2015).

Biofuels derived from marine biomasses are considered as third generation biofuels and they provide more advantages compared to biofuels generated from the previous generations. Microalgae is a photosynthetic microorganism which exists as an individual cell or chains of the cell. Microalgae, which can also grow in saline environments, transforms the sunlight, CO₂, and water to renewable algal biomass, Table 2.1 shows the oil content of algal biomass when compared to the non-edible feedstocks (Baskar and Aiswarya, 2016). Algae can be categorized into microalgae and macroalgae. Compared to microalgae, macroalgae produces superior biomass densities; however, its lipid content is very small, whereas carbohydrates and protein contents are high. Therefore, it is believed that macroalgae would not be an economically feasible source of biodiesel production (van Hal et al., 2014). Generation of biofuels from algae is promising because of the following advantages:

- Fast growth rate: it is assessed that compared to crops such as canola (200 to 450 liters per hectare) algae could yield 61,000 liters per hectare
- Ability to sustain harsh condition due to unicellular form

- Simple multicellular structure
- Short harvesting cycle (1-10 days)
- Ability to seize carbon dioxide
- Can be cultivated in non-arable lands
- No overlap with food resources
- Remarkable variety: it can produce such fuels as biodiesel, biogasoline (petrol), bio-ethanol, and even bio-jet fuel.
- Higher biocrude oil yield
- Compared to terrestrial crops with 0.5% of photosynthetic productivities, algae shows a higher range (3 to 8%).
- Algae biofuels are non-toxic, contain less sulfur and are highly biodegradable.

Table 2.1: Oil contents of different feedstocks for biofuels production (Baskar and Aiswarya, 2016)

Type of oil	Feedstock (oil)	Oil content % (w/w)
Edible	<i>Soybean</i>	15-20
	<i>Rapeseed</i>	38-46
	<i>Sunflower</i>	25-35
	<i>Peanut</i>	45-55
	<i>Coconut</i>	63-65
	<i>Palm</i>	30-60
Non-Edible	<i>Jatropha seed</i>	35-40
	<i>Pongamia pinnata</i>	27-39
	<i>Neem</i>	20-30
	<i>Castor</i>	53
Other sources	<i>Rubber seed</i>	40-50
	<i>Sea mango</i>	54
	<i>Cottonseed</i>	18-25
	<i>Microalgae</i>	30-70

Although the potential for production of algal biofuel is highly recommended, its capital and operating costs are relatively high. It requires further research and development to develop sustainable and viable methods of biofuel production on a commercial scale. Currently, as can be seen in Table 2.2, a number of companies are working on the development of algal biofuels (Saber et al., 2016). Typically, algal biomass contains three major compounds, such as lipids,

proteins, and carbohydrates in varying proportions. During photosynthesis, microalgae captures CO₂, resulting in the synthesis of carbohydrates. At this stage, lipid content can be varied based on some stress factors such as nitrogen starvation which causes the photosynthetic mechanism to switch to accumulate lipids. The productivity of algae-derived biofuels is approximately two orders of magnitude more than that from terrestrial oilseed crops. Algal biodiesel has lower melting point and better cold flow properties owing to the presence of polyunsaturated fatty acids (Demirbaş, 2008).

Table 2.2: List of representative companies working to develop algal fuels (Saber et al., 2016)

Company (Country)	Website
Algae. Tee (Australia)	http://algaetec.com.au
Algenol (USA)	www.algenol.com
Aurora Algae Inc. (USA)	www.aurorainc.com
Algae Link (Netherlands)	www.algaelink.com
ALG Western Oil (South Africa)	www.algbf.co.za
AlgaFuel (Portugal)	www.a4f.pt
BP (England)	www.bp.com
BRTeam (Iran)	http://brteam.ir
DENSO corporation (Japan)	www.denso.co.jp
Eni (Italy)	www.eni.com
Greon (Bulgaria)	www.greon.eu
Neste Oil (Finland)	www.nesteoil.com
OilFox (Argentina)	www.oilfox.com.ar
Pond Biofuels (Canada)	www.pondbiofuels.com
Total (France)	www.total.com
Varican Aqua Solutions (UK)	www.variconaqua.com

2.3 Biomass conversion technologies

Until 2010, food crops were used as a feedstocks to produce first-generation biofuels, on the other hand 0.2% of biofuels were produced from lignocellulosic materials. Biomass can be converted to biofuels through three main processes such as thermochemical process, biological process and direct combustion (Tsukahara and Sawayama, 2005). Thermochemical conversion leads to bio-methanol, biodiesel, biocrude oil, bio-syngas, and bio-hydrogen. Gasification,

pyrolysis, and liquefaction are three main routes for biomass thermochemical conversion. In comparison to biochemical technologies, thermochemical processes are preferred due to their ability to convert biomass into transportation fuels with higher heating value (Akia et al., 2014). Out of all of the processes, gasification and pyrolysis require temperature over 600 °C and dried biomass as feedstock. During gasification, biomass produces synthesis gas (a mixture of H₂ and CO), which can be converted to liquid fuel over a suitable catalyst via Fischer-Tropsch synthesis process. Pyrolysis is used to produce syngas and oil from dried biomass, where as in hydrothermal liquefaction needs the temperature lower than 400 °C in presence of water/solvents and suitable catalysts, to transform biomass into biocrude oil. Liquefaction technique is a low temperature and high-pressure process which can break down the components of the biomass into the small fragments in water/solvent medium (Dimitriadis and Bezergianni, 2017a).

2.3.1 Hydrothermal liquefaction of microalgae (HTL)

One approach to produce transportation fuels from algae is from lipid extraction following its conversion to biodiesel via esterification/transesterification reactions. Although lipid conversion technology is relatively recognized, it requires algae with a high lipid content to be economically feasible (Tian et al., 2014). Therefore, in order to employ this technology, microalgae growth conditions should be carefully controlled. Hydrothermal liquefaction of microalgae followed by hydrodeoxygenation process converts the entire microalgae components (lipid, protein and carbohydrate) to biofuel.

Rapid reaction and use of feedstocks (considering the high moisture content in algae) with no limitation in terms of lipid-content make HTL process as an appropriate method for producing biocrude oil. HTL of microalgae includes the hydrolysis of major components (lipid, protein, and carbohydrate). The biocrude oil extracted from the liquefaction has higher yield and quality, moderate oxygen concentration and, higher heating value (HHV) in the range of 25-35 MJ Kg⁻¹ as compared to those of the traditional pyrolysis biocrude oils (14-20 MJ Kg⁻¹) (Yang et al., 2016). Further, the advantage of HTL is the formation of distinct oil and water phases, whereas pyrolysis oil contains a substantial quantity of water and oxygenated compounds.

Hydrothermal liquefaction process includes three main stages, depolymerization, decomposition, and recombination. During the depolymerization of biomass, long chain macromolecules consisting of hydrogen, carbon, and oxygen, are converted to smaller macromolecules under high temperature and pressure conditions. Decomposition of biomass involves

the dehydration (the loss of water molecules), deamination (the loss of amino acid content), and decarboxylation (the loss of CO₂). Recombination of the fragments forming the compounds with high molecular weight occurs when a large number of free radicals are present during the process. As it can be seen in Figure 2.1, four phases were generated after HTL process, light gases which are principally CO₂; a solid residue (hydrochar); biocrude oil and an aqueous phase having a high organic carbon content. The relative reaction rates are strongly dependent on the nature of the feedstocks and processing conditions, such as reaction temperature, residence time and biomass loading, impacting the ultimate product distribution and composition (A R K Gollakota et al., 2018).

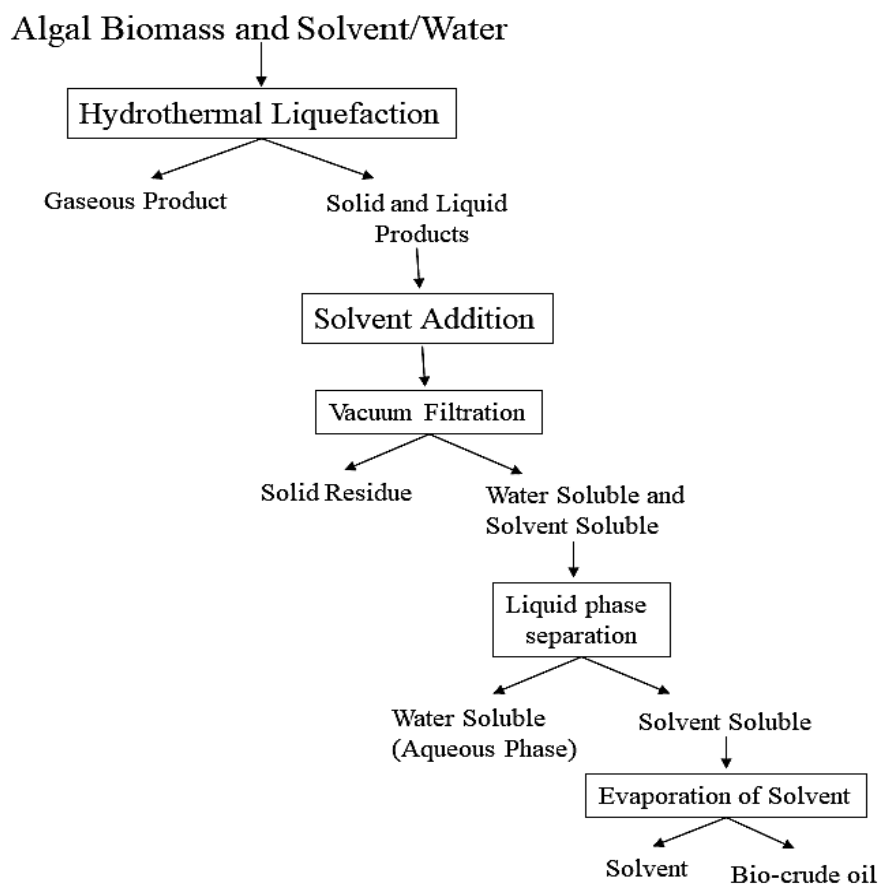


Figure 2.1: Procedures for extraction of hydrothermal liquefaction products

2.3.1.1 Hydrochar vs Biochar

Slow pyrolysis and hydrothermal carbonization (HTC) are two routes of thermochemical conversion technology for production of bio/hydrochar as main products. In fact, these thermochemical processes are employed to convert the biomass containing the organic compounds to carbon rich materials. Compared to slow pyrolysis, hydrothermal carbonization process has been considered as a promising technology due to the elimination of drying step. Also HTC is mostly considered economically viable for wet biomass (Cheng and Li, 2018).

Pyrolysis is carried out at temperature in the range of 300-650 °C in the absence of oxygen. The products are divided into biochar which is not fully carbonized, liquid phase and gas phase. Also, depending on the reaction time and heating rate, pyrolysis process is divided into different categories; fast, intermediate and slow. Slow-pyrolysis is performed with low heating rate and long residence time, resulting in higher solid product yield (Laird et al., 2009). Hydrothermal carbonization (HTC) is usually carried out in the temperature range of 180-240 °C, for 5-240 min, and the required pressure should be in the range of subcritical water condition (Masoumi and Dalai, 2020).

Hydrochar and biochar show different physicochemical properties that significantly affect their potential applications. They reveal different chemical compositions and porous characteristics as the biomass feedstock undergoes complex chemical reaction (such as degradation, dehydration and repolymerization) in different reaction conditions (temperature, time and pressure), hence, they can be significantly distinguished (Kambo and Dutta, 2015; Wiedner et al., 2013).

As hydrothermal carbonization process occurs at lower temperature, the carbon conversion is lower than that in pyrolysis, resulting in higher H/C, and O/C. Thus, hydrochar has higher atomic ratios of hydrogen to carbon and oxygen to carbon, as compared to those in biochar. Biomass contains hemicellulose, cellulose and lignin, and as the temperature increases, first hemicellulose, which has lower energy density, starts to decompose and the lignin content in the solid product increases resulting in higher HHV. During hydrothermal carbonization, which is carried out at lower temperature in water media, hemicellulose is decomposed faster (Demirbaş, 2005).

Biochar from pyrolysis produced at higher temperature (500-600 °C) contains aromatic groups and hydrochar from HTC produced at lower temperature (200-250 °C) contains more

alkyl moieties. Also, as the pyrolysis occurs at higher temperature, biochar reveals lower H/C ratio due to high carbon conversion and possesses graphite-like layers, including particles with different size ranges while surface of hydrochar samples is composed of spherical particles including more homogeneous particle sizes (Liu et al., 2013).

Hydrochars compared to biochars are slightly acidic, as hydrochars contain more oxygenated functional groups. But due to loss of carboxyl and hydroxyl groups during pyrolysis, biochars are more alkaline. The other reason for it to be alkaline is attributed to inorganic and metal compounds such as Ca and Mg. During HTC, some of the inorganics are washed away in water media resulting in acidic properties of hydrochars. Hydrochars generally show low specific surface area and porosity. But, biochars properties depend on the biomass, reaction temperature and heating rate, could exhibit the specific surface area in the wide range (Gascó et al., 2018).

2.4 Effects of hydrothermal liquefaction process parameters on biocrude oil yield

The yield and physicochemical properties of the biocrude oil obtained from liquefaction of algae are impacted by operating factors such as reaction time, process temperature, solvent type and solvent to biomass ratio, algae composition, catalyst nature and loading. This section elaborates the effects of all these process parameters on biocrude oil yield.

2.4.1 Effect of reaction temperature

Temperature is considered as an important factor in the safety and economics of industrial operation, suitable range of operating temperature relied on the nature of biomass feedstock, solvents polarity, catalysts loading, and other process factors. The ionic characteristic of water, which changes with temperature, causes different reactions to dominate. At low temperature, hydrolysis dominates dropping the biocrude oil yield. However, it is believed that the biocrude oil yield increases with increasing reaction temperature and then after reaching to the maximum, will drop. The highest biocrude oil yields can be obtained at the temperature range of 250-370 °C. Also, as the temperature increases, biocrude oils with higher quality (higher HHV) is produced, while the carbon and hydrogen contents present in the aqueous phase are reduced. Simultaneously, the nitrogen content in the biocrude oil starts to increase significantly, suggesting higher incorporation of protein-derived molecules. It is clear that maximum biocrude oil yields do not correspond to the best biocrude oil quality, and these two factors must be carefully balanced (Dimitriadis and Bezergianni, 2017a).

2.4.2 Effect of reaction time

Reaction time is considered as one of the critical factors during HTL of algae, to evaluate the process economically, sufficient reaction time is necessary to have maximum biocrude oil through the conversion of algal biomass components. If the reaction time is too long, this results in lower biocrude oil yields because of the higher production of gases and aqueous products, on the other hand, reduced reaction time leads to lower equipment and operational costs. Anastasakis and Ross, (2011) investigated the optimum reaction time to have higher biocrude oil yield. Their results showed that 15 min at a temperature of 350 °C can be considered as an appropriate condition for HTL conversion of marine algae. However, these values are generally reported at the reaction temperature and do not include heating times. Also, increase in reaction time results in increasing N/C ratios, and decreasing the oxygen and hydrogen concentrations in the oil. This shows that similar to the reaction temperatures, the holding time need to be carefully adjusted to obtain an optimal balance between biocrude oil yields and quality.

2.4.3 Effects of solvent

As can be seen in Figure 2.2, HTL is showed in the presence of subcritical water and critical point. At these conditions, water, which is considered as a polar solvent, converts to non-polar solvent due to weak hydrogen bonding within the water phase. In this situation, water as a non-polar solvent is able to extract the organic components from the biomass. Furthermore, nearby critical point, water dissociation constant (K_w) is higher in three orders of magnitude than at ambient conditions, significantly increasing the number of H^+ and OH^- ions, which may help to promote base- and acid catalyzed reactions. Singh et al. (2015) studied the effects of various solvents such as water and alcohols including methanol and ethanol on product distribution of the hydrothermal liquefaction process. The results showed that supercritical alcohol conditions used for hydrothermal liquefaction process are effective to produce liquid hydrocarbons. J. Zhang et al. (2014) studied liquefaction of algae in an ethanol-water and co-solvent system to produce biocrude oil. Their results showed that compared to mono-solvent, mixtures of solvents with different polarities yields higher biocrude oil and less solid residue.

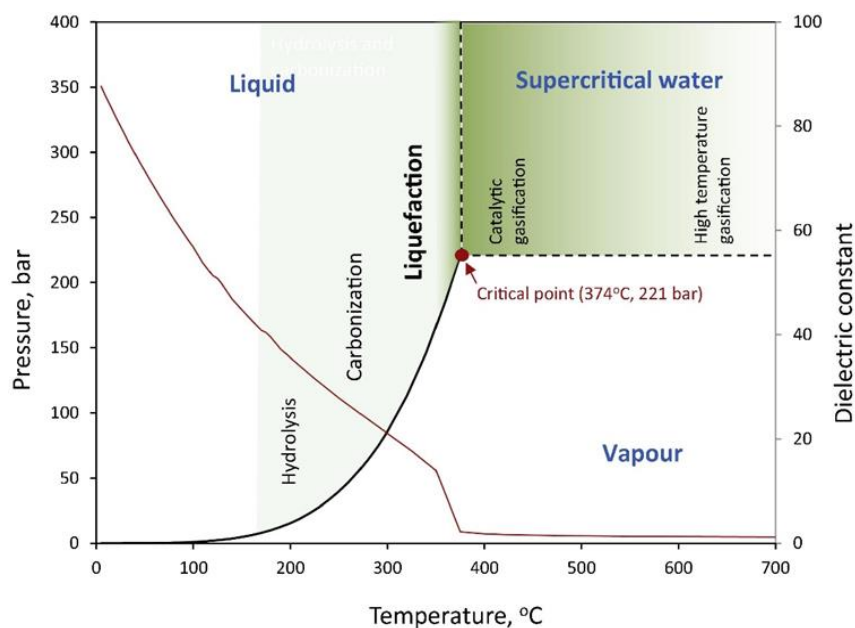


Figure 2.2: Phase diagram of water (Tran et al., 2017)

2.4.4 Effects of algal composition and loading

Microalgae are predominantly composed of three main biochemical compounds, namely proteins, lipids, and carbohydrates. Their contributions are dependent on the algae species itself and their growth conditions. Lipid-rich algae are found to have much higher oil yield than protein-rich algae and earlier studies confirmed that lipids are more readily converted into biocrude oil than proteins or carbohydrates (Gollakota et al., 2018). The research on the HTL of algae has been conducted over a wide range of biomass loadings (1 to 50 wt %)(Li et al., 2010). Peterson et al. (2008) proposed that the biomass concentrations should be in the range of 15-20 wt% for higher biocrude oil yield, whereas (López Barreiro et al., 2013) suggested slightly lower loadings ranging from 5 to 15 % and these studies were mainly focused on *Chlorella*, *Nannochloropsis*, *Dunaliella*, *Spirulina*, and *Phaeodactylum*. Biller and Ross (2011) converted a number of model compounds which showed that the highest oil yields were obtained from lipids (55 – 80%), followed by proteins (11 – 18 %) and carbohydrates (6 – 15 %). They obtained similar biocrude oil quantities from the two microalgae *Chlorella* and *Nannochloropsis*, whereas the obtained yields were different for *Porphyridium* and the cyanobacteria *Spirulina*.

2.4.5 Effects of Catalysts

Catalysts are considered as one of the most important factors for biocrude oil production, which affect the reaction rate, products chemical composition, and the quality of the biocrude

oil. Typical catalysts used in liquefaction of algal biomass are divided into two categories: homogenous and heterogeneous catalysts. Compared to heterogeneous catalysts, homogenous catalysts are economical and produce no coke. Homogenous catalysts applied for HTL are acids such as H_2SO_4 , metal ions, and alkalis (CaCO_3 , and $\text{Ca}(\text{OH})_2$) (Tian et al., 2014). Acids and alkalis are often used to weaken the bonds including C-C bond which could improve the hydrolysis of biomass during HTL, while metal ions can affect the dehydration. Jena et al. (2012) reported that hydrothermal liquefaction using catalysts increased the yield of biocrude oil up to 50 % in comparison to the non-catalytic HTL process. Besides that, catalysts play a crucial role to enhance the hydrocarbon ratio and removal of oxygen to increase the biocrude oil quality.

2.5 Algal biocrude oil upgradation techniques for liquid transportation fuels production

Algal biocrude oil produced by HTL process has similar properties as that of crude oil derived from fossils; on the other hand, biocrude oil contains higher oxygen (10-20 wt%) and nitrogen (1 to 8 wt.%). Presence of these heteroatoms cause several undesired properties that limit its direct application in engines such as:

- High viscosity, high corrosiveness (because of the high amount of fatty acids)
- The thermal and chemical instability
- Low heating value (owing to higher oxygenated compounds concentration in biocrude oil)

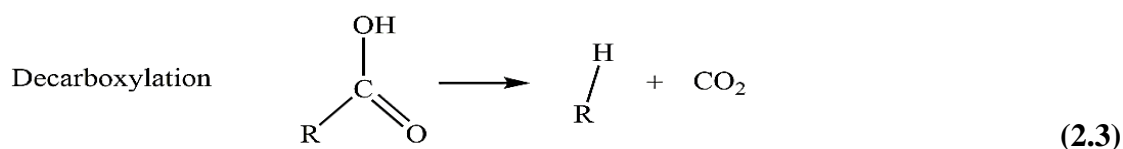
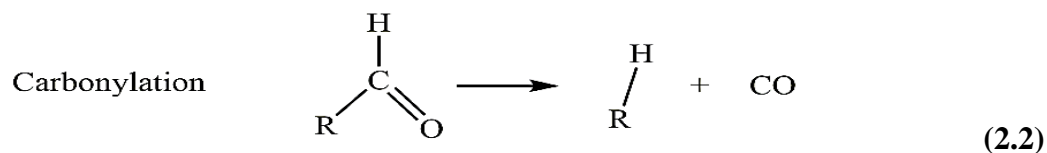
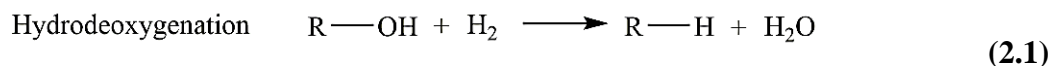
Therefore, biocrude oil quality needs to be improved in order to be used as a liquid transportation fuel. Due to the identical physicochemical properties of the vegetable oils, the technologies used for the biodiesel production from plant and vegetable seed oils can be applied to algal biocrude oils (Roussis et al., 2012). There are a variety of techniques for biocrude oil upgradation such as solvent addition, emulsification, esterification, transesterification, hydrotreating, hydrodeoxygenation, and catalytic hydrotreating. Here, hydrodeoxygenation and catalytic hydrotreating will be explored.

2.5.1 Hydrodeoxygenation, Hydrotreating and Hydrocracking

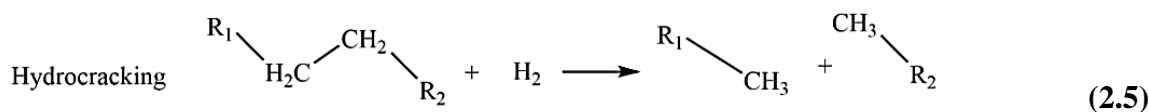
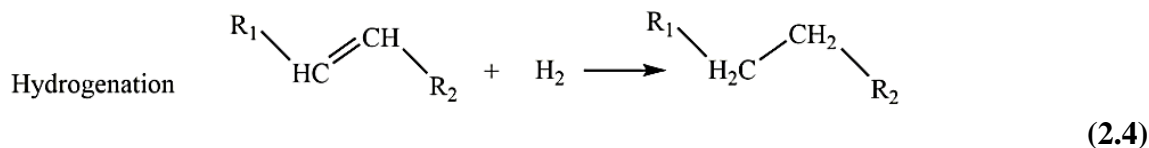
As discussed earlier, biocrude oil has high oxygen content, which leads to undesirable properties such as chemical instability and low heating value. Hydrotreating is a process used to improve heating value by increasing hydrogen content and reducing O, N, and S through catalytic reaction conditions of pressure up to 20 MPa and temperatures in the range of 300-450 °C. Following is the simplest hydrotreating reaction for biocrude oil:



The acceptable amount of oxygen present in hydrocarbon liquid fuels should be less than 1 wt%, but the oxygen content of algal biomass is around 40-60 wt.%. Therefore, the main reaction involved in hydrotreating is hydrodeoxygenation due to a significant amount of oxygenated compounds present in biocrude oil. Oxygen can be removed as water, carbon dioxide and/or carbon monoxide through a combination of decarbonylation, decarboxylation and hydrodeoxygenation reactions shown in equations (1)-(3):



Oxygen removal through CO₂ and CO formation leads to lower carbon yield, so removing oxygen as water is the preferred route. Hydrogenation can also be used to improve the biocrude oil quality. It is believed that as the content of H/C present in liquid fuel increases, the quality of the liquid hydrocarbons also increases. The partial cracking of heavy components is also expected during this process. Therefore, hydrocracking and hydrogenation also occur during hydrotreating (equations 4 and 5). Due to H₂ consumption during hydrocracking and hydrogenation, unsaturated compounds become saturated compounds.



Hydrogenation is carried out at moderate conditions followed by the operation at moderate temperature (300-450 °C) and relatively high pressure (75 to 300 bar) (Saber et al., 2016). High

pressure increases the reaction rate as well as the solubility of hydrogen in the biocrude oil, and decreases coking in the reactor. Owing to the moderate operating conditions, hydrotreating favors lower coking, increase in catalyst activity and higher yield of liquid transportation fuels. Cracking can be carried out using H-ZSM-5 as catalysts for upgrading biocrude oil. However, hydrotreating and hydrodeoxygenation using zeolite catalysts result in low-grade hydrocarbon fuels i.e. HHV of these fuels are 25% less than biocrude oils produced via catalytic hydrothermal liquefaction (Mortensen et al., 2011).

2.5.2 Catalytic hydrotreating

Biocrude oil upgrading through catalytic hydrotreatment is promising to produce hydrocarbon-rich fuel. Research has been focused on the development of catalysts with higher activity and stability for the HDO of biocrude oil especially at milder reaction conditions (Ramirez et al., 2015). Heterogenous catalysts have several advantages over the traditional homogenous catalysts such that they can be easily recovered and reused. Different heterogenous catalysts have been used in biocrude oil upgrading reactions such as zeolites, noble metals, transition metals, and carbides, mostly supported on alumina or activated carbon. CoMo and NiMo based catalysts are commercially used for industrial hydrotreating to remove oxygen, nitrogen, and sulfur. Due to their instability during the hydrotreating process, some research has been focused on noble metal (Pt, Pd, Ru) catalysts for hydrotreating of biocrude oil. This helps to convert aromatics compounds into the hydrocarbons, suitable for diesel fuel applications (Galadima and Muraza, 2018); but, due to the higher cost of noble metals, their application is limited in catalytic hydrotreating. Duan et al. (2016) evaluated the effect of zeolite catalysts on algal biocrude oil at reaction conditions of 400 °C, 6 MPa for 240 min in supercritical water. Nine zeolites were selected to investigate their effects on the product yields and the properties of the upgraded biocrude oil. Due to the acidic characteristics of zeolites, all of them improved the denitrogenation, deoxygenation, and desulfurization in comparison with non-catalytic upgrading reactions. (López Barreiro et al., 2016) studied the effect of commercial catalysts (Pt/Al₂O₃ and HZSM-5) for biocrude oil upgradation via liquefaction of *Scenedesmus almeriensis* (freshwater) and *Nannochloropsis gaditana* (marine) algae species. The uncatalyzed reaction of *S. almeriensis* revealed that the highest biocrude oil yield obtained at 4 to 8 MPa of hydrogen pressure, 400 °C of reaction temperature for 4 h in 10 mL micro autoclaves. At these process conditions, catalysts did not show significant activity and the process was promoted by

the temperature rather catalyst. The main products obtained during upgradation was found to be 50-70% of alkanes, gaseous cracking species, unsaturated fatty acids, and phenols.

Elliott et al. (2013) investigated the catalytic hydroprocessing for algal biocrude oil in a continuous-flow reactor using sulfided CoMo/ γ -Al₂O₃ and found that hydrotreating is efficient in removing S and N to undetectable levels. Konwar et al. (2014) studied hydroprocessing of rapeseed biocrude oil produced via pyrolysis using NiMo/ γ -Al₂O₃ catalyst. Their results showed that S, O and N deduction was found to be 33.3, 70.8 and 21.1 wt% respectively. Further, hydroprocessing efficiency was enhanced by removal of lighter hydrocarbons from biocrude oil through fractionation and reducing the biocrude oil LHSV to 0.5 h⁻¹. Wildschut et al. (2009) achieved 90% HDO of biocrude oil using Ru supported on carbon, which is higher conversion in comparison to commercial catalysts (sulfided NiMo/ γ -Al₂O₃ and CoMo/ γ -Al₂O₃).

2.6 Technoeconomic analysis (TEA)

Techno-economic analysis has been employed widely as a main economic assessment tool to study the potential feasibility of algal biofuel production. This method is also considered as a standard to compare different conversion process technologies in terms of cost analysis. In this study, a flowsheet of the process using a process simulation software (Aspen Plus[®]) was used to estimate capital and operating costs and ultimately determine product-selling price on the basis of dollar per liter. The economic evaluation were based on the equipment and operating cost, material and heat balances. The capital cost of equipment was calculated based on the results of simulation and also according to cost curves based on the equipment cost and their capacities (Ulrich, 1984). The MFSP, which is calculated based on total capital investment and operating costs, makes the net present value (NPV), which is the difference between the present value of cash inflow and outflow during the plant life, zero with a certain internal rate of return (IRR).

Following equation was used to adjust the total installed costs to 2019 dollars:

$$\text{Cost in 2019 \$} = \text{installed cost in reference year} \times \left(\frac{2019 \text{ cost index}=607.5}{\text{reference year cost index}} \right) \quad (2.6)$$

The reference year cost index is also called the Chemical Engineering Plant Cost Index (CEPCI). It became necessary to determine which hydrochar handling process out of chemical activation and combustion, results in lower cost estimation, equipment installed costs and products costs. Methodology applied for total plant cost estimation involved multiplying the sum of purchase prices of all the equipment by a factor known as a Lang factor (Tzanetis et al., 2017; Ulrich, 1984).

2.7 Life Cycle Assessment (LCA)

LCA is considered a useful method to analyze the environmental impacts of chemical processes such as algal biofuels production systems. As with most of the chemical process systems, the negative environmental impact is not associated with the final product, in order to have a true view of the process and its environmental performance, all stages of production such as extraction of raw materials, transportation, technologies used for production and finally distribution of final product should be accounted (Sills et al., 2020). In addition, a functional unit, which provides a reference to relate all of the inputs and outputs should be defined. It may be defined based on the volume or mass of produced biofuels or energy content of the product (Mu et al., 2020; Quinn and Davis, 2015).

LCA is a systematic set of stages of the process by considering the material and energy inputs to obtain a product through its life cycle. The real data are unavailable as there is not any large-scale industrial system for algal biofuels production. The life cycle inventory was obtained from the results of Aspen Plus simulation models based on the mass and energy streams.

A full LCA is also called the “cradle-to-grave” approach considering all stages of extraction of raw material, processing; transportation, production, recycling and distribution of final products. This analysis aims to determine areas with major GHG emissions contributors and provides the possibility of the emissions reduction compared to conventional production using petroleum resources. Therefore, LCA, which is a relative approach and requires system boundaries due to the data limitation, provides an opportunity for policy makers to decide about alternative cases that are most environmentally friendly (Tzanetis et al., 2017).

2.8 Conclusions

This chapter established that algae biomass is a potential feedstock to produce biocrude oil, biogas, and biochar via hydrothermal liquefaction for domestic and industrial applications. In recent times, there is a huge interest for the valorization of algal biomass (third generation biofuels) into liquid transportation fuels owing to the higher calorific value, hydrocarbons suitable to complement gasoline, diesel and jet fuels. However, production of biocrude oil yield and quality depends on the nature of the biomass feedstocks, liquefaction catalysts and process conditions of the liquefaction. On the other hand, produced biocrude oil is upgraded through catalytic hydrotreatment after liquefaction process via heterogeneous catalysts. This chapter discussed the various process conditions used for the removal of heteroatoms (N, S, and O) to

enhance the quality of the biocrude oil for the end application. It was reported that the maximum biocrude oil yield was in the range of 20 – 60 wt%. Further, upgrading the biocrude oil using catalytic hydrotreating technologies show a great platform for producing liquid transportation fuels. In view of this, efficient catalysts and process design need to be developed to enhance the biocrude oil yield and respective hydrocarbon yield for industrial applications.

Chapter 3: Experimental Section

This chapter includes materials section, HTL procedure, Hydrochar production procedure, catalysts synthesis section, and HDO process. Also, all the analytical techniques used to characterize the microalgae, hydrochar, catalysts, oil samples will be described.

3.1 Materials section

In this work, powdered algae called *Nannochloopsis gladina* was obtained from KeyLeaf, Saskatchewan, Canada. Certified ACS reagent-grade Methanol and Dichloromethane ($\geq 99.8\%$ of purity) were purchased from Fisher scientific (Ottawa, ON). Deionized water was prepared using arium® pro water purification system from Sartorius Co. High-purity nitrogen gas was obtained from Praxair Co. (Saskatoon, SK).

Certified ACS reagent-grade Potassium hydroxide (KOH), Potassium carbonate (K_2CO_3), Zinc Chloride ($ZnCl_2$), Sodium hydroxide (NaOH), Phosphoric acid (H_3PO_4), Nickel (II) nitrate hexahydrate ($Ni(NO_3)_2 \cdot 6H_2O$) with molecular weight of 290.79 gr/mol and Ammonium molybdate tetrahydrate ($(NH_4)_6Mo_7O_{24} \cdot 4H_2O$) with molecular weight of 1235.86 gr/mol (Sigma-Aldrich) were purchased from Fisher scientific, Canada. High-purity nitrogen, Hydrogen and methane gas were obtained from Praxair Co, Saskatoon, Canada.

3.2 Characterization methods

Lipid, Protein, Moisture and Ash content analysis

The moisture and ash content analyses for microalgae were carried out according to AOAC 930.15 and AOAC 942.05 standard test methods, respectively. For moisture content analysis, 2.0g of sample was dried to constant weight at $135 \pm 2^\circ C$ in an oven for 2h. Subsequently, the sample was heated in a muffle furnace at $600^\circ C$ for 2h with air flow circulation. Ash content of the sample was determined after a constant weight was attained.

Lipid content was determined using two methods such as Bligh and Dryer method and Swedish tube method (Troëng, 1955). The Bligh and Dyer method is considered as one of the standard analytical methods to extract the lipid content. In this method, the sample is mixed with required amount of solvents; chloroform, methanol and water, with volumetric ratios 2:2:1.8

(v/v/v) followed by filtering through a filter paper. The filtrate is separated after removing aqueous phase. In the Swedish tube method, the sample added into a Swedish tube contained three stainless steel balls and petroleum ether, which is considered as a standard solvent for this procedure. The Swedish tube was placed into a shaker unit for 30 min, and then it was filtered for collecting the solid sample, whereas solvent and extracted oil were collected in a collection flask. The solvent was removed in a rotary evaporator to retain the oil in the flask. For the calculation of the lipid content, the amount of oil retained in the flask was divided by the initial sample amount. Protein analysis was carried out based on AOAC 990.03 standard test method. In this method, the amount of nitrogen, which was released by combustion at high temperature ($\geq 950^{\circ}\text{C}$) in pure oxygen, was measured using thermal conductivity. The system was capable of measuring nitrogen content in materials. Then, the protein content was determined using appropriate numerical factor: Crude protein (wt.%) = $\% \text{N} \times 6.25$. Also, carbohydrate content was determined based on following formulae: Carbohydrate (wt.%) = $\% 100 - [\text{Lipid content} - \text{protein content} - \text{Ash content} - \text{Moisture content}]$ in wt.%.

CHNSO elemental analysis

Vario Elementar Analyzer (Elementar Americas, NY, USA) was used to measure the amount of carbon (C), nitrogen (N), hydrogen (H), sulfur (S), and the oxygen content (Oxygen (wt.%) = $100 \text{ wt.\%} - \text{C} - \text{H} - \text{N} - \text{S}$) in hydrochar samples. In this analysis, increasing temperature leads to decomposition of solid materials following their conversion into gaseous products.

Heating value measurement (HHV)

The calorific values (HHV) was measured using an oxygen bomb calorimeter with benzoic acid as a standard material for calibration (Añón et al., 1995). 1.0g of the sample was placed in a stainless-steel crucible and then mounted inside the bomb calorimeter. The reactor vessel was charged with pure compressed O_2 up to a pressure of 3.0MPa and 1.0mL of distilled water added. Subsequently, the vessel was immersed in a calorimeter filled with distilled water and then placed in an isothermal jacket maintained at constant temperature by circulating water at 25°C . The gross calorific values or the higher heating values (HHV) were also calculated from the CHNS elemental data using the Dulong equation: $[\text{HHV (MJ/kg)} = 0.338 \text{ C} + 1.428 (\text{H} - \text{O}/8) + 0.095 \text{ S}]$.

Gas chromatography (GC) analysis

The gaseous products were collected from reactor after the experiments, in tedlar bags and were analyzed in an Agilent 7890A GC using a gas autosampler. The inlet temperature, pressure and total flow of helium gas were maintained at 200°C, 4.05psig and 110mL/min with split ratio of 20.4:1, respectively. The GC was equipped with two injection ports connected to packed and capillary columns to separate the permanent gases (CO₂, CO, H₂, N₂, O₂) and hydrocarbons (ethane, ethylene, acetylene, propane, propylene, butane, butene), respectively. The packed columns were hayesep Q (1.8m long with id of 3.17mm) and molecular sieve 13X (3.04 m long with id of 3.17mm). The capillary column was CP-Al₂O₃/KCl (25m long with id of 0.53mm). The packed column was connected to a thermal conductivity detector and the capillary column was connected to a flame ionization detector. The gases from the gas collection bag were injected into both columns simultaneously by the gas autosampler and the columns were housed in the same oven. The oven temperature was initially set at 60°C, and initially held for 4min at this temperature, then was increased to 80°C at ramp rate of 5°C/min, and was finally increased to 165°C at 20°C/min and held at that temperature for 1.5min.

Simulated distillation (Sim-Dist) analysis

The boiling point distribution of the obtained biocrude oil and upgraded biocrude oil were estimated using simulated distillation (Sim-Dist) technique. The samples were dissolved in CS₂ (Fisher Scientific, Canada) to prepare the solutions for Sim-Dist analysis. Sample analyses were accomplished using ASTM D-2887 on the Varian CP-3800 gas chromatograph equipment.

Gas chromatography-mass spectrometry (GC-MS) analysis

A Trace 1310 Gas Chromatograph and a TSQ Duo Mass Spectrometer (Fisher Scientific, USA) was used to identify chemical compounds available in the biocrude oil and upgraded biocrude oil samples. The samples were dissolved in dichloromethane to prepare them for GC-MS analysis. The inlet temperature and flow rate of helium were set at 250°C and 1.2mL/min, respectively. The oven temperature was increased at 5°C/min from room temperature to 150°C, then increased to 320°C at 10°C/min and was held at this temperature for 5 min. The ion source temperature and mass spectroscopy transfer line temperatures were set at 250°C and 300°C, respectively. The peaks were recognized according to National Institute of Standards and Technology (NIST) library using Chromeleon TM 7.2 Chromatography Data System (CDS) software.

Proton Nuclear Magnetic Resonance spectroscopy

^1H -NMR analyses for the samples were performed in a 500 MHz Bruker Advance NMR spectrometer. The spectra were acquired in the Fourier Transform (FT) mode operating at a frequency of 500 MHz. Prior to data acquisition, the samples were diluted with deuterated chloroform (CDCl_3) and filtered through a $0.2\mu\text{m}$ non-pyrogenic sterilized disc filter (VWR, Canada) followed by chemical shifts measurement. The operating conditions used were as follows: the 90° pulse width was $9.5\mu\text{s}$ and the spectral width was 10 kHz. In addition, 16 scans were taken with 1 second recycle delay. The acquisition time for each sample was less than 5 minutes for the analyses.

Carbon-13 Nuclear Magnetic Resonance (NMR) Spectroscopy

A Bruker Avance 500 MHz NMR spectrometer equipped with 5 mm broadband inverse probe was used for ^{13}C -NMR analysis. Prior to analyses, 5mg of the crude oil sample was dissolved in CDCl_3 (Merck, Germany) followed by filtration using $0.2\mu\text{m}$ non-pyrogenic sterilized disc filter (VWR, Canada). During the analysis, ^{13}C NMR spectra were referenced to CDCl_3 solvent at 77.3ppm and the experimental data were processed through TopSpin version 3.5 software.

N_2 -adsorption/desorption analysis

The Micromeritics ASAP 2020 Porosity Analyzer was used to ascertain the textural properties of the bio-materials using N_2 at 77K. The specific surface area of the bio-residue samples were determined from the BET method while the pore sizes and pore volumes were estimated from the BJH method. Prior to degassing at 300°C under vacuum, the samples were heated overnight at 315°C to remove the traces of oil present in the samples post extraction. Degassing of samples was carried out at temperature of 200°C and pressure of $500\mu\text{m Hg}$ for 90 minutes. The micropore volume (V_{micro}) was calculated using t-plot method. The mesopore volume (V_{meso}) was calculated as $V_{\text{meso}} (\text{cm}^3/\text{g}) = V_{\text{total}} - V_{\text{micro}}$.

Fourier transform infra-red (FTIR) spectroscopy

The FTIR spectra of biocrude oil, upgraded biocrude oil and bio-residue samples were obtained to qualitatively determine the functional groups present. The spectroscopic analysis was carried out using a Bruker Vertex 70 FTIR spectrometer (Bruker Corporation, Billerica, MA, USA). A diamond ATR (attenuated total reflection) crystal was used in the spectrometer to obtain the infrared spectra in the range of $4500\text{--}400\text{ cm}^{-1}$ for bio-residue samples.

Thermogravimetric Analysis (TGA)

The thermal stability of bio-residue and produced activated carbons samples was evaluated via thermogravimetric analysis (TGA) method using a TGA-Q500 equipment designed by TA Instruments, USA. In a typical analysis, 10-20 mg of the sample was subjected to heating from room temperature in nitrogen atmosphere at a flow rate of 60mL/min to 800°C at a ramping rate of 10°C/min.

Scanning Electron Microscope (SEM)

The surface morphology of samples was tested using Hitachi SU8010 field emission SEM with an accelerating voltage of 3kV (Hitachi High-Technologies Corporation, Tokyo, Japan). The samples were sputter coated with 10nm thick Au films using the Quorum Q150T ES sputtering unit prior to SEM imaging.

X-Ray Diffraction (XRD) Analysis

X-ray diffractograms of the samples were collected using a Bruker D8 Advance Series II X-Ray Powder Diffractometer (Bruker Corporation, Billerica, MA, USA). Cu K- α radiation source ($\lambda = 1.5406 \text{ \AA}$) operating at voltage of 40 kV and current of 40 mA was used for analysis. The analysis was carried out in the range of $10^\circ \leq 2\theta \leq 90^\circ$ at a scan rate of $1.36^\circ \text{ min}^{-1}$.

X-ray photoelectron spectroscopy (XPS)

XPS analysis was used to study functional moieties on the samples. The analysis was carried out using a Kratos (Manchester, UK) AXIS Supra system at Saskatchewan Structural Sciences Centre (SSSC), at the University of Saskatchewan. The radiation source was a 500 mm Rowland circle monochromated Al K- α (1486.6 eV) emitter. The required voltage and current of 15 keV and 10 mA were used, respectively. High resolution C1s and O1s were collected using 0.05 eV steps and a pass energy of 20 eV. The results were given based on the average of six randomly selected points on the surface of AC.

Particle size analyzer

The particle size of algal hydrochar and chemically prepared activated carbon were studied using a Malvern Mastersizer 3000 (Malvern Instruments, Worcestershire, UK). In this setup, the concentration of the samples was set based on the specific range of obscuration when added to the water as a dispersant with refractive index of 1.33 following ultrasonicated for 10 s.

3.3 Hydrothermal liquefaction process (HTL)

Hydrothermal liquefaction (HTL) experiments were conducted in a 100mL stainless steel autoclave designed to operate at maximum temperatures and pressures of 500°C and 34.4MPa reactor, respectively. The schematic diagram of HTL system is shown in Figure 3.1. In this work, HTL system is equipped with an electrical furnace and a thermocouple to accurately measure the temperature. 5g of biomass and 25g of solvent (methanol and/or water) were taken in the reactor and sealed. Compressed nitrogen gas was used to purge the system three times to displace air in the reactor followed by temperature increments to set values with constant heating rate of 5°C/min which was controlled by a temperature controller. Reactants were agitated vertically using a magnetically coupled mechanical stirrer at 200rpm and preheated to the desired reaction temperature. First, different methanol-water mass ratio at critical temperature and pressure with constant reaction time of 60min, were applied. Second, different reaction temperature and time at constant pressure (11.5MPa) with methanol-water mass ratio of 0.75-0.25, based on CCD design were employed. During the heating period, the reactor pressure reached to the desired pressure and temperature. After the required temperature and pressure were reached, the reactor was maintained at this condition for a predetermined reaction time. Then the reactor was cooled down to 25°C by quenching quickly (less than 15 minutes) in iced-water bath in order to stop further reaction prior to depressuring to atmospheric pressure. The procedure was adapted based on the published work by Lai et al. (2018). However, in cases where the product gas analysis was required, aliquot of the gas in the reactor was carefully sampled into Tedlar bags via a control valve and subsequently analyzed using an offline GC equipped with both TCD and FID detectors. Subsequently, the reactor was thoroughly washed with dichloromethane (DCM) and the content was vacuum filtered using a separation funnel and an Erlenmeyer flask assembly with a Whatman No. 2 filter paper. Filtered cake was dried at 105°C for 12h to constant weight, and the hydrochar obtained was crushed and sieved by 1.18 mm mesh and the fraction that passed 1.18 mm sieve mesh was used for further characterizations and analytical studies. DCM and methanol were separated from liquid phase by rotary evaporator at 65°C under vacuum. Water was separated from the mixture by drying at 105°C for 2h and the remaining product was weighed and considered as biocrude oil. The yield (wt.%) of each product as well as energy recovery (ER) from HTL were calculated using the following equations:

$$Y_{\text{Biocrude oil}} (\text{wt.}\%) = \frac{\text{Mass of biocrude oil}}{\text{Mass of dry microalgae}} * 100\% \quad (3.1)$$

$$Y_{\text{Hydrochar}} (\text{wt.}\%) = \frac{\text{Mass of hydrochar}}{\text{Mass of dry microalgae}} * 100\% \quad (3.2)$$

$$Y_{\text{Gas}} (\text{wt.}\%) = 100\% - (Y_{\text{Biocrude oil}} + Y_{\text{Hydrochar}}) \quad (3.3)$$

$$\text{Energy recovery (ER) in biocrude oil (\%)} = \frac{\text{HHV}_{\text{Biocrude oil}}}{\text{HHV}_{\text{microalgae}}} \times (Y_{\text{Biocrude oil}}) \quad (3.4)$$

$$\text{Liquefaction conversion rate (wt.}\%) = \left(1 - \left(\frac{\text{Mass of dry residue}}{\text{Mass of dry microalgae}}\right)\right) 100\% \quad (3.5)$$

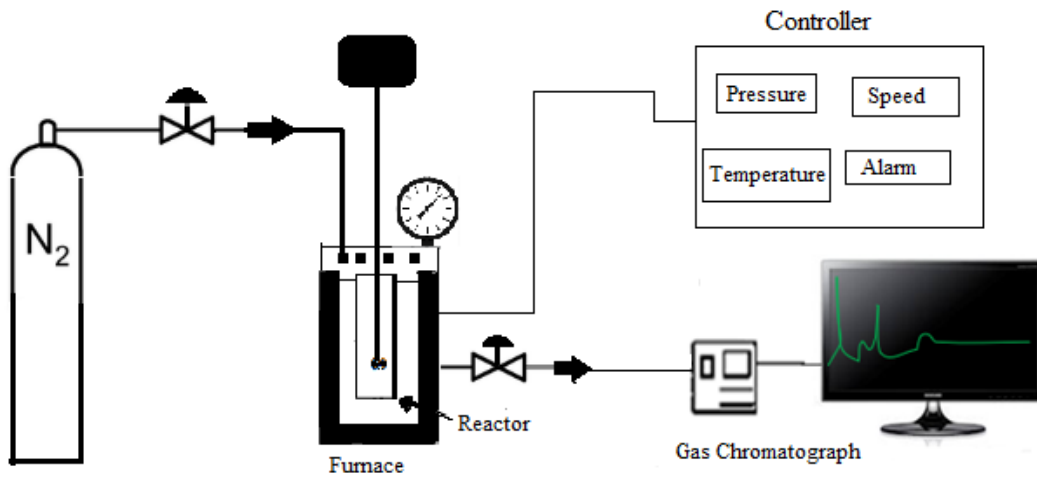


Figure 3.1: Schematic diagram of HTL process

3.4 Activated carbon production

Chemical activation of hydrochar was carried out for production of activated carbon. 5 g of hydrochar was mixed in predetermined amount of activator (based on the mass ratio of KOH/hydrochar = 0.5-2.5, defined by experimental design) to obtain uniform slurry. After immersing the hydrochar in the prepared solution, heating and stirring was continued for a slurry, then the mixture was left in the vacuum oven at 100 °C for 12 h. The prepared mixture was placed inside the reactor, heated up using a heating rate of 3°C/min to desired temperature for 2 h under nitrogen flow and was cooled down under nitrogen flow. Nitrogen flow prevented any possible hotspots in the solid bed and removed the unreacted potassium and gaseous product produced during the activation process. The schematic diagram of setup for activated carbon

production was shown in Fig. 3.2. The required temperature (525-825 °C) and flow rate of nitrogen (63-267 cc/min) were applied to investigate their effects on yield and porous characteristic of prepared activated carbons obtained. The process was carried out in a fixed-bed reactor. A k-type thermocouple was connected to the temperature controller to control and calibrate the temperature as a one of the major factors considered during activation.

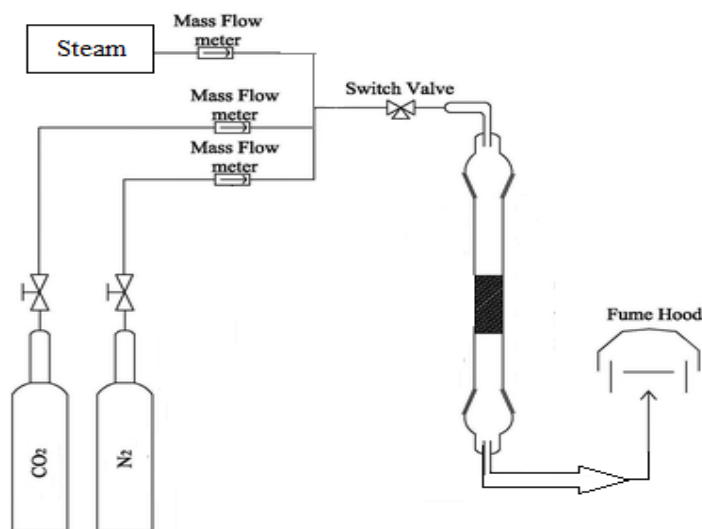


Figure 3.2: Schematic diagram of setup for activated carbon production

Then, the sample was cooled down to 25°C, collected and mixed with 0.1 M of HCl for 3 h following washing with distilled water. After removing the chemical residues, the sample was dried at 110 °C overnight to prepare activated carbon (AC). The equations (3.6) and (3.7) were used to calculate the yield and energy recovery (ER) of activated carbons:

$$\text{Yield of AC (Y}_{AC}\text{) (wt\%)} = \frac{\text{Weight of produced AC(g) after activation process}}{\text{Weight of dry impregnated algal hydrochar (g)}} \quad (3.6)$$

$$\text{Energy recovery (ER) (\%)} = \frac{\text{HHV}_{AC}}{\text{HHV}_{\text{Algal hydrochar}}} \times (\text{Y}_{AC}) \quad (3.7)$$

3.5 Methylene blue adsorption test

The adsorption behavior of samples (algal hydrochar, commercial activated carbon and chemically prepared activated carbon by K_2CO_3) was studied using adsorption of methylene blue. A commercial activated carbon with BET surface area of $1127\text{ m}^2/\text{g}$ with pore volume and pore size of $0.67\text{ cm}^3/\text{g}$ and 7.0 nm , respectively was also used. Methylene blue was purchased in analytical purity from Sigma-Aldrich with $\lambda = 668\text{ nm}$. The batch adsorption experiments were performed at room temperature using stirred flasks at a stirring speed of 500 rpm . During time intervals, the samples were filtered using $0.42\text{ }\mu\text{m}$ disposable syringe filters. The filtrate (carbon-free solution) was transferred into a clean quartz cuvette and used as a function of time for the analysis of methylene blue content using an ultraviolet spectrophotometer (Shimadzu UV Mini 1240, Sozhou instruments manufacturing, China). The experiments were performed by adding 100 mg of chemically prepared activated carbons and commercial activated carbon into 100 ml of 250 mg/L (ppm) of initial concentration of methylene blue. According to the literature the initial concentration of methylene blue as an adsorbate was in the range of $30\text{--}800\text{ mg/L}$ (Jawad et al., 2016; Karaçetin et al., 2014)

3.6 Catalyst synthesis procedure

The synthesis of Mo and NiMo carbide catalysts from Mo oxide and NiMo oxide, respectively, is described as follows. The $13\text{ wt.}\%$ Mo/AC catalyst was prepared by impregnating $13\text{ wt.}\%$ of ammonium molybdate tetrahydrate on synthesized AC from algal derived hydrochar. Also, $3.5\text{ wt.}\%$ Ni and $13\text{ wt.}\%$ Mo oxide on activated carbon was prepared by step-wise and co-impregnation of the required amount of ammonium molybdate tetrahydrate and nickel(II) nitrate hexahydrate on algae derived-activated carbon. In step-wise impregnation, the Mo precursor was added before the Ni precursor, as Mo and Ni used as an active metal and promoter, respectively (Jafarian et al., 2019). Due to porous nature of the activated carbon, both Ni and Mo species were located in the pores of the carbon support. The prepared materials were dried and calcined at $550\text{ }^\circ\text{C}$ for 4 h under a nitrogen flow rate of $100\text{ cm}^3/\text{min}$. The supported oxides using step-wise impregnation were converted to carbides in three different ways at $700\text{ }^\circ\text{C}$; temperature-programmed reaction (TPR) with $20\%\text{ CH}_4/\text{H}_2$, carbothermal hydrogen reduction (CHR) in H_2 , and carbothermal reduction (CR) in N_2 . Based on the characterization results obtained from three different reduction methods, one of them will be used to convert oxide phases of NiMo synthesized using co-impregnation method and oxide phase of Mo/AC to

carbide phase. The temperature was ramped at 5 °C/min and carbonization was done for 4 h. After that, the reactor was cooled to room temperature and the catalyst material was passivated with 1 vol.% of O₂ in N₂ for 1 h.

3.7 Hydrodeoxygenation (HDO) process

Hydrodeoxygenation of algae biocrude was performed in a 100 ml stirred tank Parr reactor unit. The reactor was loaded with algal biocrude oil and the desired amount of catalyst. After pressurizing the reactor system with hydrogen up to 3MPa, the reactor was heated to the desired temperature (350-450 °C) with a heating rate of 10 °C/min while stirring at 500 rpm. After the desired reaction time (1.5-4 h), the reactor was cooled down to room temperature, depressurized, and collected the liquid product. The upgraded product was diluted with dichloromethane (DCM) and then filtered to remove solid and catalyst particles. The upgraded products contained two phases. The aqueous phase was separated from the oil phase using a separation funnel. The oil phase was subjected to rotary evaporation to remove DCM and residual water. The yield of the aqueous phase, water-soluble compounds (WSC) and the oil phase (upgraded oil) was calculated from their respective mass divided by the mass of algal biocrude feedstock. The filter paper with solid residue and catalyst was dried at 110 °C for 12 h and the amount of solid materials (coke) was calculated by subtracting the weight of fresh catalyst loaded into the reactor from the weight of filtered materials (solid residue and spent catalyst). The procedure was adopted from C. Zhang et al., 2014. To minimize the uncertainties of the experimental results, experiments were performed in triplicate and average results reported. The Energy recovery of the upgraded biocrude oil was calculated based on the chemical energy content of feedstock and the upgraded fuel product as follow:

$$\text{Energy Recovery (\%)} = \frac{\text{The HHV of upgraded biocrude oil}}{\text{The HHV of algal biocrude oil}} \times (\text{upgraded biocrude oil yield})$$

(3.8)

Chapter 4: Biocrude oil and hydrochar production and characterization obtained from hydrothermal liquefaction of microalgae in methanol-water system

The content of this chapter has been published in Journal of Energy cited below and presented in the following conferences:

Citation:

Masoumi, S., Boahene, P.E., Dalai, A.K., 2020. Biocrude oil and hydrochar production and characterization obtained from hydrothermal liquefaction of microalgae in methanol-water system. *Energy*. 217, 119344.

Conference Proceedings:

Shima Masoumi, Ajay. K. Dalai, “Optimization of bio-crude oil production from microalgae using hydrothermal liquefaction technology in methanol-water system”, Canadian society for bioengineering, Vancouver, July 14 -17, 2019.

Shima Masoumi, Philip Effah Boahene, Venue Babu Borugadda, Ajay. K. Dalai, “Hydrothermal Liquefaction of Micro-Algae for Bio-Oil Production in Critical Methanol-Water System”, North American Catalysis Society Meeting in Chicago, Jun 23-28, 2019.

Contribution of the PhD candidate:

Experiments were designed in consultation with Dr. Philip E. Boahene, (Postdoc member of the group) under the supervision of Dr. Ajay K. Dalai and executed by Shima Masoumi. Material synthesis, catalysts characterization and data interpretation were performed out by Shima Masoumi. The manuscript was drafted by Shima Masoumi with guidance and suggestions provided by Dr. Philip E. Boahene and Dr. Ajay K. Dalai.

Contribution of this chapter to overall PhD research:

The first phase of the research is investigated in this chapter: biocrude oil and hydrochar production and characterization obtained from hydrothermal liquefaction process using methanol-water co-solvent system was studied. This chapter is the basis of the following chapters.

4.1 Abstract

Hydrothermal liquefaction of microalgae under milder reaction conditions was studied for the production and characterization of high quality biocrude oil and hydrochar confirming its feasibility as sustainable biofuel source. The present study investigates the effects of solvents, temperature and time on the yield of biocrude oil. The comparatively higher yield of biocrude oil (47wt.%) obtained in methanol-water mass ratio of 0.75:0.25 also contained higher amount of ester components resulting in higher biocrude oil quality. Methanol-water co-solvent favored higher biocrude oil yield with lower nitrogen and oxygen contents as compared to pure water. Response surface methodology was applied to study the effects of temperature (222-322°C), and reaction time (10-60min) at constant pressure of 11.5MPa for methanol-water and biomass-solvent ratios of 0.75:0.25 and 1:5, respectively. The optimum yield of biocrude oil (57.8wt.%) and highest energy recovery (85.3%) was obtained with 75wt.% of methanol in water at 272°C and reaction time of 35 min. Subcritical condition (temperature of 222°C, pressure of 11.5MPa) resulted in the highest hydrochar yield (19.5wt.%). Hydrochars were also characterized by CHNS, BET, FT-IR and TGA techniques to ascertain their prospective elemental composition, textural properties, functional groups as well as thermal stability.

Keywords: Biocrude oil, hydrochar, hydrothermal liquefaction, microalgae, co-solvent

4.2 Introduction

Over the last few decades, due to the incremental industrialization, there is a drastic increase in carbon dioxide (CO₂) emission to the environment. There is also an increase in energy consumption and the lack in the resource of environmentally friendly fuel to meet the existing demands. In response to the everlasting consumption of unsustainable fossil fuels and the effects of greenhouse-gas emissions, more attention has been paid to finding alternate sources of energy (Biswas et al., 2017; Gollakota et al., 2018; Pan et al., 2018). Renewable energy as a sustainable and secure resource, obtained from biomass feedstocks (which are rich in carbon and hydrogen) can be converted to value-added products through thermochemical and biochemical technologies (Dimitriadis and Bezergianni, 2017; Valdez et al., 2011; Zhu et al., 2018). As compared to the conventional first generation solid biomass sources such as agricultural crops, which require enormous acreage of arable lands and consequently compete with food production, microalgae as the third generation of feedstock has attracted much attention due to its advantages such as an

effective CO₂ capture, fast growth rate and lack of arable land supplies (Chiaramonti et al., 2017; Galadima and Muraza, 2018; López Barreiro et al., 2013).

Hydrothermal liquefaction (HTL) of microalgae as a thermochemical conversion method is a promising technology for the production biocrude oil. Low energy cost for processing due to the elimination of wet biomass drying steps and high energy efficiency are some of the beneficial effects of this technology (Elliott et al., 2013; Toor et al., 2011). Production of algal biofuels by the HTL technique results in the co-generation of significant amounts of residues as co-products known as bio- or hydrochar. The suitable utilization of the hydrochar obtained from the HTL process will improve the overall economics of algal biofuel production (Broch et al., 2014; Safari et al., 2018).

Recently, research has been focused on replacing water by reactive organic solvents or using co-solvent for HTL process to improve the reaction conditions and process efficiency. The critical temperature and pressure of organic solvents such as ethanol are much lower than that of water due to its lower polarity (Lai et al., 2018; J. Zhang et al., 2014). One of the objectives of this research was to investigate the hydrothermal liquefaction of algae with methanol and water as the co-solvent. Methanol was introduced into the hydrothermal liquefaction process due to several advantages: Methanol is the only alcohol which is a little bit more acidic than water (pK_a value for methanol (15.5) is slightly lower than pK_a value for water (15.7)), because it is the conjugate acid of a weak base (OMe^-) while water is the conjugate acid of a strong base (OH^-). According to the Bronsted-Lowry concept, the conjugate acid of a weak base is a strong acid and vice versa. Moreover, lipid content would be more soluble in methanol as a reactive organic solvent in less severe reaction conditions which favors liquefaction process. In addition, methanol can react with acidic compounds by transesterification reaction and produce the biodiesel-like product (Feng et al., 2018; Patel and Hellgardt, 2016).

The influence of methanol-water mass ratio, reaction temperature, time and their interactions on biocrude oil and hydrochar yield and their characterizations in methanol-water system have rarely been investigated in the literature. In this study, firstly the effects of methanol to water mass ratios at critical conditions were investigated to determine the maximum biocrude oil production. Secondly, Design Expert (Central Composite Design, CCD) was employed to investigate the effects of time and temperature (subcritical-supercritical conditions) as crucial factors on biocrude oil and hydrochar yields, and these materials were extensively characterized.

The influence of these parameters and their combined interactions on biocrude oil yield was also statistically evaluated using Analysis of Variance (ANOVA). Quadratic models as a function of time and temperature during HTL process were generated for the maximum biocrude oil yield and carbon contents in the biocrude oil. The chemical compositions (CHNSO) of the biocrude oil and its physical properties (boiling point distributions, higher heating values, etc.) were also analyzed. The solid by-product (algal hydrochar) obtained from the HTL process was thoroughly analyzed by characterization techniques such as CHNS, BET, FTIR and TGA to investigate the effects of methanol/water mass ratio, time and temperature on its physico-chemical properties. It should be highlighted that the reason for studying the impact of critical conditions of different mass ratios of methanol-water system is that there is only one single critical point for each mass ratio of methanol and water. After optimizing the mass ratio, at constant pressure, the effects of subcritical and supercritical conditions on products yield and their characterizations were investigated thoroughly by changing the temperature and time using response surface methodology. Systematic study as described above is rare in the literature.

4.3 Materials and methods

Materials, HTL process and characterization methods used in this study explained previously in Chapter 3, Sections 3.1, 3.2, and 3.3.

4.4 Results and discussion

Table 4.1 presents the results of elemental analysis, biochemical composition, and HHV of microalgae used for HTL process. For this study, the amount of lipids reported based on the Bligh and Dryer method used for the extraction. During HTL process, proteins and carbohydrates as well as lipids can be converted to biocrude oil. It can be considered as one the advantages of HTL compared to solvent extraction technique.

Table 4.1: Biochemical properties, elemental analysis and HHV of microalgae

Proximate analysis (dry-basis) (wt %)				Elemental analysis (wt %)					HHV(MJ/kg)
Lipid	protein	Carbohydrate*	Ash	C	H	N	S	O*	
18.9	44.2	25.7	6.7	50.2	6.8	7.2	0.8	35	21.2

*Calculated by difference

4.4.1 Effects of different mass ratios of methanol/water in critical reaction condition

4.4.1.1 The effects of methanol/water mass ratios on product distributions

As can be seen in Table 4.2, solvent with five different mass ratios of methanol and water was used for the HTL process. The critical temperature and pressure (T_c , P_c) for solvents used with different methanol-water mass ratios are also given in the Table. Each of these five experiments was performed at critical points for 60min at 200rpm. Compared to traditional HTL process with water (Run 1), adding methanol as co-solvent to the HTL system resulted in lowering the severity of the reaction conditions (temperature and pressure) due to lower critical point of methanol.

Table 4.2: Biocrude oil yield and product compositions

Run	Water (wt.%)	Methanol (wt.%)	T_c (°C)	P_c (MPa)	Biocrude oil yield (wt.%)	Gas yield (wt.%)	Gas composition (mol.%)		
							CO ₂	CH ₄	C2 ⁺
1	100	0	374	22.0	15.9±0.5	56.2	97.5	2.1	0.7
2	75	25	340	18.5	34.1±0.7	42.5	91.0	6.3	2.7
3	50	50	306	15.0	43.1±0.3	34.6	91.5	5.4	2.1
4	25	75	272	11.5	47.5±0.4	23.5	91.6	7.1	1.3
5	0	100	239	8.0	45.1±0.3	24.1	90.5	5.1	4.4

These experiments were carried out at least three times to determine the repeatability of the collected data. Biocrude oil samples obtained from HTL are viscous with strong aromatic fragrance and their color change from green to dark brown as the temperature increased. The yield of biocrude oil was lowest for the experiment carried out with pure water as solvent (15 wt.%), and then it obviously increased with increasing the amount of methanol as co-solvent; reaching a maximum of 47wt.% at methanol-water mass ratio of 0.75:0.25. According to GC analysis, light gas molecules were formed, which were mainly CO₂ and CH₄. As it can be seen in Table 3.2, for HTL process, over 90 mol.% of the gas products was CO₂.

Figure 4.1 revealed that compared to pure water (Run 1) and pure methanol (Run 5) as the solvent medium for HTL process, using methanol-water co-solvent results in higher biocrude oil. Use of pure methanol as solvent resulted in higher biocrude oil yield as compared to its pure water counterpart. Due to the lower dielectric constant and less polar nature of methanol as

compared to water, the diffusion of solvent into the biomass was enhanced; consequently, increasing biocrude oil yield. Also, methanol is slightly more acidic than water which served as hydrogen donor, resulting in catalyzing the HTL process; thus, resulting in increased yields of biocrude oil obtained.

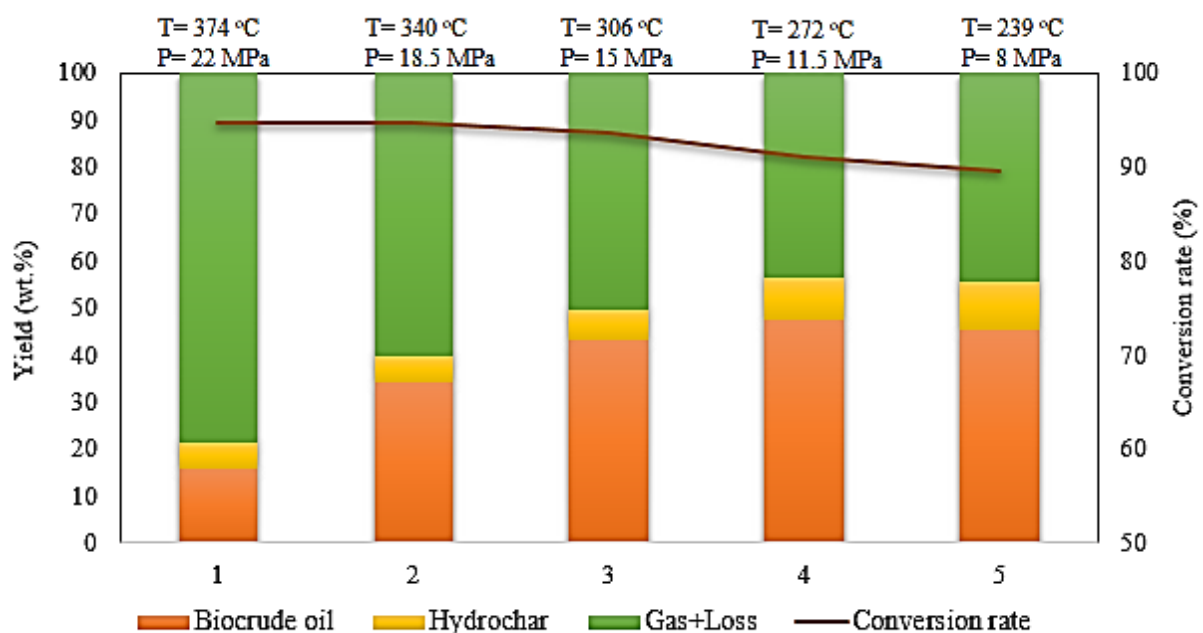


Figure 4.1: Effect of methanol/water ratio on liquefaction product distribution (Numbers 1,2,3,4 and 5 indicate the biocrude oil obtained by pure water, 25 wt.% of methanol, 50 wt.% of methanol, 75 wt.% of methanol and pure methanol as solvent at constant reaction time of 60 min)

The change in the conversion rate from 100:0 methanol water ratio to 50:50 was low, and the lowest value appeared for Run 5, with pure methanol. This observation can be ascribed to the fact that methanol is less polar than water with much lower critical temperature and pressure; thus, leading to insufficient conversion of biomass. Therefore, highest hydrochar (solid residue) yield was obtained from Run 5 with pure methanol at lowest temperature (239 °C) compared to other experiments. It may have occurred because of re-polymerization reaction of free radicals and incomplete hydrolysis. Higher gas yield was obtained from HTL with pure water compared to HTL with pure methanol and methanol-water as medium solvent. It means that the reaction conditions (T= 374°C and P= 22MPa) favor decarboxylation and gasification reactions of intermediates, leading to more gas yield. Therefore, addition of methanol as solvent or co-solvent in HTL process resulted in lower gas production.

4.4.1.2 The effects of methanol/water ratios on elemental composition of biocrude oil

The elemental compositions of biocrude oils obtained from different mass ratios of methanol-water at critical points are given in Table 4.3. Similarly, the corresponding HHV and energy recovery of HTL for different runs are also listed in Table 4.3. Carbon is considered as the major contribution to the higher heating value. Hydrogen is another major constituent of microalgae which greatly contributed to the higher heating value (Dimitriadis and Bezergianni, 2017). The carbon and hydrogen contents in biocrude oils increased and the oxygen content decreased, in comparison with elemental composition of raw microalgae (Table 4.1). It is noteworthy to mention that biocrude oils obtained from HTL of algae have high contents of oxygen and nitrogen as compared to amounts in a typical conventional petroleum crude oil with 0.05-1.5% O and 0.1-2% N, respectively (Jarvis et al., 2017). In this regard, biocrude oils have limited usage as fuel for transportation due to their detrimental properties such as thermal instability and low calorific value.

The highest contents of oxygen and nitrogen was obtained with pure water as solvent for the HTL process. The addition of methanol lowered the contents of oxygen and nitrogen as well as increased the hydrogen and carbon contents resulting in increasing the higher heating value. It can be related to the fact that methanol performs well as an efficient hydrogen donor solvent, which can enhance hydration reactions. Therefore, the addition of methanol up to 75wt.% resulted in decreasing H/C and O/C, and increasing the HHV as depicted in Table 4.3. For the various ratios investigated, the highest C and H contents with the lowest O content was recorded for the biocrude oil with MeOH/H₂O ratio of 0.75:0.25, resulting in HHV of 32.2MJ/kg. The sulfur content of biocrude oil from H₂O only and MeOH-H₂O systems did not change indicating that different solvents investigated were unable to significantly change the sulfur contents. Interestingly, as can be seen in Table 4.3, solvent environment plays a significant role in ER of HTL process. The ER of HTL process in methanol-water co solvent and in pure methanol were obviously higher than that with pure water. The maximum ER (71.3%) was achieved with HTL process using MeOH/H₂O ratio of 0.75:0.25 as solvent due to high yield and HHV of the biocrude oil.

Table 4.3: Elemental composition and HHV of biocrude oils

Run	Elemental composition (wt.%)					H/C	O/C	HHV (MJ/kg)	ER* (%)
	C	H	N	S	O*				
1	65.2	7.9	6.1	0.3	20.5	1.45	0.23	24.7	17.4
2	65.8	8	5.4	0.3	20.5	1.45	0.23	25.2	40.4
3	67.1	8	4.5	0.3	20.1	1.43	0.22	26.7	54.1
4	72.3	8.3	4.1	0.3	15.0	1.37	0.15	32.2	71.3
5	69.1	8.1	4.1	0.3	18.4	1.40	0.19	29.1	61.7

$$*\text{Energy recovery (ER) in biocrude oil (\%)} = \frac{\text{HHV}_{\text{Biocrude oil}}}{\text{HHV}_{\text{microalgae}}} \times (Y_{\text{Biocrude oil}})$$

4.4.1.3 The effects of methanol/water ratios on boiling point distribution of biocrude oils

Simulated distillation (Sim-Dist) was employed to evaluate the boiling point distribution for HTL biocrude oils, which is a function of structure of compounds in the range of C₁₀ – C₆₀. Figure 4.2 shows a quantitative comparison based on calibration of Sim-Dist using n-alkane standards. For all the biocrude oil samples, boiling cuts of fractions were predominantly in the range of vacuum gas oil (343-538°C), with its carbon range of C₂₀-C₄₀. Biocrude oil obtained from pure water revealed the highest percentage (~79%) of compounds belonged to the high-boiler category (with C ≥ 20), and the largest amount of residue (23%), compared with MeOH only sample or MeOH-H₂O co-solvent system. It can be correlated to the fact that biocrude oil using pure water would self-polymerize into materials with higher molecular weight (Lai et al., 2018). The biocrude oil obtained from HTL process in pure methanol and methanol-water ratio of 0.75:0.25 has large amount of materials with carbon chain ≤ 20 than produced from pure water. Although, addition of methanol as co-solvent into the system resulted in higher amounts of low boiling point compounds, the need for upgrading of HTL biocrude oils seems important for its use as transportation fuel.

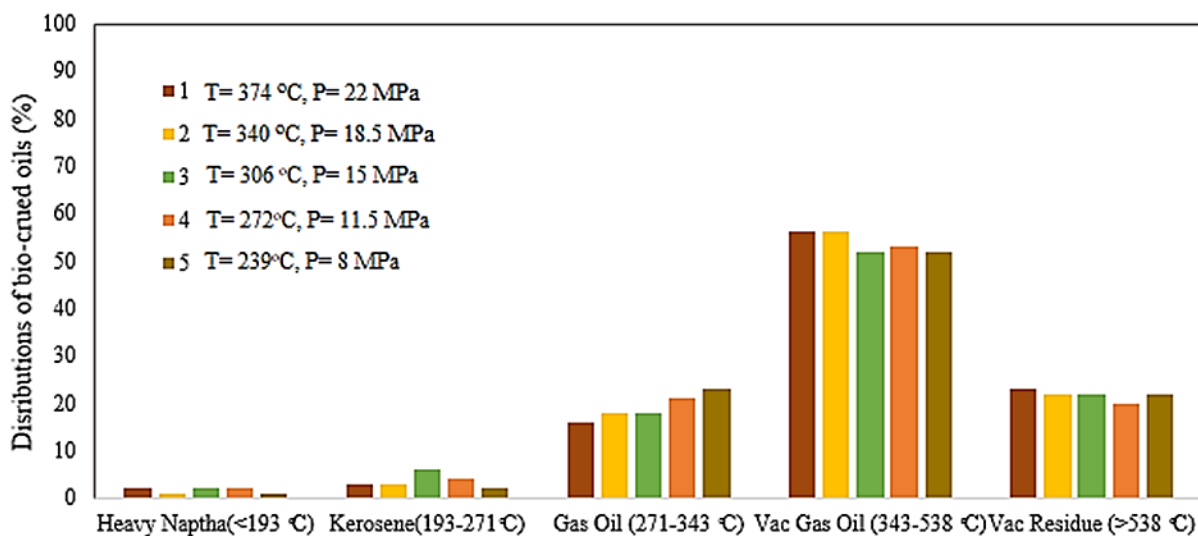


Figure 4.2: Sim-Dist boiling point fractions of HTL biocrude oils (Numbers 1,2,3,4 and 5 indicate the biocrude oil obtained by pure water, 25 wt.% of methanol, 50 wt.% of methanol, 75 wt.% of methanol and pure methanol as solvent at constant reaction time of 60 min)

4.4.1.4 The effects of methanol/water ratios on chemical compositions of biocrude oils

GC-MS analysis was used to identify different chemical compounds of biocrude oils obtained from HTL in different mass ratios of methanol-water system (Figure 4.3). From the results, it was found that biocrude oil obtained using pure water contained large amount of nitrogenous compounds, which agrees with the data from CHNS analysis, and phenolic compounds such as phenol, 3-methyl, nanofin, 1H-indole, 7-methyl, and rescinamine. Addition of methanol as a co-solvent resulted in lowering nitrogenous compounds. The major peaks are related to tridecanoic acid, 9-octadecanoic acid and to large amount of hexadecanoic acid.

The potential reaction pathways for biomolecules for hydrothermal liquefaction of microalgae in the methanol-water co-solvent system is presented in Figure 4.4. Through hydrothermal liquefaction process, firstly, biomolecules (lipid, protein and carbohydrates) hydrolyze to form triglyceride (the common form of lipid), and nitrogenous compounds such as amino acids and sugars(Gai et al., 2015; Zhang and Zhang, 2014). It is clear that addition of methanol in water through liquefaction results in esterification reactions leading to more ester content, which is in a good agreement with GC-MS analysis. Amino acids were degraded via decarboxylation and deamination reactions, and having methanol in system may increase the possibility of esterification reactions resulting in lower amount of phenolic and nitrogenous

compounds. It can be seen in Fig 4.3 that the GC-MS results for biocrude oil obtained from water system confirmed the presence of phenolic and nitrogenous compounds in the product sample.

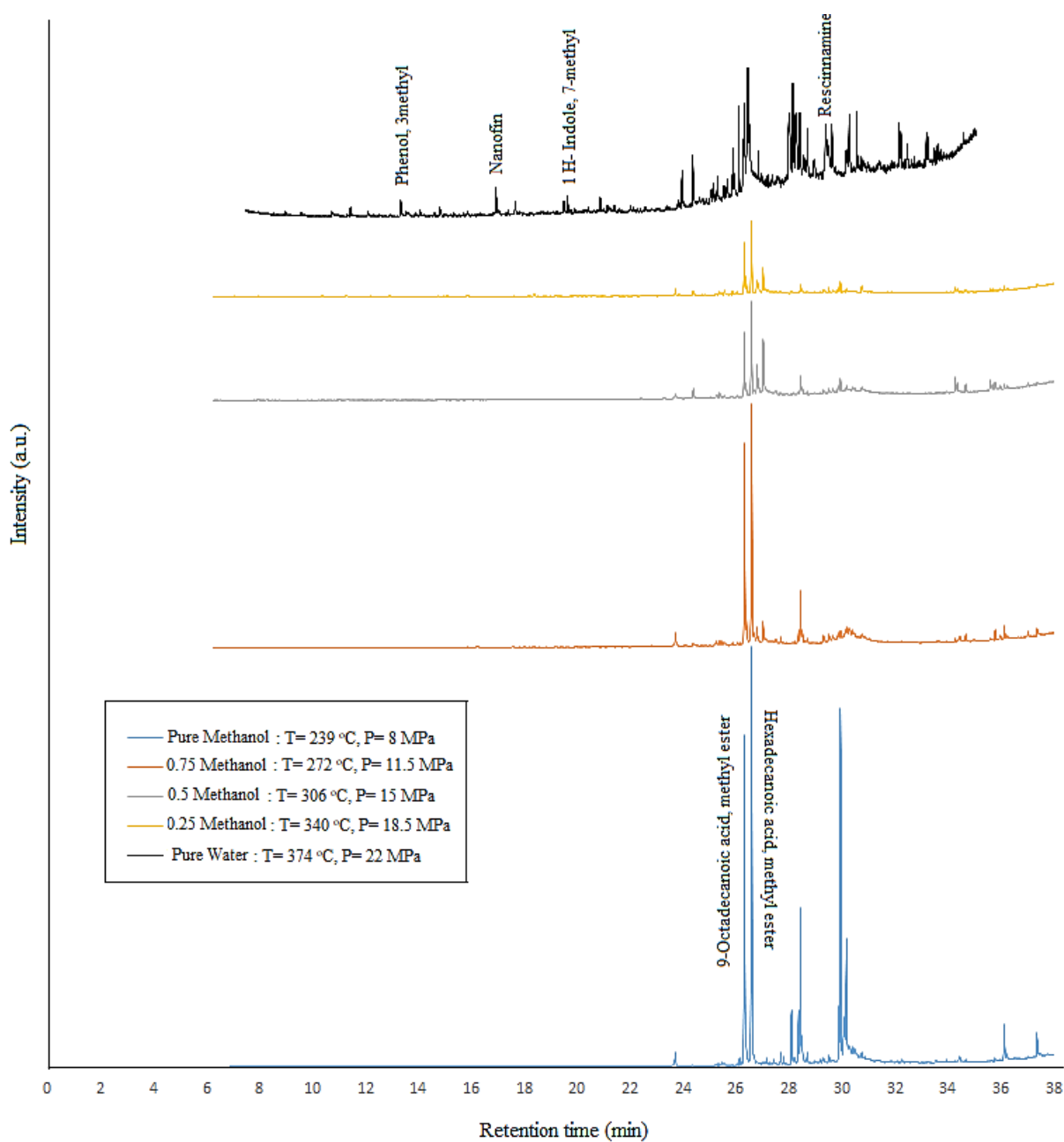


Figure 4.3: GC-MS analysis of biocrude oils obtained from different mass ratios of methanol and water

4.4.1.5 NMR spectroscopy for biocrude oils obtained from different ratios of methanol-water

NMR spectra provided quantitative functional group information for biocrude oils obtained with the different liquefaction solvents. As depicted in Figure 4.5, the ^1H NMR for all biocrude oil samples revealed high percentages of aliphatic functional groups related to the resonances between 0.5 – 3 ppm. The chemical shifts from 0.5 to 1.5 ppm is attributed to protons on aliphatic carbon atoms away from heteroatom or C=C, while, resonances between 1.5-3 ppm correspond to the protons on aliphatic carbon atoms that may be bonded to carbon or heteroatom with a double bond (Pan et al., 2018). The percentage of protons with 0-1.5 ppm chemical shifts in the biocrude oil obtained by methanol-water co-solvent and pure methanol is higher than that derived from pure water. The biocrude oil derived from methanol-water mass ratio of 0.75:0.25 contained the highest percentage ($\approx 69\%$) of alkane functional groups (0-1.5 ppm), which may be attributed to the high decomposition of triglycerides under HTL conditions. However, the percentage of protons bonded to unsaturated carbons or heteroatoms (N, S, and O) in the region of 1.5-3 ppm for the biocrude oil obtained from pure water as solvent was the highest ($\approx 46\%$). This observation can be correlated to the large number of nitrogen and oxygenate compounds as a result of high protein contents (44.2 wt.%) of the microalgae used. Results obtained from CHNS analysis also corroborate the presence of high percentages of nitrogen and oxygen contents in the biocrude oil obtained from pure water. The low percentage ($\leq 5\%$) of carbohydrates functionality for all biocrude oils confirmed that most of the oil from HTL of microalgae was contributed by the decomposition of lipid-derived compounds (Duan and Savage, 2011a).

^{13}C NMR spectra provided more details about C-related chemical functional groups due to its larger chemical shift region. As can be seen in Figure 4.6, all the biocrude oils obtained from MeOH- H_2O co-solvent systems and pure methanol had high aliphatic content (0-55ppm). Aliphatics were sub-divided into short and long-branched aliphatics which are in the range of 0-28ppm and 28-55ppm, respectively. Biocrude oil obtained with pure methanol exhibited the highest proportion of short aliphatics, followed by that obtained from methanol-water mass ratio of 0.75:0.25. On the contrary, the aromatics-olefins range was the highest for biocrude oil obtained from pure water, which corroborates observation of the highest unsaturated functional groups (1.5-3 ppm) as evidenced by ^1H NMR for the same sample. Low percentages of

alcohols/carbohydrates were also observed in all ^{13}C NMR spectra, which is consistent with the low carbohydrates of the microalgae that can be converted into biocrude oil. Percentage of esters/carboxylic acids with chemical shifts of 165-180 ppm for biocrude oil with methanol-water ratio of 0.75:0.25 was the highest. The peaks in the region of 180-215 ppm arise from ketone and aldehydes. Based on the literature (Pan et al., 2018; Vardon et al., 2011), low amounts of ketone and aldehyde are present in biocrude oils.

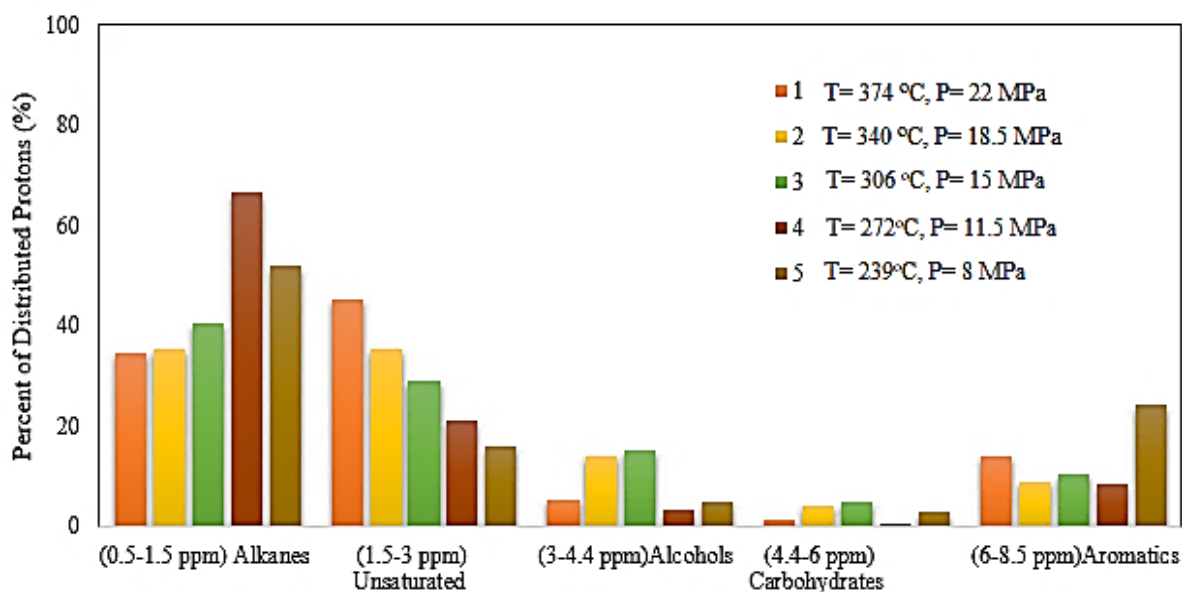


Figure 4.5: ^1H NMR distribution of functional groups present in biocrude oils (Numbers 1,2,3,4 and 5 indicate the biocrude oil obtained by pure water, 25 wt.% of methanol, 50 wt.% of methanol, 75 wt.% of methanol and pure methanol as solvent at constant reaction time of 60 min)

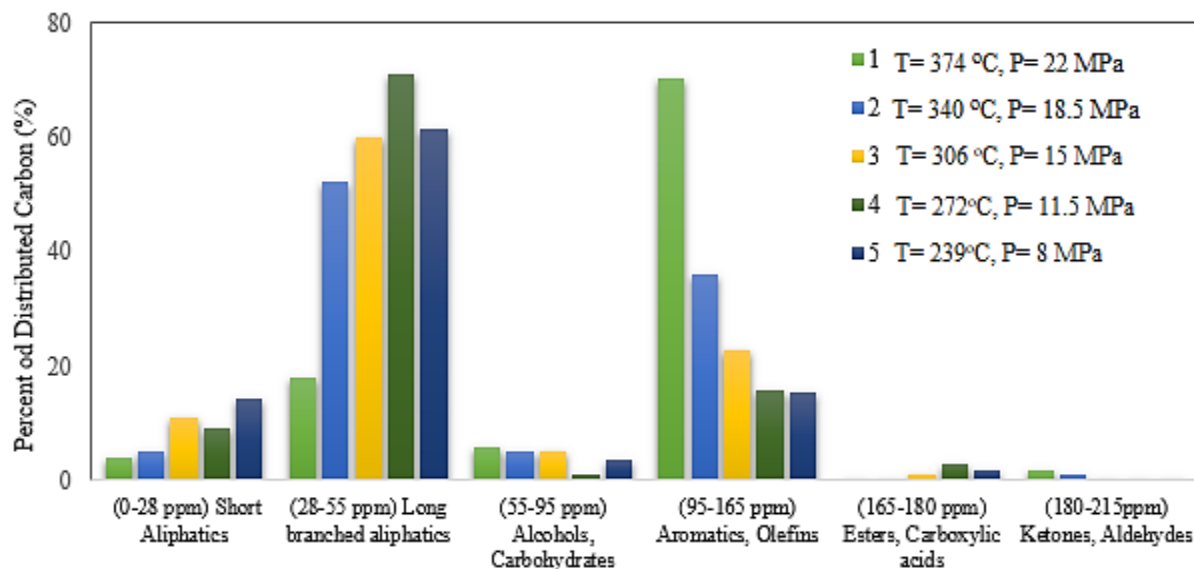


Figure 4.6: ¹³C NMR distribution of functional groups present in biocrude oils ((Numbers 1,2,3,4 and 5 indicate the biocrude oil obtained by pure water, 25 wt.% of methanol, 50 wt.% of methanol, 75 wt.% of methanol and pure methanol as solvent at reaction time of 60 min)

4.4.2 Effects of operating condition on HTL of microalgae using methanol-water system

Process parameters such as time and temperature play important roles on biocrude oil yield derived from HTL of microalgae. In addition, these parameters are essential for the safety and economics of industrial application of HTL to ensure the maximum biocrude oil yields. The influence of temperature and reaction time on biocrude oil yield carried out at methanol-water mass ratio of 0.75:0.25 with biomass-solvent ratio of 1:5 at constant pressure of 11.5MPa was studied to ascertain the suitable reaction conditions. HTL under milder conditions may validate the feasibility of the process to sustainably generate biofuels from micro-algal biomass feedstocks.

Elemental compositions of biocrude oils obtained at different temperatures and times, at constant pressure of 11.5MPa are shown in Table 4.4. The HHV and ER of the biocrude oils are also listed in Table 4.4. It can be observed that increasing temperature resulted in increased HHVs due to higher carbon contents and correspondingly decreased oxygen content associated with temperature rise. Compared to traditional pyrolysis, where oxygen contents and HHVs are in the range of 17-35% and 21-31MJ/kg, respectively (de Caprariis et al., 2017), biocrude oil obtained by HTL process exhibited superior quality of oil.

Table 4.4: Elemental analysis and HHV of biocrude oils obtained at different reaction conditions

Run	Temperature (°C)	Time (min)	Biocrude oil yield (wt.%)	Elemental analysis (wt.%)					HHV (MJ/kg)	ERR (%)
				C	H	N	S	O*		
S1	222	10	39.9	60.9	8.2	6.6	0.3	24	26.6	50.0
S2	272	10	44.4	66.6	8.3	6.9	0.2	18	29.5	61.9
S3	322	10	32.2	72.7	8.6	5.4	0.0	13.3	32.7	49.6
S4	222	35	48.3	62.2	8.2	6.8	0.2	22.6	27.2	62.0
S5	272	35	57.8	71.2	8.0	6.5	0.2	14.1	31.2	85.3
S6	322	35	21.1	73.4	8.2	5.5	0.1	12.9	32.4	32.3
S7	222	60	43.1	70.3	8.5	6.9	0.2	14.1	31.7	64.4
S8	272	60	47.2	72.3	8.4	5.5	0.0	13.8	32.2	71.3
S9	322	60	20.2	73.5	8.1	5.2	0.1	13.1	32.3	30.8

^a Calculated by difference

The biocrude oil obtained from supercritical and critical conditions showed lower amount of oxygen compared to the experiments performed at subcritical condition ($T = 222^{\circ}\text{C}$). Moreover, for all the data sets evaluated at constant temperature and increasing reaction time in the range of 10 - 60min, one can observe a decrease in the amount of oxygen and increase in carbon content. The maximum biocrude oil heating value was obtained from the test performed at reaction temperature of 322°C and time of 10 minutes. The maximum ER (85.3 %) was obtained from biocrude oil produced at reaction temperature of 272°C after 35 minutes.

Figure 4.7 shows the biocrude oil yield obtained at different temperatures and reaction times. It can be noted that sufficient reaction time was a pre-requisite to improve the yield of biocrude oil. This allows smaller molecules from decomposition and to rearrange and maximize the hydrolysis and re-polymerization reactions during HTL process. Therefore, low reaction time resulted in lower biocrude oil yield at subcritical and critical conditions ($T = 222$ and 272°C , respectively). Also, longer reaction time causes large volumes of gaseous products and lower biocrude oil production. Lower reaction temperature in subcritical conditions of methanol-water system are not sufficient for HTL reactions to obtain the high biocrude oil yield. Increasing temperature up to 272°C results in the increase of biocrude oil yield. The biocrude oil sample obtained from methanol-water mass ratio of 0.75:0.25 at critical condition after 35 minutes exhibited the highest biocrude oil yield (57.8wt.%). It can be noted that in supercritical

conditions, gasification reactions dominate after 10 minutes; resulting in lower yields of biocrude oil.

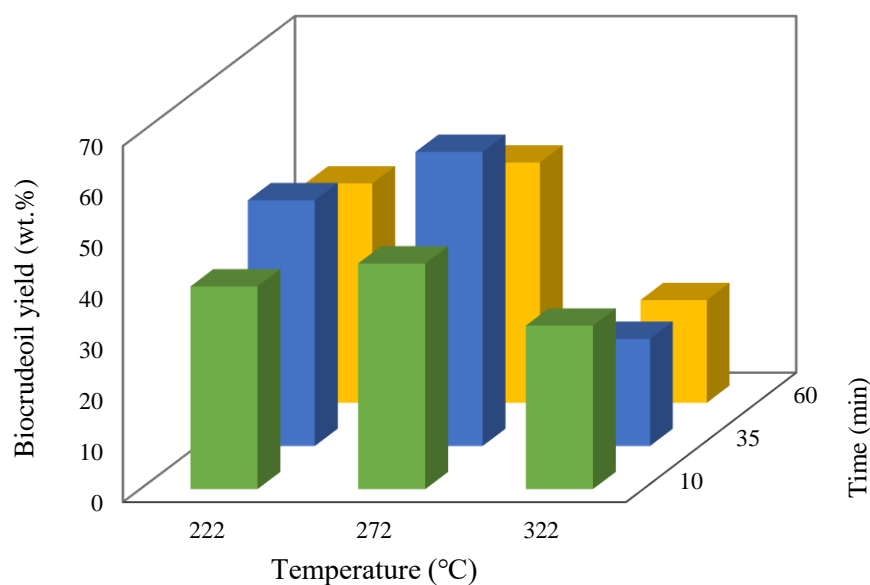


Figure 4.7: Biocrude oil yields obtained from different reaction conditions at constant pressure of 11.5 MPa

Central composite design (CCD) was used for designing a second order (quadratic) response surface model to study the effects of two independent variables namely, temperature (A) and time (B) on biocrude oils yield and their C content. The independent factors (A and B) were coded as +1, 0, and -1 to denote high levels, center value, and low levels, respectively, as depicted in Table 4.5. At the center point in design experiment, four experiments were conducted to determine the reproducibility of the experimental results and estimate the experimental error. The results showed that the biocrude yields were within ± 1 wt.% error.

Table 4.5: Variables and their examined levels used in experimental design

Factor	Level		
	-1	0	+1
A-Temperature (°C)	222	272	322
B-Time (min)	10	35	60

Also, the CHNS analysis was performed at least for three times to obtain the carbon content available in biocrude oil and the error involved in the experimental measurements was $\pm 1.5\text{wt.}\%$. Quadratic polynomial equation is given to compute the influence of process parameters (independent variables) on the response:

$$Y = \beta_0 + \sum_{i=1}^k \beta_i X_i + \sum_{i=1}^k \beta_{ii} X_i^2 + \sum_{i=1}^k \sum_{i < j}^k \beta_{ij} X_i X_j \quad (4.1)$$

Where Y is the calculated response, k is the number of parameters, and β_0 , β_j , β_{jj} , β_{ij} , are the constant, linear, squared, and interaction coefficient, respectively. X_i and X_j are also independent parameters.

As can be seen in Tables 4.6 and 4.7, ANOVA was used to investigate the significance of temperature and time (main process parameters) and their interactions considering F and p values. Independent variables in the model are considered significant, if P values are less than 0.05. The greater value of F, which is defined as $F = \text{MSF}/\text{MSE}$, indicates that the effect of the variables or the model is statistically more significant. MSF indicates the mean squares of factors or interactions and MSE is defined as the mean squares of errors (Hang et al., 2011).

According to ANOVA results for biocrude oil yield, compared to factor B (time), the factor A (temperature) and interactions A^2 were statistically more significant effects on the biocrude oil yield. The quadratic model for biocrude oil yield as a function of actual variables is given in Eq. (4.2). As can be seen in Table 4.6, the model is highly significant. Also, coefficient of determination (R^2) of Eq. (7) is 0.93; suggesting that within the parameters investigated, this model can be used to describe the experimental data of biocrude oil yield (see Eq. (3.7)).

$$\text{Biocrude oil yield} = -441.6 + 3.66X_A + 1.4X_B - 3.04 \times 10^{-3}X_A X_B - 0.007X_A^2 - 0.01X_B^2 \quad (4.2)$$

Where X_A and X_B denote actual variables of temperature and time, respectively.

The three-dimensional response surface for biocrude oil yield based on reaction temperature and time are given in Figure 4.8. The impact of temperature and time resulted in changing the biocrude oil yield in the range of 28-57wt.% and 50-56%, respectively. These values confirm that reaction temperature for the HTL processing of microalgae has maximum effect on biocrude oil yield in comparison with reaction time.

It is observed that low levels of temperature and time during HTL process correlated with high biocrude oil yield. Increasing temperature up to 272°C led to increase in biocrude oil yield, reaching a maximum (about 58wt.%) and then dropping. In general, at low temperature, hydrolysis of macro-molecules into smaller fragments controls the reactions during HTL process. As the temperature increases, competition between hydrolysis and re-polymerization increases, therefore the biocrude oil yield can reach a maximum. At higher temperature, conditions favor decarboxylation, dehydration and gasification reactions, resulting in higher gas yield and lower biocrude oil yield (Y. Guo et al., 2015) .

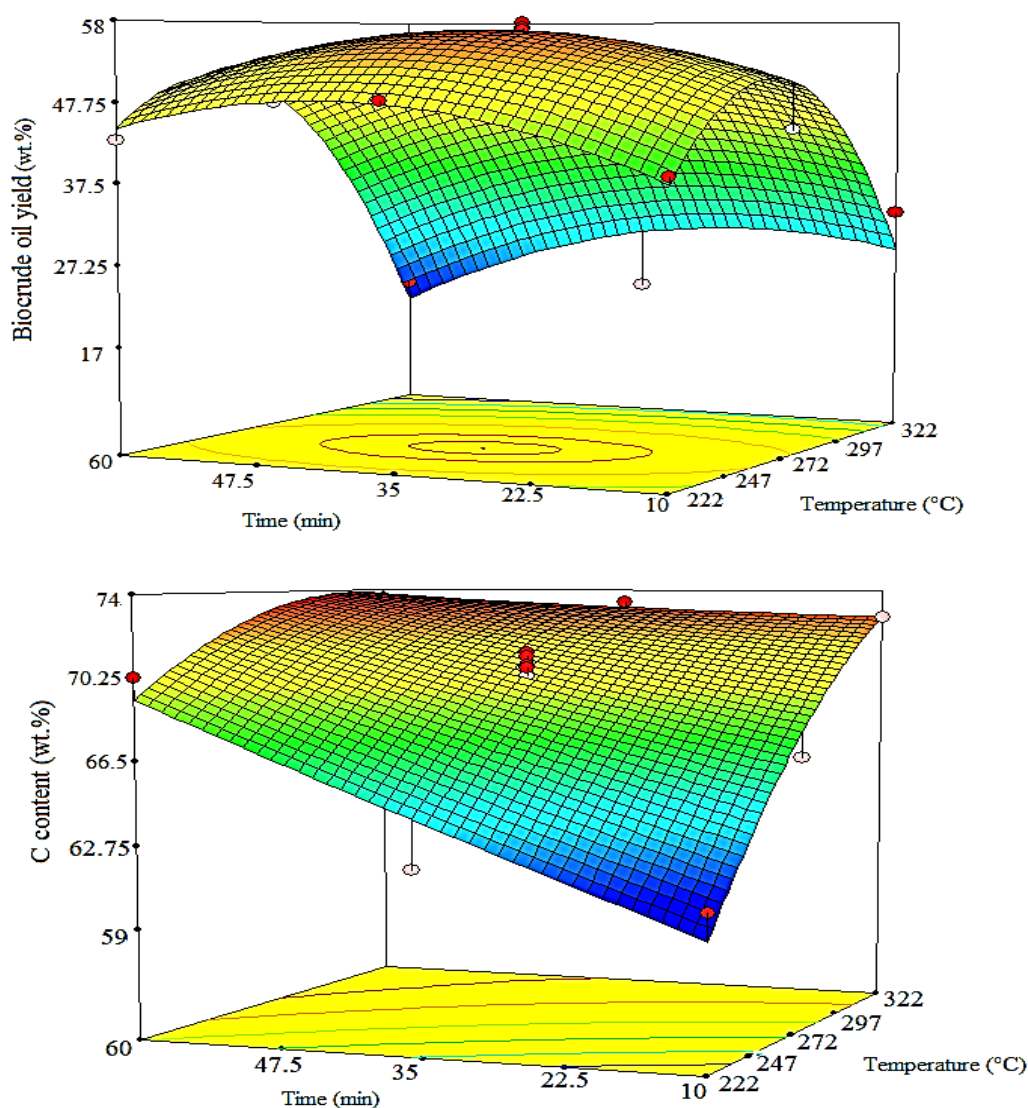


Figure 4.8: The response surface for biocrude oil yield (wt.%) and carbon content (wt.%) as a function of temperature and time at constant pressure of 11.5 MPa

According to Table 4.6, the F values for A and A² recorded as 28.16 and 41.47, respectively, corresponded to the temperature effects on biocrude oil yield, and their impacts were more than those of other terms. As shown in Fig 4.8, biocrude oil yield increased with increasing temperature and time up to 272°C and 35min, respectively. Thus, the main components of microalgae could be completely hydrolyzed and depolymerized during this range; leading to higher biocrude oil yield. At higher temperature ($\approx 320^{\circ}\text{C}$), biocrude oil might be further converted to ash by polymerization and to higher gas yield due to gasification. Gasification reactions would restrain biocrude oil production and favor gaseous product formation. Therefore, the addition of methanol as co-solvent to HTL resulted in higher biocrude oil yield at lower temperature.

Table 4.6: Analysis of variance (ANOVA) for biocrude oil yield (wt.%)

Source	Sum of Squares	df	Mean Square	F Value	P-Value
Model	1961.30	5	392.26	19.84	0.0005
A-Temperature	556.81	1	556.81	28.16	0.0011
B-Time	6.00	1	6.00	0.30	0.5989
AB	57.76	1	57.76	2.92	0.1312
A ²	820.03	1	820.03	41.47	0.0004
B ²	103.82	1	103.82	5.25	0.0557
Error	2.05	4	0.51		
Core total	2099.73	12			

From the ANOVA results for carbon content (wt.%) in biocrude oils (Table 4.7), the factors A (temperature) and B (time) and their interactions, AB, have statistically significant effects on carbon content (wt.%) present in biocrude oil yield (see Eq. (4.3)).

$$\text{C-content (wt.\%)} = -18.8 + 0.48 X_A + 0.56 X_B - 1.7 \times 10^{-3} X_A X_B - 0.0006 X_A^2 + 0.0001 X_B^2 \quad (4.3)$$

Where X_A and X_B indicate actual variables of temperature (°C) and time (min), respectively. The R^2 value of Eq. (4.3) is 0.95; indicating experimental data can be correlated with predicted values and of C content present in biocrude oil.

Graphical representation of experimental design is shown in Figure 4.8 to investigate the effects of variables (time and temperature) on C content (wt.%) in biocrude oils. According to Figure 4.8, although factor B (time) is statistically significant, temperature has the predominant effect on C content (%) in biocrude oils as confirmed by results in Table 4.7. The amount of carbon (wt.%) in biocrude oils increases with the increase of reaction temperature and time. Thus, as observed, supercritical conditions ($T \approx 322^\circ\text{C}$) led to maximum carbon content (wt.%) and as a consequence minimum oxygen content and higher heating values of biocrude oil.

Table 4.7: Analysis of variance (ANOVA) for C content (%) presents in biocrude oils

Source	Sum of Squares	df	Mean Square	F Value	P-Value
Model	182.29	5	36.46	23.72	0.0003
A- Temperature	114.41	1	114.41	74.42	<0.0001
B-Time	42.14	1	42.14	27.41	0.0012
AB	18.49	1	18.49	12.03	0.0104
A^2	6.53	1	6.53	4.25	0.0782
B^2	0.03	1	0.03	0.02	0.8848
Error	0.75	4	0.19		
Core total	193.05	12			

4.4.3 Hydrochar characterization

4.4.3.1 Elemental analysis and surface properties of hydrochars

The characteristics of hydrochars obtained from different solvents and reaction conditions ($T=222$ - 272°C , and time of 10-60 min) were also investigated. According to CHNSO analysis, carbon content of hydrochars obtained from systems such as pure water, pure methanol and methanol-water ratio of 0.75:0.25 at 60 min was similar, which indicated that liquefaction solvents had little influence on C contents in hydrochar. Therefore, the effects of reaction time and temperature on hydrochar characteristics were only considered for samples obtained from methanol-water co-solvent mass ratio of 0.75:0.25.

The elemental analysis and surface properties of hydrochars in different reaction temperature and time as well as their yields are given in Table 4.8. The highest C content (60.3wt.%) in hydrochar was obtained from reaction temperature of 322°C and 10 minutes. As the temperature increased, the contents of C in hydrochars increased and oxygen content decreased resulting in higher calorific values. As can be seen in Table 4.8 and Figure 4.9, increasing the reaction time and temperature resulted in lowering the hydrochar yield. Maximum hydrochar yield (19.5wt.%) was obtained from subcritical condition in temperature and of 222°C , 11.5MPa after 10 minutes. After 35 minutes and temperature of 322°C , hydrochar was not formed.

Table 4.8: Elemental analysis and surface properties of hydrochars from different reaction conditions

Run	Temperature ($^{\circ}\text{C}$)	Time (min)	Hydrochar yield (wt.%)	Elemental analysis (wt.%)				
				C	H	N	S	O
S1	222	10	19.5	52.1	7.4	4.7	0.9	34.9
S2	272	10	12.1	54.3	6.8	4.3	0.4	34.2
S3	322	10	8.2	60.3	7.3	4.4	0.5	27.5
S4	222	35	15.4	55.6	6.9	3.9	0.7	32.9
S5	272	35	10	57.2	7.2	4.6	0.4	30.6
S6	322	35	0	-	-	-	-	-
S7	222	60	10.1	58.4	7.0	4.6	0.2	29.8
S8	272	60	8.1	59.2	6.2	4.9	0.5	29.2
S9	322	60	0	-	-	-	-	-

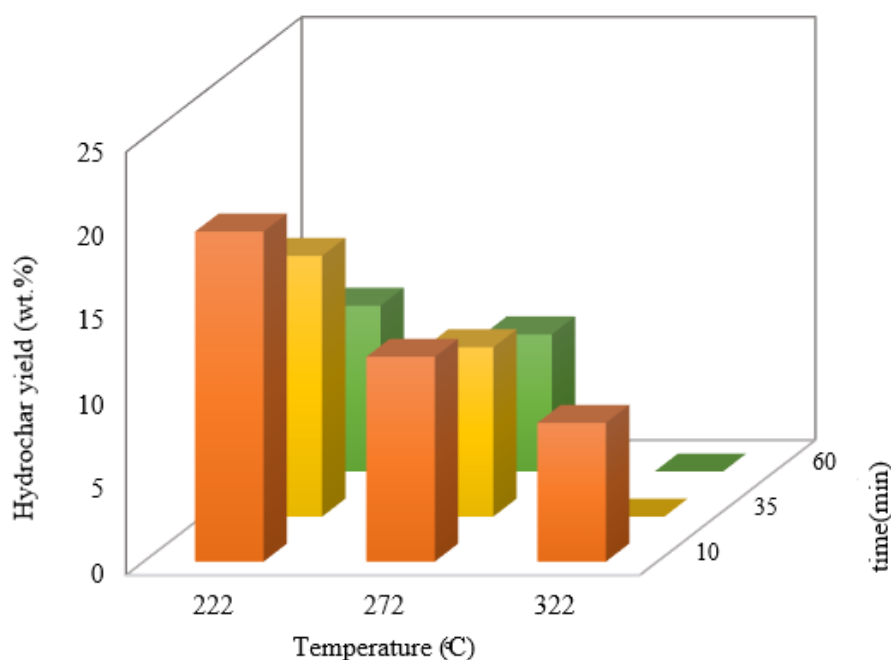


Figure 4.9: Effects of reaction time and temperature on hydrochar yield at constant pressure of 11.5 MPa

By increasing temperatures in supercritical conditions, the yield of hydrochar and biocrude oil significantly decreased, which might probably be related to gasification reactions converting products to ash and gaseous product. All the hydrochars revealed low BET surface area ($\leq 4 \text{ m}^2/\text{g}$) and low pore volume ($\leq 0.02 \text{ cm}^3/\text{g}$), which rendered its adsorption or catalytic applications. In order to improve the physico-chemical properties of hydrochars such as BET surface area and porous structure characteristics, physical and chemical activation are needed (Cheng and Li, 2018).

4.4.3.2 FT-IR of hydrochars

Figure 4.10 depicts the FT-IR spectra of microalgae and hydrochars obtained from different solvents and reaction conditions. FT-IR spectra of hydrochars obtained from methanol-water ratio of 0.75:0.25 in different reaction time and temperatures were similar. However, the intensity of the peaks at around 3400 cm^{-1} attributing to hydroxyl functionalities decreased at 322°C . It means that a significant amount of hydroxyl groups are decomposed at this temperature after 10 minutes of reaction. Regarding the effects of methanol and water on FT-IR spectra of hydrochars, the peak intensity around 1700 cm^{-1} attributed to C=O stretching present in carboxylic acid/ester, was higher for hydrochar obtained from pure methanol. The peak intensity

at 3400 cm^{-1} decreased for hydrochar obtained from pure water. The peaks present in the range of $1400\text{--}1600\text{ cm}^{-1}$, may be attributed to the band of benzene ring, CH_3 vibrations and groups of amides related to the presence of protein in microalgae and hydrochar (Biswas et al., 2017). The intensity of the peaks in the range of $1000\text{--}1300\text{ cm}^{-1}$, which are related to the C-O stretching or C-H bending, is higher for hydrochar obtained from pure methanol than pure water. Also, vibration peaks in the range of $500\text{--}700\text{ cm}^{-1}$, in FT-IR spectra may be ascribed to C-Cl, C-Br or C-I (Pan et al., 2018) present in the sample.

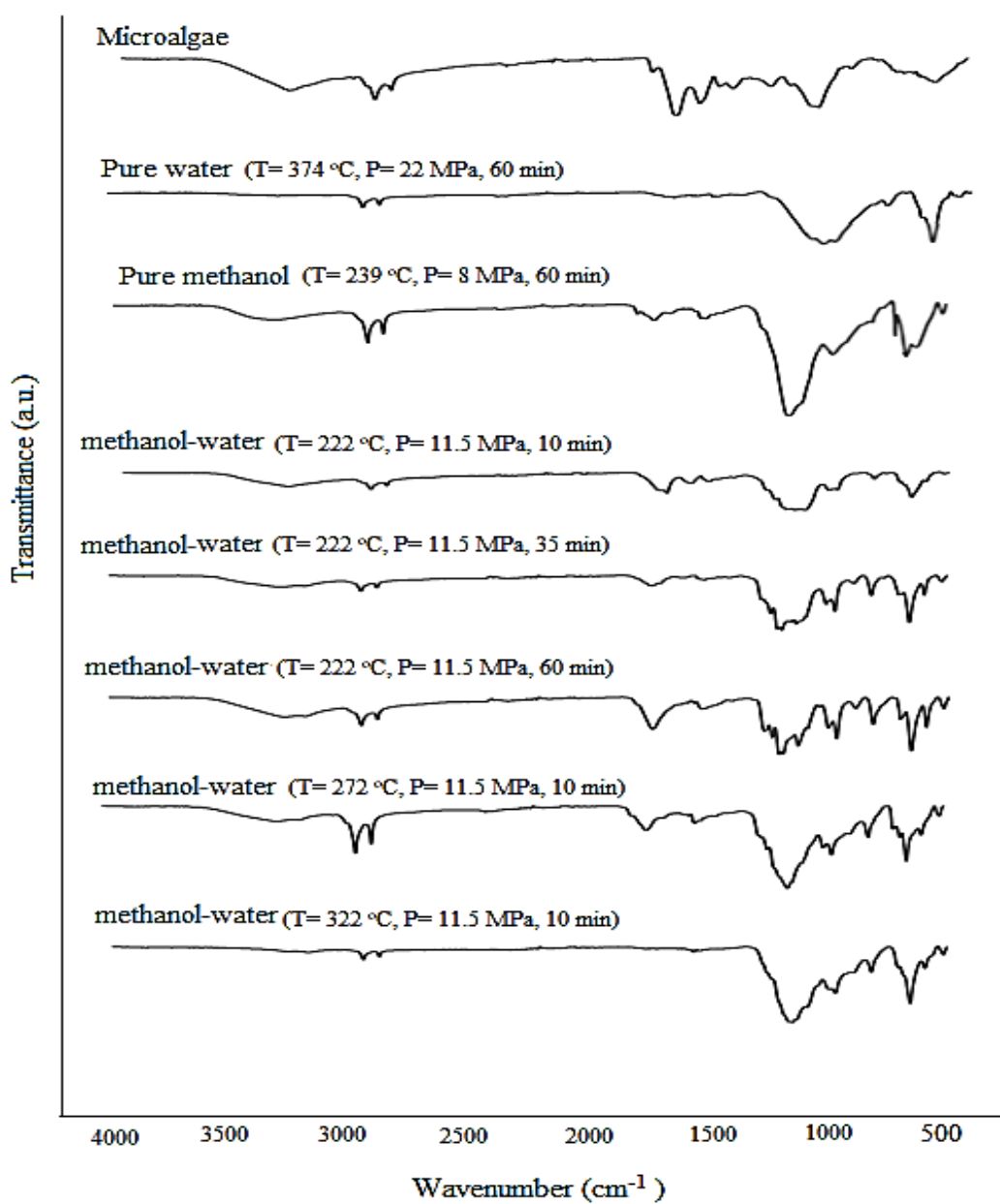


Figure 4.10: FT-IR spectra of hydrochar obtained from HTL of microalgae

4.4.3.3 Thermal stability of hydrochars

Figure 4.11 and 4.12 demonstrates the thermal behavior of the microalgae and hydrochars obtained from HTL, determined by thermogravimetric analysis (TG) and differential thermogravimetric analysis (DTG). There are usually three main steps of decomposition for the microalgae and its hydrochars. The initial mass loss in the range of 40- 200°C, caused by the loss of water bound to bio-molecules and alterations of lipid structure (Pane et al., 2001). The second mass loss in the range of 200-400°C, was related to the decomposition of proteins and carbohydrates. And, the third step occurred at temperature above 400°C, due to complete decomposition and oxidation of organic matters (Y. Guo et al., 2015). Application of different solvents and co-solvent affects thermal stability of hydrochars. The analysis of the TGA showed that the thermal stability of hydrochar obtained from HTL in pure methanol is slightly higher than that obtained with pure water. Therefore, the application of methanol as compared to water as solvent can improve the thermal stability of hydrochars. TGA results also suggested that HTL temperature effectively imputed thermal stability of hydrochars, in a way that increasing process temperature increases thermal stability. As a result, the thermal stability of hydrochars followed the order: 322 °C > 272 °C > 222°C. It can be concluded that methanol-water co-solvent system improved the release of volatile compounds result in higher fixed carbon and higher stability which agrees with the results of CHNS.

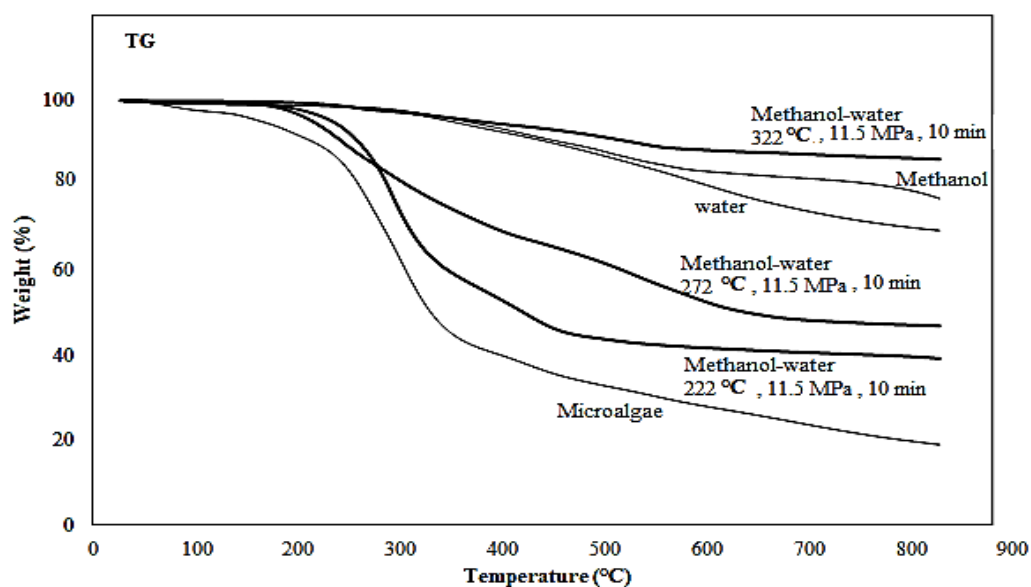


Figure 4.11: Thermogravimetric analysis of hydrochars obtained from HTL

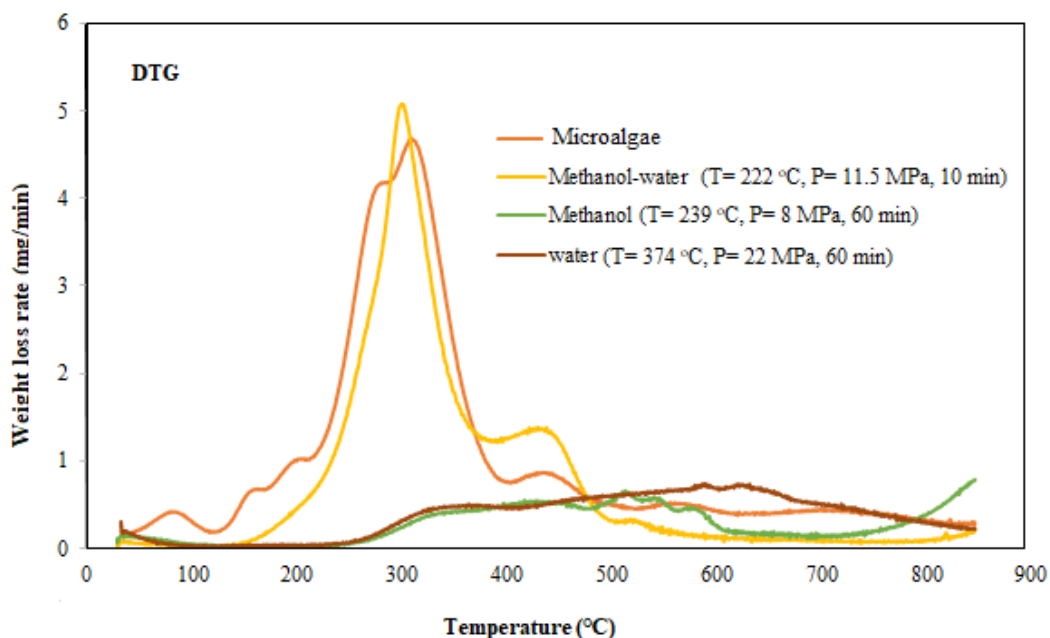


Figure 4.12: Differential thermogravimetric analysis of hydrochars obtained from HTL

4.5 Conclusions

In this study, hydrothermal liquefaction of microalgae using methanol-water system was investigated to produce renewable biocrude oil. Compared with pure water as solvent for HTL process, the addition of methanol lowered the contents of oxygen and nitrogen as well as increased the amounts of low-boiling compounds. The maximum biocrude oil yield (57.8wt.%) was obtained with 75 wt.% of methanol in water at $T= 272^{\circ}\text{C}$ $P=11.5\text{MPa}$ and reaction time of 35 min. This sample also revealed the highest energy recovery (85.3 %), and HHV of 31.2 MJ/Kg with higher ester components resulting in higher biocrude oil quality. According to RSM results, compared to time, the temperature was proved statistically to have more significant effect on the biocrude oil yields. Increasing process temperature decreased the hydrochar yield, however increased its thermal stability.

The utilization of by-product, hydrochar, may improve the overall process economics. In the next phase, hydrochar is utilized to produce highly porous activated carbon, which is used as catalysts/catalyst support.

Chapter 5: Optimized production and characterization of highly porous activated carbon from algal-derived hydrochar

The content of this chapter has been published in Journal of Cleaner Production cited below and presented in the following conferences:

Citation:

Masoumi, S., Dalai, A.K., 2020. Optimized production and characterization of highly porous activated carbon from algal-derived hydrochar. J. Clean. Prod. 263, 121427.

Conference Proceedings

Shima Masoumi, Philip E. Boahene, Ajay. K. Dalai, “Hydrothermal conversion of microalgae to bio-crude oil and hydro-char, and hydro-char upgradation to activated carbons”, 69th Canadian Chemical Engineering Conference, Halifax, October 20-23, 2019.

Contribution of the PhD candidate:

Experiments were designed in consultation with Dr. Ajay K. Dalai and executed by Shima Masoumi. Material synthesis, catalysts characterization and data interpretation were performed out by the student. The manuscript was drafted by Shima Masoumi with guidance and suggestions provided by Dr. Ajay K. Dalai.

Contribution of this chapter to overall PhD research:

The second phase of the research is investigated in this chapter: hydrochar as a co-product of HTL of microalgae was activated through chemical activation process to produce highly porous activated carbon to be used as a catalyst support for the next phase.

5.1 Abstract

Preparation of porous activated carbon from algal hydrochar obtained from hydrothermal carbonization, using chemical activation method has been conducted in this study. This study focused on the effects of different activation parameters as well as different chemical activators such as alkali activators, carbonate, acid and mixture of alkali activators on prepared activated

carbon. Response surface methodology applying central composite design was employed to investigate the effects of activation temperature ($525 \leq T \leq 825$ °C), mass ratios of potassium hydroxide as an activator and hydrochar ($0.3 \leq R \leq 2.7$) and nitrogen flow rate ($63 \leq F \leq 267$ cc/min) at constant heating rate of 3°C/min on BET surface area and yield of the produced activated carbons. The chemically prepared activated carbons at optimum process conditions of $T=675$ °C, $R=1.5$ and $F=267$ cc/min, using potassium carbonate or potassium hydroxide as a chemical agent, revealed high surface area (≥ 2100 m²/g) with the maximum yield of 61.3 wt.%, pore volume in the range of (1.2-1.5 cm³/g) and average pore size of (5.9-8.3 nm). 100% methylene blue removal was achieved from a solution with methylene blue concentration of 250 mg/L, with chemically activated carbon dosage of 1 g/L within 5 min at room temperature.

Keywords: Hydrothermal carbonization, algal hydrochar, chemical activation, activated carbon, adsorption

5.2 Introduction

High cost of activated carbon (AC) production using non-renewable precursors is one of the most challenges for commercialization of AC, while, global demand for production of activated carbon using alternative environmentally friendly sources has annually increased (Ayinla et al., 2019, Namazi et al., 2016). Recently, the use of inexpensive, abundantly available and renewable raw materials to produce valuable activated carbon has attracted a lot of attention (Cheng and Li, 2018, Hu et al., 2010).

The AC can be used as adsorbent and catalysts or catalysts support for various industrial applications (e.g. wastewater treatment, discoloration and recovery of chemicals) due to its remarkable properties such as porous structure and high thermal stability (Basta et al., 2019). Bio/hydrochar, which can be obtained as a by-product of thermochemical conversion of biomass, is considered as a renewable carbonaceous material compared to activated carbon from traditional non-renewable fossil sources (Cao et al., 2017; Pallarés et al., 2018). Bio/hydrochars show a low surface area and porosity due to the formation and condensation of hydrocarbons on the surface and blocking the pores. In order to improve the physico-chemical properties of bio/hydrochars such as BET surface area and porous structure characteristics, physical and chemical activation methods become necessary (Kołtowski et al., 2017, Tan et al., 2017)

Chemical activation is performed through the impregnation of hydrochar with one or a mixture of chemical agent (s) and subsequently activation under nitrogen atmosphere (Ao et al., 2018). Phosphoric acid (H_3PO_4), Zinc chloride (ZnCl_2), sodium hydroxide (NaOH) and potassium hydroxide (KOH) are the mostly used chemical activating agents (Moralı et al., 2018, Sulaiman et al., 2018). KOH was used to synthesize nanoporous carbons with high surface area ($2682 \text{ m}^2/\text{g}$) from jute biomass (Khan et al., 2019). High surface area carbon materials ($2959 \text{ m}^2/\text{g}$) were produced from high ash content biochar, which is a waste material from thermochemical biomass conversion processes (Jin et al., 2013). In another study, AC with high surface area ($1704 \text{ m}^2/\text{g}$) was produced from fibers of oil palm using KOH as the chemical activation agent (Farma et al., 2013). The production of AC with high surface area ($850\text{-}1100 \text{ m}^2/\text{g}$) for different biomass feedstocks with KOH was demonstrated in another study (González-García et al., 2013). In a similar study, AC produced by KOH -assisted chemical activation of rice-straw and sewage char as the raw materials increased the surface areas from 14 to 772 and from 18 to $783 \text{ m}^2/\text{g}$, respectively (Cha et al., 2010).

Physical or thermal activation which can be done in two stages involving carbonization and subsequently activation or in one stage, is achieved by gasification with a reactive steam, gas (mostly CO_2) or mixture of steam and CO_2 as an oxidizing agent (Cha et al., 2016, Xiong et al., 2017). Compared with physical activation, chemical agents through chemical activation dehydrate the samples resulting in enhancing the yield of carbonization due to the increase of removing volatile compounds (Azargohar and Dalai, 2008). Also, chemical activation can create highly porous structures at a relatively lower temperature and shorter time (Angin et al., 2013).

Although, for over 20 years, many researchers have focused on activation of biochars obtained from pyrolysis of agricultural residues and waste biomasses (Pallarés et al., 2018; Ros et al., 2006), comprehensive study for hydrochar as a sustainable raw material and its conversion to activated carbon for its applications is limited. Compared to biochar obtained from pyrolysis process, hydrochar, which is obtained from hydrothermal carbonization (HTC), can be produced in lower temperature because the decomposition of biomass can occur more easily in an aqueous environment (Kambo and Dutta, 2015; Kim et al., 2016). According to the literature, many studies have focused on HTC as a suitable process for feedstocks with high moisture contents such as microalgae, food waste and animal manure (Cha et al., 2016; Wilk et al., 2019). The advantages of using microalgae as a feedstock are fast growth rate due to its high photosynthetic

efficiency and lack of large arable land area without competition with food crops (Galadima and Muraza, 2018).

In this study, for the first time, systematic approach is employed to examine hydrochar from microalgae through hydrothermal process as a source of activated carbons and then to study the effects of different process conditions on the characteristics of prepared activated carbon obtained from hydrothermal algal-derived hydrochar. The process parameters include temperature, impregnation ratio of KOH and hydrochar, nitrogen flow rate, and different chemical activators such as NaOH, K_2CO_3 , $ZnCl_2$, H_3PO_4 , and mixture of alkali activators. In this regard, response surface methodology was employed to study the impact of temperature ($525 \leq T \leq 825$ °C), nitrogen flow rate ($63 \leq F \leq 267$ cc/min) and mass ratios of KOH as an activator-hydrochar ($0.3 \leq R \leq 2.7$) on the yield, BET surface area and porosity of activated carbon. Analysis of Variance (ANOVA) was applied to study the effects of the main factors and their interactions on yield and BET surface area. The morphology, specific surface area, thermal gravimetric, surface functional group, higher heating value, elemental and proximate analysis of prepared activated carbon were characterized by several advanced structural chemistry tools. The second purpose of this work is to study the potential of AC prepared from algal hydrochar for methylene blue adsorption to contribute to environmental pollution control.

5.3 Materials and methodology

Materials used in this section, hydrochar production procedure, chemical activation process used for production of activated carbon, and also methylene blue adsorption tests were previously explained in Chapter 3.

5.4 Results and discussion

5.4.1 Physiochemical properties of algae biomass and algal hydrochar

The results of elemental analysis, biochemical composition, proximate analysis and HHV of algae biomass and algal hydrochar used for activation process are presented in Table 5.1. The results of elemental composition analysis (ultimate analysis) revealed that the carbon and hydrogen

Table 5.1: Physico-chemical properties of microalgae and algal hydrochar

Sample	Elemental Contents (wt.%)					Proximate analysis (wt.%)				Biochemical composition (wt.%)			HHV (MJ/Kg)
	C	H	N	S	O ^a	Moisture	Volatile matter	Fixed ^a carbon	Ash	Cellulose	Hemicellulose	Lignin	
Algae biomass	50.2	6.8	7.2	0.8	35	4.5	73.4	15.4	6.7	6.1	4.3	23.0	21.2
Algal Hydrochar	52.1	7.4	6.2	0.5	33.8	4.5	57.1	33.3	5.1	4.9	2.1	22.1	22.1

^aCalculated by difference

content of algal hydrochar produced from HTC at 222 °C for 15 min, increased while the oxygen content decreased. It could be due to decomposition of carbon band and removing oxygen as volatile compounds. Increasing the content of carbon and hydrogen led to an increase in the higher heating value of algal hydrochar compared to algal biomass. Also, compared to microalgae with lipid, protein and carbohydrate contents of 10.8 wt.%, 44.2 wt.% and 33.8 wt.%, respectively, hydrochar contains lower protein (38.78 wt.%) and carbohydrate (34.86 wt.%) contents and consequently higher lipid content (26.36 wt.%). This is in agreement with elemental analysis (Table 5.1), since lower nitrogen content of hydrochar compared with microalgae shows that hydrochar contains less protein compounds. Also, higher carbon content of hydrochar compared with microalgae, is related to higher carbon denser products (lipids compounds) (Du et al., 2012).

Based on proximate analysis results, the other advantage of HTC process compared to torrefaction process includes less ash content of algal biomass due to reduction of the inorganic content (Dieguez-Alonso et al., 2018). Ash content causes corrosion problems, in which can increase the expenses such as maintenance of equipment and affects the fuel efficiency (Zhang et al., 2018). For HTC process, at temperature of 222 °C, hemicellulose and cellulose started to hydrolyze while lignin needs higher temperature for hydrolysis (Reza et al., 2014). According to the ADF (ANKOM 08-16-06), NDF (ANKOM 08-16-06), lignin (ANKOM 08/05), the content of cellulose, hemicellulose and lignin in microalgae and algal hydrochar are given in Table 5.1. Hemicellulose content was calculated by the difference of ADF and NDF; cellulose content was calculated by the difference of ADF and lignin. Biochemical compositions of algae biomass and

algal hydrochar confirmed that the hemicellulose and cellulose contents decreased during HTC process.

5.4.2 Effects of different process variables on porous structure and yield of activated carbons

To investigate the effects of three independent variables namely, temperature (X_1) and nitrogen flow rate (X_2) and impregnation ratio (mass ratio of KOH and algal hydrochar) (X_3) on dependent variables (yield and BET surface area), response surface methodology (RSM) using central composite design (CCD) was used to design a second order response surface model. RSM is a combination of mathematical and statistical techniques for empirical model building to optimize the response (dependent variable) influenced by several independent variables. Design-Expert software was used to build the design matrix. The factors and corresponding response can be seen in Table 5.2.

Table 5.2: Independent process variables and their examined levels used in experimental design

Factor	Level				
	-1.2	-1	0	+1	+1.2
X₁ -Temperature (°C)	525	550	675	800	825
X₂ - Nitrogen flow rate (cc/min)	63	80	165	250	267
X₃- Mass ratio of KOH/Algal hydrochar	0.3	0.5	1.5	2.5	2.7

The most significant parameters and their interactions were evaluated and identified by experimental design and statistical analysis with the minimum number of experiments. The three independent factors (X_1 , X_2 and X_3) were coded at five different levels as $-\alpha$, -1, 0, +1, and $+\alpha$. The value of alpha (1.2) is defined the rotatability and orthogonality in the design (Oz et al., 2019). The center point in design experiment was applied to estimate the standard deviation which is a measure of amount of variation of set of values. The center point in this study is at temperature of 675 °C, KOH/algal hydrochar mass ratio of 1.5 and nitrogen flow rate of 165 cm³/min, and the average values are given in Table 5.3. The standard deviation for BET surface area and yield of activated carbons produced at this condition was calculated as 1.8 and 2.9, respectively. As the calculated standard deviation is not high so the values are close to the mean value.

Quadratic polynomial equation is given to study the linear, quadratic and interactive effects of process parameters (independent variables) on the response:

$$Y = \beta_0 + \beta_1 X_1 + \beta_2 X_2 + \beta_3 X_3 + \beta_{11} X_1^2 + \beta_{22} X_2^2 + \beta_{33} X_3^2 + \beta_{12} X_1 X_2 + \beta_{13} X_1 X_3 + \beta_{23} X_2 X_3 \quad (5.1)$$

Where Y is the calculated response, and β_0 , β_j , β_{ij} , β_{ij} , are the intercept value (constant), linear, squared, and interaction coefficient, respectively. X_1 , X_2 and X_3 are also independent parameters. The applied different process parameters in the defined range based on experimental design, the porous characteristics of the algal hydrochar and the activated carbons produced from chemical activation of algal hydrochar are summarized in Table 5.3. KOH is a strong base, which leads to elimination of pre-carbonization of hydrochar at high temperature. Therefore, it supports single step activation, which means that chemical activation and carbonization can be processed at the same time at lower temperature (Shu Hui and Abbas Ahmad Zaini, 2015). In this method, hydrochar was activated chemically at a desired impregnation ratio. During carbonization, KOH acts as a dehydrating agent, to eliminate the presence of volatile compounds in hydrochar which leads to form porous structure. Further carbonization would also lead to the formation of tar which could clog the pores. According to classification of International Union of Pure Applied Chemistry (IUPAC), pores are classified into micropore (<2 nm), mesopore (2-50 nm) and macropore (>50 nm) (Sing, 1985).

Compared to hydrochar (BET surface area of 4 m²/g), KOH chemical activation enhanced the specific surface area and improved porous characteristics. The effect of temperature, nitrogen flow and mass ratio of chemical agent and algal hydrochar on the porous structure and porosity development was investigated and the results are given in Table 5.3. The results obtained from chemical activation in different activation conditions revealed the BET surface area in the range of 502- 2099 m²/g with a high level of micropore development. Also, chemically activated carbons obtained from algal hydrochar in this study revealed total pore volume, and average pore size in the range of 0.29-1.2 cm³/g and 4.3-12.7 nm, respectively. The prepared activated carbons contained higher mesopore volumes (0.15-0.79 cm³/g) compared to micropore volume (0.14-0.68 cm³/g). The highest BET surface area of 2099 m²/g corresponds to the chemically prepared ACs at temperature of 675°C, with KOH/ algal hydrochar mass ratio of 1.5 using flow rate of nitrogen of 267 cc/min. This also led to higher pore volume (1.2 cm³/g) due to higher probability

of chemical reaction with KOH, compared to the other prepared activated carbons. The adsorption desorption isotherm is used to study the pore characteristics of the activated carbons. It is defined as standard amount of nitrogen adsorbed as a function of relative pressure (nitrogen gas partial pressure/ standard vapor pressure).

Table 5.3: Porous characteristic of chemically activated carbons using different process parameters

Sample	Process Parameters			BET surface area (m ² g ⁻¹)	Total pore volume (cm ³ g ⁻¹)	Micropore volume (cm ³ g ⁻¹)	Mesopore ² volume (cm ³ g ⁻¹)	Average pore size (nm)	Yield (wt.%)
	X ₁ ¹	X ₂ ¹	X ₃ ¹						
1	800	250	2.5	1147	0.89	0.37	0.52	8.2	8.7
2	550	80	2.5	502	0.29	0.14	0.15	5.4	39.8
3	675	165	0.3	1241	0.94	0.40	0.54	8.9	61.2
4	800	80	0.5	1302	1.0	0.42	0.58	6.9	27.4
5	550	80	0.5	844	0.5	0.22	0.28	12.7	67.3
6	675	165	1.5	1935	1.18	0.44	0.74	9.6	49.8
7	525	165	1.5	663	0.47	0.2	0.27	9.2	57.2
8	825	165	1.5	906	0.54	0.22	0.34	6.6	9.4
9	675	165	2.7	989	0.56	0.2	0.35	4.3	25.1
10	800	250	0.5	1338	1.1	0.44	0.65	9.0	15.9
11	800	80	2.5	1057	0.75	0.24	0.51	4.8	13.1
12	550	250	2.5	535	0.35	0.2	0.15	6.5	35.1
13	550	250	0.5	1136	0.75	0.24	0.51	10.7	58.8
14	675	267	1.5	2099	1.2	0.58	0.62	5.9	42.3
15	675	63	1.5	1369	1.12	0.44	0.68	10.1	53.7

¹ X₁, X₂, and X₃ represent different process variables which are temperature, nitrogen flow rate and mass ratio of KOH/algal hydrochar (impregnation ratio), respectively.

² obtained by the difference

Figure 5.1, shows the isotherm plot of prepared activated carbon at activation temperature, impregnation ratio and flow rate of nitrogen of 675°C, 1.5 and 267 cc/min. The isotherm plot is categorized into type IV according to IUPAC classification and its characteristics features are its hysteresis loop. Type IV isotherms are related to capillary condensation taking place in many mesoporous industrial adsorbents (Sing, 1985).

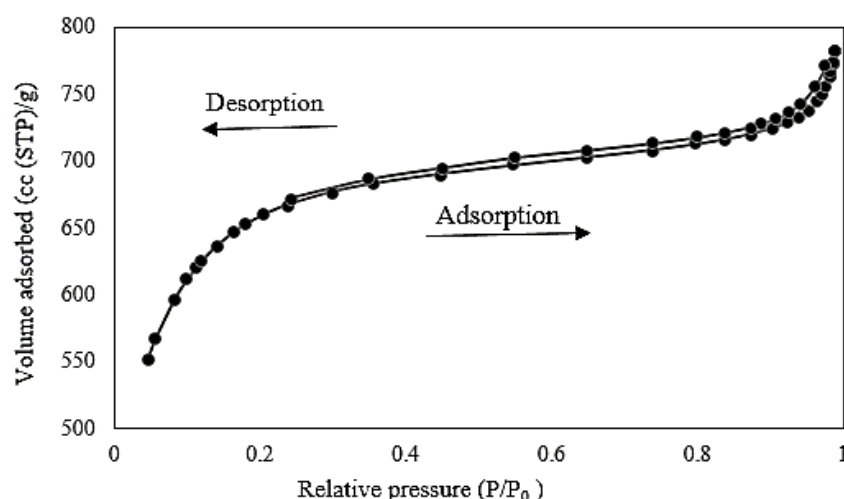


Figure 5.1: Typical isotherm of chemically activated carbons produced from algal hydrochar

According to the Tables 5.4 and 5.5, ANOVA was used to study the effects of the independent process parameters (temperature, nitrogen flow rate and mass ratio of KOH/hydrochar) on the responses (yield and BET surface area) and their interactions. The F and P value are considered to reveal the significance of model and independent process parameters. Independent variables in the model are considered significant, if P values are below 0.05. The greater value of F, which is defined as $F = MSF/MSE$, indicates that the effect of the variables or the model is statistically more significant. MSF and MSE indicates the mean squares of factors or interactions and the mean squares of errors, respectively (Ba and Boyaci, 2007; Hang et al., 2011). Through this work, the experiments were performed multiple times and the error involved in the experimental measurements are $\leq 3\%$.

ANOVA results revealed that for BET surface area, compared to the nitrogen flow rate as one of the independent variable (X_2), temperature (X_1) and mass ratio of KOH/algal hydrochar has statistically more significant influence on the BET surface area. Regarding the chemically prepared ACs yield, all the independent variables were highly significant. Based on the results

of ANOVA, the given quadratic model for BET surface area and yield were significant. The models for BET surface area and yield are given in equations (5.2) and (5.3), respectively.

Also, coefficient of determination (R^2) of Equation (5.2) and (5.3) which were 0.91 and 0.98, confirmed that these suggested quadratic models that within the parameters investigated, this model can be used to explain the effect of process parameters on experimental data of BET surface area and chemically activated carbon yield.

$$\text{BET surface area: } -17281.1 + 53.35 X_1 + 0.92 X_2 + 675.99 X_3 - 2.33 \times 10^{-3} X_1 X_2 + 0.5 X_1 X_3 - 0.3 X_2 X_3 - 0.03 X_1^2 + 7.7 \times 10^{-3} X_2^2 - 374.19 X_3^2 \quad (5.2)$$

$$\text{AC yield: } -139.77 + 0.78 X_1 - 0.00442 X_2 - 20.33 X_3 - 3.17 \times 10^{-5} X_1 X_2 + 0.03 X_1 X_3 + 0.016 X_2 X_3 - 0.0007 X_1^2 + -0.0001 X_2^2 - 4.3 X_3^2 \quad (5.3)$$

Table 5.4: Analysis of variance (ANOVA) for BET surface area of chemically activated carbon

Source	Sum of Squares	df	Mean Square	F Value	P-Value
Model	4753000	9	528100	10.97	0.0004 (Significant)
X ₁ -Temperature	412000	1	412000	8.56	0.0152
X ₂ -Nitrogen flow	161900	1	161900	3.36	0.0965
X ₃ - KOH/Hydrochar mass ratio	260100	1	260100	5.40	0.0425
X ₁ X ₂	4935.21	1	4935.21	0.10	0.7554
X ₁ X ₃	32042.46	1	32042.46	0.67	0.4336
X ₂ X ₃	5258.25	1	5258.25	0.11	0.7478
X ₁ ²	1891000	1	1891000	39.29	<0.0001
X ₂ ²	16090.14	1	16090.14	0.33	0.5759
X ₃ ²	726100	1	726100	15.09	0.0030
Residual	481400	10	48136.42		
Error	0	5	0		
Core total	52	19			

Table 5.5: Analysis of variance (ANOVA) for chemically activated carbons yield

Source	Sum of Squares	df	Mean Square	F Value	P-Value
Model	5750.41	9	638.93	32.24	<0.0001 (Significant)
X ₁ -Temperature	2633.18	1	2633.18	132.86	<0.0001
X ₂ -Nitrogen flow	168.21	1	168.21	8.49	0.0155
X ₃ - KOH/Hydrochar mass ratio	1237.19	1	1237.19	62.43	<0.0001
X ₁ X ₂	0.91	1	0.91	0.046	0.8345
X ₁ X ₃	110.26	1	110.26	5.56	0.0400
X ₂ X ₃	14.85	1	14.85	0.75	0.4070
X ₁ ²	1276.29	1	1276.29	64.40	<0.0001
X ₂ ²	11.13	1	11.13	0.56	0.4709
X ₃ ²	18.78	1	18.78	0.95	0.3533
Residual	198.19	10	19.82		
Error	0	5	0		
Core total	5948.60	19			

Figures 5.3 and 5.4 are the three-dimensional response surface of product yield and BET surface area (dependent variables or responses) of prepared ACs at different activation conditions (independent variables). It was observed that the responses were significantly affected by independent factors. The impregnation ratio (mass ratio of KOH/ algal hydrochar) and activation temperature were found as the most important independent process parameters, which affect significantly on yield and porous structures of chemically activated carbons.

According to Figure 5.3, increasing temperature up to 675 °C, and mass ratio of KOH/algal hydrochar up to 1.5 during activation process led to a higher BET surface area, which can be related to pore volume development and chemical reactions between activation agent and algal hydrochar. Higher activation temperature and impregnation ratio (mass ratio of KOH/algal hydrochar) during activation process, lowered the BET surface area of prepared chemically activated carbon. It may happen due to higher extent of chemical reactions with in the carbon

material resulting in the destruction of the pores. Experimental data showed that as flow rate of nitrogen increased the BET surface area increased due to higher removal of volatile compounds which favored activation process. According to Table 5.3, chemically ACs produced at temperature of 647 °C and chemical activating agent impregnation ratio of 1.5, with different flow rates for nitrogen (63, 165, and 267 cc/min) revealed different BET surface areas of 1369, 1935 and 2099, respectively. Prepared activated carbons at constant impregnation ratio of 1.5 and 165 cc/min for flow rate of nitrogen, had product yield of 57.2, 49.8 and 9.4 wt.% at reaction temperature of 525, 675 and 825 °C, respectively.

Higher impregnation ratio (higher KOH concentration) progressively produced products with higher external surface area, which may trap inside the pores and lower BET surface area of chemically activated carbons (Adinata et al., 2007).

The results of activated carbon yield calculated by equation (3.1), are also presented in Table 5.3 and Figure 5.4. As the activation temperature and impregnation ratio increased, the yield of chemically prepared activated carbons decreased due to gasification of hydrochar by KOH and release of volatile compounds. The maximum yield (61.2 wt.%) of activated carbon was obtained at optimum conditions of activation temperature of 675 °C, mass ratio of KOH to hydrochar of 0.3 with nitrogen flow rate of 165 cc/min. This shows that during overall carbonization and activation process, the maximum product yield was about 25 wt.% from microalgae.

5.4.3 Effects of different chemical agents on properties of activated carbons

5.4.3.1 Yield and porous characteristics of prepared activated carbons

In this study, the effects of different chemical agents such as alkali activators (KOH, NaOH, K₂CO₃) and the mixture of alkali activators (KOH+ NaOH and KOH+K₂CO₃), ZnCl₂, and H₃PO₄ on the yield and BET surface area are investigated. The results of porous characteristics and the yield of prepared activated carbons are given in Table 5.6. The process parameters used for production of activated carbons from different chemical agents are based on the obtained optimum

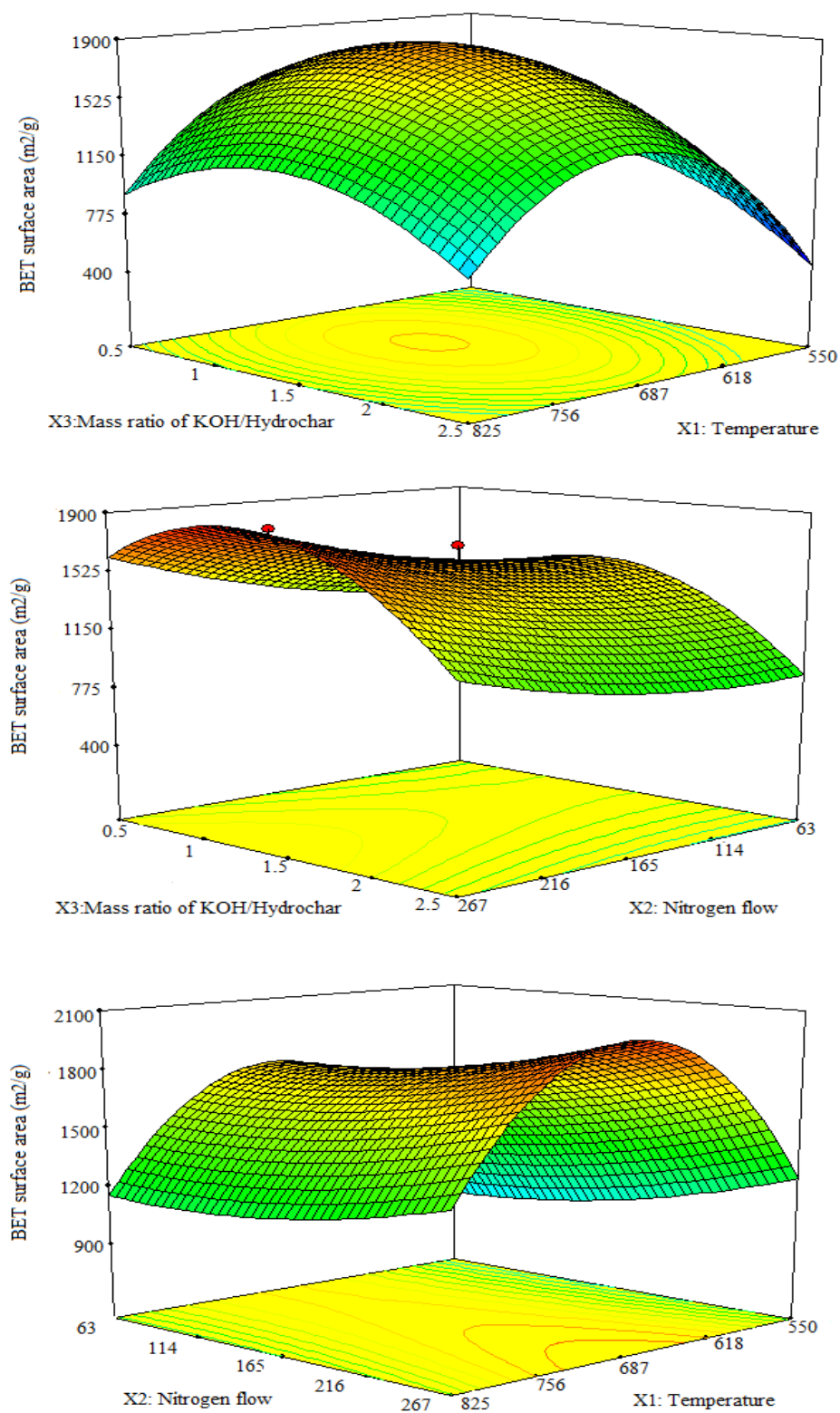


Figure 5.2: Three-dimensional plot of BET surface area model of activated carbons prepared by chemical activation of algal hydrochar

process conditions (at temperature of 647 °C, impregnation ratio of 1.5 and F= 267 cc/min); discussed previously. The yields of all the prepared ACs through chemical activation were lower than the one produced by thermal method (Run #1) without chemical agents at optimum flow rate of nitrogen of 267 cc/min and temperature of 647 °C. This shows that all the chemical agents worked well through chemical reactions during activation process, although using different chemical agents result in different yields of AC. Compared to thermally prepared activated carbon with BET surface area of carbons, chemical activation showed higher BET surface area. The average pore size of the thermally and chemically prepared activated carbon were 5.3-10.9 nm which were in the range of mesoporous materials (2-50 nm).

Among, all the chemical agents, alkali activators revealed higher BET surface area in the range of 793-2638 m²/g. K₂CO₃ was found more effective than NaOH and KOH as a chemical agent under identical conditions in terms of porosity characteristics and yield of the activated carbons. Maximum product yield of 63.1 wt.% with the highest BET surface area of 2638 m²/g and total pore volume of 1.7 cm³/g corresponded to the chemically prepared activated carbons using K₂CO₃.

This material also revealed micropore and mesopore volume of 0.61 and 0.89 cm³/g, respectively. Also, compared to KOH and NaOH, which are considered corrosive and hazardous alkali hydroxides, K₂CO₃ is not a hazardous chemical agent (Adinata et al., 2007). It was found that the microporosity was well developed for the activated carbon produced by mixed-alkali (K₂CO₃ + KOH) compared to chemically activated carbon using K₂CO₃ as a chemical agent. The micropore volume of activated carbon prepared using the mixture of K₂CO₃ + KOH was 0.64 cm³/g, which was higher than activated carbon prepared using K₂CO₃ (0.61 cm³/g). Compared to the results of BET surface area reported in the literature such as AC from sunflower extracted meal (1534.9 m²/g using ZnCl₂) (Morali et al., 2018), AC from Cocoa pod husk (1800 m²/g using KOH) (Tsai et al., 2019) , AC from tobacco stem (1347 m²/g using ZnCl₂) (Chen et al., 2017) chemically prepared activated carbon using K₂CO₃ from algal hydrochar revealed much higher BET surface area.

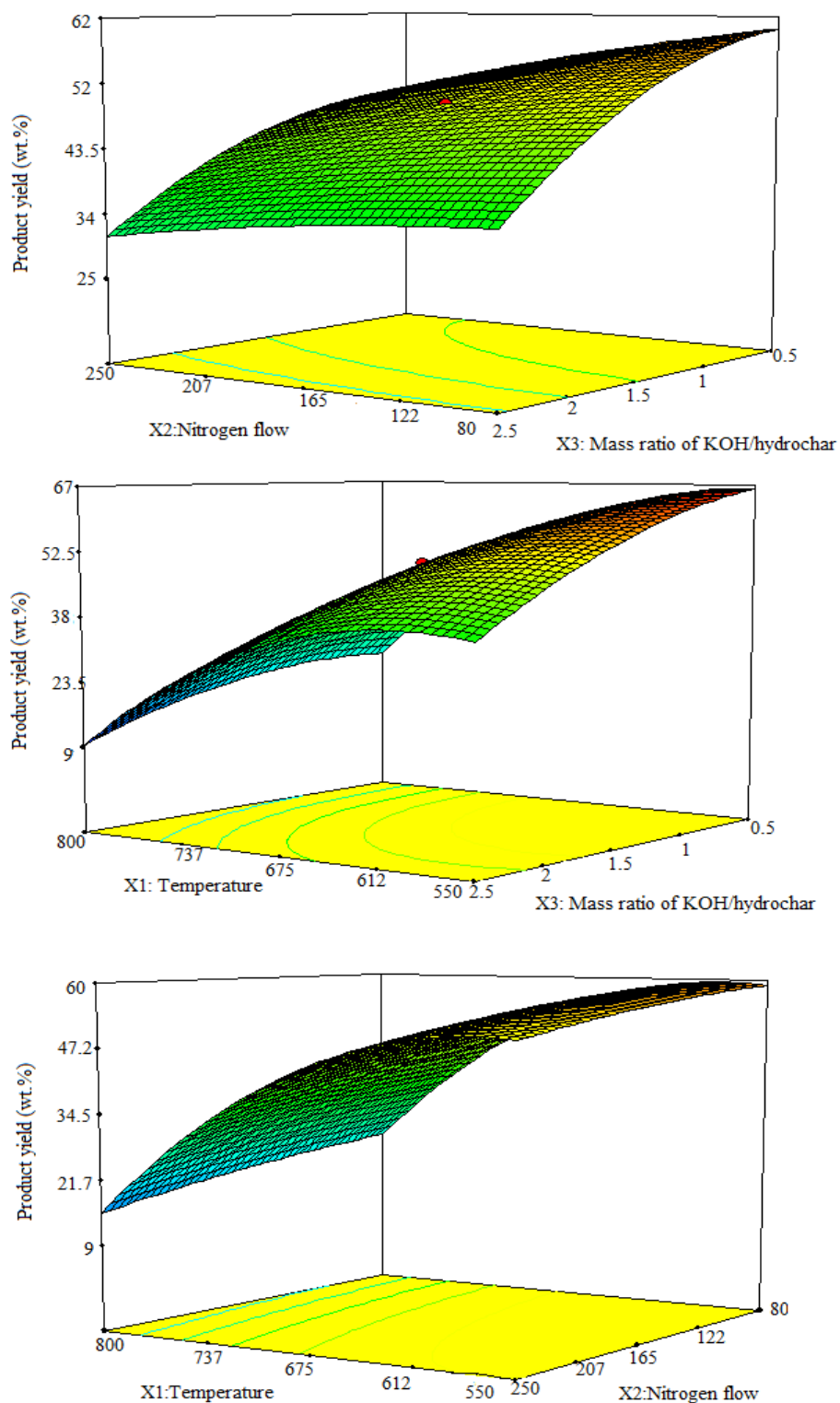


Figure 5.3: Three-dimensional plot of product yield model of activated carbons prepared by chemical activation of algal hydrochar

Table 5.6: Porous characteristics of activated carbons prepared by different chemical agents

Sample	Chemical agent	BET surface area (m ² /g)	Total pore volume (cm ³ /g)	Micropore volume (cm ³ /g)	Mesopore volume (cm ³ /g)	Average pore size (nm)	Yield (wt.%)
AC-1	-	366	0.2	0.07	0.13	5.6	75.6
AC-2	KOH	2099	1.2	0.58	0.62	5.9	42.3
AC-3	K ₂ CO ₃	2638	1.5	0.61	0.89	8.3	63.1
AC-4	NaOH	793	0.28	0.13	0.15	5.3	25.4
AC-5	H ₃ PO ₄	406	0.28	0.14	0.14	10.9	41.2
AC-6	ZnCl ₂	502	0.29	0.17	0.12	5.4	49.5
AC-7	KOH+NaOH	1348	1.1	0.41	0.7	6.1	31.2
AC-8	KOH+K ₂ CO ₃	2223	1.36	0.64	0.72	7.5	52.3

5.4.3.2 Elemental and proximate analysis of AC

The results of elemental and proximate analyses of prepared activated carbons chemically and thermally, are given in Table 5.7. Based on elemental analysis, chemical agents had a strong impact on production of carbon-dense activated carbon. The carbon content available in AC produced by alkali activator was higher than the amount of AC produced by thermal method or chemically AC produced by ZnCl₂ and H₃PO₄. It may happen due to the conversion of oxygen available in compounds present in algal hydrochar into volatile compounds resulting decrease in oxygen content in produced AC. HHV and energy recovery (ER) of activated carbons prepared thermally and chemically are also listed in Table 5.7. In this Table AC-1 to AC-8 are the same from Table 5.6. As carbon is considered as the major element to contribute to HHV, ACs prepared by alkali activators revealed higher heating value. Also, oxygen and hydrogen removal during the activation process can be contributed to the increase in calorific value of the prepared activated carbons. Chemically activated carbon prepared by K₂CO₃ revealed the highest amount of carbon (78.9 wt.%), and subsequently highest HHV (29.4 MJ/Kg), and ER (83.8 %).

Table 5.7: Elemental analysis, proximate contents and HHV of activated carbons

Run	Elemental analysis (wt.%)					Proximate analysis (wt.%)				HHV ^b (MJ/kg)	ER (wt.%)
	C	H	N	S	O ^a	Volatile matter	Fixed carbon ^a	Moisture	Ash		
AC-1	60.1	5.5	3.5	0.7	30.2	25.9	64.7	4.5	4.9	22.8	77.8
AC-2	70.4	4.3	3.1	0.6	21.6	14.5	75.7	5.3	4.5	26.1	49.8
AC-3	78.9	3.7	3.1	0.3	14	13.8	76.6	5.8	3.8	29.4	83.8
AC-4	65.2	4.1	3.3	0.4	27	22.0	67.7	5.5	4.8	23.1	26.4
AC-5	60.5	5.3	3.5	0.4	30.3	22.5	67.1	5.9	4.5	22.6	42.0
AC-6	63.2	5.5	4.1	0.5	26.7	18.2	72.1	4.8	4.9	24.4	54.6
AC-7	69.4	4.7	3	0.3	22.6	20.1	70.9	5.1	3.9	26.1	36.7
AC-8	72.1	4.9	2.9	0.3	19.8	15.2	76.1	4.9	3.8	27.8	65.6

^a Calculated by the mass difference

^b Calculated by Dulong equation: $[\text{HHV (MJ/kg)} = 0.338 \text{ C} + 1.428 (\text{H} - \text{O}/8) + 0.095 \text{ S}]$

According to proximate analysis, prepared activated carbons contain fixed carbon in the range of (64.7-76.6 wt.%) as the major contents, volatile matter, moisture and ash content in the range of (14.5-25.9 wt.%), (4.5-5.9 wt.%) and (3.8-4.9 wt.%), respectively. The ash contents of all the chemically and thermally activated carbons are lower than the ash content of algal hydrochar. It shows that the ash content was reduced during acid treatment with HCl. The ash content was also in the range of commercially accepted value (< 5 wt.%). It should be considered as an important property of activated carbon as a catalyst since higher ash content leads to compromising the porous structure of the activated carbons due to undesired reactions. Figure 5.5 reveals the thermal behavior of the microalgae, algal hydrochar and chemically prepared activated carbon with K₂CO₃ which is determined by thermogravimetric analysis (TG) and differential thermogravimetric analysis (DTG). According to the literature (Hassan et al., 2013; Tongpoothorn et al., 2011), the first stage of mass loss in DTG curves corresponds to the elimination of moisture (up to 180 °C). The second stage considered as a significant weight loss stage, which is related to the evolution of volatile compounds due to the decomposition of cellulose and hemicellulose (180 – 400 °C). The third stage corresponds to the decomposition of

lignin which showed higher thermal stability ($> 400\text{ }^{\circ}\text{C}$). Compared to microalgae, algal hydrochar obtained from HTC at $222\text{ }^{\circ}\text{C}$, showed weight loss around the reaction temperature due to decomposition of hemicellulose. The chemically activated carbon was not significantly affected by temperature due to its higher thermal stability. There was weight loss under $180\text{ }^{\circ}\text{C}$, due to the removal of moisture. Compared to microalgae and algal hydrochar, the moisture weight loss was significant due to its higher surface area and higher moisture adsorption (Hassan et al., 2013).

5.4.3.3 Surface morphology and particle size distributions of AC

Figure 5.6 shows SEM images of microalgae, algal hydrochar and prepared activated carbons to investigate their surface topography. Spherical particles with a limited porosity was observed in the surface of microalgae. Also, it can be seen that there is a significant difference between the surface structure of algal hydrochar and prepared activated carbons specially the one that were prepared chemically. The chemically activated carbon prepared with mixed-alkali ($\text{K}_2\text{CO}_3 + \text{KOH}$) and the one prepared with K_2CO_3 demonstrated well porous structure which is in a good agreement with the results of BET analysis as earlier discussed.

Table 5.8: Particle size distributions of thermally and chemically activated carbons

Sample	Volume fraction (%)		
	D10 (μm)	D50 (μm)	D90 (μm)
Algal hydrochar	38.4 ± 3.56	409 ± 43.1	1170 ± 127
AC-1	62.1 ± 4.2	253 ± 19.9	517 ± 66.9
AC-2	16.1 ± 0.31	62.8 ± 1.25	191 ± 42.3
AC-3	9.95 ± 0.24	42.4 ± 2.34	178 ± 48.9
AC-4	29 ± 0.7	133 ± 5.4	335 ± 3.1
AC-5	21.1 ± 0.9	103 ± 10.8	403 ± 91.6
AC-6	17.2 ± 0.8	102 ± 6.7	332 ± 47.5
AC-7	24.9 ± 0.5	91.8 ± 0.8	196 ± 5.1
AC-8	20 ± 0.7	70.2 ± 4.3	239 ± 18.3

*D10, D50 and D90 is the diameter at which 10%, 50% and 90% of a sample's volume are comprised of smaller particles, respectively.

The particle size distributions of algal hydrochar and chemically prepared activated carbons are given in Table 5.8. Compared to algal hydrochar, which 50% of its particles volume are in the range of $409 \pm 43.1 \mu\text{m}$, all the thermally and chemically prepared activated carbons revealed lower particle size distributions. Smaller particle sizes of activated carbons can result in faster reaction rate as they can be used as an adsorbent or catalyst, due to shorter mass transfer area. According to Figure 5.7, for chemically activated carbon prepared with K_2CO_3 , the particles ranged with sizes $191 \pm 42.3 \mu\text{m}$, which also 50% volume of its particles are in the range of $62.8 \pm 1.25 \mu\text{m}$.

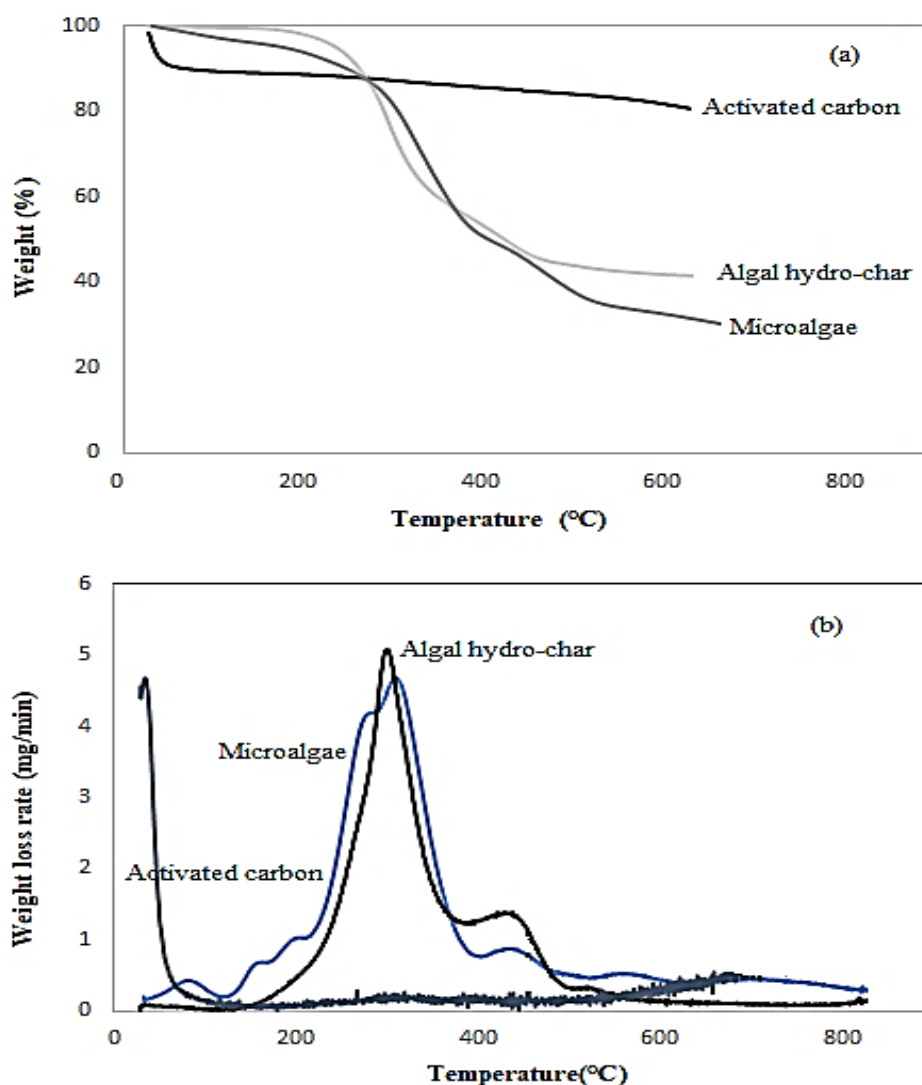


Figure 5.4: Thermal behaviors of microalgae, algal hydrochar and chemically activated ((a) indicates thermogravimetric analysis and (b) indicates differential thermogravimetric analysis)

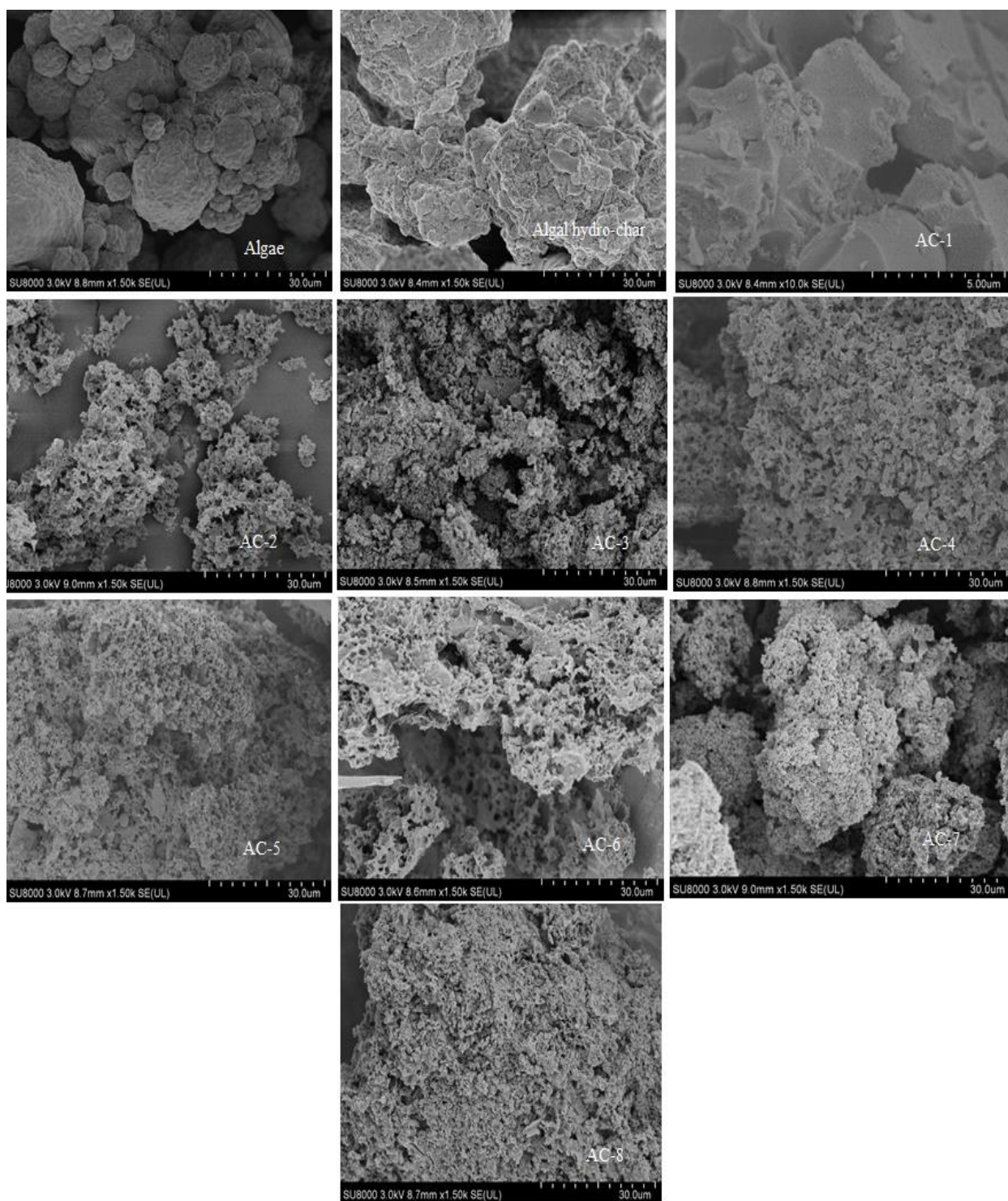


Figure 5.5: SEM images of microalgae, algal hydrochar and prepared activated carbons

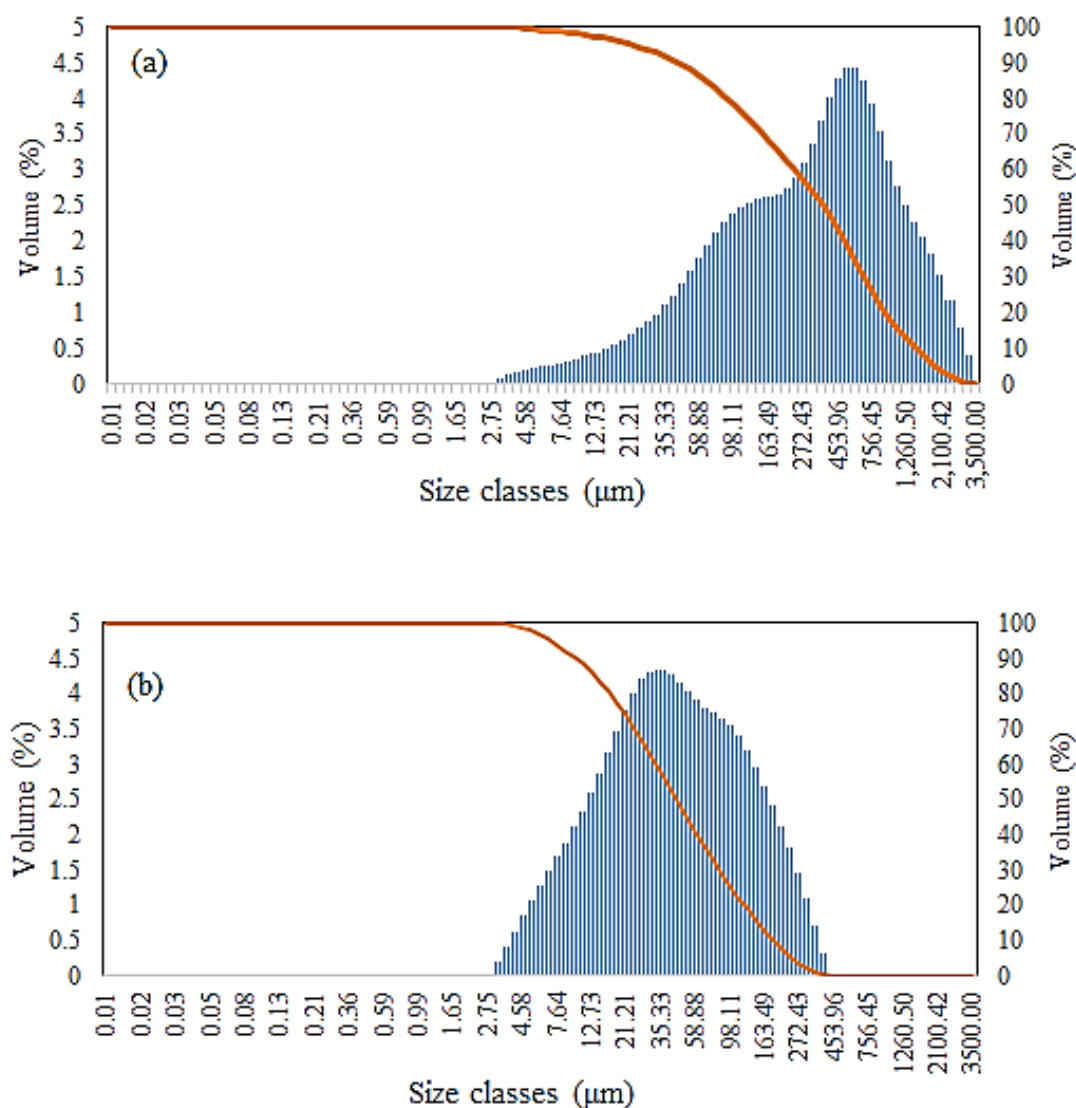


Figure 5.6: Particle size distribution of algal hydrochar and chemically prepared activated carbon

5.4.3.4 XRD analysis

Figure 5.8 shows XRD patterns of microalgae, algal hydrochar and chemically activated carbon prepared by K_2CO_3 . It is observed that there are no sharp peaks in the XRD patterns of microalgae and algal hydrochar. These broad peaks reveal the amorphous nature of the materials. Cellulose fraction has a peak around $2\theta = 13.5^\circ$, related to lattice plane (1 0 1). The intensity of

the peak related to cellulose fraction in microalgae is higher than that for algal hydrochar due to decomposition of the compounds during hydrothermal carbonization of microalgae. Two broad peaks around 26° and 43° confirmed the formation of carbon layer planes. It showed the signs of graphitic crystallite in the low (peaks around $2\theta = 26^\circ$) and high angle region (peaks around $2\theta = 43^\circ$) corresponding to lattice plane (0 0 2) and (1 0 0), respectively. Hence, the prepared chemically activated carbon by K_2CO_3 can be considered as a crystalline carbonaceous structured material. Similar results are reported by other researchers (Pechyen et al., 2007, Tongpoothorn et al., 2011).

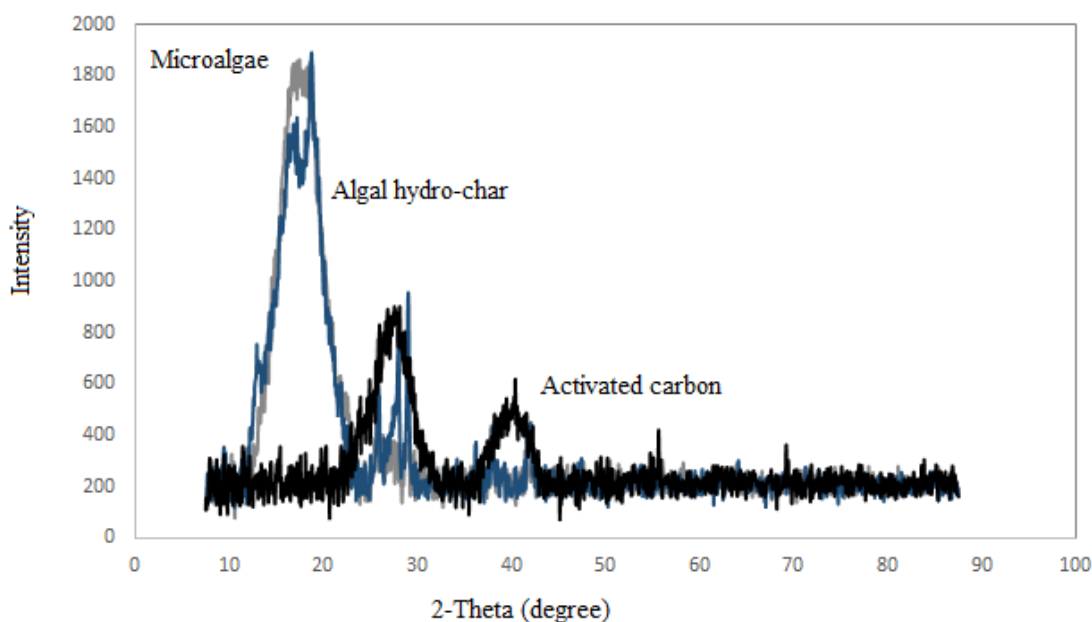


Figure 5.7: X-ray diffraction pattern of microalgae, algal hydrochar and prepared activated carbon

5.4.3.5 Chemical composition of AC (XPS)

The C1s peak from XPS spectra of chemically activated carbon prepared with K_2CO_3 and the relative content of its functional group are presented in Figure 5.9. Algal derived-hydrochar XPS data revealed two major peaks about 285.3 eV (21%) and 287.9 eV (79%), related to C–H and C=O bands, respectively. According to Fig. 5.8, five peaks related to carbon- contains functional group and surface acidity were recognized: peak 1 around 284.4 eV is related to graphitic carbon (–C=C–) or (C–C) (61.2%); Peak 2 around 285.7 is correlated with C–H band (14.6%); peak 3 which is about 286.8 eV corresponded to –C–O band (9.8%); peak 4 (287.7 eV)

is correlated with double bond of carbon and oxygen, C=O (8.1%); and peak 5 (289.3 eV) is related to the carboxyl acid groups (–COOH) (6.3%) (Gao et al., 2013; Shen et al., 2012).

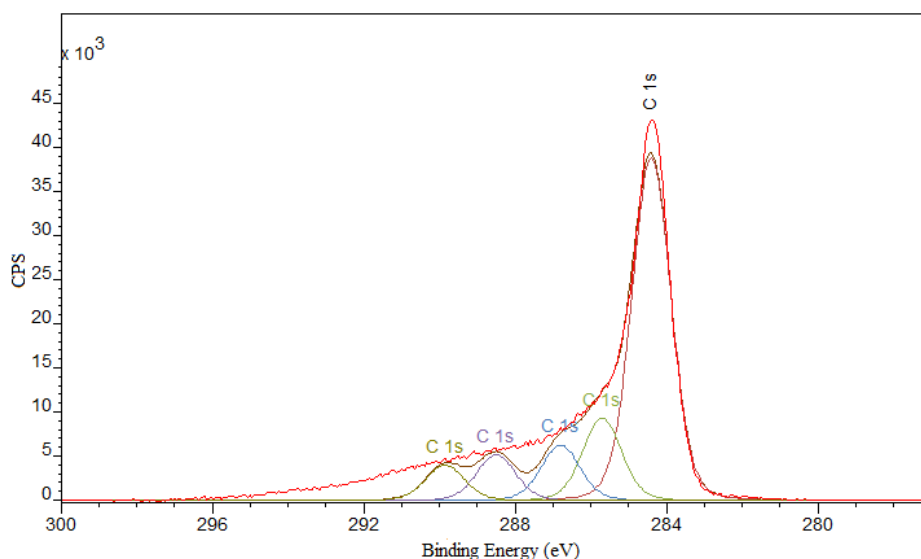


Figure 5.8: C 1s XPS spectra of the chemically prepared activated carbon

5.4.3.6 FT-IR analysis

FT-IR technique was employed to study the available functional groups on the surface of the materials. The FT-IR spectra of microalgae, algal hydrochar and prepared activated carbon by K_2CO_3 are shown in Figure 5.9. The peaks in the range of $800\text{--}1300\text{ cm}^{-1}$ assigned to C–O stretching or C–H bending (Biswas et al., 2017). The bands between 1500 and 1725 cm^{-1} are related to C=C and C=O stretching present in carboxylic acid. The bands between 3200 and 3500 cm^{-1} can be attributed to O–H groups indicating the presence of alcohols and phenolic groups (Pan et al., 2018, Shu et al., 2017). The intensity of the peaks related to C–H and C=O band for algal hydrochar is higher than AC which agrees with the results of XPS.

5.4.4 Methylene blue adsorption

The methylene blue adsorption behavior for algal hydrochar, commercial activated carbon and prepared activated carbon through chemical activation of algal hydrochar is shown in Figure 5.10. For algal hydrochar, there was no removal of methylene blue because as mentioned earlier, of its low surface area ($4\text{ m}^2/\text{g}$). For 1 g/L adsorbent dosage, 100% of methylene blue from 100 ml volume of solution with 250 mg/L of concentration, was removed within the first 5 min for chemically prepared activated carbon by K_2CO_3 or KOH due to its highly porous structure with

BET surface area ($\geq 2100 \text{ m}^2/\text{g}$) which is almost twice as that of commercially activated carbon ($1127 \text{ m}^2/\text{g}$) used for adsorption. Figure 5.11 shows that even 0.5 g/L dosage of chemically prepared activated carbon by KOH had better performance compared to 1 g/L dosage of commercial activated carbon.

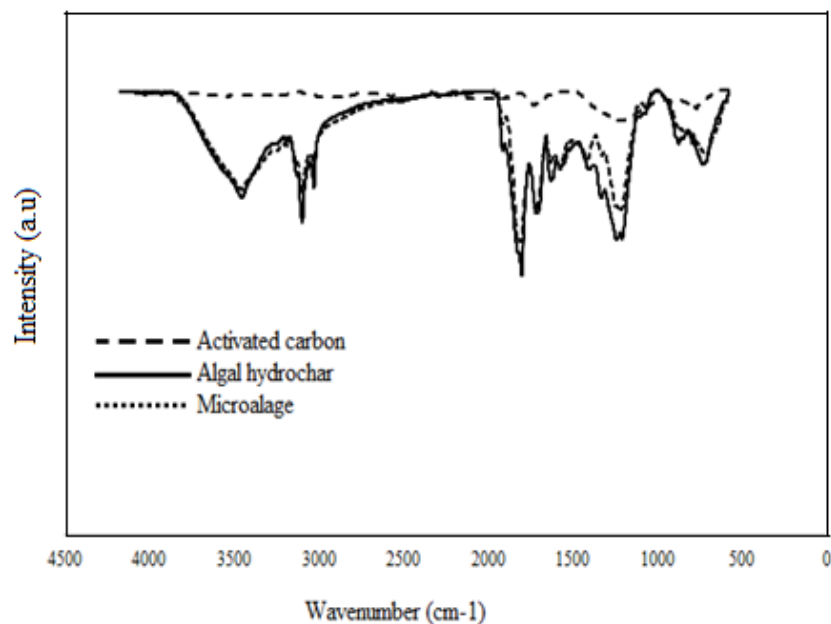


Figure 5.9: FT-IR spectra of AC, hydrochar and microalgae

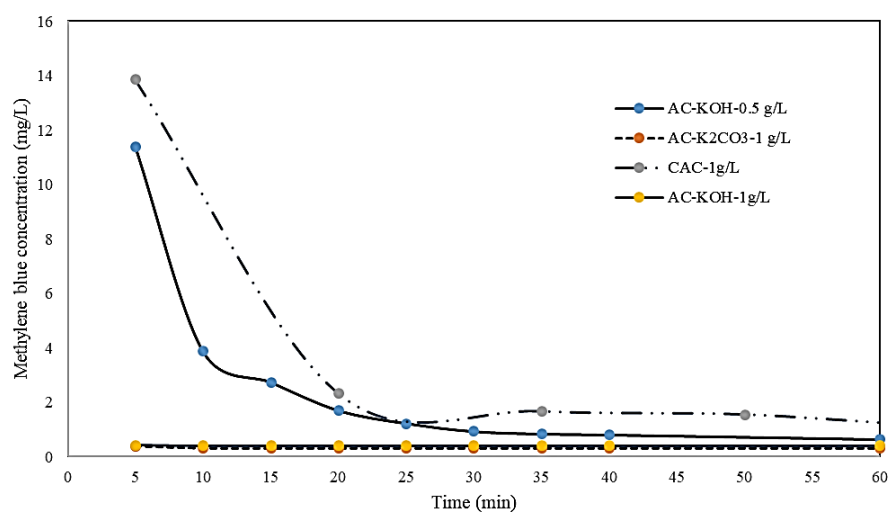


Figure 5.10: Methylene blue adsorption profiles for CAC and AC

5.5 Conclusions

In this study, chemical activation method was applied for porous activated carbon production from algal hydrochar. High BET surface areas of activated carbon were produced using algal hydrochar having BET surface area of $4 \text{ m}^2/\text{g}$. Response surface methodology applying central composite design (CCD) was employed to develop two quadratic models to evaluate the effect of process variables on BET surface area and products yield. The chemically activated carbon prepared at activation temperature of 675°C , impregnation ratio of 1.5 and flow rate of nitrogen of 267 cc/min , revealed high surface area ($\geq 2100 \text{ m}^2/\text{g}$) using KOH or K_2CO_3 as a chemical agent which showed micropore (V_{micro}) and mesopore (V_{meso}) volume in the range of $0.58\text{-}0.61$ and $0.62\text{-}0.89 \text{ cm}^3/\text{g}$, respectively. Hence, activated algal hydrochar as a carbon rich material revealed high surface area, and better porous structures which make it suitable as an environmental adsorbent for the removal of methylene blue from aqueous solution. 100% of methylene blue from aqueous solution of 250 mg/L was removed by using 1 g/L of chemically prepared activated carbon at room temperature within 5 min. A systematic approach was made to chemically activate algal hydrochar as a clean source for high quality activated carbon having high surface area with pore volume of $1.5 \text{ cm}^3/\text{g}$ and average pore diameter of 8.3 nm . This activated carbon was applied as a sustainable adsorbent material. It is recommended that this chemically prepared activated carbon can be applied as an adsorbent for wide variety of industrial pollutants. We have initiated new research on kinetic studies and equilibrium studies for certain pollutants to calculate adsorption capacity of activated carbon obtained from algal hydrochar.

Algal biocrude oil requires to be upgraded in order to be used as transportation fuel. Catalytic hydrodeoxygenation over hydrochar based catalysts is studied in the next phase to remove oxygenated compounds from algal biocrude oil.

Chapter 6: NiMo carbide supported on algal derived activated carbon for hydrodeoxygenation of algal biocrude oil

The content of this chapter has been published in the journal of Energy Conversion and Management cited below and presented in the following conferences:

Citation:

Masoumi, S., Dalai, A.K., 2021. NiMo carbide supported on algal derived activated carbon for hydrodeoxygenation of algal biocrude oil. Energy Convers. Manag. 231, 113834.

Conference Proceedings

Shima Masoumi, Ajay. K. Dalai, “Techno-economic and life cycle analysis of algal biofuel production via hydrothermal liquefaction of microalgae in a methanol-water system and catalytic hydrotreatment using hydrochar as a catalyst support”, 70th Canadian Chemical Engineering Conference,(Virtual), Ottawa , October 2020

Contribution of the PhD candidate:

Experiments were designed in consultation with Dr. Ajay K. Dalai and executed by Shima Masoumi. Material synthesis, catalysts characterization and data interpretation were performed out by the student. The manuscript was drafted by Shima Masoumi with guidance and suggestions provided by Dr. Ajay K. Dalai.

Contribution of this chapter to overall PhD research:

The third phase of the research is investigated in this chapter: hydrodeoxygenation reactions of algal biocrude oil obtained from HTL (first phase) are carried out over hydrochar-based catalysts impregnated with Mo and NiMo.

6.1 Abstract

The use of novel algae-derived activated carbon supported NiMo carbide catalysts for upgrading algal biocrude oil by hydrodeoxygenation was investigated. The carbide catalysts

were prepared in a two-step process involving sequential impregnation or co-impregnation of NiMo on activated carbon and followed by carbonization through three different methods namely temperature-programmed reaction with 20%CH₄-80%H₂, carbothermal hydrogen reduction in H₂, and carbothermal reduction in N₂. The synthesized carbide catalysts were characterized using XRD, BET, TPD-NH₃, TGA, and XPS techniques. The catalysts were screened for hydrodeoxygenation (HDO) of algal biocrude at various process conditions in a stirred tank reactor to produce liquid hydrocarbon fuels. The liquid hydrocarbon product was analyzed by ¹HNMR, ¹³CNMR, Sim-dist, CHNS, and GC-MS to gain insight into algal biofuel properties. The NiMo carbide synthesized through co-impregnation and carbothermal reduction in N₂ showed optimal activity for oxygen removal due to its high acidity and specific surface area and a greater amount of Mo₂C as active phases on the surface. Response surface methodology was applied for NiMoC catalyst to optimize the effects of temperature (350-450°C), catalyst loadings (5-15wt.%), and reaction time (1.5-4h) at a constant pressure of 3MPa. The upgraded biocrude oil revealed an oxygen reduction percentage of 94% with HHV of 43.9 MJ/kg.

Keywords: Algal biocrude, algal derived-activated carbon, NiMocarbide catalyst, hydrodeoxygenation, biofuel

6.2 Introduction

The increase in petroleum fuel prices, environmental concerns of CO₂ emission, and incremental demand for transportation fuels have gained much attention to find alternative renewable fuels (Horáček et al., 2020; Obeid et al., 2019). Biofuel obtained from biomass as a renewable source of energy is considered the most promising substitute for petroleum fuels (Q. Guo et al., 2015; C. Zhang et al., 2014). Algal biofuel as the third generation biofuel has been explored over the past decade since algae grows in a saline environment and sequesters carbon dioxide (Bahadar and Bilal Khan, 2013).

Hydrothermal liquefaction (HTL) is one of the promising technologies to convert wet biomass, particularly microalgae, into high-quality biocrude (Masoumi et al., 2020a; Palomino et al., 2020). HTL of algae generates the solid residue called hydrochar as a by-product. The

utilization of hydrochar as a catalyst/catalyst support can improve the overall process economy (Naderi and Vesali-Naseh, 2019). Algal biocrude obtained from the HTL process has undesired low heating value due to the presence of oxygen compounds such as acids, aldehydes, esters, ketones, and phenols. Therefore, it cannot be used directly as a transportation fuel and requires further processing to remove heteroatoms. Sulfur removal is not an issue as algal biocrude oil contains a low amount of sulfur content (Haider et al., 2018; Yang et al., 2016). It has been suggested that compared with the direct catalytic hydrothermal liquefaction (HTL) process, a two-step upgrading method including non-catalytic HTL followed by catalytic upgrading can be more effective to increase the quality of biocrude oil (Gu et al., 2020).

Out of all techniques used for upgrading biocrude, hydrodeoxygenation (HDO) reveals higher selectivity towards hydrocarbons and higher deoxygenation (Duan et al., 2016; Kazemi Shariat Panahi et al., 2019; Xu et al., 2018). The most significant challenge in HDO of biocrude is the development of a cost-effective catalyst with high activity, stability, and long lifetime. Different catalysts have been tested in biocrude upgrading. These catalysts contain transition metals or noble metals supported mostly on alumina, activated carbon, and zeolites. The carbon-based supports have shown better stability in water and high resistance to poisoning and coking than Al_2O_3 support (Yang et al., 2018; Zou et al., 2017).

Sulfided NiMo and CoMo supported on γ -alumina are the most well-known industrial catalysts for hydrotreating of petroleum oil (Anthonykutty et al., 2015). Since algal biocrude does not contain too many sulfur compounds, co-feeding of a sulfur source is required to keep the catalyst active [10]. On the other hand, noble metal catalysts can be used for biocrude hydrotreating as they do not require the co-feeding of sulfur. However, the high cost of noble metals, as well as their scarcity, limit their application in biocrude hydrotreating (Zhou and Hu, 2020).

Like transition metal sulfides, transition metal carbides were found to be active for hydrodeoxygenation because of their unique electronic structure and high thermal stability (Liang et al., 2017; Masoumi and Dalai, 2020a; Zou et al., 2016). Also, for HDO of aliphatic and cyclic oxygenate compounds available in biocrude, NiMo catalysts are more preferred than CoMo due to their better performance for decarboxylation and C-O bond cleavage. Besides, NiMo catalysts form less coke and consume less H_2 for hydrotreating than noble metal-based hydrotreating catalysts (Yang et al., 2018; Zhou and Lawal, 2016, 2015).

The objective of this study is to develop a novel NiMo carbide hydrodeoxygenation catalyst using algal-derived activated carbon as a support and upgrade algal biocrude into transportation fuels. In this regard, for the first time, algal-derived activated carbon supported NiMo carbide catalysts were prepared by different metal impregnation (incipient or co-impregnation), and different carbonization processes, and screened for hydrodeoxygenation of algal biocrude, which was obtained by HTL. The catalysts were analyzed by BET, XPS, XRD, TGA and TPD-NH₃. After catalysts screening, experimental design, response surface technology (RSM) was applied to optimize the hydrodeoxygenation process conditions including time, temperature and catalyst loading. Analysis of Variance (ANOVA) was employed to statistically evaluate the effect of these process parameters on the oxygen content through HDO process of algal biocrude oil. Quadratic model was developed as a function of temperature, time and catalyst loading to obtain oxygen content (wt.%) in algal biofuels produced through HDO process. The chemical compositions (CHNSO & GC-MS) of biocrude oil and biofuels and their physical properties (boiling point distributions, higher heating values, etc.) were also analyzed.

6.3 Materials and methods

Materials used for this section, also catalyst synthesis procedure was explained in Chapter 3. It should be mentioned that for synthesizing the catalysts, KOH/hydrochar ratio of 0.5 was used for activated carbon production and during the chemical activation process, nitrogen gas was purged at 80 cm³/min to remove gaseous products, and the reactants were heated at 3°C/min to the temperature of 550 °C, and remained in this temperature for 2 h. As, in this process condition, the produced activated carbon revealed higher yield and relatively high surface area suitable for its usage as catalysts support.

6.4 Results and discussion

6.4.1 Physical and chemical characterizations of synthesized carbide catalysts

Since one of the objectives of this research was to study the effects of catalysts in algal biofuels production through HDO of algal biocrude oil, detailed characterizations of NiMo and Mo supported on chemically activated carbon derived from algal hydrochar was conducted to gain more insight of catalysts structure.

The XRD patterns of the activated carbon support and various carbide catalysts are shown in Figure 6.1. As mentioned before, the activated carbon support was produced by chemical activation of hydrochar that was obtained from microalgae by HTL. Two diffractions around

$2\Theta = 28$ and 43° represent the graphite crystallites related to the lattice plane (002) and (100), respectively (Masoumi and Dalai, 2020a). The activated carbon supported Mo carbide catalyst shows diffraction peaks at $2\Theta = 34.4, 38.0, 39.4, 52.1, 61.5$ and 69.6° . These peaks correspond to the Mo_2C crystal planes of (100), (002), (101), (102), (110) and (103) (Liang et al., 2017). The NiMo carbides contain additional diffraction peaks at $2\Theta = 44.3, 51.7, 76.1^\circ$, which correspond to Ni^0 species (Zou et al., 2017). There is a peak around $2\Theta = 26^\circ$ in NiMo carbides prepared by step-wise impregnation. This is attributed due to the NiMoO_4 phase. The intensity of this peak for different methods of carbonization was in the order of, TPR method > CHR method > CR method. It means, using CR method, Ni was incorporated in Mo oxides phase easily and facilitate the reduction process resulted in increasing the NiC and Mo_2C phases. Thus, CR method was used to convert oxide phases of NiMo/AC synthesized using co-impregnation method and Mo/AC catalyst to carbide phase. It should be also mentioned that one of the advantages of this method is, the use of N_2 gas as an inexpensive gas to carbidation of the catalysts supported on porous AC derived from algal hydrochar. According to the XRD pattern of the sample synthesized by co-impregnation and CR carbonization, the peak around 26° , completely disappeared, and the intensity of peaks related to Mo_2C increased. It means that co-impregnation and CR method, is not only inexpensive method among them, also facilitate reduction process.

The porous characteristics of the support and catalyst samples are listed in Table 6.1. The hydrochar obtained from HTL possessed very poor textural properties and a low surface area of $4 \text{ m}^2/\text{g}$. Hydrochar porous characteristics were improved by chemical activation. The activated carbon derived from hydrochar has a surface area of $631 \text{ m}^2/\text{g}$ and mesopores with a mean pore diameter of 8.2 nm . The NiMoC/AC prepared by TPR showed the lowest surface area and pore size of $384 \text{ m}^2/\text{g}$ and 8 nm , respectively. This might be due to the formation of carbonaceous deposits inside the pores of AC by CH_4/H_2 . The highest surface area of $570 \text{ m}^2/\text{g}$ was obtained with the sample prepared through a combination of step-wise impregnation and carbonization with nitrogen gas. This sample possessed higher pore volume and pore size compared to the AC support. It may be related to the pore widening due to the removal of volatile compounds from the AC support in the N_2 atmosphere.

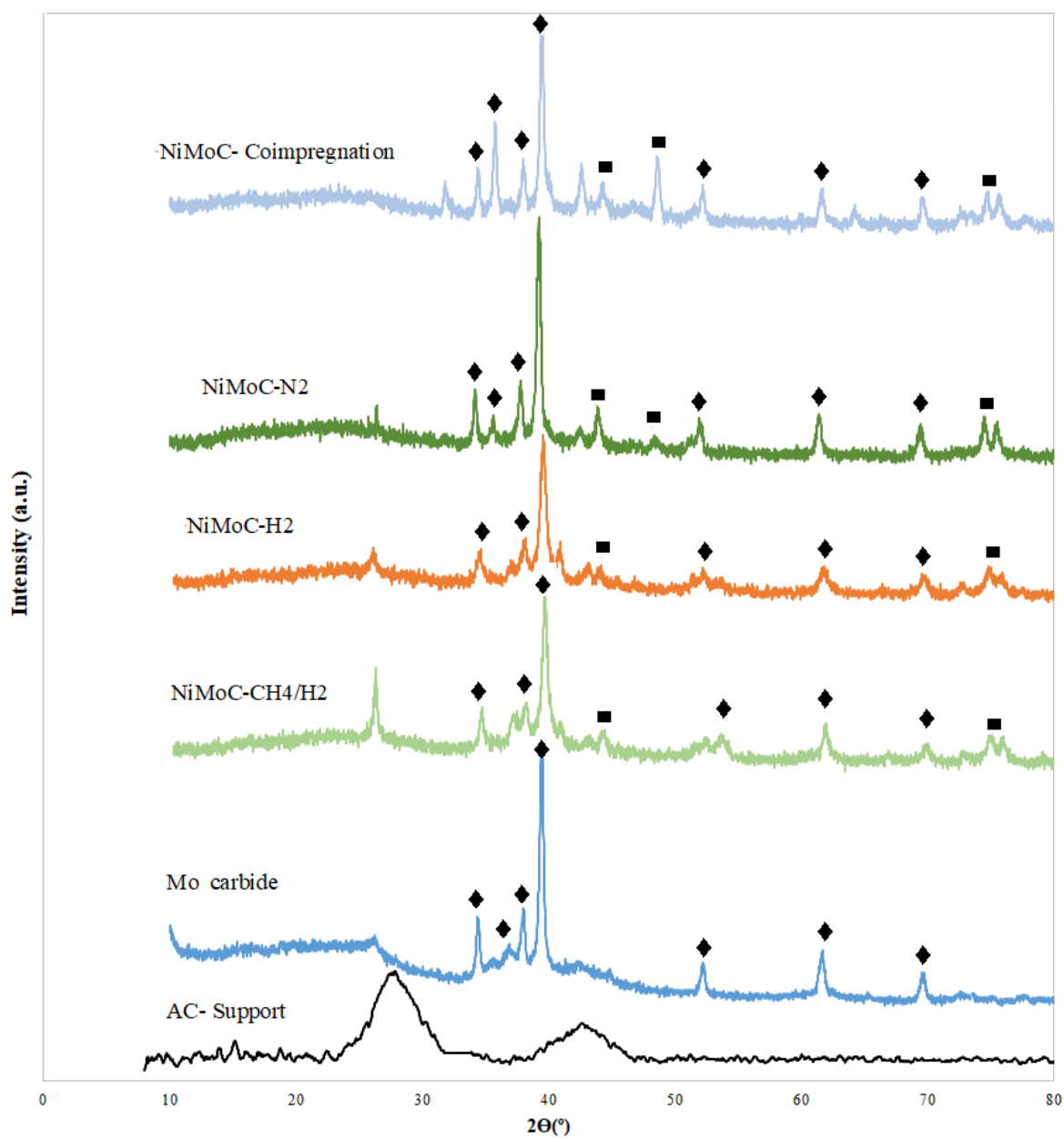


Figure 6.1: XRD pattern of AC and synthesized catalysts

(♦ indicating Mo_2C and ■ indicating NiC)

Table 6.1: Porous characteristics of synthesized catalysts

Sample	Specific surface area (m ² /g)	Pore volume (Cm ³ /g)	Pore size (nm)
AC- Support	631	0.36	8.2
Mo Carbide	450	0.3	8.0
NiMoC-CH₄/H₂	384	0.30	8.0
NiMoC-H₂	498	0.35	8.8
NiMoC-N₂	570	0.37	10.8
NiMoC-Coimpregnation	505	0.36	9.1

The XPS analysis was used to determine the Mo 3d spectra and its relative oxidation states of the synthesized catalysts and the results are shown in Figure 6.2, and Table 6.2. Mo 3d spectra consist of two peaks resulting from spin-orbit (j-j) coupling: Mo 3d_{5/2} and Mo 3d_{3/2} with area ratio of 3:2. The peak distance between 3d_{5/2} and 3d_{3/2} equal to 3.2 eV. Mo 3d_{5/2} peaks of Mo²⁺, Mo^{δ+}, Mo⁴⁺, and Mo⁶⁺ species were centered at 228.2 ± 0.1 eV, 229.0 ± 0.1 eV, 229.6 ± 0.1 eV and 232.4 ± 0.1 eV, respectively. The Mo₂C, MoOxCy (an intermediate oxidation state between Mo²⁺ and Mo⁴⁺), MoO₂, and MoO₃ phase corresponded to Mo²⁺, Mo^{δ+}, Mo⁴⁺, and Mo⁶⁺, respectively (Zou et al., 2016). The sample synthesized using temperature programmed reaction (TPR) with 20% CH₄/H₂ showed low amount of Mo₂C. This indicates that the carbidation process using methane, which could decompose and block the pores, was not completed. MoOxCy, The total amount of Mo⁺² and Mo^{+δ} corresponded to Mo carbide and oxycarbide species for the NiMoC-coimpregnated sample were about 54.53%, which were more than those for other carbide catalysts. It can be related to the presence of NiMoO₄ species in the co-impregnated oxidic precursors, which during the carbonization process was more easily reduced to Mo²⁺ and Mo^{δ+} compared to MoO₃ and MoO₂.

Table 6.2: XPS data of synthesized catalysts

Sample	Mo²⁺	Mo^{δ+}	Mo⁴⁺	Mo⁶⁺
	Content (%)	Content (%)	Content (%)	Content (%)
Mo Carbide	3.85	46.76	12.17	37.22
NiMoC-CH₄/H₂	0.05	12.5	15.92	71.56
NiMoC-H₂	3.32	13.14	37.55	45.98
NiMoC-N₂	12.55	19.92	10.24	57.3
NiMoC- Coimpregnation	33.39	21.14	9.69	35.78

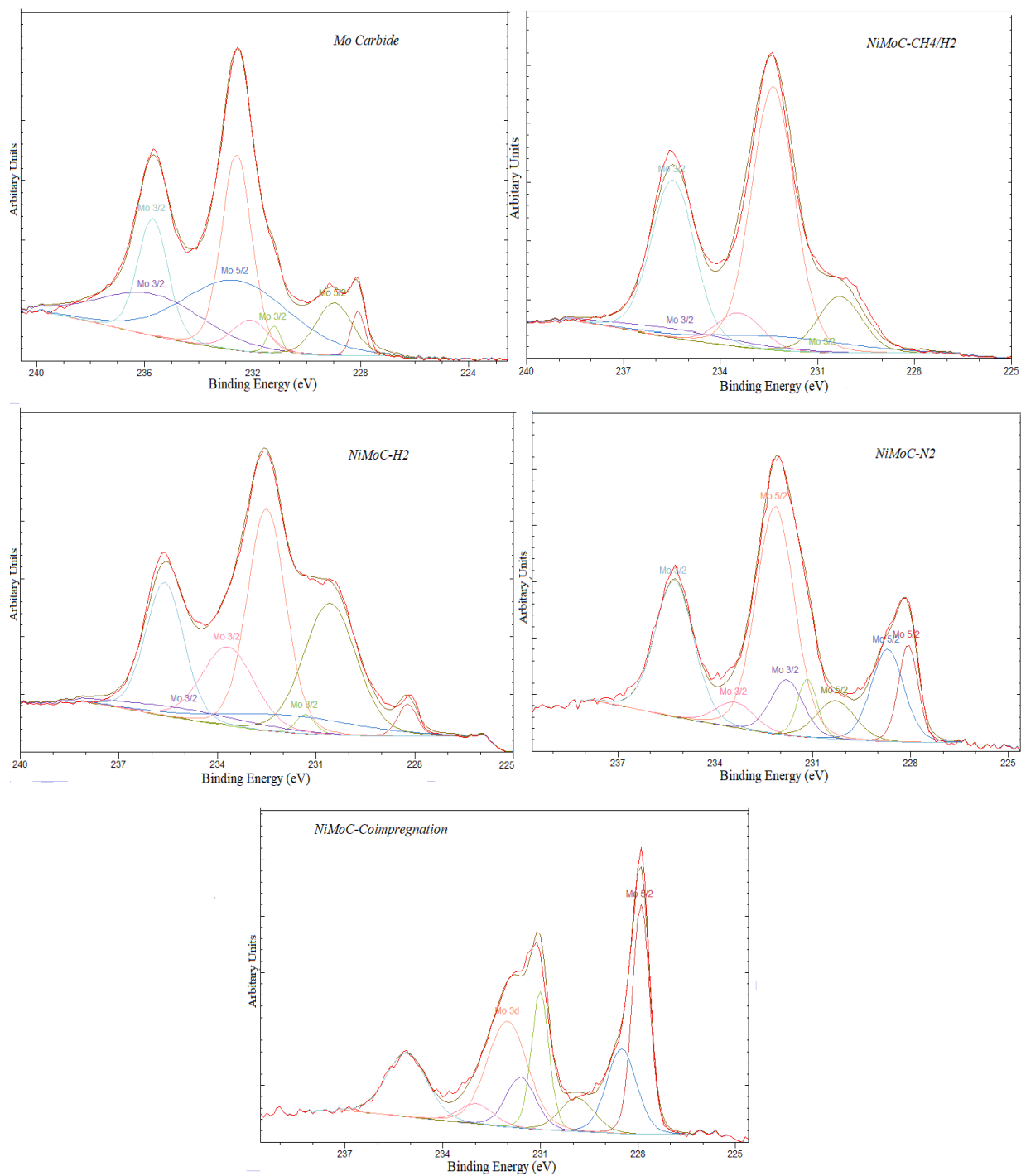


Figure 6.2: XPS patterns of synthesized catalysts

The strength of acidic sites on the surface of prepared catalysts was analyzed by NH₃-TPD analysis based on the adsorption strength of ammonia molecule on acidic sites, which depends on the desorption temperature. The acidic sites are classified as weak ($\leq 200^{\circ}\text{C}$), moderate ($200\text{--}400^{\circ}\text{C}$) and strong ($\geq 400^{\circ}\text{C}$) acid sites (Duan et al., 2016). Figure 6.3, shows the results of the analysis for MoC and NiMoC catalysts. Those catalyst samples exhibited major peaks above 700°C , which is the characteristic of very strong acid sites. It seems that Ni as a chemical promotor could affect support and active metal (Mo) resulting in higher acid sites. The amount of ammonia desorbed, which also indicate the amount of acid sites, was determined based on the area under the curves. It is about 0.33 and 0.56 mmol/g for the MoC and NiMoC, respectively.

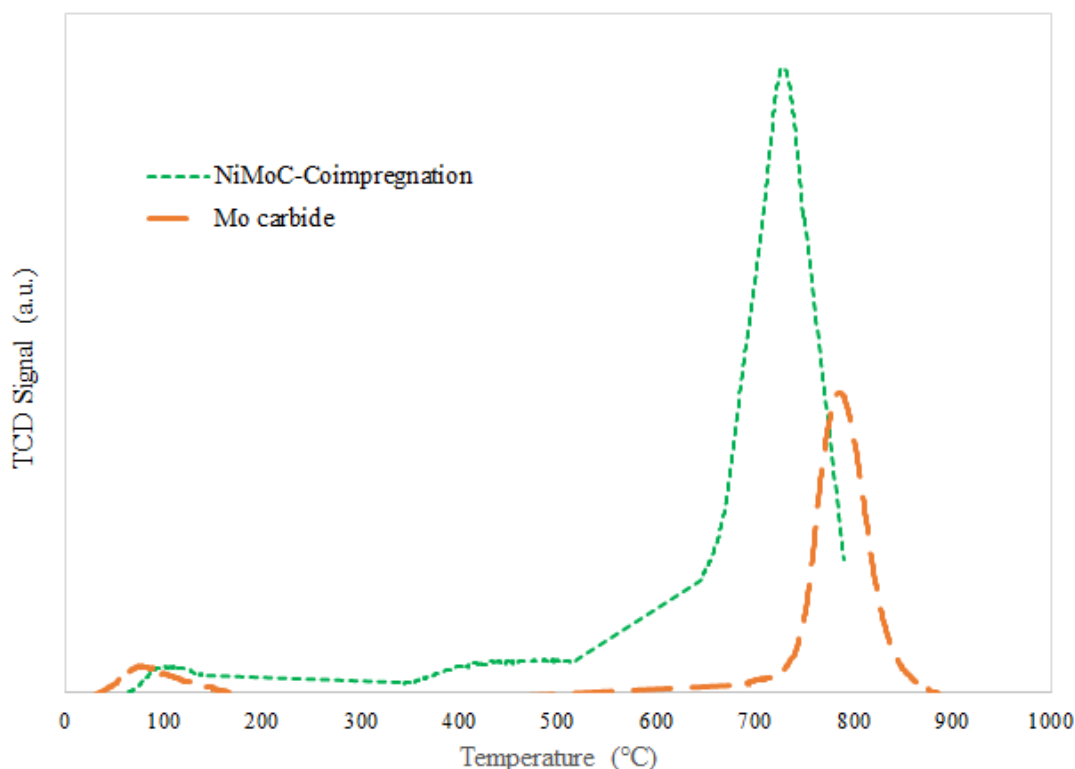


Figure 6.3: TPD-NH₃ results for MoC and NiMoC

6.4.2 Effects of catalysts on product distributions and algal biofuels characteristics

Algal-derived biocrude contains 5.4, and 15.3 wt.% of total nitrogen and oxygen, respectively. The presence of large amount of nitrogen and oxygenated compounds emphasizes the necessity of HDO of algal-derived biocrude to upgrade into transportation fuels. HDO of algae-derived biocrude over Mo and NiMo carbides supported on algae-derived activated carbon

was investigated at a reaction temperature of 400 °C, time of 2 h, and catalyst loading of 5 wt.%. The gaseous products were analyzed by GC. The gas mixture contained over 90 % unreacted H₂, with balanced CH₄, CO₂, CO, ethane, propane, ethylene, and propylene. Compared to algal biocrude oil, upgraded biocrude was lighter in color and showed a lower viscosity at room temperature. Table 6.3, shows the effects of different catalysts on the yields of products, elemental composition, and HHV of upgraded biocrude oil.

Among catalysts screened, the percentage of oxygen removal is the lowest over NiMoC/AC synthesized using the TPR method. As evidenced by XPS, this catalyst contains the lowest presence of Mo₂C species, as a result, it showed very poor performance for HDO. NiMo/AC carbide prepared through co-impregnation and carbothermal reduction exhibits an optimal catalytic activity for HDO. The upgraded oil obtained with this catalyst contains the nitrogen and oxygen content of 3.9 and 2.6 wt.%, respectively. Among all catalysts evaluated, the above catalyst showed a maximum of 83% of oxygen reduction. The better deoxygenation activity of this catalyst is related to the presence of more amount of Mo carbide active phase in NiMo/AC catalyst than

that in Mo/AC catalyst, as evidenced by XPS. Higher activity of NiMo/AC is also related to its higher acidity as compared to the MoC/AC (Nava et al., 2009). Besides that, comparing the catalytic activity of NiMoC/AC and MoC/AC which was reduced to carbide phase using the same method, Ni as a promoter can dissociate H₂ and provide active hydrogen for Mo impregnated on AC, resulting in higher deoxygenation activity of oxygenated compounds (Zou et al., 2016). The algal biocrude contains an HHV of 33.4 MJ/kg. After the removal of N, S, and O compounds, the upgraded oil had HHV of 42.8 MJ/kg, which is quite close to that (45 MJ/kg) petroleum diesel.

Table 6.3: Product distribution and elemental analysis of upgraded oil over synthesized catalysts

Sample	Upgraded oil yield (wt.%)	Gas Yield (wt.%)	Coke Yield (wt.%)	WSC Yield (wt.%)	C (wt.%)	H (wt.%)	N (wt.%)	S (wt.%)	O (wt.%)	HHV (MJ/kg)	ER (%)
Biocrude oil	-	-	-	-	70.5	8.6	5.4	0.2	15.3	33.4	-
Mo Carbide	71.3	5.9	13.9	8.9	81.2	10.2	4.5	0.1	3.8	41.3	88.4
NiMoC-CH ₄ /H ₂	67.8	8.4	20.9	2.9	76.1	8.8	5.2	0.1	9.8	36.5	74.4
NiMoC-H ₂	69.9	7.4	15.1	7.6	80.7	9.8	4.9	0.1	4.5	40.4	84.9
NiMoC-N ₂	70.4	6.1	14.2	9.3	81.5	10.3	4.2	0.1	3.9	41.5	87.8
NiMoC- Coimpregnation	72.5	6.5	11.3	9.7	82.6	10.8	3.9	0.1	2.6	42.8	93.3

The boiling point distributions of algal-derived biocrude feedstock and upgraded biocrude oil over the optimal NiMoC/AC catalyst (prepared via co-impregnation and carbothermal reduction) and MoC were determined using a simulated distillation (Sim-Dist) method and the results are given in Figure 6.4. It is a function of the chemical compounds structure in the range of C₁₀-C₆₀ and used to determine the relative portion of light and heavy compounds in the bio oil samples. The boiling ranges of gasoline, diesel cut 1, diesel cut 2, vacuum gas oil, and vacuum residue as depicted in Figure 5 are <190 °C, 190-290 °C, 290-340 °C, 340-538 °C, and > 538 °C, respectively. The biocrude feedstock contains around 70 % compounds in the range of vacuum gas oil and vacuum residue. Catalytic hydrodeoxygenation increased the number of compounds with lower boiling points, as a result, NiMoC catalyst showed more favorable results with 13 and 47% in the range of gasoline and diesel 1 and 2 cuts. It seems that during the HDO process, cracking was also involved and it increased the low boiling point compounds in the upgraded oil.

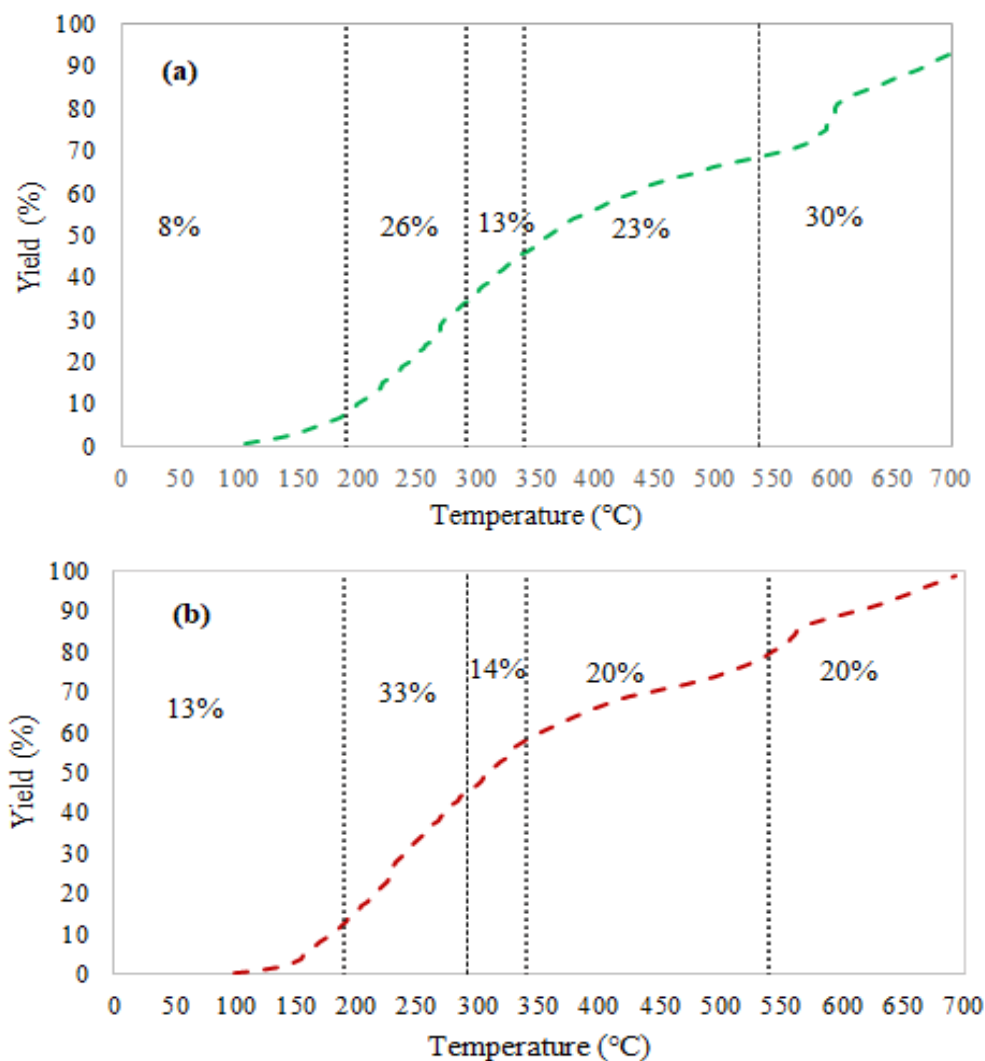


Figure 6.4: Boiling point distribution of upgraded oil obtained from HDO over a) MoC b) NiMoC catalysts

The GC-MS spectra of biocrude feedstock, upgraded liquid product over the optimal catalyst are shown in Figure 6.5. The feedstock contains nitrogen and oxygen containing compounds such as fatty acids, esters, amines, phenolic compounds. The two major peaks in GC-MS spectra of feedstock are related to octadecanoic acid and hexadecanoic acid. After HDO, the oil contains mostly saturated hydrocarbons. The HDO process not only removed the unwanted heteroatom compounds but also increased the stability of biocrude by forming saturated compounds.

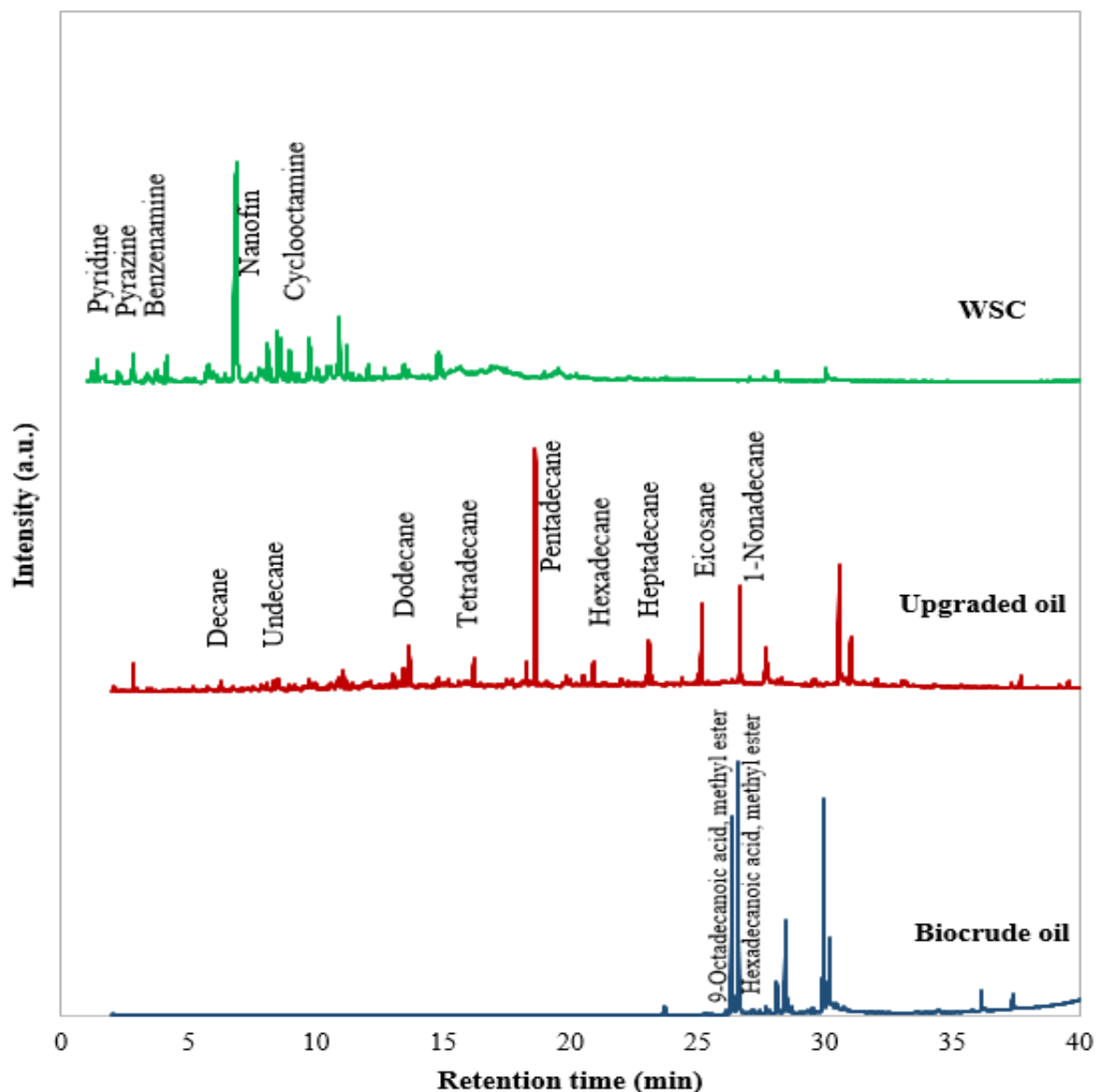


Figure 6.5: GC-MS patterns of biocrude oil and upgraded oil and WSC

FT-IR analysis was performed for determining the functional groups present in the feedstock and the product oil. As shown in Figure 6.6, the feedstock possesses a band around 3400 cm^{-1} which is related to O—H stretching vibration. This band might be associated with phenolic and carboxylic acid compounds, which were found to be rich in biocrude by GC-MS. There is also a band in the range of $1760\text{--}1690\text{ cm}^{-1}$, which is correlated to C=O stretching vibrations. The intensities of these two bands drop in the upgraded oil. This result supports the GC-MS result of the reduction of oxygenated compounds in upgraded biocrude oil. The band in the range of 1450--

1360 cm^{-1} is related to C—H stretch. The intensity of this band is significantly higher in the upgraded oil than that of the feedstock. It confirms the increase of saturated hydrocarbons after HDO.

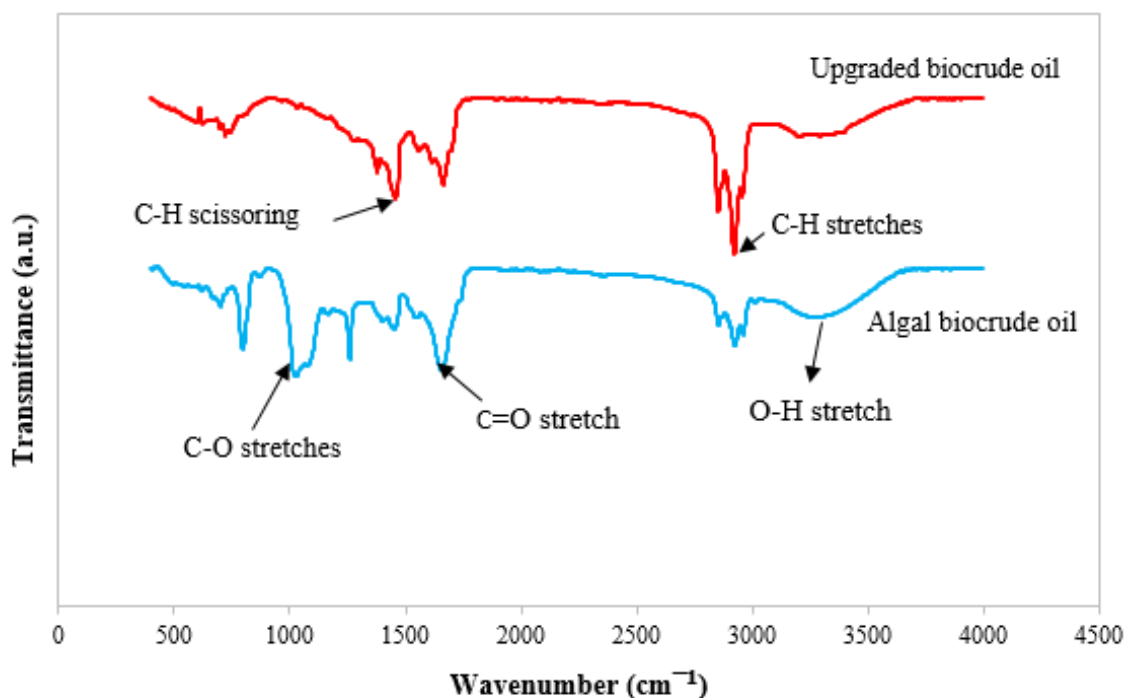


Figure 6.6: FTIR analysis results of algal biocrude oil and upgraded oil

The results of ^1H NMR analysis of the feedstock and the product oil from the optimal catalyst are given in Table 6.4. The number of alkane protons (0.5-1.5 ppm) is more in the upgraded oil than that of feedstock. It corroborates the results of GC-MS and FTIR and points out that the saturated hydrocarbons are the main compounds in upgraded oil. The proton chemical shift in the range of 1.5-3 ppm is related to the heteroatoms and unsaturated compounds (Masoumi et al., 2020a). The number of above protons dropped by 33 % after HDO. This supports the results of CHNSO, which also evidenced the reduction of nitrogenous and oxygenated compounds on HDO of biocrude oil.

Table 6.4: ^1H NMR and ^{13}C NMR analysis results for algal biocrude oil and upgraded oil

NMR/Chemical shift		Algal biocrude oil (%)	Upgraded biocrude oil (%)
¹ H NMR	Alkanes (0.5-1.5 ppm)	64.9	80.3
	Aliphatics (unsaturated or heteroatoms) (1.5-3 ppm)	23.9	15.8
	Alcohols (3-4.4 ppm)	-	-
	Carbohydrates (4.4-6 ppm)	-	-
	Aromatics (6-8.5 ppm)	11.2	3.9
¹³ C NMR	Short aliphatics (0-28 ppm)	15	25.1
	Long branched aliphatics (28-55 ppm)	68.2	65.2
	Alcohols, carbohydrates (55-95 ppm)	-	-
	Aromatics, Olefins (95-165 ppm)	16.8	9.7
	Esters, Carboxylic acids, Ketones, aldehydes (165-215ppm)	-	-

6.4.3 Effects of operating conditions of HDO to oxygen removal from algal biocrude oil

The catalytic hydrodeoxygenation of algal-derived biocrude over the optimal NiMo/AC carbide (synthesized using co-impregnation and reduction in N₂) was performed by varying reaction temperature (350-450 °C), time (1.5-4 h), and catalytic loading (5-15wt.%) at a constant pressure of 3 MPa. Response surface methodology (RSM) as an experimental design technology, using central composite design (CCD) was applied to obtain a model to study how the independent factors of this study; temperature (X₁), time (X₂), and catalyst loading (X₃) and their interaction affect the percentage of oxygen reduction. In Table 5.5, the independent variables, which are coded as $-\alpha$, -1, 0, +1, and $+\alpha$, ($\alpha=1.3$) related to the rotatability and orthogonality in the CCD design are given.

Table 6.5: Independent process variables and their examined levels used in experimental design

Factor	Level				
	-1.3	-1	0	+1	+1.3
X₁ -Temperature (°C)	335	350	400	450	465
X₂ – time (h)	1.1	1.5	2.75	4	4.3
X₃- catalyst loading (wt.%)	3.5	5	10	15	16.5

To better understand the influence of process parameters on the response (oxygen reduction percentage), the below quadratic polynomial equation (5.1) was used.

$$Y = \beta_0 + \beta_1 X_1 + \beta_2 X_2 + \beta_3 X_3 + \beta_{11} X_1^2 + \beta_{22} X_2^2 + \beta_{33} X_3^2 + \beta_{12} X_1 X_2 + \beta_{13} X_1 X_3 + \beta_{23} X_2 X_3 \quad (6.1)$$

Where Y is the calculated response which is the oxygen content (wt.%) in the upgraded product oil. The oxygen removal percentage was calculated using the equation (5.2):

$$\text{Oxygen removal percentage: (OR)} = \left[1 - \frac{\text{oxygen content (wt.\%) in upgraded oil}}{\text{oxygen content (wt.\%) in algal biocrude}} \right] \times 100 \quad (6.2)$$

And β_0 , β_j , β_{jj} , β_{ij} , are the constant values as linear, squared, and interaction coefficients, respectively. Based on experimental design, the different independent process parameters (X_1 , X_2 , and X_3) were applied, and the oxygen content and oxygen reduction percentage based on the results of CHNSO analysis are summarized in Table 6.6. Due to the statistical design of the experiments, three experiments were conducted at the center point in the design experiment to determine the reproducibility of the results and estimate the errors, which were within ± 0.3 wt.%. The result were given in the central point ($X_1 = 400$ °C, $X_2 = 2.75$ h, $X_3 = 10$ wt.%), were the mean of the results obtained from the three experimental runs.

According to Table 6.7, ANOVA was applied to investigate the process parameters and their interactions influences on the response (the oxygen content in upgraded biocrude oil) during the HDO process. Two parameters of F and P values are employed to investigate if the process parameters and their interaction as well as the model are significant. F value defines as MSF

divided by MSE, in which MSF indicates the mean squares of factors or interactions and MSE defines the mean squares of errors. The higher F value is related to the more significant model [24].

Table 6.6: Elemental analysis results of upgraded biocrude oil in different process conditions

Sample	Process Parameters			CHNSO (wt.%)					Oxygen reduction (%)	HHV(MJ/kg)
	X ₁ ¹	X ₂ ¹	X ₃ ¹	C	H	N	S	O ²		
1	335	2.75	10	75.1	10.1	5.1	0.1	9.6	37	38.1
2	350	4	5	75.2	10.2	5.1	0.1	9.4	38	38.3
3	400	2.75	10	84.1	11.0	3.9	0.1	0.9	94	43.9
4	450	1.5	15	74.4	9.8	3.7	0.1	12	21	37.0
5	450	1.5	5	77.5	10.1	3.8	0.1	8.5	44	39.1
6	400	2.75	16.5	77.4	10.4	4.1	0.1	8	47	39.5
7	450	4	5	78.2	10.8	4.0	0.1	6.9	54	40.6
8	400	4.38	10	81.2	11.1	3.8	0.1	3.8	74	42.6
9	350	1.5	15	74.5	10.3	5.2	0.1	9.9	35	38.1
10	400	1.13	10	79.9	10.9	4.9	0.1	4.2	72	41.8
11	350	4	15	72.4	9.8	5.2	0.1	12.5	18	36.2
12	400	2.75	3.5	79.4	10.8	3.9	0.1	5.8	62	41.2
13	350	1.5	5	76.3	10.2	5.3	0.1	8.1	47	38.9
14	450	4	15	72.9	9.8	4.5	0.1	12.7	16	36.3
15	465	2.75	10	78.9	9.7	4.3	0.1	7	54	39.2

¹ X₁, X₂, and X₃ represent different process variables which are temperature, time and catalyst loading, respectively.

² obtained by the difference

ANOVA results revealed that when compared to the time and temperature, the catalyst loading is statistically the most significant factor that influences the removal of oxygen during HDO. The model for calculating the oxygen content of biocrude is given in equation (5.3). Keeping all the terms, the coefficient of determination (R^2) calculated using design expert software for the final equation in terms of actual factors is 0.97, confirmed that the suggested

quadratic model could be able to investigate the effects of HDO process parameters on oxygen content of upgraded biocrude oil samples.

$$\text{Oxygen content (wt.\%)} = +284.76423 - 1.31740 * X_1 - 2.22776 * X_2 - 3.40568 * X_3 - 0.0096 X_1 X_2 + 0.0022 X_1 X_3 + 0.072 * X_2 X_3 + 0.001645267 X_1^2 + 1.00402 X_2^2 + 0.13139 * X_3^2$$

(6.3)

The lack of fit test is shown in Table 6.7, and as the P-value (0.0760) is higher than 0.05, means that lack of fit is insignificant, and the model is in a good fit with experimental data.

Table 6.7: ANOVA table obtained from response surface methodology

Source	Sum of Squares	df	Mean Square	F Value	P-Value
Model	238.18	9	25.84	31.17	<0.0001 (Significant)
X₁-Temperature	0.89	1	0.89	1.07	0.3369
X₂-time	0.54	1	1.26	1.51	0.4479
X₃- catalyst loading	25.58	1	25.58	30.85	0.0009
X₁X₂	2.88	1	2.88	3.44	0.1059
X₁X₃	2.42	1	2.42	2.89	0.1327
X₂X₃	1.62	1	1.62	1.94	0.2066
X₁²	102.83	1	102.83	122.97	<0.0001
X₂²	15.07	1	15.07	18.03	<0.0001
X₃²	65.66	1	65.66	78.52	0.0038
Residual	6.00	7	0.86		
Lack of fit	5.81	5	1.16	12.46	0.0760 (not significant)
Pure Error	0.19	2	0.093		
Core total	244.03	16			

Figure 6.7 shows the three-dimensional response surface of oxygen content (wt.%) available in upgraded biocrude oil at different reaction conditions (temperature, time and catalyst loading). It seems that increasing the time, temperature and catalyst loading lead to reduction of the oxygen content. Maximum reduction of oxygen (94%) was obtained at temperature of 400 °C, catalyst loading of 10 wt.%, and time of 2.75 h. Increasing temperature up to 400°C increased the

cracking of larger molecules, and kinetic energy of the reactant resulted in higher HDO rate, leading to higher oxygen removal. However, increasing the temperature more than 400°C leads to increase in the rate of secondary reactions such as cracking of light compounds and oligomerization/ polymerization (Ayodele and Daud, 2015). Increase in the catalyst loading up to 10 wt.% leads to reduction of oxygen content available in upgraded biocrude oil. However, increasing the catalyst loading above 10 wt.% increased the repolymerization of molecules leading to coke formation. Duan and Savage, (2011b) had studied the effect of process parameters (catalyst loading, time and temperature) on the algal biocrude oil treatment. Their results showed that the catalyst loading (using Mo_2C) was important for the oxygen content of upgraded biocrude oil. However, they reported that the type of the catalyst is a more important factor than catalyst loading and time for the chemical composition of treated oil.

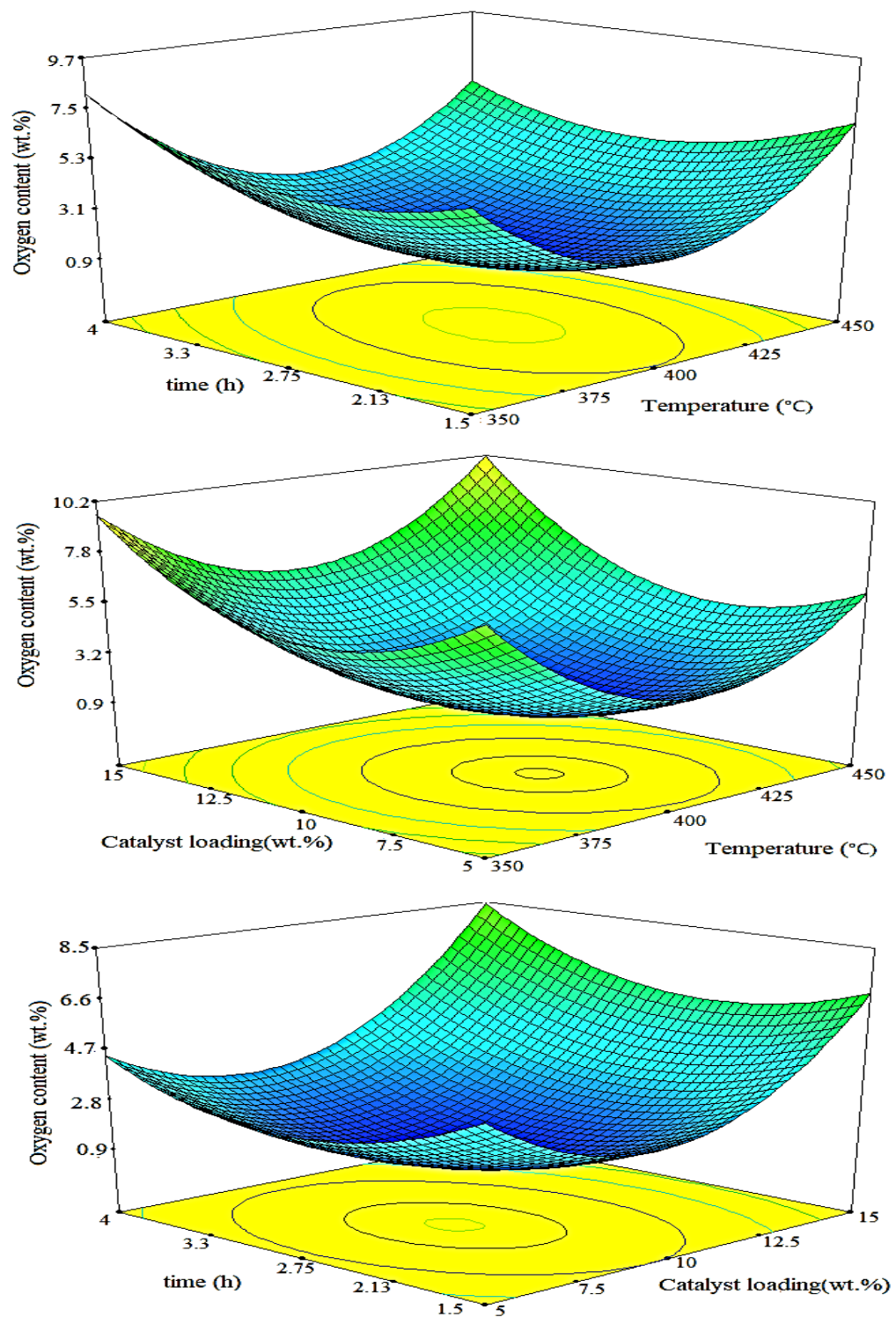


Figure 6.7: The response surface for oxygen content (wt.%)

6.5 Conclusions

In this study, catalytic hydrodeoxygenation of algal biocrude oil over novel hydrochar-based catalysts was investigated to produce renewable hydrocarbon biofuels. NiMo carbide supported activated carbon using co-impregnation method to synthesize the oxide phase and carbothermal reduction method, exhibited higher catalytic activity result in reduction of more oxygen content from oxygenated compounds. It can be related to its high pore size, high acidity and higher amount of active phase (Mo_2C) during reaction, as NiMoO_4 phase could be reduced easier. According to the response surface technology, the most significant factor affecting the oxygen removal during hydrodeoxygenation reaction was catalyst loading following by time and temperature. Also, the significant model was offered with $R^2=0.97$ to estimate the oxygen content of upgraded biocrude oil. At reaction condition of $T=400\text{ }^\circ\text{C}$, $t=2.75\text{ h}$ and 10 wt.% of catalyst loading, the maximum oxygen removal of 94% was achieved using NiMoC catalyst. Thus, two stage of HTL and catalytic HDO studied in this research could be a promising technology for production of high quality algal biofuels. It is recommended to perform more blending studies to find the optimum blending ratio of the algal upgraded oil with petroleum diesel.

The two stages of HTL and catalytic HDO over hydrochar-based catalysts for algal biofuels production were studied. The next phase is focused on technoeconomic analysis (TEA) and life cycle assessment (LCA) of the overall process of algal biofuels production to evaluate the feasibility of the developed technology.

Chapter 7: Techno-economic and life cycle analysis of algal biofuel production via hydrothermal liquefaction of microalgae in methanol-water system and catalytic hydrotreatment using hydrochar as a catalyst support

The content of this chapter is submitted to the journal of Biomass & Bioenergy to be reviewed and published as an original research article.

Contribution of the PhD candidate:

Experiments and simulation were designed in consultation with Dr. Ajay K. Dalai and executed by Shima Masoumi. Aspen plus simulation and Sima pro design were performed out by the student. The manuscript was drafted by Shima Masoumi with guidance and suggestions provided by Dr. Ajay K. Dalai.

Contribution of this chapter to overall PhD research:

The forth phase of the research is investigated in this chapter. Techno-economic analysis using Aspen plus simulation, also life cycle assessment using Sima pro software were employed to study the feasibility and greenhouse gas emission of HTL and HDO processes applied in two methods of utilizing hydrochar as a catalyst or through combustion to provide heat for overall process.

7.1 Abstract

The hydrochar, a byproduct of hydrothermal liquefaction (HTL) of algal biomass, was utilized through two methods; combustion and activation, to produce high quality activated carbon for its use as a support for nickel and molybdenum for hydrodeoxygenation (HDO) process for algal biofuels production. In this study, techno-economic analysis (TEA) and life cycle analysis (LCA) of algal biofuels production in a two stage process such as HTL and HDO were investigated. Aspen plus simulation and SimaPro software were used to analyze process economics and greenhouse gas (GHG) emissions. Microalgae at 200 dry metric tonnes/day was the basis for its

conversion to biocrude oil through hydrothermal liquefaction (HTL) in the methanol-water system followed by catalytic upgrading to produce biofuels. According to HTL experimental results, maximum biocrude oil yield of 57.8 wt.% was obtained at reaction conditions of $T=275^{\circ}\text{C}$, $P=11.5\text{ MPa}$ using microalgae-solvent mass ratio and methanol-water mass ratio of 1:5 and 3:1, respectively. Produced biocrude oil contained 14.5 wt.% of oxygen and HHV of 33.4 MJ/kg_{biocrude oil} which required upgrading to be utilized as a transportation fuel. The minimum fuel selling price (MFSP) for using method #2 (activation) was \$8.8/gal to breakeven the cost of operation, which was 15% lower than that from method #1. The GHG emissions performance was estimated at -1.13 gCO_{2-eq}/MJ indicating the significant GHG emissions reduction compared to petroleum-based fuels production (91 gCO_{2-eq}/MJ).

Keywords: Algal biofuels, Hydrothermal liquefaction, Hydroprocessing, Techno-economic analysis, Life cycle assessment

7.2 Introduction

In recent years, the increasing price of petroleum fuels and chemicals, the rapid increase in global energy demand, and its negative impact of the fossil fuel utilization on the environment due to greenhouse gas (GHG) emissions have led to an increase interest in finding renewable and sustainable alternatives of energy. Biomass is considered the most important renewable alternative with the high potential to replace petroleum transportation fuels (A R K Gollakota et al., 2018).

Of the biomass candidates, microalgae is considered as a third biofuel feedstock with no competition with food supplies. It is promising due to its ability to faster sequestration and conversion of CO₂ and water into biomass resulting in enhancing CO₂ mitigation and producing up to 30 times more oil per unit land mass compared to terrestrial biomass (Masoumi et al., 2020b).

Thermochemical processes such as hydrothermal gasification, hydrothermal liquefaction (HTL), and hydrothermal carbonization are more suitable for the conversion of wet feedstocks such as microalgae by eliminating the drying step. HTL process is considered the most promising technology for the production of high-quality biocrude oil from wet biomass and it requires process conditions of temperature range from 200 to 350 °C and pressure of 10-20 MPa with reaction time from 5 to 60 min (Han et al., 2019). Through this process, all the components in

microalgae (lipid, carbohydrate and protein) can convert to biocrude oil resulting in higher liquid yield. The use of co-solvent for the HTL process such as reactive organic solvents mixed with water at moderate reaction conditions has raised a lot of interest (Feng et al., 2018). Hydrochar as a by-product of HTL process can be utilized as a carbon-based catalyst/adsorbent leading to improve economics and feasibility of algal biofuels production (Masoumi and Dalai, 2020b).

Algal biocrude oil obtained from HTL process contains higher levels of heteroatoms such as oxygen and nitrogen compared to petroleum crude oil, up to 20 and 6 wt.%, respectively. Therefore, biocrude oil has undesired properties such as high viscosity and thermal instability which limit its applications (Biller et al., 2015). Consequently, the subsequent upgradation is required to decrease the level of heteroatoms and produce algal biofuels more similar to conventional hydrocarbon fuels. Of all the techniques used for upgrading of biocrude oil such as hydrodeoxygenation (HDO), hydrocracking, supercritical fluids treatment, HDO seems to be one of the most promising techniques for biocrude oil upgrading for fuel (Xu et al., 2018).

The main challenge regarding the commercialization of algal biofuels production is economics. Techno-economic analysis (TEA) is considered the most useful and fundamental tool to determine the feasibility of the new process. Algal biofuels can be employed as one of the alternatives to reduce climate change, however, it has environmental impacts as well. Life cycle assessment (LCA) is the most useful and accepted method to determine and quantify these impacts. Many researchers have focused on economic analysis reporting the biofuels selling cost and life cycle assessment of algal biofuels that range between \$1.64-30/gal and -75-534 gCO_{2-eq}/MJ, respectively (Quinn and Davis, 2015). The variable results are due to various systems used for the cultivation of algae, different reaction pathways, product distributions and handling the byproduct utilization.

Pankratz et al., 2020 studied the environmental performances of HTL and pyrolysis of microalgae to produce diluents. The GHG emissions from HTL process were estimated at -5.9 and -11.5 gCO_{2-eq}/MJ using microalgae cultivation through photobioreactor and open race pond technology, respectively. GHG emissions through pyrolysis were estimated at 45.65 and 40.05 gCO_{2-eq}/MJ for microalgae cultivation method of photobioreactor and open race pond, respectively. DeRose et al., 2019 studied the economic viability of two pathways of biochemical and thermochemical conversion of modeled low lipid algae to produce economically viable biofuels. Results from TEA showed MFSP of \$12.85/gal and \$10.41/gal for the biochemical and

thermal-chemical pathways, respectively. In addition, their study demonstrated that MFSP could be reduced by reducing ash content, biomass feedstock cost and improving HTL fuel yields.

Gu et al., 2020 studied the two different reaction pathways for the HTL process; two-stage sequential hydrothermal liquefaction (SEQHTL) and one-stage direct hydrothermal liquefaction (DHTL). Their results showed that compared to DHTL, SEQHTL facilitates the production of co-products and biocrude oil at less severe reaction conditions. Also, compared to DHTL with MSFP of \$8.07/gal, SEQHTL revealed lower MFSP of \$6.19/gal. Zhu et al., 2019, evaluated three aqueous phase treatment; direct recycle to the algae farm, catalytic hydrothermal gasification and anaerobic digestion. In this study, *Chlorella* sp. with a feed rate of 170 MT/d under HTL process temperature and pressure of 350 °C and 21 MPa were selected. Direct recycle had the lowest MFSP of \$12.5/gal, compared to two other cases. Xin et al., 2016 studied the techno-economic analysis of algal biofuels production using wastewater- based algal feedstock and they reported the minimum fuel selling price (MFSP) of \$2.23/gal.

In this study, a techno-economic analysis including sensitivity analysis of algal biofuels production through two stages of non-catalytic HTL in the methanol-water co-solvent system and catalytic hydroprocessing was investigated. For the first time, two different scenarios were investigated to study the effects of two methods (activation and combustion) to utilize hydrochar as a byproduct. The goal of this study is to compare the performances of two different methods of by-products utilization and to determine the economics of algal biofuels production process. These methods were studied to identify the promising production pathway to achieve commercial feasibility. Aspen plus simulation was applied based on laboratory research results to develop the TEA model for their consideration of the feasibility and economics of this process. In addition, life cycle analysis (LCA) was used to determine greenhouse gas (GHG) emissions and environmental impact in the case of utilizing hydrochar as a by-product through chemical activation and combustion methods.

7.3 Materials and Methods

A process simulation model for algal biocrude oil and its upgrading through the hydrotreating process was developed using Aspen Plus[®] according to experimental data. In the first step, algal biocrude oil and hydrochar obtained from hydrothermal liquefaction of microalgae in the methanol-water system were simulated and their techno-economic performance was assessed. In the next step, the two methods, i.e. method #1; combustion and method #2 i.e. chemical

activation were used to utilize hydrochar as a by-product of HTL process to determine the effects of by-product treatment on energy-saving and overall process economic. In the following subsection, the details on these two methods are provided. Also, the process simulation for biocrude oil upgradation by hydrodeoxygenation was developed. As mentioned above, the purpose and focus of this study are related to the conversion of microalgae to fuel. The simulation and cost related to the algae growth and its harvesting are not investigated. Finally, the life cycle assessment and GHG emissions performance were evaluated

7.3.1 Algal feedstock

According to the literature related to the economic analysis and viability of algal derived biofuels, the cost of algal feedstock is one of the most important variables for the overall economics. The cost of algae feedstock for the traditional cultivation system in open raceway ponds (ORP) varies in range from \$445 to \$3711 per ash-free dry weight tonnes. Photobioreactors (PBR) system is considered as an alternative cultivation system. However, both technologies impact the algae production, lipid content and extraction cost (DeRose et al., 2019). There are still challenges to provide resource requirements including water, CO₂, and nutrient. Consequently, wastewater-based algal systems have received much attention recently. This system is designed to treat wastewater and at the same time, provides nutrient needs to grow microalgae (such as C, N, and P). In the countries like Canada with cold climate condition, using ORP system to cultivate the algae feedstock is limited to a short period of time when the suitable conditions (temperature and light) for algae growth can be provided. Pankratz et al. (Pankratz et al., 2019) developed the cost models of algae production in a cold climate using OPR and PBR systems. The minimum biomass selling price (MBSP) for algae cultivation at the same site was \$1288 tonne⁻¹, and \$550 tonne⁻¹, for the OPR and PBR systems, respectively.

In terms of modeling the biomass in Aspen Plus[®], microalgae is defined as a non-conventional solid, which requires characterization of its properties such as enthalpy and density. These properties are calculated based on the ultimate and proximate analysis given in Table 7.1.

Table 7.1: Proximate and ultimate analyses of microalgae

Proximate analysis	(wt.%)	Ultimate analysis	(wt.%)	Higher heating value	(MJ/kg)
Fixed carbon	15.4	Carbon	50.2	(HHV)	21.2
Volatiles	73.4	Hydrogen	6.8		
Moisture	4.5	Nitrogen	7.2		
Ash content	6.7	Sulphur	0.8		
		Oxygen*	35		

*Calculated by difference

7.3.2 Process overview

The algal biofuels production includes three main sections: microalgae cultivation (which is not included in this study), a thermochemical conversion, which is the HTL process, and upgrading of biocrude oil obtain from HTL, which is hydrodeoxygenation (HDO) process (please see Figure 7.1). Through HTL, microalgae is converted to three phases of products: liquid which includes biocrude oil, solid (called hydrochar) and gas. Solvent (mixture of methanol and water) was used for the hydrothermal process as a reaction medium. To improve the overall economics of biocrude oil production, utilization of hydrochar as a by-product of HTL could be beneficial.

In this study, two methods were considered to utilize hydrochar; method #1 involves heat generation for HTL process by using furnace as a combustion chamber and method #2 is related to the production of AC through chemical activation of hydrochar, which can be used as a catalyst/ catalyst support to upgrade the biocrude oil. Due to the high amount of heteroatoms present in biocrude oil, it needs to be upgraded through hydrodeoxygenation to remove oxygen and increase the higher heating value of the final product. The vented gas contains large amount of hydrogen, which can be separated and recycled for upgrading section.

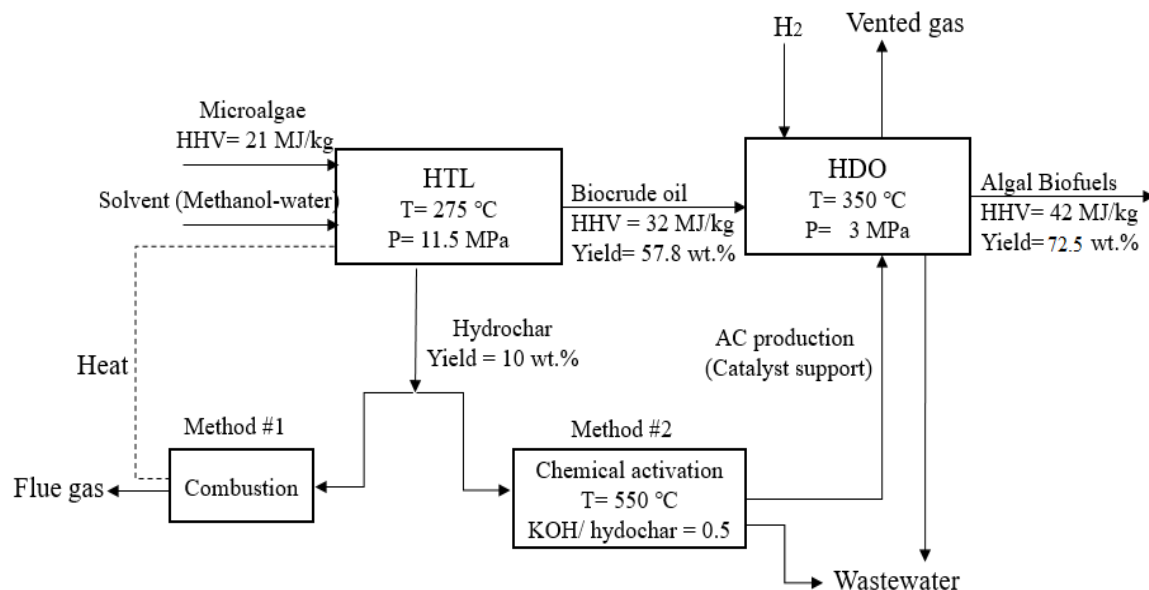


Figure 7.1: Process flow diagram of algal biofuels production

7.3.3 Hydrothermal liquefaction process

Generally, hydrothermal liquefaction process (HTL) is carried out in a hot compressed water system with temperature ranges from 200-370 °C and pressure of 4-20 MPa for 10-60 min in sub to supercritical conditions with or without the presence of catalysts (Masoumi et al., 2020b). In our HTL process, the impacts of different mass ratios of methanol-water and different reaction conditions (up to maximum temperature and pressure of 500 °C and 34.4 MPa) were studied in a 100 mL stainless steel autoclave. Design expert software was used to study the effects of key process parameters (temperature, time and solvent mass ratio) at sub to supercritical conditions. In this study, methanol was introduced along with water to take advantage of using it as a reactive organic co-solvent through the HTL process (Feng et al., 2018; Han et al., 2019). As the critical temperature and pressure of alcohol are less than water due to its lower polarity, it resulted in less severe reaction conditions. In addition, as lipid present in microalgae is more soluble in methanol, the biocrude oil yield and the amount of biodiesel-like product was increased.

First, the effects of methanol-water mass ratio in critical condition system were investigated and the higher yield of biocrude oil (47 wt.%) was obtained at the methanol-water mass ratio of 0.75:0.25. Compared to pure water as a solvent, the yield of biocrude oil was higher and its

quality was better due to higher amount of ester components according to the results of GC-MS and NMR.

In the next step, the effects of temperature and time at a constant pressure of 11.5 MPa at the mass ratio of microalgae to solvent and methanol to water of 1:5 and 0.75:0.25, respectively, were investigated. The optimum biocrude oil yield (57.8 wt.%) and highest energy recovery (85.3 %) were obtained with 75 wt.% of methanol in water at 272°C and reaction time of 35 min. The process conditions used for simulation and the optimum product yield are given in Table 7.2. The overall yield of products was calculated based on the mass of the final product with respect to the mass of dry microalgae.

Table 7.2: HTL process conditions and products yield

Microalgae-solvent mass ratio	1:5
Methanol-water mass ratio	0.75:0.25
Catalyst	-
Temperature, °C	275
Pressure, MPa	11.5
HHV of Biocrude oil, MJ/kg	31.8
Biocrude oil yield, wt.%	57.8
Hydrochar yield, wt.%	10
Gas yield, wt.%	16.1

7.3.4 Utilization of hydrochar

Hydrochar is a by-product of HTL process and can be utilized as a catalyst/catalyst support or as an energy source for an economically viable process. In this study, two different methods; method #1: combustion process and method #2: chemical activation process were investigated. In method #1, Combustion of hydrochar as a by-product solid fuels, results in heat generation for HTL process and the increase in the sustainability of energy production. For HTL at the reaction temperature of 275 °C, hydrochar can be considered as a solid fuel. According to the literature (Mau and Gross, 2018), hydrochar can potentially replace coal for the generation of electricity resulting in significant decrease in greenhouse gas emissions. Hydrochar produced at a reaction temperature of >250 °C, has high energy density, which leads to higher energy

generation. Generally, the main gaseous emission during the combustion of hydrochar is CO₂, while several other gases are emitted including CO, CH₄, NO, and NH₃ (Tsukahara and Sawayama, 2005).

Recently, high cost of production of carbon materials such as activated carbon using non-renewable petroleum precursors as well as their environmental issues have received much attention. So, global demand for the production of carbon materials using alternative environmentally friendly sources has increased with an annual rate of 10.3 % (Masoumi and Dalai, 2020b; Namazi et al., 2016).

Hydrochar has received much attention because its feedstock is abundantly available, renewable and inexpensive. The other advantages of utilizing of bio/hydrochar for production of the carbon materials can be related to the future concerns such as CO₂ emission reduction, pollution control, sustainable land use, and energy storage (Mau and Gross, 2018). However, hydrochar has a low surface area and porosity due to the formation of hydrocarbons on the surface, which hinders its application as contaminant adsorbents and catalysts/catalysts support (Masoumi and Dalai, 2020b). The physicochemical properties of hydrochar and its porous structure characteristics can be improved by using various modification methods including surface functionalization and physical or chemical activation. Hydrochar contains surface functional groups and can be very effective for bio/hydrochar functionalization such as sulfonating or metal dispersion for catalysis applications. Chemical activation is carried out over the impregnation of bio/hydrochar with one or a mixture of chemical agent (s) followed by the activation process in a fixed-bed reactor under the nitrogen flow rate. Zinc chloride (ZnCl₂), phosphoric acid (H₃PO₄), sodium hydroxide (NaOH), potassium carbonate (K₂CO₃) and potassium hydroxide (KOH) are the most used chemical activating agents for the chemical activation process. Physical or thermal activation can be done through gasification with reactive steam, CO₂ or a mixture of steam and CO₂ as an oxidizing agent. A lot of studies have shown that use of KOH as an activation agent can increase the porosity and specific surface area up to 3000 m²/g (Cao et al., 2017; Khan et al., 2019)

In our previous work, the effects of activation temperature, mass ratios of KOH and hydrochar and nitrogen flow rate on the specific surface area were investigated (Masoumi and Dalai, 2020b). In this study, produced AC with specific surface area of 800 m²/g and production yield of 67.3 wt.% at activation temperature of 550 °C, KOH/hydrochar mass ratio of 0.5 and

nitrogen flow rate of 80 cm³/min, was utilized as catalyst support for hydro treating of biocrude oil.

7.3.5 Hydrotreating process description

Biocrude oil obtained from HTL contains large amount of oxygen and cannot be used as transportation fuel due to its undesired properties such as high viscosity and corrosiveness, low heating value, thermal and chemical instability. Therefore, biocrude oil needs to be upgraded to meet the requirements of transportation liquid fuels. Hydrodeoxygenation (HDO) is considered as the most promising technique for the upgrading of biocrude oil to enhance the quality of biocrude oil with decrease in oxygen content and an increase in heating value.

This upgradation techniques typically occurs at high temperature and pressure range of 250- 450 °C and 0.75-30 MPa, respectively, in the presence of a catalyst. HDO reactions were performed in a Parr reactor (100 ml stainless steel autoclave). The impacts of different reaction conditions such as reaction temperature, time and catalysts loading on quality and yield of upgraded biofuel were studied. The reactor was loaded with algal biocrude oil and desired amount of catalyst, and was pressured with hydrogen up to 3 MPa, and heated to 350-450 °C with a heating rate of 5 °C while stirring at 500 rpm, for reaction time of 2-6 h. More information can be found in our previous study (Masoumi and Dalai, 2021). For the simulation purposes, the optimum conditions used for HDO as well as the yield of upgraded biofuel are presented in Table 7.3. Chemically prepared activated carbon using KOH as a chemical agent as discussed in section 7.3.4 was used as catalyst support. As noble metals are costly and rare, their application is limited, although, they show high activity for HDO. Recently, transition metal carbide, due to its high thermal stability and tenable electronic structure, have shown high catalytic activity (Smirnov et al., 2017). In this study, the carbide phase of activated algal derived hydrochar-supported NiMo was used as a catalyst for upgrading of algal biocrude oil using HDO.

Table 7.3: Major inputs and products for HDO system

Catalyst	NiMo/ AC
Catalyst loading, wt. %	5
Temperature, °C	350
Pressure, MPa	3
upgraded oil to microalgae yield, wt. %	41.9
Upgraded oil to biocrude oil yield, wt. %	72.5
Higher heating value of upgraded oil, MJ/kg	42
Oxygen content, wt. %	3.1
Water soluble compounds, wt. %	7.5
Density, kg/L	0.75

7.3.6 Economic evaluation

In this study, fixed capital investment (FCI) and total capital investment (TCI) were estimated using Lang factor based on installed equipment costs, which are given in Table 7.4, besides the cost parameters used for economic analysis of algal biofuels production. The Lang factor of 5.04 for FCI and capital charge of 12% of FCI were considered to calculate total production cost using an interest rate of 10% and a project life of 20 years.

The plant was assumed to operate for 8000 hours per year (i.e. 24 hours per day during 333 days per year, remaining 32 days for maintenance tasks) on a three eight-hour shifts cycle. In this plant, 25 people were employed contributing to the cost of operating labor and supervisor. The hourly wage rate usually depends on the time and place, however, the typical U.S. rate of \$12/h was assumed. Also, in this study, all of the expenses regarding hydrogen plant to provide required hydrogen for HDO reactions was not considered.

7.3.7 Life cycle assessment (LCA)

Figure 7.2, shows the steps taken for algal biofuel production, which includes all the algae cultivation and collection, transportation of prepared raw material, production of algal biocrude oil using HTL process, production of algal biofuels using HDO process over catalysts obtained from hydrochar as a by-product of HTL. Finally, transportation of algal biofuels was considered for the production of synthetic transportation fuel.

Table 7.4: Cost parameters and assumptions for economic analysis of algal biofuels production

Plant life	10 years
Internal rate of return	10%
Operating hours per year	8000
Lang factor	5.04 for FCI
Working capital cost	15% of FCI
Operating labor	\$24000/year per employee
Supervisory and clerical labor	15% of labor cost
Maintenance and repairs	6% of FCI
Operating supplies	15% of maintenance and repairs
Local taxes	1% of FCI
Insurance	1% of FCI
Overhead (payroll and packaging, storage)	60% of (operating labor, supervision and maintenance)
Capital charge	12% of FCI
Depreciation	10% of FCI
Administrative cost	25% of overhead
Distribution and selling costs	10% of total expenses
Research and development	5% of total expenses
Raw materials	
Microalgae	\$550/tonnes
Solvent	\$300/tonnes
KOH	\$280/tonnes
Combustion gas	\$170/tonnes
Catalyst	
Activated carbon	\$3000/tonnes
Nickel(II) nitrate hexahydrate	\$10000/tonnes
Ammonium molybdate tetrahydrate	\$20000/tonnes
Utilities	
Electricity	\$180/MWh
Cooling water	\$1/MWh
Wastewater treatment	\$300/ton

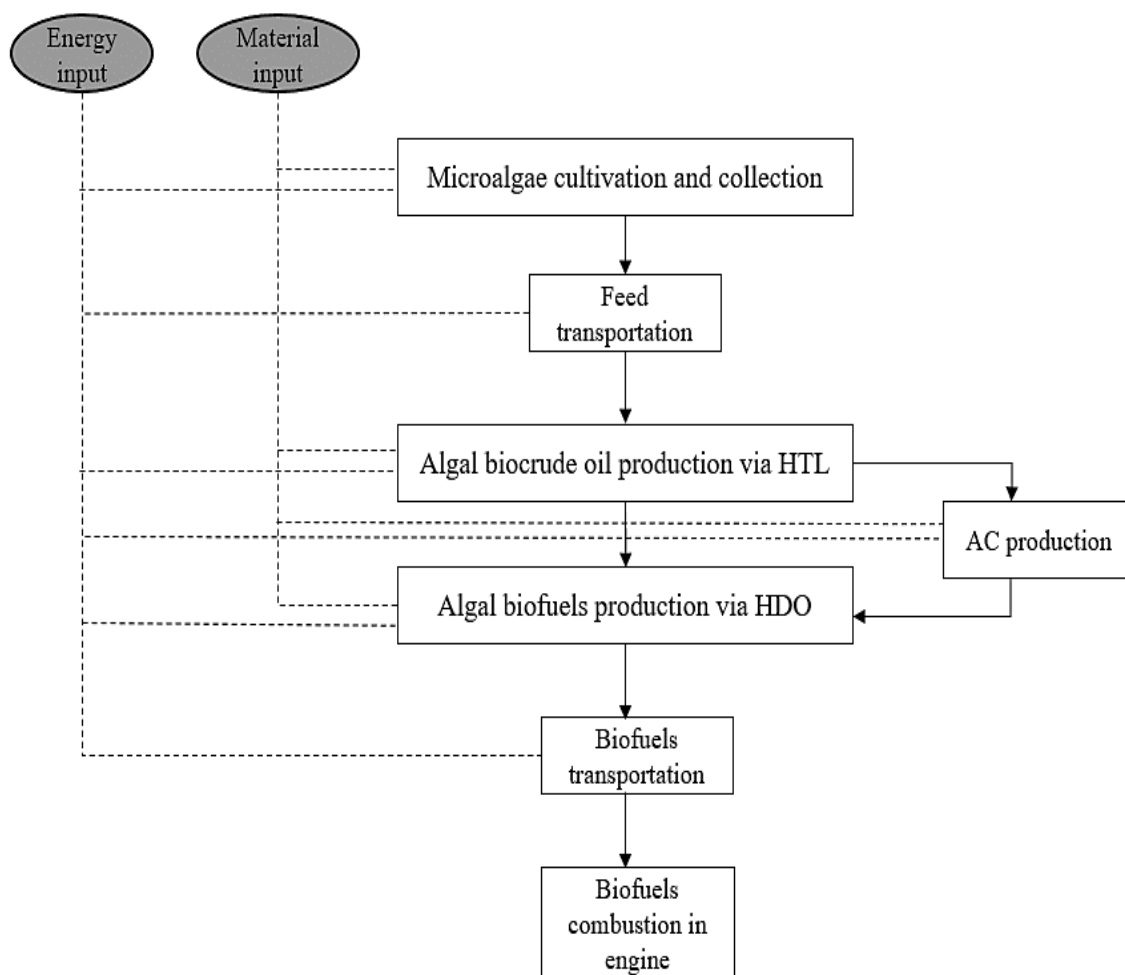


Figure 7.2: Schematic block diagram for LCA of algal biofuels

7.4 Results and discussion

7.4.1 Techno-economic analysis of algal biocrude oil production

The process flow diagram for HTL of microalgae in the methanol-water system is shown in Figure 7.3. The Predictive Soave-Redlich-Kwang (PSRK) and IDEAL model were selected as suitable methods to predict the thermodynamic properties of conventional components. Microalgae on the basis of 200 tonnes/day was used for all the calculations and was defined as a nonconventional component using HCOALGEN and DCOALIGT/DCHARIGT through

product gas was carefully sampled into Tedlar bags via a control valve and subsequently analyzed, which resulted in 91.6 wt.% of CO₂ and 7.1wt.% of CH₄. To obtain the light gases with high recovery fraction, they were separated in a flash drum at 60 °C and 1 atm.

Table 7.5: Main components used to represent biocrude oil

Functional group	Representative compound(s)	Yield (wt.%)
Aliphatic	Octadecanoic acid (C ₁₈ H ₃₆ O ₂)	8.2
	Hexadecanoic acid (C ₁₆ H ₃₂ O ₂)	9.1
	Recinoleic acid (C ₁₈ H ₃₄ O ₃)	6.9
Aromatic	Cholesteryl Benzoate (C ₃₄ H ₅₀ O ₂)	15.3
Alcohols	Oleyl alcohol (C ₁₈ H ₃₆ O ₂)	8.4
Phenols	Bisphenol (C ₁₅ H ₁₆ O ₂)	5.8
Furan	Dibenzofuran (C ₁₂ H ₈ O)	4.1

7.4.1.1 Utilization of hydrochar as a by-product of HTL

As discussed earlier, the solid residues called hydrochar are considered as a by-product of HTL. To be economically viable, in addition to algal biocrude oil and biofuels production, algal biorefineries will require to utilize the produced by-products (Mau and Gross, 2018; Sills et al., 2020). In this study, hydrochar was utilized through (1) combustion to generate heat for the HTL process and (2) chemical activation to produce highly porous activated carbon used as catalyst support, which are shown in Fig. 7.4 and 7.5, respectively.

According to Figure 7.4, hydrochar, which was removed from the reactor with solid separator, was fed to the furnace for combustion and heat generation. In this simulation, the adiabatic furnace was used to operate at a temperature of 550 °C and to achieve the complete combustion. For this, airflow with 5 wt.% of excess oxygen was used. All generated heat was transferred to the HTL reactor and the flue gas generated contained only carbon dioxide. The generated heat was used to provide the energy to meet the desired temperature of 275 °C in the HTL reactor.

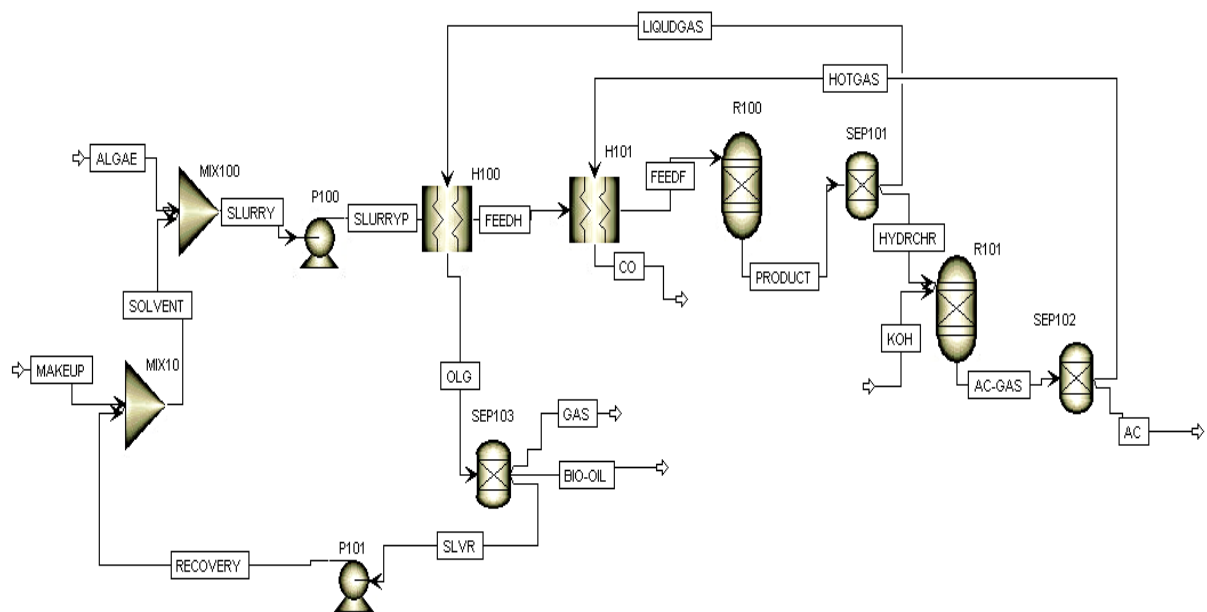


Figure 7.5: HTL process and utilization of hydrochar through chemical activation

The results of economic analysis for biocrude oil production and the utilization of hydrochar through methods #1 and #2 are summarized in Table 7.7. Total equipment cost was calculated using simulation of HTL and HDO processes, results in 10.25 and 10.01 \$M for method #1 and #2, respectively. Fixed and total capital investment were calculated using total equipment cost and Lang factor of 5.04 for each method. There is extra cost for gas consumption in furnace through combustion for method #1, providing chemical agent (KOH) and wastewater treatment after acid washing to produce highly porous activated carbon for method #2. Also, by-product credits was considered for method #2, due to production of highly porous activated carbon used as a catalyst support for HDO process. Regarding consumption of cooling water, electricity for method #1, the amount of 15, 3.2 MW and for method #2, the amount of 15 and 2.6 MW were considered.

7.4.2 Techno-economic evaluation of algal biofuel production

The carbide phase of activated carbon-supported NiMo was used as a heterogeneous catalyst for HDO reactions. The amounts of Ni and Mo in the heterogeneous catalyst were 3.5 and 13 wt.%, respectively. The reactions for HDO of biocrude oil are given in Table 7.6.

Table 7.6: Hydrodeoxygenation reactions based on model compounds

Functional group	Assumed reaction
Aliphatic	$C_{18}H_{36}O_2 + 2H_2 \rightarrow C_{18}H_{36} + 2H_2O$
	$C_{16}H_{32}O_2 + 2H_2 \rightarrow C_{16}H_{32} + 2H_2O$
	$C_{18}H_{34}O_3 + 3H_2 \rightarrow C_{18}H_{34} + 3H_2O$
Aromatic	$C_{34}H_{50}O_2 + 2H_2 \rightarrow C_{34}H_{50} + 2H_2O$
Alcohols	$C_{18}H_{36}O_2 + 2H_2 \rightarrow C_{18}H_{36} + 2H_2O$
Phenols	$C_{15}H_{16}O_2 + 2H_2 \rightarrow C_{15}H_{16} + 2H_2O$
Furan	$C_{12}H_8O + H_2 \rightarrow C_{12}H_8 + H_2O$

Some of the main oxygenate compounds (such as Octadecanoic acid, Hexadecanoic acid, ...) produced through HTL of algae which already used for describing biocrude oil were considered for hydrodeoxygenation reaction (such as Octadecane, Hexadecane, ...).

The process flow diagram for algal biocrude oil through hydrodeoxygenation (HDO) is shown in Figure 7.6. A single hydrodeoxygenation unit was used for obtaining the experimental data and hence for process simulation. In addition, a Stoichiometric reactor (RStoic) was used to model the HDO reactor, operating at constant temperature and pressure of 350 °C and 13 MPa, respectively. The hydrogen required for the hydrodeoxygenation reactor was 23 moles/kg of biocrude oil.

The reactor products were depressurized, cooled down and separated into a gas, liquid phase and solid phase. The removed gas contained mostly unreacted hydrogen, which can be recovered to the hydrotreating reactor.

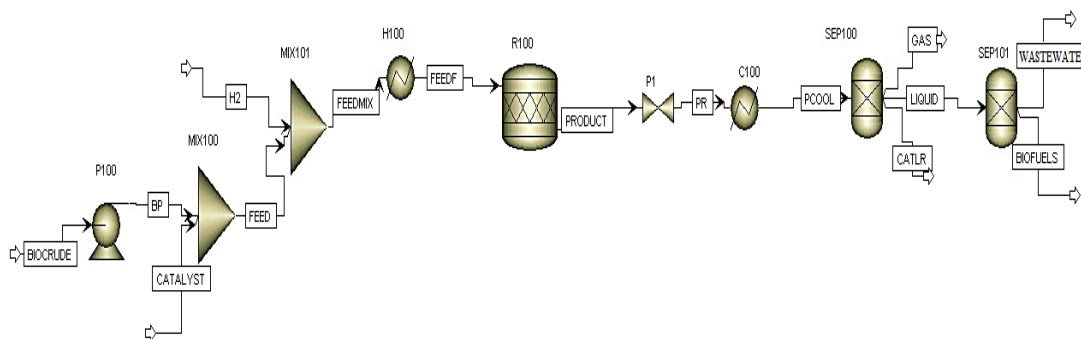


Figure 7.6: HDO process simulation with Aspen plus

Based on laboratory data, the composition of the gas product was calculated using GC after sampling the product. This resulted in 92 wt.% of hydrogen and 2 wt.% of methane and the rest contained small amounts of ethane, ethylene, propane, propylene, butane, and CO₂. Based on the reactions that occurred through HDO, a significant amount of water was generated, which can be recycled back through the separation unit. The results of economic analysis based on the simulated data in terms of total equipment cost for biofuels production through hydrotreating, are given in Table 7.7. In this table, the unit conversion of 0.26 is used to convert L to gal.

As it was mentioned before, the plant capacity was estimated to be 200 tonnes/day of dry microalgae which considering the yield of biocrude oil (57.8 wt.%) and biofuels (72.5 wt.%), results in biofuels production of 83.81 tonnes/day. According to Table 7.7, the total production costs for biofuels production varied due to hydrochar utilization. It was concluded that hydrochar activation to produce highly porous activated carbon as catalysts support for the hydrotreating process resulted in lowering total production cost (\$3083/t) due to providing valuable by-product credits compared to that used (\$3505/t) for combustion thus improving the overall economics of algal biofuel production. MFSP for algal biofuels production using method #2, is 8.8 \$/gal, which is 14% lower than method #1 with MFSP of 10.1 \$/gal.

Table 7.7: Comparison of total production costs for algal biofuel production

Parameter, units	Method #1	Method #2
Equipment cost, \$M		
HTL plant	8.6	8.36
HDO plant	1.65	1.65
Total equipment cost, \$M	10.25	10.01
Fixed capital investment, \$M	51.66	50.45
Working capital, \$M	7.74	7.56
Total capital investment, \$M	59.4	58.01
Production costs, \$M		
Microalgae feedstock	36.6	
Gas consumption in Furnace	0.51	-
Electricity	4.71	3.82
Cooling water	0.12	0.12
Wastewater treatment	0.8	2.7
By-product credits	-	-10.8
Solvents	8.2	8.2
Chemical agent	-	0.9
Catalysts	10.6	10.6
Operating labor and supervisory	0.7	0.7
Maintenance and repair	3.1	3.0
Operating supplies	0.46	0.45
Local taxes	0.51	0.5
Insurance	0.51	0.5
Overhead(payroll and packaging, storage)	2.3	2.3
Capital charge	7.1	6.9
Depreciation	5.9	5.8
Administrative cost	0.57	0.57
Distribution and selling costs	9.7	8.5
Research development	4.9	4.2
Total production costs, \$M/y	97.29	85.56
MFSP, \$/t	3486.1	3065.7
MFSP, \$/L	2.6	2.2
MFSP, \$/gal	10.1	8.8

7.4.3 Discounted cash flow analysis

The plot of cumulative discounted cash flow versus the years of plant operation is given in Figure 7.7, which provides the profitability criteria of discounted cash flow rate of return (DCFROR), net present value (NPV), discounted break-even point (DBEP) and payback period (PBP). In this study, the plant is constructed in one year with investment of 58.01 \$M (fixed capital cost of 50.45 \$M + working capital cost of 7.56 M\$) and annual sell income is projected to be 100 \$M, except for the first year which is 80 \$M. For this study DCFROR is 23%, greater than the internal discount rate, which means the project is profitable. Also, payback period (PBP) and discounted break- even point (DBEP) are 3.5 years and 6 years, respectively.

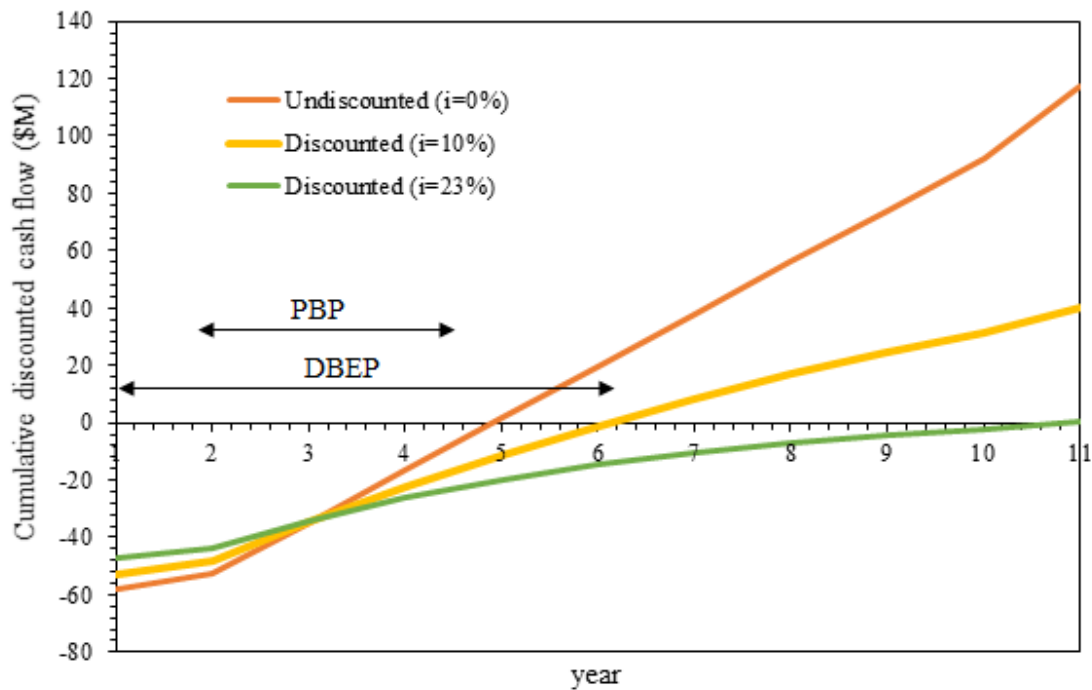


Figure 7.7: Cash flow diagram for algal biofuels production plant

7.4.4 Sensitivity analysis

Feedstock cost and fuel yield were recognized as the crucial parameters to which MFSP is most sensitive (Gu et al., 2020; Ou et al., 2015). Obviously, as the yield of biofuels produced through HTL and HDO process increases, the MFSP will decrease. Ou et al. (Ou et al., 2015)

investigated the impact of fuel yield on MFSP. Their results showed that a 20% increase on fuel yield resulted in lowering of approximately 19.3% in fuels selling price.

Regarding the feedstock cost, Albrecht et al., 2016 studied the TEA of biofuels production through HTL and catalytic hydrotreating of microalgae. Their results showed that the feedstock price affects significantly MFSP in a way that by changing the feedstock price from \$0 to \$1200/ton, MFSP varies from \$3.5 to \$22/ gal. Davis et al., 2014 studied the TEA and LCA of combined system of algal cultivation and process conversion to produce liquid fuels. Their results showed that seasonal variation in algal growth could impact on the price and consequently change the MFSP in the range of \$10.7/gal and \$14.1/gal.

In this study, sensitivity analysis was employed to determine how changes to the most important input factor affect the MFSP. The algae production system was not modeled and the algae feedstock cost used for calculation of MFSP, was obtained from the model developed by Pankratz (Pankratz et al., 2019). They modeled a photobioreactor (PBR) cultivation system located at a site near Fort Saskatchewan, a northern city in the province of Alberta, Canada. Their results showed that algae production has a minimum biomass selling price (MBSP) of \$550 T⁻¹.

This study only focused on the conversion of microalgae to biofuels through hydrothermal liquefaction followed by catalytic hydroprocessing. The process conditions and results of the products yield used for simulation were obtained based on the optimum conditions of laboratory data. As discussed in section 7.3.1, algae feedstock cost is considered as one of the most significant factor to determine the fuels selling price. In order to analyze its impact on the overall economic performance of algal biofuel production and fuel selling price, this parameter was varied in the range of $\pm 50\%$ and the results was shown in Figure 7.8.

Considering method #2, which showed lower MFSP compared to method #1, due to the utilization of hydrochar as catalyst support and also providing heat for final feed before feeding to the reactor, if the cost of algal feedstock reduces by 50% ,the MFSP decreases to 6.51 \$/gal. Thus, a 50% decrease on algae feedstock price (from 550 to 275 \$/tonne), will result in approximately 27 % decrease on MFSP (please see Figure 7.7).

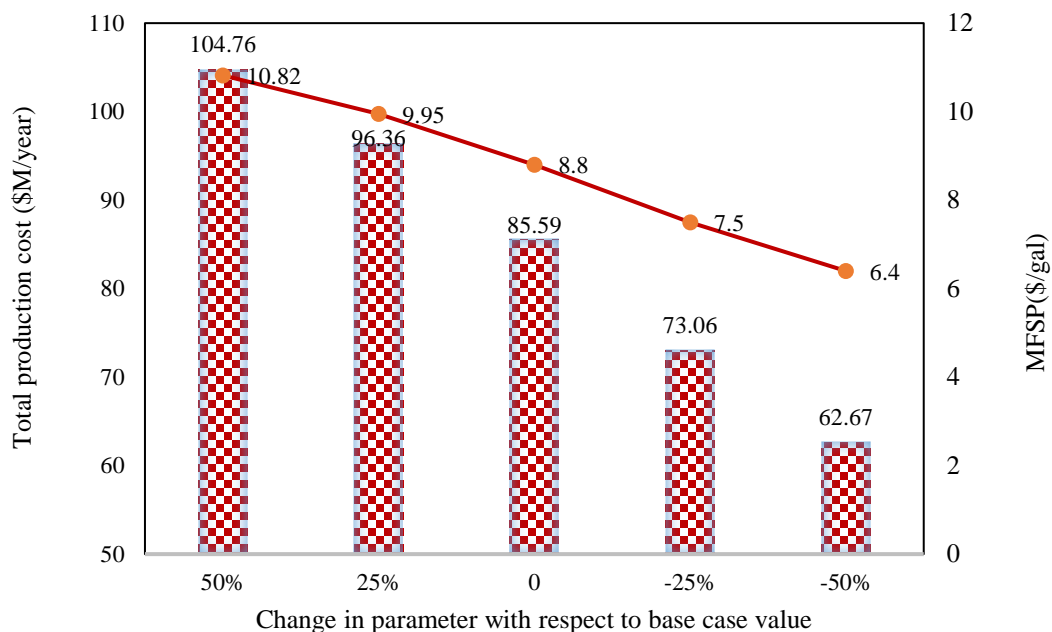


Figure 7.8: Effect of algae feedstock cost on total production cost and MFSP

7.4.5 Life cycle assessment for hydrochar utilization using two different methods

Life cycle assessment (LCA) of algal biofuels has been widely studied and due to the production of multiple products and by-products, different technologies and boundaries, the results varied (Quinn and Davis, 2015; Sills et al., 2020). In this study, two different methods (method #1; combustion and method #2; chemical activation of hydrochar) were employed for utilizing hydrochar as a by-product of the HTL process for LCA analysis. In this study, the effects of these methods resulted in different environmental impacts and climate change for algal biofuels production.

In the current LCA analysis, GHG emissions were used to compare the performances of these two methods utilizing the hydrochar along with algal biofuels production. The LCA was conducted based on the Global Warming Potential (GWP) characterization factor. The characterization factors per substance are identical to the IPCC 2007 GWP (100a) which contains the climate change factors of IPCC with a timeframe of 100 years. To quantify the GHG emissions related to two applied methods, a “cradle-to-gate” based-life cycle analysis was employed, in which the system boundary including all the steps from microalgae cultivation to algal biofuels production through HTL process and catalytic hydroprocessing.

The information concerning microalgae cultivation was obtained from the model developed by Pankratz et. al (Pankratz et al., 2020) which was based on the modeled growth of microalgae at Fort Saskatchewan and through consultation with industry experts for the cultivation of microalgae using National Research council of Canada (NRC) facilities located in Halifax, Nova Scotia. In the photobioreactor (PBR) system, CO₂ is injected along with the continuous mixing of media to exchange the nutrients. To optimize the growth of microalgae, lighting using LEDs were provided. 0.9 kg CO₂-eq/kg microalgae of GHG emission was estimated for the PBR system used to produce algal biomass. Since the production of 1 kg of algal biomass requires 1.8 kg of CO₂, 66,600 tonnes of microalgae resulted in sequestering of ~59,940 tonnes of CO₂ for algal biofuels production (51.13 g CO₂-eq/MJ).

In this analysis, it was assumed that the facilities used for cultivation of microalgae, and its conversion to biofuels through HTL and HDO reaction pathways are located near each other and the effects of transportation of raw materials and products are negligible. The energy and material requirements for microalgae production are assumed to be the same for both methods.

The main differences between the two methods used for biofuels production are due to the results in differences in hydrochar utilization and the production of activated carbon as a catalyst support for the HDO process. The overall process conditions, reactions, inputs and outputs used for method#1 and method #2, for production of biocrude oil through HTL, utilization of algal hydrochar as a by-product of HTL and production of algal biofuels were presented in sections 3.1 and 3.2 in detail. The mass balances of method#1 and method#2, were estimated using the results obtained from the process model in Aspen Plus®.

45.2 g CO₂-eq/MJ of GHG emission was estimated for method #1, which was lower than that (50 g CO₂-eq/MJ) obtained in method # 2. The GHG emissions from petroleum-based fuel products are about 91 g CO₂-eq/MJ, which are approximately 50% and 45% higher than those from method #1 and method #2, respectively.

As it can be seen in Fig 7.9, GHG emission for method#1 and method #2, were estimated at 1.9 and 2.1 KgCO₂-eq/Kgbiofuel, respectively. Based on higher heating value of biofuel (42 MJ/Kg), GHG emission for method #1 were calculated at 45.2 gCO₂-eq/MJ which was lower than that (50 gCO₂-eq/MJ) obtained in method # 2. The GHG emissions from petroleum-based fuel products are about 91 gCO₂-eq/MJ, which are approximately 50% and 45% higher than those from method #1 and method #2, respectively.

Considering all of the steps of cultivation of microalgae, production of biofuels and utilization of hydrochar through two different methods, the GHG emissions from method #1 and #2, were estimated at -5.93 and -1.13, respectively. It should be also noted that the results of this analysis are given with some level of uncertainties due to the system boundary, data used from literature and theoretical conditions, and also modeling approach.

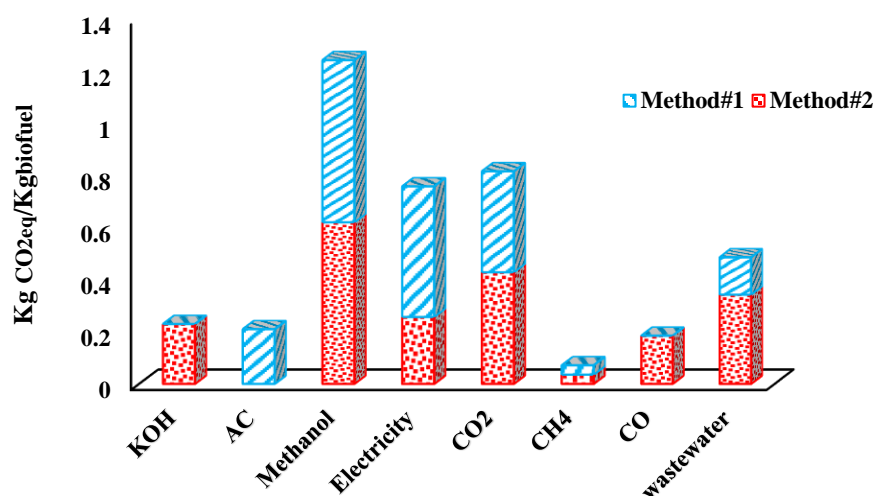


Figure 7.9: GHG emissions from method #1 and method #2

7.5 Conclusions

The comparative techno-economic analysis GHG emissions performance for algal biofuels production through two methods (method #1; combustion and method #2; chemical activation) to utilize hydrochar as a by-product of HTL process was studied. Based on experimental results, optimum reaction conditions of $T = 275\text{ }^{\circ}\text{C}$, $P = 11.5\text{ MPa}$ for production of maximum biocrude oil yield (57 wt.%) was selected. The algal biocrude oil has large amount of oxygen (14.5 wt.%), which required upgrading through hydrodeoxygenation process for transportation liquid fuels. Compared to method #1, with MFSP of \$10.1/gal, method # 2 resulted in lower MFSP of \$8.89/gal. In this method, hydrochar was utilized through chemical activation process to obtain activated carbon for catalyst support in hydrotreating of biocrude oil. The effects of different methods on climate change through algal biofuels production was investigated using LCA analysis. 45.2 g CO₂-eq/MJ of GHG emission was estimated for method #1, which was lower than that (50 g CO₂-eq/MJ) obtained with method # 2.

Chapter 8: Conclusions and Recommendations

8.1 Summary

Due to the environmental concerns and the lack of adequate renewable energy supply, finding a sustainable alternative source of energy has received much attention. Through this study, microalgae was used as a source of sustainable energy to produce liquid biofuels due to its high growth rate and the high CO₂ capture ability as compared to other biomasses. Hydrothermal liquefaction (HTL) process was employed as a promising technology to convert microalgae to high quality biocrude oil as a main product and hydrochar as a by-product. As suitable utilization of by-product such as hydrochar could improve the overall economics of algal biofuels production, hydrochar was activated through chemical activation process to produce highly porous activated carbon. The chemically produced activated carbon was impregnated with 3.5 wt.% Ni and 13 wt.% Mo and this material was reduced through carbothermal reduction method to produce NiMoC catalyst. Since algal biocrude oil from HTL process has higher amount of oxygenated compounds, it cannot be used directly as a transportation fuel and requires further upgradation to remove heteroatoms. Hydrodeoxygenation of algal biocrude over NiMoC catalyst was successfully carried out to remove oxygenated compounds and produce biofuels containing more hydrocarbons in the range of gasoline and diesel. One of the main challenges regarding the commercialization of algal biofuels production is economics. Techno-economic analysis (TEA) is considered the most useful and fundamental tool to determine the feasibility of a two-stage process of algal biofuels production. Both TEA and Life cycle assessment (LCA) were employed to determine and quantify the environmental impacts of the process. Overall conclusions drawn from this study are given in the following section.

8.2 Conclusions

The overall aim of this research was to aid the development of commercially feasible technology for the production of sustainable fuels from microalgae. Thus, the study focused on the production of biocrude oil from hydrothermal liquefaction of microalgae, and upgradation of biocrude oil using novel hydrochar-based catalysts through hydrodeoxygenation process.

Literature review helped to identify the knowledge gaps associated with this research. Based on the literature, moderate reaction conditions for the production of biocrude oil and highly

active catalysts for hydrodeoxygenation of biocrude oil were identified in a way to have the process economically feasible.

Thus, the production of high quality biocrude oil and hydrochar through hydrothermal liquefaction (HTL) process in sub- super critical condition using methanol-water co-solvent system was studied in Chapter 3. The effects of solvents, temperature and time on the yield and characteristics of biocrude oil and hydrochar were investigated. It was found that, compared to pure water, adding methanol as an organic reactive solvent with lower critical temperature and pressure, moderated the reaction conditions of HTL process, which helped the process with energy saving. Methanol-water co-solvent favored higher biocrude oil yield with lower nitrogen and oxygen contents as compared to pure water. The optimum yield of biocrude oil (57.8 wt.%) and highest energy recovery (85.3%) was obtained with 75 wt.% of methanol in water at 272 °C and reaction time of 35 min. The characteristic of hydrochar as a co-product of HTL process was studied to consider this as the potential support to produce novel heterogeneous catalysts for HDO process. The application of methanol as compared to water as solvent improved the thermal stability of hydrochar. Subcritical condition (temperature of 222 °C, pressure of 11.5 MPa) resulted in the highest hydrochar yield (19.5 wt.%).

Hydrochar revealed low specific surface area ($\leq 4 \text{ m}^2/\text{g}$) and low pore volume ($\leq 0.02 \text{ cm}^3/\text{g}$). In order to improve the physico-chemical properties of hydrochars such as BET surface area and porous structure characteristics, chemical activation was applied. Porous activated carbon was prepared from algal hydro-char using chemical activation method. The effects of different activation parameters as well as different chemical activators such as alkali hydroxides, carbonate, acid and mixture of alkali activators on prepared activated carbon were studied. Mesoporous activated carbon prepared from different activation conditions using potassium hydroxide as a chemical agent revealed high surface area up to $2100 \text{ m}^2/\text{g}$. Furthermore, hydro-char was activated by using different chemical activators under obtained optimum condition. Based on the optimum condition of temperature of 675 °C, KOH/algal hydrochar mass ration of 1.5 and nitrogen flow rate of $267 \text{ cm}^3/\text{min}$, using potassium carbonate as a chemical agent, highest BET surface area of $2638 \text{ m}^2/\text{g}$ was obtained, which also revealed micro pore and mesopore volume of 0.68 and $1.02 \text{ cm}^3/\text{g}$, respectively. The activated carbons obtained from different process conditions were physicochemically characterized by advanced structural chemistry tools, which showed that activated algal hydrochar is a low-cost carbon rich material

that revealed high surface area, and better porous structures thus making it suitable as a catalyst support.

Activated carbon with relatively high surface area of 800 m²/g and high yield of 67.5 wt.% as catalysts support, was prepared at moderate reaction condition (temperature of 550 °C, KOH/algal hydrochar mass ratio of 0.5 and nitrogen flow of 80 cm³/min.

NiMo carbide catalysts (13 wt.% Mo and 3.5 wt.%) were prepared in a two-step process involving sequential impregnation or co-impregnation of NiMo on activated carbon followed by carbonization through three different methods namely temperature-programmed reaction with 20%CH₄-80%H₂, carbothermal hydrogen reduction in H₂, and carbothermal reduction in N₂. The catalysts were screened for hydrodeoxygenation (HDO) of algal biocrude at various process conditions in a stirred tank reactor to produce liquid hydrocarbon fuels. The NiMo carbide synthesized through co-impregnation and carbothermal reduction in N₂ showed optimal activity for oxygen removal due to its high acidity and specific surface area and a greater amount of Mo₂C as active phases on the surface. At reaction condition of T=400 °C, t=2.75 h and 10 wt.% of catalyst loading, the maximum oxygen removal of 94% was achieved using NiMoC catalyst. Thus, two stage of HTL and catalytic HDO was found to be promising technology for production of high quality algal biofuels. Finally, technoeconomic analysis and life cycle assessment of overall HTL and HDO process were investigated. It was found that the minimum fuel selling price (MFSP) for two stages of algal biofuels production using hydrochar utilization as catalysts support was \$8.8/gal, which was 15% lower than the case study used hydrochar combustion to provide heat for the process. The effects of process conditions for biofuels production on the GHG emissions performance were estimated at 50 g CO_{2-eq}/MJ, which was 45 % lower than fossil fuel-based products.

8.3 Recommendations

For the future research work, it is recommended that:

- Different reactive organic compounds such as different alcohols or mixture of water and alcohols may be employed along with water for HTL process in co-solvent system.
- Different heterogeneous and homogenous catalysts can be evaluated for HTL process.
- The chemically prepared activated carbon can be obtained with different surface area based on different chemical activation condition, as a catalyst support which can have different physico-chemical properties.

- Different activation conditions and their impacts on the catalysts' activities and product selectivities could be investigated.
- Different amounts of active metal (Mo) and promoter (Ni) can be applied for synthesizing the catalysts for HDO process.
- Research on *in situ* characterization during HDO reactions can assist in predicting the behavior of these novel heterogeneous catalysts during HDO process.
- More experiments may be employed to focus and discuss on the hydrodenitrogenization (HDN) reactions.
- The spent catalyst can be characterized and regenerated for reusability study.
- The upgraded oil can be blended with petroleum diesel since its heating value is comparable to that of petroleum diesel, to find the optimum blending ratio.

Reference

- Abdelhafez, A. A., Abbas, M. H., & Li, J. (2017). Biochar: the black diamond for soil sustainability, contamination control and agricultural production. Engineering applications of biochar, 2.
- Adinata, D., Wan Daud, W.M.A., Aroua, M.K., 2007. Preparation and characterization of activated carbon from palm shell by chemical activation with K_2CO_3 . Bioresour. Technol. 98 (1), 145-149.
- Akia, M., Yazdani, F., Motaei, E., Han, D., Arandiyani, H., 2014. A review on conversion of biomass to biofuel by nanocatalysts. Biofuel Res. J.1 , 16-25.
- Albrecht, K.O., Zhu, Y., Schmidt, A.J., Billing, J.M., Hart, T.R., Jones, S.B., Maupin, G., Hallen, R., Ahrens, T., Anderson, D., 2016. Impact of heterotrophically stressed algae for biofuel production via hydrothermal liquefaction and catalytic hydrotreating in continuous-flow reactors. Algal Res. 14, 17-27.
- Anastasakis, K., Ross, A.B., 2011. Hydrothermal liquefaction of the brown macro-alga *Laminaria Saccharina*: Effect of reaction conditions on product distribution and composition. Bioresour. Technol. 102 (7), 4876-4883.
- Angin, D., Altintig, E., Köse, T.E., 2013. Influence of process parameters on the surface and chemical properties of activated carbon obtained from biochar by chemical activation. Bioresour. Technol. 148, 542-549.
- Añón, J.A.R., López, F.F., Castiñeiras, J.P., Ledo, J.P., Regueira, L.N., 1995. Calorific values and flammability for forest wastes during the seasons of the year. Bioresour. Technol. 52, 269–274.
- Anthonykutty, J.M., Linnekoski, J., Harlin, A., Lehtonen, J., 2015. Hydrotreating reactions of tall oils over commercial NiMo catalyst. Energy Sci. Eng. 3 (4), 286-299.
- Ao, W., Fu, J., Mao, X., Kang, Q., Ran, C., Liu, Y., Zhang, H., Gao, Z., Li, J., Liu, G., Dai, J., 2018. Microwave assisted preparation of activated carbon from biomass: A review. Renew. Sustain. Energy Rev. 92, 958-979.

- Ayinla, R.T., Dennis, J.O., Zaid, H.M., Sanusi, Y.K., Usman, F., Adebayo, L.L., 2019. A review of technical advances of recent palm bio-waste conversion to activated carbon for energy storage. *J. Clean. Prod.* 229, 1427-1442.
- Ayodele, O.B., Daud, W.M.A.W., 2015. Optimization of catalytic hydrodeoxygenation of oleic acid into biofuel using fluoroplatinum oxalate zeolite supported catalyst. *J. Taiwan Inst. Chem. Eng.* 47, 113-124.
- Azad, A.K., Rasul, M.G., Khan, M.M.K., Sharma, S.C., Hazrat, M.A., 2015. Prospect of biofuels as an alternative transport fuel in Australia. *Renew. Sustain. Energy Rev.* 43, 331–351.
- Azargohar, R., Dalai, A.K., 2008. Steam and KOH activation of biochar: Experimental and modeling studies. *Microporous Mesoporous Mater.* 110, 413-421.
- Ba, D., Boyaci, I.H., 2007. Modeling and optimization i: Usability of response surface methodology. *J. Food Eng.* 78 (3), 836-845.
- Bahadar, A., Bilal Khan, M., 2013. Progress in energy from microalgae: A review. *Renew. Sustain. Energy Rev.* 27, 128-148.
- Baskar, G., Aiswarya, R., 2016. Trends in catalytic production of biodiesel from various feedstocks. *Renew. Sustain. Energy Rev.* 57, 496–504.
- Basta, A.H., Lotfy, V.F., Hasanin, M.S., Trens, P., El-Saied, H., 2019. Efficient treatment of rice byproducts for preparing high-performance activated carbons. *J. Clean. Prod.* 207, 284-295.
- Biller, P., Ross, A.B., 2011. Potential yields and properties of oil from the hydrothermal liquefaction of microalgae with different biochemical content. *Bioresour. Technol.* 102 (1), 215-225.
- Biller, P., Sharma, B.K., Kunwar, B., Ross, A.B., 2015. Hydroprocessing of bio-crude from continuous hydrothermal liquefaction of microalgae. *Fuel*. 159, 197-205.
- Biswas, B., Arun Kumar, A., Bisht, Y., Singh, R., Kumar, J., Bhaskar, T., 2017. Effects of temperature and solvent on hydrothermal liquefaction of *Sargassum tenerrimum* algae. *Bioresour. Technol.* 242, 344-350.
- Broch, A., Jena, U., Hoekman, S.K., Langford, J., 2014. Analysis of solid and aqueous phase

- products from hydrothermal carbonization of whole and lipid-extracted algae. *Energies*. 7(1), 62-79
- Cao, X., Sun, S., Sun, R., 2017. Application of biochar-based catalysts in biomass upgrading: A review. *RSC Adv.* 7, 48793-48805.
- Cha, J.S., Choi, J.-C., Ko, J.H., Park, Y.-K., Park, S.H., Jeong, K.-E., Kim, S.-S., Jeon, J.-K., 2010. The low-temperature SCR of NO over rice straw and sewage sludge derived char. *Chem. Eng. J.* 156, 321–327.
- Cha, J.S., Park, S.H., Jung, S.C., Ryu, C., Jeon, J.K., Shin, M.C., Park, Y.K., 2016. Production and utilization of biochar: A review. *J. Ind. Eng. Chem.* 40, 1-15.
- Chen, R., Li, L., Liu, Z., Lu, M., Wang, C., Li, H., Ma, W., Wang, S., 2017. Preparation and characterization of activated carbons from tobacco stem by chemical activation. *J. Air Waste Manage. Assoc.* 67, 713–724.
- Cheng, F., Li, X., 2018. Preparation and Application of Biochar-Based Catalysts for Biofuel Production. *Catalysts*. 8 (9), 346.
- Chiaramonti, D., Prussi, M., Buffi, M., Rizzo, A.M., Pari, L., 2017. Review and experimental study on pyrolysis and hydrothermal liquefaction of microalgae for biofuel production. *Appl. Energy*. 185, 963-972.
- Davis, R.E., Fishman, D.B., Frank, E.D., Johnson, M.C., Jones, S.B., Kinchin, C.M., Skaggs, R.L., Venteris, E.R., Wigmosta, M.S., 2014. Integrated evaluation of cost, emissions, and resource potential for algal biofuels at the national scale. *Environ. Sci. Technol.* 48 (10), 6035-6042.
- de Caprariis, B., De Filippis, P., Petrullo, A., Scarsella, M., 2017. Hydrothermal liquefaction of biomass: Influence of temperature and biomass composition on the bio-oil production. *Fuel*. 208, 618-625.
- Demirbaş, A., 2008. Production of biodiesel from algae oils. *Energy Sources, Part A Recover. Util. Environ. Eff.* 31 (2), 163–168.

- Demirbaş, A., 2005. Estimating of structural composition of wood and non-wood biomass samples. *Energy Sources*. 27 (8), 761-767.
- DeRose, K., DeMill, C., Davis, R.W., Quinn, J.C., 2019. Integrated techno economic and life cycle assessment of the conversion of high productivity, low lipid algae to renewable fuels. *Algal Res*. 38, 101412.
- Dieguez-Alonso, A., Funke, A., Anca-Couce, A., Rombolà, A.G., Ojeda, G., Bachmann, J., Behrendt, F., 2018. Towards biochar and hydrochar engineering-influence of process conditions on surface physical and chemical properties, thermal stability, nutrient availability, toxicity and wettability. *Energies*. 11(3), 496.
- Dimitriadis, A., Bezergianni, S., 2017. Hydrothermal liquefaction of various biomass and waste feedstocks for biocrude production: A state of the art review. *Renew. Sustain. Energy Rev*. 68, 113-125.
- Du, Z., Hu, B., Shi, A., Ma, X., Cheng, Y., Chen, P., Liu, Y., Lin, X., Ruan, R., 2012. Cultivation of a microalga *Chlorella vulgaris* using recycled aqueous phase nutrients from hydrothermal carbonization process, *Bioresource Technology*. 126, 354-357.
- Duan, P., Savage, P.E., 2011a. Hydrothermal liquefaction of a microalga with heterogeneous catalysts. *Ind. Eng. Chem. Res*. 50 (1), 52-61.
- Duan, P., Savage, P.E., 2011b. Catalytic treatment of crude algal bio-oil in supercritical water: Optimization studies. *Energy Environ. Sci*. 4, 1447-1456.
- Duan, P., Xu, Y., Wang, F., Wang, B., Yan, W., 2016. Catalytic upgrading of pretreated algal bio-oil over zeolite catalysts in supercritical water. *Biochem. Eng. J*. 116, 105-112.
- Elliott, D.C., Hart, T.R., Schmidt, A.J., Neuenschwander, G.G., Rotness, L.J., Olarte, M. V, Zacher, A.H., Albrecht, K.O., Hallen, R.T., Holladay, J.E., 2013. Process development for hydrothermal liquefaction of algae feedstocks in a continuous-flow reactor. *Algal Res*. 2, 445-454.
- Farma, R., Deraman, M., Awitdrus, A., Talib, I.A., Taer, E., Basri, N.H., Manjunatha, J.G., Ishak, M.M., Dollah, B.N.M., Hashmi, S.A., 2013. Preparation of highly porous binderless activated carbon electrodes from fibres of oil palm empty fruit bunches for application in

- supercapacitors. *Bioresour. Technol.* 132, 254–261.
- Feng, H., Zhang, B., He, Z., Wang, S., Salih, O., Wang, Q., 2018. Study on co-liquefaction of *Spirulina* and *Spartina alterniflora* in ethanol-water co-solvent for bio-oil. *Energy*. 155, 1093-1101.
- Gai, C., Zhang, Y., Chen, W.T., Zhang, P., Dong, Y., 2015. An investigation of reaction pathways of hydrothermal liquefaction using *Chlorella pyrenoidosa* and *Spirulina platensis*. *Energy Convers. Manag.* 96, 330-339.
- Galadima, A., Muraza, O., 2018. Hydrothermal liquefaction of algae and bio-oil upgrading into liquid fuels: Role of heterogeneous catalysts. *Renew. Sustain. Energy Rev.* 81, 1037-1048.
- Gao, Y., Wang, X., Wang, J., Li, X., Cheng, J., Yang, H., Chen, H., 2013. Effect of residence time on chemical and structural properties of hydrochar obtained by hydrothermal carbonization of water hyacinth. *Energy*. 58, 376-383.
- Gascó, G., Paz-Ferreiro, J., Álvarez, M.L., Saa, A., Méndez, A., 2018. Biochars and hydrochars prepared by pyrolysis and hydrothermal carbonisation of pig manure. *Waste Manag.* 79, 395-403.
- Gollakota, A. R.K., Kishore, N., Gu, S., 2018. A review on hydrothermal liquefaction of biomass. *Renew. Sustain. Energy Rev.* 81, 1378-1392.
- González-García, P., Centeno, T.A., Urones-Garrote, E., Ávila-Brandé, D., Otero-Díaz, L.C., 2013. Microstructure and surface properties of lignocellulosic-based activated carbons. *Appl. Surf. Sci.* 265, 731–737.
- Gu, X., Yu, L., Pang, N., Martinez-Fernandez, J.S., Fu, X., Chen, S., 2020. Comparative techno-economic analysis of algal biofuel production via hydrothermal liquefaction: One stage versus two stages. *Appl. Energy*. 259, 114115.
- Guo, Q., Wu, M., Wang, K., Zhang, L., Xu, X., 2015. Catalytic hydrodeoxygenation of algae bio-oil over bimetallic Ni-Cu/ZrO₂ catalysts. *Ind. Eng. Chem. Res.* 54 (3), 890-899.
- Guo, Y., Yeh, T., Song, W., Xu, D., Wang, S., 2015. A review of bio-oil production from hydrothermal liquefaction of algae. *Renew. Sustain. Energy Rev.* 48, 776-790.

- Haider, M.S., Castello, D., Michalski, K.M., Pedersen, T.H., Rosendahl, L.A., 2018. Catalytic hydrotreatment of microalgae biocrude from continuous hydrothermal liquefaction: Heteroatom removal and their distribution in distillation cuts. *Energies*.48, 776-790.
- Han, Y., Hoekman, S.K., Cui, Z., Jena, U., Das, P., 2019. Hydrothermal liquefaction of marine microalgae biomass using co-solvents. *Algal Res.* 38, 101421.
- Hang, Y., Qu, M., Ukkusuri, S., 2011. Optimizing the design of a solar cooling system using central composite design techniques. *Energy Build.* 43 (4), 988-994.
- Hassan, A.F., Youssef, A.M., Prielcel, P., 2013. Removal of deltamethrin insecticide over highly porous activated carbon prepared from pistachio nutshells. *Carbon Lett.* 14 (4), 234-242.
- Hoekman, S.K., Broch, A., Robbins, C., Zielinska, B., Felix, L., 2013. Hydrothermal carbonization (HTC) of selected woody and herbaceous biomass feedstocks. *Biomass Convers. Biorefinery.* 3 (2), 113-126.
- Horáček, J., Akhmetzyanova, U., Skuhrovcová, L., Tišler, Z., de Paz Carmona, H., 2020. Alumina-supported MoNx, MoCx and MoPx catalysts for the hydrotreatment of rapeseed oil. *Appl. Catal. B Environ.* 263, 118328.
- Hu, B., Wang, K., Wu, L., Yu, S.H., Antonietti, M., Titirici, M.M., 2010. Engineering carbon materials from the hydrothermal carbonization process of biomass. *Adv. Mater.* 22 (7), 813-823
- Jafarian, S., Tavasoli, A., Nikkhah, H., 2019. Catalytic hydrotreating of pyro-oil derived from green microalgae spirulina the (*Arthrospira*) *plantensis* over NiMo catalysts impregnated over a novel hybrid support. *Int. J. Hydrogen Energy.* 44, 19855-19867.
- Jarvis, J.M., Billing, J.M., Hallen, R.T., Schmidt, A.J., Schaub, T.M., 2017. Hydrothermal Liquefaction Biocrude Compositions Compared to Petroleum Crude and Shale Oil. *Energy and Fuels.* 31 (3), 2896-2906.
- Jawad, A.H., Rashid, R.A., Ishak, M.A.M., Wilson, L.D., 2016. Adsorption of methylene blue onto activated carbon developed from biomass waste by H₂SO₄ activation: kinetic, equilibrium and thermodynamic studies. *Desalin. Water Treat.* 57 (52), 25194-25206.

- Jena, U., Das, K.C., Kastner, J.R., 2012. Comparison of the effects of Na_2CO_3 , $\text{Ca}_3(\text{PO}_4)_2$, and NiO catalysts on the thermochemical liquefaction of microalga *Spirulina platensis*. *Appl. Energy*. 98, 368-375.
- Jin, H., Wang, X., Gu, Z., Polin, J., 2013. Carbon materials from high ash biochar for supercapacitor and improvement of capacitance with HNO_3 surface oxidation. *J. Power Sources*. 236, 285–292.
- Kambo, H.S., Dutta, A., 2015. A comparative review of biochar and hydrochar in terms of production, physico-chemical properties and applications. *Renew. Sustain. Energy Rev.* 45, 359-378.
- Karaçetin, G., Sivrikaya, S., Imamoğlu, M., 2014. Adsorption of methylene blue from aqueous solutions by activated carbon prepared from hazelnut husk using zinc chloride. *J. Anal. Appl. Pyrolysis*. 110, 270-276.
- Kazemi Shariat Panahi, H., Tabatabaei, M., Aghbashlo, M., Dehghani, M., Rehan, M., Nizami, A.S., 2019. Recent updates on the production and upgrading of bio-crude oil from microalgae. *Bioresour. Technol. Reports*. 7, 100216.
- Khan, J.H., Marpaung, F., Young, C., Lin, J., Islam, M.T., Alsheri, S.M., Ahamad, T., Alhokbany, N., Ariga, K., Shrestha, L.K., 2019. Jute-derived microporous/mesoporous carbon with ultra-high surface area using a chemical activation process. *Microporous Mesoporous Mater.* 274, 251–256.
- Kim, D., Lee, K., Park, K.Y., 2016. Upgrading the characteristics of biochar from cellulose, lignin, and xylan for solid biofuel production from biomass by hydrothermal carbonization. *J. Ind. Eng. Chem.* 42, 95-100.
- Kołtowski, M., Hilber, I., Bucheli, T.D., Charmas, B., Skubiszewska-Zięba, J., Oleszczuk, P., 2017. Activated biochars reduce the exposure of polycyclic aromatic hydrocarbons in industrially contaminated soils. *Chem. Eng. J.* 310, 33-40.
- Konwar, L.J., Boro, J., Deka, D., 2014. Review on latest developments in biodiesel production using carbon-based catalysts. *Renew. Sustain. Energy Rev.* 29, 546-564.

- Lai, F. ying, Chang, Y. chao, Huang, H. jun, Wu, G. qiang, Xiong, J. bo, Pan, Z. qian, Zhou, C. fei, 2018. Liquefaction of sewage sludge in ethanol-water mixed solvents for bio-oil and biochar products. *Energy*. 29, 546-564.
- Laird, D.A., Brown, R.C., Amonette, J.E., Lehmann, J., 2009. Review of the pyrolysis platform for coproducing bio-oil and biochar. *Biofuels, Bioprod. Biorefining*. 3 (5), 547-562.
- Li, Y., Wang, T., Liang, W., Wu, C., Ma, L., Zhang, Q., Zhang, X., Jiang, T., 2010. Ultrasonic preparation of emulsions derived from aqueous bio-oil fraction and 0# diesel and combustion characteristics in diesel generator. *Energy and Fuels*. 24 (3), 1987-1995.
- Liang, P., Gao, H., Yao, Z., Jia, R., Shi, Y., Sun, Y., Fan, Q., Wang, H., 2017. Simple synthesis of ultrasmall β -Mo₂C and α -MoCl_{1-x} nanoparticles and new insights into their catalytic mechanisms for dry reforming of methane. *Catal. Sci. Technol*. 7, 3312-3324.
- Libra, J.A., Ro, K.S., Kammann, C., Funke, A., Berge, N.D., Neubauer, Y., Titirici, M.M., Fühner, C., Bens, O., Kern, J., Emmerich, K.H., 2011. Hydrothermal carbonization of biomass residuals: A comparative review of the chemistry, processes and applications of wet and dry pyrolysis. *Biofuels*. 2 (1), 71-106.
- Liu, Z., Quek, A., Kent Hoekman, S., Balasubramanian, R., 2013. Production of solid biochar fuel from waste biomass by hydrothermal carbonization, *Fuel*. 103, 943-949.
- López Barreiro, D., Gómez, B.R., Ronsse, F., Hornung, U., Kruse, A., Prins, W., 2016. Heterogeneous catalytic upgrading of biocrude oil produced by hydrothermal liquefaction of microalgae: State of the art and own experiments. *Fuel Process. Technol*. 148, 117-127.
- López Barreiro, D., Prins, W., Ronsse, F., Brilman, W., 2013. Hydrothermal liquefaction (HTL) of microalgae for biofuel production: State of the art review and future prospects. *Biomass and Bioenergy*. 53, 113-127.
- Manayil, J.C., Inocencio, C.V.M., Lee, A.F., Wilson, K., 2016. Mesoporous sulfonic acid silicas for pyrolysis bio-oil upgrading via acetic acid esterification. *Green Chem*. 18, 1387-1394.
- Masoumi, S., Boahene, P.E., Dalai, A.K., 2020a. Biocrude oil and hydrochar production and

- characterization obtained from hydrothermal liquefaction of microalgae in methanol-water system. *Energy*. 217, 119344.
- Masoumi, S., Borugadda, V.B., Dalai, A.K., 2020b. Biocrude Oil Production via Hydrothermal Liquefaction of Algae and Upgradation Techniques to Liquid Transportation Fuels, in: *Biorefinery of Alternative Resources: Targeting Green Fuels and Platform Chemicals*. Springer, Singapore, 249-270.
- Masoumi, S., Dalai, A.K., 2021. NiMo carbide supported on algal derived activated carbon for hydrodeoxygenation of algal biocrude oil. *Energy Convers. Manag.* 231, 113834.
- Masoumi, S., Dalai, A.K., 2020. Optimized production and characterization of highly porous activated carbon from algal-derived hydrochar. *J. Clean. Prod.* 263, 121427.
- Mau, V., Gross, A., 2018. Energy conversion and gas emissions from production and combustion of poultry-litter-derived hydrochar and biochar. *Appl. Energy*. 213, 510-519.
- Morali, U., Demiral, H., Şensöz, S., 2018. Optimization of activated carbon production from sunflower seed extracted meal: Taguchi design of experiment approach and analysis of variance. *J. Clean. Prod.* 189, 602-611.
- Mortensen, P.M., Grunwaldt, J.D., Jensen, P.A., Knudsen, K.G., Jensen, A.D., 2011. A review of catalytic upgrading of bio-oil to engine fuels. *Appl. Catal. A Gen.* 407 (1-2) 1-19.
- Mu, D., Xin, C., Zhou, W., 2020. Life Cycle Assessment and Techno-Economic Analysis of Algal Biofuel Production, *Microalgae Cultivation for Biofuels Production*. 281-292
- Mumme, J., Eckervogt, L., Pielert, J., Diakité, M., Rupp, F., Kern, J., 2011. Hydrothermal carbonization of anaerobically digested maize silage. *Bioresour. Technol.* 102 (19), 9255-9260.
- Naderi, M., Vesali-Naseh, M., 2019. Hydrochar-derived fuels from waste walnut shell through hydrothermal carbonization: characterization and effect of processing parameters. *Biomass Convers. Biorefinery* 1–9.
- Namazi, A.B., Allen, D.G., Jia, C.Q., 2016. Benefits of microwave heating method in production of activated carbon. *Can. J. Chem. Eng.* 94, 1262–1268.

- Nava, R., Pawelec, B., Castaño, P., Álvarez-Galván, M.C., Loricera, C. V., Fierro, J.L.G., 2009. Upgrading of bio-liquids on different mesoporous silica-supported CoMo catalysts. *Appl. Catal. B Environ.* 92 (1-2), 154-167.
- Obeid, F., Chu Van, T., Brown, R., Rainey, T., 2019. Nitrogen and sulphur in algal biocrude: A review of the HTL process, upgrading, engine performance and emissions. *Energy Convers. Manag.* 181, 105-119.
- Onay, O., Kockar, O.M., 2003. Slow, fast and flash pyrolysis of rapeseed. *Renew. Energy.* 28 (15), 2417-2433.
- Ou, L., Thilakaratne, R., Brown, R.C., Wright, M.M., 2015. Techno-economic analysis of transportation fuels from defatted microalgae via hydrothermal liquefaction and hydroprocessing. *Biomass and Bioenergy.* 72, 45-54.
- Oz, U.C., Küçüktürkmen, B., Devrim, B., Saka, O.M., Bozkir, A., 2019. Development and Optimization of Alendronat Sodium Loaded PLGA Nanoparticles by Central Composite Design. *Macromol. Res.* 27 (9), 857-866.
- Pallarés, J., González-Cencerrado, A., Arauzo, I., 2018. Production and characterization of activated carbon from barley straw by physical activation with carbon dioxide and steam. *Biomass and Bioenergy.* 115, 64-73.
- Palomino, A., Godoy-Silva, R.D., Raikova, S., Chuck, C.J., 2020. The storage stability of biocrude obtained by the hydrothermal liquefaction of microalgae. *Renew. Energy.* 145, 1720-1729.
- Pan, Z. qian, Huang, H. jun, Zhou, C. fei, Xiao, X. feng, He, X. wu, Lai, F. ying, Xiong, J. bo, 2018. Highly efficient conversion of camphor tree sawdust into bio-oil and biochar products by liquefaction in ethanol-water cosolvent. *J. Anal. Appl. Pyrolysis.* 136, 186-198.
- Pane, L., Franceschi, E., De Nuccio, L., Carli, A., 2001. Applications of thermal analysis on the marine phytoplankton, *Tetraselmis suecica*. *J. Therm. Anal. Calorim.* 66, 145–154.
- Pankratz, S., Kumar, M., Oyedun, A.O., Gemechu, E., Kumar, A., 2020. Environmental performances of diluents and hydrogen production pathways from microalgae in cold climates: Open raceway ponds and photobioreactors coupled with thermochemical

- conversion. *Algal Res.* 47, 101815.
- Pankratz, S., Oyedun, A.O., Kumar, A., 2019. Development of cost models of algae production in a cold climate using different production systems. *Biofuels, Bioprod. Biorefining.* 13 (5), 1246-1260.
- Patel, B., Hellgardt, K., 2016. Hydrothermal liquefaction and: In situ supercritical transesterification of algae paste. *RSC Adv.* 6(89), 86560-86568.
- Pechyen, C., Atong, D., Aht-ong, D., Sricharoenchaikul, V., 2007. Investigation of Pyrolyzed Chars from Physic Nut Waste for the Preparation of Activated Carbon. *J. Solid Mech. Mater. Eng.* 1 (4), 498-507.
- Peterson, A.A., Vogel, F., Lachance, R.P., Fröling, M., Antal, M.J., Tester, J.W., 2008. Thermochemical biofuel production in hydrothermal media: A review of sub- and supercritical water technologies. *Energy Environ. Sci.* 1 (1), 32-65.
- Quinn, J.C., Davis, R., 2015. The potentials and challenges of algae based biofuels: A review of the techno-economic, life cycle, and resource assessment modeling. *Bioresour. Technol.* 184, 444-452.
- Ramirez, J.A., Brown, R.J., Rainey, T.J., 2015. A review of hydrothermal liquefaction bio-crude properties and prospects for upgrading to transportation fuels. *Energies.* 8 (7), 6765-6794.
- Reza, M.T., Andert, J., Wirth, B., Busch, D., Pielert, J., Lynam, J.G., Mumme, J., 2014. Hydrothermal Carbonization of Biomass for Energy and Crop Production. *Appl. Bioenergy.* 1 (1), 11-29.
- Ros, A., Lillo-Ródenas, M.A., Fuente, E., Montes-Morán, M.A., Martín, M.J., Linares-Solano, A., 2006. High surface area materials prepared from sewage sludge-based precursors. *Chemosphere.* 65 (1) 132-140.
- Roussis, S.G., Cranford, R., Sytkovetskiy, N., 2012. Thermal treatment of crude algae oils prepared under hydrothermal extraction conditions, *Energy and Fuels.* 26 (8), 5294-5299.
- Saber, M., Nakhshiniev, B., Yoshikawa, K., 2016. A review of production and upgrading of algal bio-oil. *Renew. Sustain. Energy Rev.* 58, 918-930.

- Safari, F., Javani, N., Yumurtaci, Z., 2018. Hydrogen production via supercritical water gasification of almond shell over algal and agricultural hydrochars as catalysts. *Int. J. Hydrogen Energy*. 143 (2), 1071-1080.
- Shen, W., Li, Z., Liu, Y., 2012. Surface Chemical Functional Groups Modification of Porous Carbon. *Recent Patents Chem. Eng.* 1 (1), 27-40.
- Shu Hui, T., Abbas Ahmad Zaini, M., 2015. Potassium hydroxide activation of activated carbon: a commentary. *Carbon Lett.* 16 (4), 275-280.
- Shu, J., Cheng, S., Xia, H., Zhang, L., Peng, J., Li, C., Zhang, S., 2017. Copper loaded on activated carbon as an efficient adsorbent for removal of methylene blue. *RSC Adv.* 7 (24), 14395-14405.
- Sills, D.L., Van Doren, L.G., Beal, C., Raynor, E., 2020. The effect of functional unit and co-product handling methods on life cycle assessment of an algal biorefinery. *Algal Res.* 46, 101770.
- Sing, K.S.W., 1985. Reporting physisorption data for gas/solid systems with special reference to the determination of surface area and porosity (Recommendations 1984). *Pure Appl. Chem.* 57, 603–619.
- Singh, R., Bhaskar, T., Balagurumurthy, B., 2015. Effect of solvent on the hydrothermal liquefaction of macro algae *Ulva fasciata*. *Process Saf. Environ. Prot.* 93, 154-160.
- Smirnov, A.A., Geng, Z., Khromova, S.A., Zavarukhin, S.G., Bulavchenko, O.A., Saraev, A.A., Kaichev, V. V., Ermakov, D.Y., Yakovlev, V.A., 2017. Nickel molybdenum carbides: Synthesis, characterization, and catalytic activity in hydrodeoxygenation of anisole and ethyl caprate. *J. Catal.* 354, 61-77.
- Sulaiman, N.S., Hashim, R., Mohamad Amini, M.H., Danish, M., Sulaiman, O., 2018. Optimization of activated carbon preparation from cassava stem using response surface methodology on surface area and yield. *J. Clean. Prod.* 198, 1422-1430.
- Tan, X. fei, Liu, S. bo, Liu, Y. guo, Gu, Y. ling, Zeng, G. ming, Hu, X. jiang, Wang, X., Liu, S. heng, Jiang, L. hua, 2017. Biochar as potential sustainable precursors for activated carbon production: Multiple applications in environmental protection and energy storage.

- Bioresour. Technol. 227, 359-372.
- Tian, C., Li, B., Liu, Z., Zhang, Y., Lu, H., 2014. Hydrothermal liquefaction for algal biorefinery: A critical review. *Renew. Sustain. Energy Rev.* 38, 933-950.
- Tongpoothorn, W., Sriuttha, M., Homchan, P., Chanthai, S., Ruangviriyachai, C., 2011. Preparation of activated carbon derived from *Jatropha curcas* fruit shell by simple thermo-chemical activation and characterization of their physico-chemical properties. *Chem. Eng. Res. Des.* 89 (3), 335-340.
- Toor, S.S., Rosendahl, L., Rudolf, A., 2011. Hydrothermal liquefaction of biomass: A review of subcritical water technologies. *Energy*. 36 (5), 2328-2342.
- Tran, D.T., Chang, J.S., Lee, D.J., 2017. Recent insights into continuous-flow biodiesel production via catalytic and non-catalytic transesterification processes. *Appl. Energy*. 185, 376-409.
- Troëng, S., 1955. Oil determination of oilseed. Gravimetric routine method. *J. Am. Oil Chem. Soc.* 32 (3), 124-126.
- Tsai, W.-T., Bai, Y.-C., Lin, Y.-Q., Lai, Y.-C., Tsai, C.-H., 2019. Porous and adsorption properties of activated carbon prepared from cocoa pod husk by chemical activation. *Biomass Convers. Biorefinery*, 10 (1), 35-43.
- Tsukahara, K., Sawayama, S., 2005. Liquid fuel production using microalgae. *J. Japan Pet. Inst.* 48 (5), 251-259.
- Tzanetis, K.F., Posada, J.A., Ramirez, A., 2017. Analysis of biomass hydrothermal liquefaction and biocrude-oil upgrading for renewable jet fuel production: The impact of reaction conditions on production costs and GHG emissions performance. *Renew. Energy*. 113, 1388-1398.
- Ulrich, G.D., 1984. A guide to chemical engineering process design and economics. Wiley New York.
- Valdez, P.J., Dickinson, J.G., Savage, P.E., 2011. Characterization of product fractions from hydrothermal liquefaction of *Nannochloropsis* sp. and the influence of solvents, Energy and

- Fuels. 25 (7), 3235-3243.
- van Hal, J.W., Huijgen, W.J.J., López-Contreras, A.M., 2014. Opportunities and challenges for seaweed in the biobased economy. *Trends Biotechnol.* 32 (5), 231–233.
- Vardon, D.R., Sharma, B.K., Scott, J., Yu, G., Wang, Z., Schideman, L., Zhang, Y., Strathmann, T.J., 2011. Chemical properties of biocrude oil from the hydrothermal liquefaction of *Spirulina* algae, swine manure, and digested anaerobic sludge. *Bioresour. Technol.* 102 (17), 8295-8303.
- Wiedner, K., Rumpel, C., Steiner, C., Pozzi, A., Maas, R., Glaser, B., 2013. Chemical evaluation of chars produced by thermochemical conversion (gasification, pyrolysis and hydrothermal carbonization) of agro-industrial biomass on a commercial scale. *Biomass and Bioenergy.* 59, 264-278.
- Wildschut, J., Mahfud, F.H., Venderbosch, R.H., Heeres, H.J., 2009. Hydrotreatment of fast pyrolysis oil using heterogeneous noble-metal catalysts. *Ind. Eng. Chem. Res.* 48 (23), 10324-10334.
- Wilk, M., Magdziarz, A., Jayaraman, K., Szymańska-Chargot, M., Gökalp, I., 2019. Hydrothermal carbonization characteristics of sewage sludge and lignocellulosic biomass. A comparative study. *Biomass and Bioenergy.* 120, 166-175.
- Wu, L., Hu, X., Wang, S., Mahmudul Hasan, M.D., Jiang, S., Li, T., Li, C.Z., 2018. Acid-treatment of bio-oil in methanol: The distinct catalytic behaviours of a mineral acid catalyst and a solid acid catalyst. *Fuel.* 212, 412-421.
- Xiao, L.P., Shi, Z.J., Xu, F., Sun, R.C., 2012. Hydrothermal carbonization of lignocellulosic biomass. *Bioresour. Technol.* 118, 619-623.
- Xin, C., Addy, M.M., Zhao, J., Cheng, Y., Cheng, S., Mu, D., Liu, Y., Ding, R., Chen, P., Ruan, R., 2016. Comprehensive techno-economic analysis of wastewater-based algal biofuel production: A case study. *Bioresour.* 211, 584-593.
- Xiong, X., Yu, I.K.M., Cao, L., Tsang, D.C.W., Zhang, S., Ok, Y.S., 2017. A review of biochar-based catalysts for chemical synthesis, biofuel production, and pollution control. *Bioresour. Technol.* 246, 254-270.

- Xu, D., Lin, G., Guo, S., Wang, S., Guo, Y., Jing, Z., 2018. Catalytic hydrothermal liquefaction of algae and upgrading of biocrude: A critical review. *Renew. Sustain. Energy Rev.* 97, 103-118.
- Xu, Y., Wang, Q., Hu, X., Li, C., Zhu, X., 2010. Characterization of the lubricity of bio-oil/diesel fuel blends by high frequency reciprocating test rig. *Energy* 35, 283–287.
- Yan, W., Acharjee, T.C., Coronella, C.J., Vásquez, V.R., 2009. Thermal pretreatment of lignocellulosic biomass. *Environ. Prog. Sustain. Energy.* 28 (3), 435-440.
- Yang, C., Li, R., Cui, C., Liu, S., Qiu, Q., Ding, Y., Wu, Y., Zhang, B., 2016. Catalytic hydroprocessing of microalgae-derived biofuels: A review. *Green Chem.* 18 (13), 3684-3699.
- Yang, C., Zhang, B., Li, R., Qiu, Q., 2018. Hydroprocessing Catalysts for Algal Biofuels. *Hydroprocessing Catal. Process. Challenges Biofuels Prod.* 17, 129-173.
- Zhang, B., Heidari, M., Regmi, B., Salaudeen, S., Arku, P., Thimmannagari, M., Dutta, A., 2018. Hydrothermal carbonization of fruit wastes: A promising technique for generating hydrochar. 11(8), 2022.
- Zhang, C., Duan, P., Xu, Y., Wang, B., Wang, F., Zhang, L., 2014. Catalytic upgrading of duckweed biocrude in subcritical water. *Bioresour. Technol.* 166, 37-44.
- Zhang, J., Zhang, Y., 2014. Hydrothermal liquefaction of microalgae in an ethanol-water Co-solvent to produce biocrude oil. *Energy and Fuels.* 28 (8), 5178-5183.
- Zhang, J., Zhang, Y., Luo, Z., 2014. Hydrothermal liquefaction of chlorella pyrenoidosa in ethanol-water for bio-crude production. *Energy Procedia* 61, 1961–1964.
- Zhou, L., Lawal, A., 2016. Hydrodeoxygenation of microalgae oil to green diesel over Pt, Rh and presulfided NiMo catalysts. *Catal. Sci. Technol.* 6 (5), 1442-1454.
- Zhou, L., Lawal, A., 2015. Evaluation of presulfided NiMo/ γ -Al₂O₃ for hydrodeoxygenation of microalgae oil to produce green diesel. *Energy & Fuels* 29 (1), 262–272.
- Zhou, Y., Hu, C., 2020. Catalytic thermochemical conversion of algae and upgrading of algal oil for the production of high-grade liquid fuel: A review. *Catalysts.* 10 (2), 145.

- Zhu, Y., Jones, S.B., Schmidt, A.J., Albrecht, K.O., Edmundson, S.J., Anderson, D.B., 2019. Techno-economic analysis of alternative aqueous phase treatment methods for microalgae hydrothermal liquefaction and biocrude upgrading system. *Algal Res.* 39, 101467.
- Zhu, Z., Rosendahl, L., Toor, S.S., Chen, G., 2018. Optimizing the conditions for hydrothermal liquefaction of barley straw for bio-crude oil production using response surface methodology. *Sci. Total Environ.* 630, 560-569.
- Zou, H., Chen, S., Huang, J., Zhao, Z., 2017. Effect of impregnation sequence on the catalytic performance of NiMo carbides for the tri-reforming of methane. *Int. J. Hydrogen Energy.* 42 (32), 20401-20409.
- Zou, H., Chen, S., Huang, J., Zhao, Z., 2016. Effect of additives on the properties of nickel molybdenum carbides for the tri-reforming of methane. *Int. J. Hydrogen Energy.* 41 (38), 16842-16850.

Appendix A: Analytical data for microalgae

Table A.1: Analytical data for microalgae

Analysis	Nannochloopsis gaditana (Wet broth, ~30% solid)			Nannochloopsis gaditana-dry powder
	95% EtOH	Isohexane	IPA*	
Extracted Solvent	95% EtOH	Isohexane	IPA*	IPA
Lipid Content of biomass (%)	26.45	11.12	15.42	10.79
Glycolipids				
Monogalatosyl diacylglycerol (%)	0.72	0.74	1.54	
Steryl Glucoside (%)	<0.01	<0.01	<0.01	
Digalactosyl diacylglycerol (%)	4.05	3.61	5.41	
Neutral lipid (%)	17.7	56.8	41.3	
Phospholipids				
N-acylphosphatidylethanolamine	<0.01	<0.01	<0.01	
Phosphatidic Acid	4.74	3.96	8.77	
Phosphatidylethanolamine	4.08	3.37	5.61	
Phosphatidylcholine	4.17	3.68	3.93	
Phosphatidylinositol	3.23	1.54	3.89	
Lysophosphatidylcholine	0.13	0.09	0.11	
Total Phospholipids	16.4	12.6	22.3	

*Isopropyl Alcohol

Appendix B: Process outline for HTL, Chemical activation, synthesis of the catalysts and HDO process

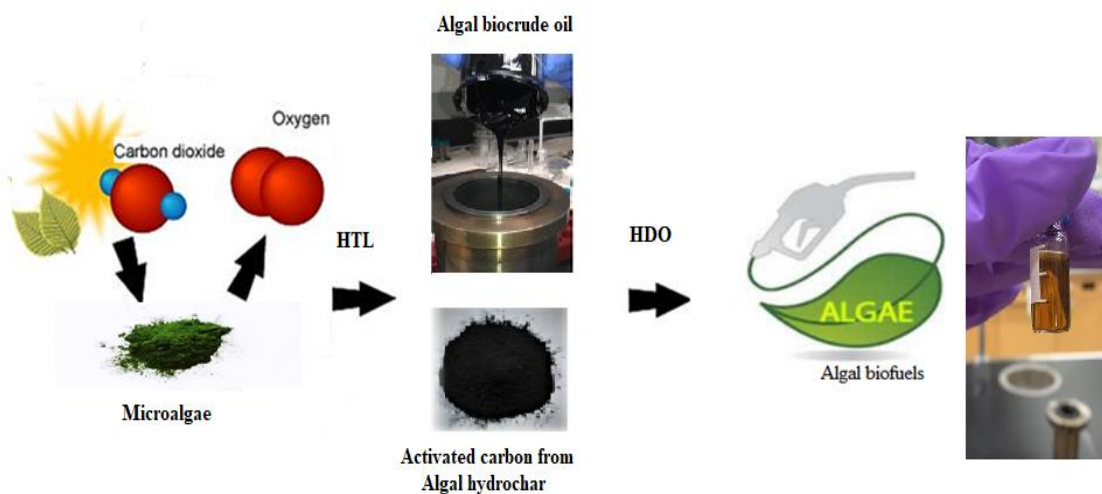


Figure B.1 Process outline for the production of algal biofuels

Synthesis of NiMo/AC catalysts (Basis: 1 g)

Ni: 3.5 wt.% = 0.035 g ,

Precursor: Nickel (II) nitrate hexahydrate ($\text{Ni}(\text{NO}_3)_2 \cdot 6\text{H}_2\text{O}$) with 290.79 g/mol

Mo: 13 wt.% = 0.13 g

Precursor: Ammonium molybdate tetrahydrate ($(\text{NH}_4)_6\text{Mo}_7\text{O}_{24} \cdot 4\text{H}_2\text{O}$) with 1235.86 gr/mol

AC = 0.835 g

$$0.035 \text{ g Ni} \times \frac{1 \text{ mol of Ni}}{58.69 \text{ g Ni}} \times \frac{1 \text{ mol Ni}(\text{NO}_3)_2 \cdot 6\text{H}_2\text{O}}{1 \text{ mol Ni}} \times \frac{290.79 \text{ g}}{1 \text{ mol Ni}(\text{NO}_3)_2 \cdot 6\text{H}_2\text{O}} = 0.17 \text{ g Ni}(\text{NO}_3)_2 \cdot 6\text{H}_2\text{O}$$

$$0.13 \text{ g Mo} \times \frac{1 \text{ mol of Mo}}{95.95 \text{ g Mo}} \times \frac{1 \text{ mol } (\text{NH}_4)_6\text{Mo}_7\text{O}_{24} \cdot 4\text{H}_2\text{O}}{7 \text{ mol Mo}} \times \frac{1235.86 \text{ g}}{1 \text{ mol } (\text{NH}_4)_6\text{Mo}_7\text{O}_{24} \cdot 4\text{H}_2\text{O}} = 0.23 \text{ g } (\text{NH}_4)_6\text{Mo}_7\text{O}_{24} \cdot 4\text{H}_2\text{O}$$

Appendix C: Temperature profile of furnace

To obtain the temperature profile inside the stainless steel reactor used for production of AC and catalysts (synthesis and passivation), various temperatures were set on the furnace while N_2 gas was passing through the reactor. The inside temperature of the reactor was measured and recorded at various positions using a K-type thermocouple. Figure B.1 shows the schematic of the furnace and set-up. Temperature at each position was recorded three times and then the average value was used to calibrate the temperature. The calibration curve is shown in Figure B.2.

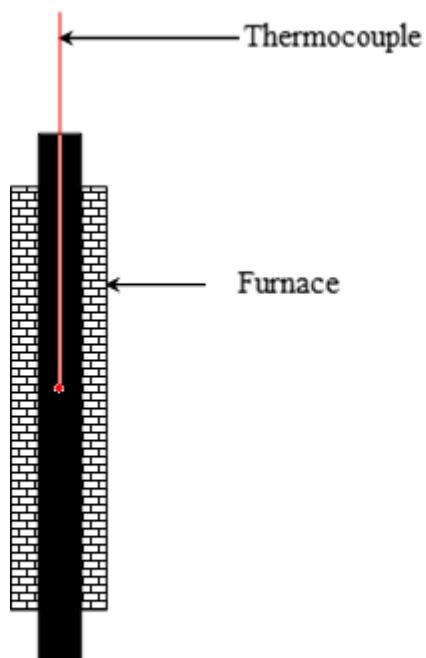


Figure C.1: Schematic diagram of the furnace and thermocouple

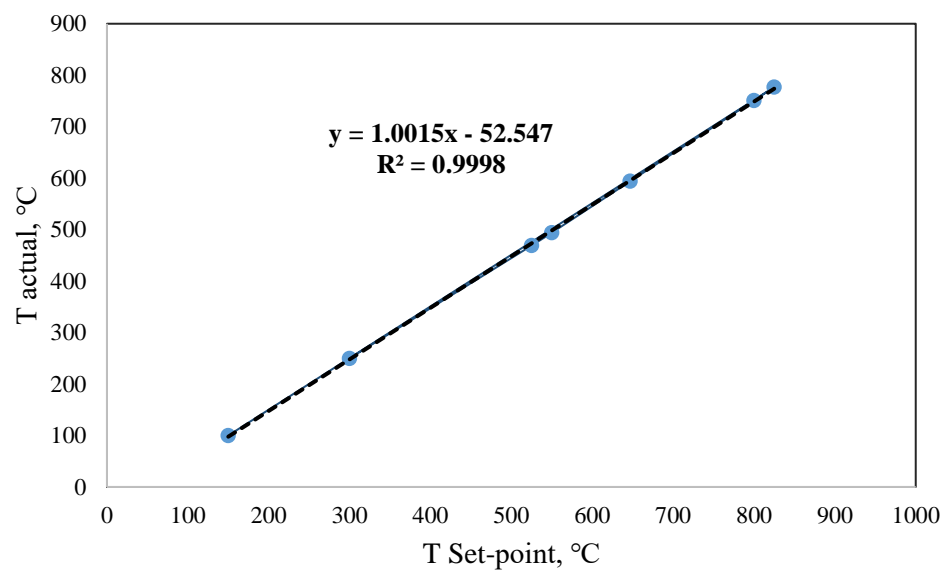


Figure C.2: Calibration curve for furnace temperature

Appendix D: GC-MS results for biocrude oil, water soluble compounds and upgraded biocrude oil

Results of GC-MS based on different library are shown in the following Table C1-C3, confirming the large amount of compounds present in oil samples.

Table D.1: Algal biocrude oil compounds

1	0.55	Methylene Chloride
2	0.58	Acetic acid, dichloro-
3	0.92	Cyclohexane
12	6.89	N,N-Bis(2-hydroxyethyl)-2-aminoethanesulfonic acid
29	11.06	Cyclohexanone, 2-nitro-
54	19.25	10-Undecenoic acid, methyl ester
58	19.89	9-Tetradecen-1-ol, (E)-
69	22.61	Cyclohexanone, 2-nitro-
71	23.65	Tridecanoic acid, methyl ester
72	24.26	Azelaoyl chloride
73	24.39	Undecylenic Acid
82	25.67	9-Tetradecen-1-ol, (E)-
83	26.09	9-Tetradecen-1-ol, (E)-
87	26.52	3-Cyclohexene-1-acetaldehyde, α ,4-dimethyl-
88	26.74	9-Octadecenoic acid (Z)-, methyl ester
89	27.09	Hexadecanoic acid, methyl ester
90	27.37	Undecanoic acid, hydroxy-, lactone
91	27.7	? Dodecalactone
96	29.1	Oleyl Alcohol
98	29.45	9-Tetradecen-1-ol, (E)-

99	29.55	9-Octadecenoic acid (Z)-, methyl ester
100	29.7	9-Hexadecen-1-ol, (Z)-
105	31.53	Vitamin A aldehyde
106	31.61	Vitamin A aldehyde
108	33.21	Vitamin A aldehyde
109	33.58	Vitamin A aldehyde
110	34.17	Ricinoleic acid
112	34.67	Vitamin A aldehyde
118	37.95	Vitamin A aldehyde
122	40.2	Retinol, acetate
124	41.03	β Carotene
129	41.96	Gibberellic acid
130	42.8	Gibberellic acid
134	43.41	Digitoxin
135	43.63	Beclomethasone
136	43.88	β Carotene
137	44.02	Beclomethasone
138	44.59	Phenol, 2,4-bis(1,1-dimethylethyl)-
140	45.04	Rescinnamine
145	45.46	Beclomethasone
146	46.08	Rescinnamine
147	46.52	Beclomethasone
149	46.75	Phenol, 2,4-bis(1,1-dimethylethyl)-
150	47.43	Beclomethasone
151	47.48	Prednisolone Acetate
153	47.87	Beclomethasone
155	48.5	Ergoline-8-carboxamide, 9,10-didehydro-6-methyl-, (8 β)-
156	48.58	Beclomethasone
157	48.98	Beclomethasone

158	49.22	Beclomethasone
161	50.78	Beclomethasone
162	50.85	Beclomethasone
163	51.23	Beclomethasone
164	51.41	Ergoline-8-carboxamide, 9,10-didehydro-6-methyl-, (8 β)-
167	52.5	Beclomethasone
168	52.55	Beclomethasone
169	52.74	Beclomethasone
170	52.9	Beclomethasone
171	53.14	Beclomethasone
172	53.31	Beclomethasone
173	55.26	Beclomethasone
174	55.34	Beclomethasone
176	56.81	Beclomethasone
177	57.03	Beclomethasone
179	57.2	Beclomethasone
184	59.05	Beclomethasone
185	59.25	Ergoline-8-carboxamide, 9,10-didehydro-6-methyl-, (8 β)-
186	59.63	Ergoline-8-carboxamide, 9,10-didehydro-6-methyl-, (8 β)-
188	60.72	Beclomethasone
189	61.01	Beclomethasone
191	63.58	Beclomethasone
192	63.73	Beclomethasone
193	64.05	Beclomethasone

Table D.2: Upgraded biocrude oil compounds

Peak	Ret.Time	Library Compound
No.	min	
TIC	TIC	TIC
6	2.82	Ethylbenzene
21	4.75	1H-Pyrrole, 3-ethyl-2,4-dimethyl-
25	5.2	Aniline
27	5.51	Phosphonic acid, (p-hydroxyphenyl)-
30	5.75	1,6-Octadien-3-ol, 3,7-dimethyl-
33	6.09	Benzenamine, N,3-dimethyl-
35	6.27	1H-Pyrrole, 3-ethyl-2,4-dimethyl-
38	6.69	Nanofin
40	7.1	1,2-Ethanediamine, N-(phenylmethyl)-
42	7.3	Phenol, 2-methyl-
43	7.47	Benzenamine, 3,5-dimethyl-
44	7.54	Benzenamine, 3-methyl-
45	7.59	Phenol, 3,5-dimethyl-
48	7.86	Phenol, 3-methyl-
49	7.91	1H-Pyrrole, 3-ethyl-2,4-dimethyl-
51	8.07	Phenol, 3,5-dimethyl-
53	8.34	1H-Pyrrole, 3-ethyl-2,4-dimethyl-
54	8.45	1H-Pyrrole, 3-ethyl-2,4-dimethyl-
55	8.51	Phenol, 2,3-dimethyl-
58	8.92	Cyclooctanamine
61	9.14	Phenol, 3,5-dimethyl-
62	9.28	Vitamin A aldehyde
64	9.58	Benzenemethanol, 4-ethyl-
65	9.75	Phenol, 2,3-dimethyl-
66	9.93	3,4-Dimethyl-o-phenylenediamine
67	10.16	Benzenamine, 4-methoxy-N-methyl-

69	10.33	Phenol, 3-ethyl-
70	10.4	Benzenamine, 4-methoxy-N-methyl-
71	10.58	Phenol, 2,3,6-trimethyl-
72	10.67	Vitamin A aldehyde
73	10.84	Benzenamine, 4-methoxy-N-methyl-
74	11.03	Dodecane
75	11.09	Phenol, 2,4,5-trimethyl-
76	11.19	Gibberellic acid
77	11.29	4a,7-Methano-4aH-naphth[1,8a-b]oxirene, octahydro- 4,4,8,8-tetramethyl-
78	11.4	Oxacyclododecan-2-one
79	11.5	1H-Pyrrole, 3-ethyl-2,4-dimethyl-
82	11.78	Gibberellic acid
83	11.93	Phenol, 2,3,5-trimethyl-
84	12.03	Oxacyclododecan-2-one
85	12.16	Phenol, 2,4,5-trimethyl-
86	12.29	4,5-Dimethyl-ortho-phenylenediamine
88	12.53	4,5-Dimethyl-ortho-phenylenediamine
89	12.78	Pyrazine, 2,5-dimethyl-3-propyl-
90	12.86	4a,7-Methano-4aH-naphth[1,8a-b]oxirene, octahydro- 4,4,8,8-tetramethyl-
91	12.96	Cholest-5-en-3-ol (3 β)-, tetradecanoate
92	13.05	Phenol, 2,3,5,6-tetramethyl-
93	13.14	4a,7-Methano-4aH-naphth[1,8a-b]oxirene, octahydro- 4,4,8,8-tetramethyl-
94	13.24	Naphthalene, 1-methyl-
95	13.36	1,4-Methanoazulen-7(1H)-one, octahydro-1,5,5,8a- tetramethyl-
96	13.45	Phenol, 2-methyl-5-(1-methylethyl)-
99	13.66	Pentadecane

100	13.73	Pyrazine, 2,5-dimethyl-3-propyl-
101	13.81	4a,7-Methano-4aH-naphth[1,8a-b]oxirene, octahydro-4,4,8,8-tetramethyl-
103	14.02	Gibberellic acid
104	14.13	Gibberellic acid
105	14.26	Gibberellic acid
106	14.35	1,4-Methanoazulen-7(1H)-one, octahydro-1,5,5,8a-tetramethyl-
107	14.43	Gibberellic acid
108	14.49	Gibberellic acid
109	14.59	Gibberellic acid
110	14.78	Gibberellic acid
113	15	Gibberellic acid
114	15.09	Gibberellic acid
115	15.21	Benzene, 1-methoxy-4-methyl-2-(1-methylethyl)-
116	15.3	Gibberellic acid
117	15.45	Pregn-4-ene-3,20-dione, 11-hydroxy-, (11a)-
118	15.59	Cholest-5-en-3-ol (3 β)-, tetradecanoate
119	15.79	1H-Indole-3-methanamine, N,N-dimethyl-
121	15.99	Gibberellic acid
122	16.2	Tetradecane
123	16.28	Pyrazine, 2,5-dimethyl-3-propyl-
124	16.45	Gibberellic acid
125	16.55	4a,7-Methano-4aH-naphth[1,8a-b]oxirene, octahydro-4,4,8,8-tetramethyl-
126	16.69	Pregn-4-ene-3,20-dione, 11-hydroxy-, (11a)-
127	16.82	Gibberellic acid
128	17.1	Pregn-4-ene-3,20-dione, 11-hydroxy-, (11a)-
129	17.22	Gibberellic acid
131	17.48	Gibberellic acid

132	17.61	Gibberellic acid
133	17.7	Cholest-5-en-3-ol (3 β)-, tetradecanoate
134	17.84	Gibberellic acid
135	17.92	Gibberellic acid
136	17.99	Gibberellic acid
137	18.12	Gibberellic acid
138	18.27	2-Cyclohexen-1-one, 3-phenyl-
139	18.42	Digitoxin
140	18.51	Gibberellic acid
141	18.65	Pentadecane
142	18.75	Digitoxin
143	18.87	Gibberellic acid
144	18.97	β Carotene
145	19.07	Gibberellic acid
146	19.22	Retinol, acetate
147	19.47	Gibberellic acid
148	19.76	Gibberellic acid
149	19.84	Gibberellic acid
150	19.97	Estriol
151	20.13	Gibberellic acid
152	20.23	Retinal, 9-cis-
153	20.29	Retinal, 9-cis-
154	20.39	Gibberellic acid
155	20.51	Retinol, acetate
156	20.67	Gibberellic acid
157	20.91	Hexadecane
158	21.01	Retinal, 9-cis-
160	21.29	Gibberellic acid
161	21.44	Gibberellic acid
162	21.61	Retinal, 9-cis-

163	21.75	Gibberellic acid
164	21.9	Gibberellic acid
165	21.99	Cholest-5-en-3-ol (3 β)-, tetradecanoate
166	22.1	Retinal, 9-cis-
167	22.29	Retinoic acid, methyl ester
168	22.44	Gibberellic acid
169	22.53	Retinal, 9-cis-
170	22.62	Retinal, 9-cis-
171	22.84	Retinal, 9-cis-
172	22.96	Retinal, 9-cis-
173	23.08	Heptadecane
174	23.2	Digitoxin
175	23.32	Gibberellic acid
176	23.39	Gibberellic acid
177	23.54	Retinoic acid, methyl ester
178	23.69	Retinoic acid, methyl ester
179	23.77	Gibberellic acid
180	23.98	Gibberellic acid
181	24.16	Retinal, 9-cis-
182	24.22	Retinoic acid, methyl ester
183	24.38	Retinoic acid, methyl ester
184	24.49	Digitoxin
185	24.77	Digitoxin
187	25	Digitoxin
188	25.16	Eicosane
189	25.41	Vobassan-17-oic acid, 4-demethyl-3-oxo-, methyl ester
190	25.55	Digitoxin
192	25.78	Digitoxin
193	25.87	Gibberellic acid
194	25.91	Retinoic acid, methyl ester

195	26.01	Gibberellic acid
196	26.08	Digitoxin
197	26.24	Gibberellic acid
198	26.34	Gibberellic acid
199	26.54	Gibberellic acid
200	26.66	Ricinoleic acid
202	26.91	Gibberellic acid
203	27.08	Gibberellic acid
205	27.21	Gibberellic acid
207	27.42	Gibberellic acid
208	27.56	Gibberellic acid
209	27.76	Octadecanoic acid
210	27.97	Vobassan-17-oic acid, 4-demethyl-3-oxo-, methyl ester
211	28.14	Digitoxin
212	28.3	Rescinamine
214	28.5	Vobassan-17-oic acid, 4-demethyl-3-oxo-, methyl ester
215	28.69	Vobassan-17-oic acid, 4-demethyl-3-oxo-, methyl ester
217	29.08	Gamabufotalin
218	29.21	Vobassan-17-oic acid, 4-demethyl-3-oxo-, methyl ester
220	29.52	Rescinamine
221	29.6	Rescinamine
223	29.81	Gibberellic acid
224	29.9	Hydrocortisone Acetate
225	30.04	Rescinamine
228	30.59	Pentadecylamine
229	30.81	Digitoxin
231	31.03	1,3-Dioxolane, 2-heptyl-
232	31.12	Vobassan-17-oic acid, 4-demethyl-3-oxo-, methyl ester
233	31.27	Vobassan-17-oic acid, 4-demethyl-3-oxo-, methyl ester
234	31.36	Beclomethasone

235	31.53	Beclomethasone
237	31.82	Vobassan-17-oic acid, 4-demethyl-3-oxo-, methyl ester
238	32.02	Digitoxin
246	32.65	Vobassan-17-oic acid, 4-demethyl-3-oxo-, methyl ester
247	32.76	Vobassan-17-oic acid, 4-demethyl-3-oxo-, methyl ester
248	32.86	Hydrocortisone Acetate
249	33.06	Vobassan-17-oic acid, 4-demethyl-3-oxo-, methyl ester
250	33.18	Digitoxin
251	33.44	Digitoxin
252	33.61	Hydrocortisone Acetate
253	33.73	Rescinamine
255	34.18	Hydrocortisone Acetate
256	34.34	Rescinamine
257	34.52	Hydrocortisone Acetate
260	34.99	Hydrocortisone Acetate
262	35.36	Digitoxin
264	35.54	Hydrocortisone Acetate
265	36.38	Digitoxin
268	37.31	Hydrocortisone Acetate
269	37.37	Digitoxin
270	37.54	Hydrocortisone Acetate
271	37.69	Dehydrocholic acid
275	38.33	Octacosane
277	38.63	Hydrocortisone Acetate
278	39	Hydrocortisone Acetate
281	39.25	Octacosane
282	39.55	Hydrocortisone Acetate
285	40.14	Digitoxin
286	40.6	Vobassan-17-oic acid, 4-demethyl-3-oxo-, methyl ester
289	41.02	Octacosane

293	41.87	Rescinnamine
311	46.51	Gamabufotalin
313	47.26	Gamabufotalin
317	48.49	Colchicine
318	48.73	Colchicine
319	49.21	Colchicine
320	49.54	Beclomethasone
321	49.73	Beclomethasone
322	49.89	Colchicine
323	50.16	Colchicine
328	52.49	Colchicine
339	54.66	Prednisolone Acetate
341	55.28	Beclomethasone

Table D.3: Water soluble compounds

Peak	Ret.Time	Library Compound
No.	min	
TIC	TIC	TIC
2	1.22	Formic acid hydrazide
3	1.42	Pyridine
4	1.55	Ethanamine, N,N-dimethyl-
5	1.74	1,2:5,6-Dianhydrogalactitol
7	2.21	Pyridine, 2-methyl-
11	2.84	a-Chloroethyltrimethylsilane
12	3.3	Ethane, isothiocyanato-
13	3.75	Pyrimidine, 4,6-dimethyl-
14	3.82	Pyrimidine, 4,6-dimethyl-
15	4.14	1,3-Dioxane
17	4.82	N,N-Bis(2-hydroxyethyl)-2-aminoethanesulfonic acid
18	4.9	a-D-Glucopyranoside, a-D-glucopyranosyl
19	5.2	Benzenamine, 3-methyl-
20	5.61	Digitoxin
21	5.7	Pyrazine, 2-ethyl-5-methyl-
22	5.78	Pyrazine, trimethyl-
23	5.98	5-Chlorovaleric acid
24	6.29	1H-Pyrrole, 3-ethyl-2,4-dimethyl-
25	6.46	2,3-Butanediol, 2,3-dimethyl-
26	6.61	11-Bromoundecanoic acid
27	6.7	Cyclohexanone, 2-nitro-
28	6.89	Nanofin
30	7.33	Ethanone, 1-(1-cyclohexen-1-yl)-
31	7.42	Piperidine, 3,5-dimethyl-
32	7.79	Adenosine 3',5'-cyclic monophosphate
33	7.91	? Dodecalactone

35	8.12	1,5-Dimethyl-2-pyrrolidinone
37	8.41	a-D-Glucopyranoside, a-D-glucopyranosyl
38	8.5	Piperidine, 3,5-dimethyl-
39	8.63	Octadecane, 1-isocyanato-
40	8.74	2-Cyclopenten-1-one, 2-hydroxy-3-methyl-
41	8.99	Cyclooctanamine
42	9.15	Phenol, 3,5-dimethyl-
43	9.31	2-Cyclopenten-1-one, 2-hydroxy-3-methyl-
44	9.54	Oxacyclododecan-2-one
45	9.67	Oxacyclododecan-2-one
46	10.03	Piperidine, 2,2,6,6-tetramethyl-
47	10.31	2-Cyclopenten-1-one, 2-hydroxy-3-methyl-
48	10.82	Oxacyclododecan-2-one
49	10.93	Caprolactam
50	10.98	Nanofin
51	11.09	Oxacyclododecan-2-one
52	11.23	Octadecane, 1-isocyanato-
54	11.44	2-Cyclopenten-1-one, 2-hydroxy-3-methyl-
56	11.73	Oxacyclododecan-2-one
57	12.06	1-(3-Aminopropyl)-2-pipecoline
58	12.27	Oxacyclododecan-2-one
60	12.59	Oxacyclododecan-2-one
61	12.71	Atropine
62	12.96	Ricinoleic acid
63	13.26	Oxacyclododecan-2-one
64	13.46	Oxacyclododecan-2-one
65	13.63	Oxacyclododecan-2-one
66	13.74	Ricinoleic acid
67	14.22	Ricinoleic acid
68	14.34	Ricinoleic acid

70	14.62	Ricinoleic acid
72	14.81	Octadecane, 1-isocyanato-
73	14.88	Benzene, 1-(1-methylethyl)-4-nitro-
74	14.99	Oxacyclododecan-2-one
75	15.22	3-Buten-2-one, 4-(2,2,6-trimethyl-7-oxabicyclo[4.1.0]hept-1-yl)-
76	15.33	Ricinoleic acid
77	15.52	3-Buten-2-one, 4-(2,2,6-trimethyl-7-oxabicyclo[4.1.0]hept-1-yl)-
78	15.7	3-Buten-2-one, 4-(2,2,6-trimethyl-7-oxabicyclo[4.1.0]hept-1-yl)-
79	16.09	Ricinoleic acid
80	16.15	Ricinoleic acid
81	16.34	Ricinoleic acid
82	16.53	Ricinoleic acid
83	16.8	Ricinoleic acid
84	17.09	Digitoxin
85	17.49	Undecylenic Acid
86	17.6	Oxacyclododecan-2-one
88	18.96	Phenol, 2-methoxy-4-(1-propenyl)-, (E)-
89	19.21	Digitoxin
91	19.51	Pregn-4-ene-3,20-dione, 11-hydroxy-, (11a)-
92	20.04	Digitoxin
93	20.26	4a,7-Methano-4aH-naphth[1,8a-b]oxirene, octahydro-4,4,8,8-tetramethyl-
96	20.7	Digitoxin
97	21.31	Digitoxin
98	21.82	Digitoxin
101	22.92	Digitoxin
102	23.63	Gibberellic acid

103	23.78	Digitoxin
104	24.46	Retinal, 9-cis-
105	24.65	Cholest-5-en-3-ol (3 β)-, tetradecanoate
106	24.75	Digitoxin
107	25.17	Digitoxin
108	25.29	Digitoxin
109	25.77	Digitoxin
111	26.7	Digitoxin
113	27.05	Ricinoleic acid
120	27.62	Digitoxin
123	28.12	N,N-Bis(2-hydroxyethyl)-2-aminoethanesulfonic acid
124	28.39	Digitoxin
128	30.05	Ricinoleic acid
129	30.37	Digitoxin
131	31.82	Digitoxin
132	31.92	Digitoxin
134	33.25	Gibberellic acid
137	34.83	Rescinamine
143	36.18	Digitoxin
150	38.28	β Carotene
152	39.16	Digitoxin
154	39.66	β Carotene
160	43.14	Beclomethasone
164	45.01	Beclomethasone
166	45.47	Beclomethasone
167	45.94	Beclomethasone
168	46.15	Beclomethasone
169	46.56	Beclomethasone
170	46.89	Beclomethasone
171	46.96	Beclomethasone

174	47.57	Beclomethasone
175	48.2	Beclomethasone
176	48.44	Beclomethasone
177	49.64	Beclomethasone
179	50.68	Beclomethasone
180	50.84	Beclomethasone
181	51.25	Beclomethasone
182	51.5	Beclomethasone
183	52.89	Digitoxin
184	53.02	Digitoxin
185	53.13	Beclomethasone
186	53.23	Digitoxin
187	54.24	Digitoxin
188	54.39	Digitoxin
189	54.63	Digitoxin
190	54.96	Beclomethasone
191	55.19	Beclomethasone
192	55.52	Beclomethasone
193	55.58	Beclomethasone
194	57.12	Beclomethasone
197	57.66	Beclomethasone
198	59.09	Beclomethasone
199	59.45	Beclomethasone
200	60.57	Beclomethasone
202	61.84	Beclomethasone
203	62.83	Beclomethasone

Appendix E: Calibration curve for NH₃-TPD analysis

The strength of acidic sites on the surface of prepared catalysts was analyzed by NH₃-TPD analysis based on the adsorption strength of ammonia molecule on acidic sites, which depends on the desorption temperature. The setup was calibrated based on the ammonia (mmol/g) injected using the injection port and the area under the curve. Based on the area under the curve, the acidic sites are classified as weak ($\leq 200^{\circ}\text{C}$), moderate ($200\text{--}400^{\circ}\text{C}$) and strong ($\geq 400^{\circ}\text{C}$) acid sites.

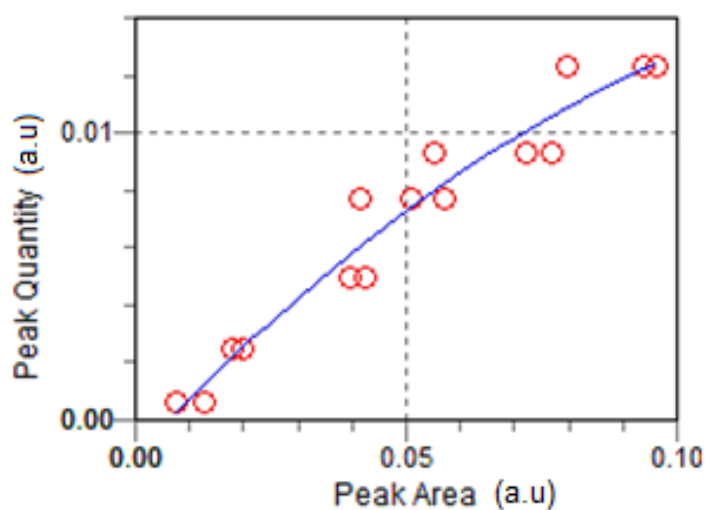


Figure E.1: Calibration curve for NH₃-TPD analysis

Appendix F: XPS results from Casa-XPS software

The XPS analysis was used to determine the Mo 3d spectra and its relative oxidation states of the synthesized catalysts and the results are shown in Table E.1. Mo 3d spectra consist of two peaks resulting from spin-orbit (j-j) coupling: Mo 3d_{5/2} and Mo 3d_{3/2} with area ratio of 3:2. The peak distance between 3d_{5/2} and 3d_{3/2} equal to 3.1 eV. The XPS spectra were obtained from Kratos AXIS Supra XPS instrument and analysed using Casa-XPS software. The instrument was equipped with a hemispherical analyser to capture the photoelectrons ejected from the sample after irradiation by Al k-(alpha) radiation. As, the curves are not smooth for reducing the errors, full width half maximum (FWHM) for area calculation is counted.

Table F.1: XPS results for NiMoC/AC obtained from Casa-XPS software

Component	A	B	C	D	E	F	G	H
Name	Mo 5/2	Mo 3/2	Mo 5/2	Mo 3/2	Mo 5/2	Mo 3/2	Mo 3d	Mo 3d
R.S.F.	9.5	9.5	9.5	9.5	9.5	9.5	9.5	9.5
Line Shape	LA(1.53,243)	LA(1.53,243)	LA(1.53,243)	LA(1.53,243)	LA(1.53,243)	LA(1.53,243)	LA(1.53,243)	LA(1.53,243)
Area	1530.6	918.3	969.2	581.5	444.9	266.9	1645.0	987.0
Area Constr.	0.0, 57701.3	A * 0.6	0.0, 57701.3	C * 0.6	0.0, 57701.3	E * 0.6	0.0, 57701.3	G * 0.6
fwhm	0.629541	0.629541	1.08137	1.08137	1.2577	1.2577	1.46893	1.46893
fwhm Constr.	0.2, 5	A * 1	0.2, 5	C * 1	0.2, 5	E * 1	0.2, 5	G * 1
Position	227.9054	231.0054	228.5011	231.6011	229.8711	232.9711	232.0162	235.1162
Pos. Constr.	237.19, 226....	A + 3.1	237.19, 226....	C + 3.1	237.19, 226....	E + 3.1	237.19, 226....	G + 3.1
Tag	Mo 3d	Mo 3d	Mo 3d	Mo 3d	Mo 3d	Mo 3d	Mo 3d	Mo 3d
Comp Index	-1	-1	-1	-1	-1	-1	-1	-1
Asymmetry Index	-0.0000	-0.0000	-0.0000	-0.0000	-0.0000	-0.0000	-0.0000	-0.0000
% Concentr.	20.89	12.50	13.22	7.92	6.06	3.63	22.38	13.40

Appendix G: Calibration results for GC

Regarding gas product analysis, aliquot of the gas in the reactor was carefully sampled into Tedlar bags via a control valve and subsequently analyzed using an offline GC equipped with both TCD and FID detectors. The peaks were recognized according to National Institute of Standards and Technology (NIST) library using Chromeleon TM 7.2 Chromatography Data System (CDS) software.

Table G.1: Calibration results for GC

RetTime [min]	Lvl Sig	Amount [mol %]	Area	Amt/Area	Ref Grp Name
-----	-- --	-----	-----	-----	-----
1.002	1 2	7.41000	1.06923e4	6.93021e-4	methane
	1	15.00000	2.21210e4	6.78088e-4	
1.109	3 2	35.53700	1.10510e4	3.21572e-3	H2
	1	38.28700	1.28643e4	2.97622e-3	
1.127	1 2	3.44000	9354.44434	3.67740e-4	ethane
	1	7.02000	1.92692e4	3.64312e-4	
1.251	1 2	3.68000	1.01540e4	3.62419e-4	ethylene
	1	7.50000	2.09794e4	3.57494e-4	
1.672	1 2	3.94000	1.63354e4	2.41195e-4	propane
	1	8.04000	3.02248e4	2.66007e-4	
2.586	1 1	3.05000	1.15068e4	2.65062e-4	propylene
	2	4.48000	1.80867e4	2.47696e-4	
3.200	2 1	3.01000	1746.59204	1.72336e-3	CO2
	2	6.10000	3407.61670	1.79011e-3	
3.716	1 1	1.00000	3259.30330	3.06814e-4	acetylene
	2	1.96000	6399.30000	3.06283e-4	
4.195	1 1	2.04000	8235.84017	2.47698e-4	I-butane
	2	4.96000	2.73700e4	1.81220e-4	
4.773	2 1	31.60000	2.75010e4	1.14905e-3	O2
	2	95.00000	4.05974e4	2.34005e-3	
5.240	2 1	3.96000	1873.18164	2.11405e-3	N2
	2	3.97000	2005.63782	1.97942e-3	
	3	95.00000	4.41212e4	2.15316e-3	
7.016	2 1	2.01000	844.35203	2.38052e-3	CO
	2	3.92000	1699.57117	2.30646e-3	

Signal 1: FID 1 A, front signal, Signal 2: TCD2 B, back Signal, and Signal 3: TCD3 C, Aux Signal

Appendix H: ASPEN Plus results

Table H.1: Aspen plus results for HDO process

	Units	BIOCRUDE	BIOFUELS	BP	CATALYST	FINALF	H2	WATER
Description								
From			B11	B1		B4		B11
To		B1		B2	B4	B3	B2	
Stream Class		CONVEN	CONVEN	CONVEN	CONVEN	CONVEN	CONVEN	CONVEN
Maximum Relative Error								
Cost Flow	\$/hr							
MIXED Substream								
Phase		Liquid Phase	Liquid Phase	Liquid Phase	Solid Phase		Vapor Phase	Liquid Phase
Temperature	C	25	25	39.898538	25	45.8460774	25	25
Pressure	MPa	0.101325	0.101325	13	0.101325	0.101325	13	0.101325
Molar Vapor Fraction		0	0	0	0	0.04418136	1	0
Molar Liquid Fraction		1	1	1	0	0.58798345	0	1
Molar Solid Fraction		0	0	0	1	0.36783519	0	0
Mass Vapor Fraction		0	0	0	0	0.00242338	1	0
Mass Liquid Fraction		1	1	1	0	0.95916912	0	1
Mass Solid Fraction		0	0	0	1	0.0384075	0	0
Molar Enthalpy	cal/mol	-129212.67	-134580.67	-127230	1.24E-13	-76265.16	20.74	-68725.84
Mass Enthalpy	cal/gm	-700.64	-638.68	-689.89	1.04E-14	-662.99432	10.28	-3814.88
Molar Entropy	cal/mol-K	-284.01	-324.15	-280.06	3.12E-16	-166.37485	-9.6970	-40.11
Mass Entropy	cal/gm-K	-1.54	-1.54	-1.51	2.60E-17	-1.44	-4.810	-2.226
Molar Density	mol/cc	0.005	0.005	0.004	0.18733	0.0007777	0.004	0.055
Mass Density	gm/cc	0.89	0.87	0.864	2.250	0.08946778	0.009	0.993
Enthalpy Flow	kcal/hr	-3374766.86	3011217.13	-3322985	1.99E-12	-3322955.1	29.57	-282998.4
Average MW		184.42	210.72	184.4	12.011	115.03	2.01588	18.015
Mole Flows	kmol/hr	26.12	22.37	26.117	16.02698	43.57	0.069	4.117
Mass Flows	tonne/day	115.6	83.81	115.6	4.62	120.289	0.07	1.78
H2	tons/day	0	0	0	0	0.07	2.875	0
WATER	tons/day	1.61	0	1.61	0	1.6184	0	1.78
N-HEX-01	tonne/day	69.36	56.29	69.36	0	69.36	0	0
1-HEX-01	tonne/day	0	2.69	0	0	0	0	0
PALMI-01	tonne/day	23.12	5.99	23.12	0	23.12	0	0
N-CYC-01	tons/day	0	6.32	0	0	0	0	0
O-ETH-01	tons/day	23.71	12.89	23.70	0	23.7014569	0	0
ETHYL-01	tonne/day	0	1.67	0	0	0	0	0
CARBON	tonne/year	0	0	0	4.62	4.62	0	0
OXYGEN	tonne/day	0	0	0	0	0	0	0
Volume Flow	l/hr	5506.19	5425.54	5569.80	85.55477	56020.6346	289.562335	74.634

Table H.2: Aspen plus results for HTL + method #1

	Units	ALGAE	SOLVENT	FEEDF	MAKEUP
Description					
From			B6	B2	
To		B1	B1	B3	B6
Stream Class		MIXCINC	MIXCINC	MIXCINC	MIXCINC
Temperature	C	25	55.36	275	25
Pressure	MPa	0.101325	0.101325	11	0.101325
Mass Vapor Fraction		0	0	0.073	0
Mass Liquid Fraction		0	1	0.75	1
Mass Solid Fraction		1	0	0.16	0
Mass Enthalpy	cal/gm	-980.109	-2255.81	-1735.357917	-2691.63
Mass Density	gm/cc	1.21	0.79	0.274547446	0.86
Enthalpy Flow	kcal/hr	-8167583.039	-93992331.91	-86767895.83	-15420829.78
Mass Flows	tonne/day	200	1000	1200	137.5
ALGAE	tonne/day	200	0	200	0
H2O	tonne/day	0	250	250	62.5
METHANOL	tonne/day	0	750	750	75
CO2	tonne/day	0	0	0	0
CH4	tonne/day	0	0	0	0
STEARICA	tonne/day	0	0	0	0
ETHYL-01	tonne/day	0	0	0	0
RICIN-01	tonne/day	0	0	0	0
C18H36O	tonne/day	0	0	0	0
C15H16O2	tonne/day	0	0	0	0
C12H8O	tonne/day	0	0	0	0
CARBON	tonne/day	0	0	0	0
OXYGEN	tonne/day	0	0	0	0

	Units	GAS	BIO-OIL	CHAR	PRODUCT	RECOVERY
Description						
From		B19	B7	B17	B3	B5
To				B4	B17	B6
Stream Class		MIXCINC	MIXCINC	MIXCINC	MIXCINC	MIXCINC
Temperature	C	60	60	275	275	60.23238185
Pressure	MPa	0.101325	0.101325	11.5	11.5	0.506625
Mass Vapor Fraction		1	0.017	0	0.211382045	0
Mass Liquid Fraction		0	0.98	0	0.771332866	1
Mass Solid Fraction		0	0	1	0.017285089	0
Mass Enthalpy	cal/gm	-1815.819216	-1706.42	62.59	-1721.61	-2186.34
Mass Density	gm/cc	0.00123129	0.069	2.25	0.192461004	0.78
Enthalpy Flow	kcal/hr	-4569039.51	18227994.37	54094.39	86080516.21	78571502.13
Mass Flows	tonne/day	60.38	256.36	20.74210648	1200	862.5
ALGAE	tonne/day	0	0	0	0	0
H2O	tonne/day	2.361	65.95	0	255.81	187.5
METHANOL	tonne/day	29.419	69.95	0	774.31	675
CO2	tonne/day	26.21408098	4.20	0	30.427	0
CH4	tonne/day	2.394409044	0.094	0	2.48	0
STEARICA	tonne/day	1.88E-08	19.35	0	19.35	0
ETHYL-01	tonne/day	1.22E-07	19.35	0	19.35	0
RICIN-01	tonne/day	2.30E-09	19.35	0	19.35	0
C18H36O	tonne/day	1.82E-06	19.3	0	19.35	0
C15H16O2	tonne/day	3.35E-09	19.35	0	19.359	0
C12H8O	tonne/day	0.000167172	19.356	0	19.359	0
CARBON	tonne/day	0	0	20.74210648	20.74	0
OXYGEN	tonne/day	0	0	0	0	0

Table H.3: Aspen plus results for HTL + method #2

	Units	ALGAE	SOLVENT	FEEDF	PRODUCT	CHAR
Description						
From			B9	B4	B3	B17
To		B1	B1	B3	B17	B8
Stream Class		MIXCINC	MIXCINC	MIXCINC	MIXCINC	MIXCINC
Maximum Relative Error						
Cost Flow	\$/hr					
Total Stream						
Temperature	C	25	55.36579964	275	275	275
Pressure	MPa	0.101325	0.101325	11.5	11.5	11.5
Mass Vapor Fraction		0	0	0	0.21	0
Mass Liquid Fraction		0	1	0.83	0.77	0
Mass Solid Fraction		1	0	0.166	0.017	1
Mass Enthalpy	cal/gm	-980.109	-2255.81	-1738.95	-1721.61	62.59
Mass Density	gm/cc	1.26	0.79	0.348	0.192	2.25
Enthalpy Flow	kcal/hr	-	-	-	-	-
Mass Flows	tonne/day	8167583.039	93992331.61	86947790.74	86080516.21	54094.39
ALGAE	tonne/day	200	1000	1200	1200	20.742
H2O	tonne/day	200	0	200	0	0
METHANOL	tonne/day	0	250	250	255.819	0
CO2	tonne/day	0	750	750	774.3	0
CH4	tonne/day	0	0	0	30.42	0
STEARICA	tonne/day	0	0	0	2.48	0
ETHYL-01	tonne/day	0	0	0	19.35	0
RICIN-01	tonne/day	0	0	0	19.35	0
C18H36O	tonne/day	0	0	0	19.35	0
C15H16O2	tonne/day	0	0	0	19.36	0
C12H8O	tonne/day	0	0	0	19.356	0
CARBON	tonne/day	0	0	0	19.35	0
CO	tonne/day	0	0	0	20.74	20.74
K	tonne/day	0	0	0	0	0
KOH	tonne/day	0	0	0	0	0
HYDROGEN	kg/hr	0	0	0	0	0

	Units	GAS	MAKEUP	BIO-OIL	KOH
Description					
From		B19		B7	
To			B9		B8
Stream Class		MIXCINC	MIXCINC	MIXCINC	MIXCINC
Maximum Relative Error					
Cost Flow	\$/hr				
Total Stream					
Temperature	C	60	25	60	25
Pressure	MPa	0.101325	0.101325	0.101325	0.101325
Mass Vapor Fraction		1	0	0.017533461	0
Mass Liquid Fraction		0	1	0.982466539	1
Mass Solid Fraction		0	0	0	0
Mass Enthalpy	cal/gm	-1815.816	-2691.6357	-1706.420	-1931.14
Mass Density	gm/cc	0.00123129	0.866	0.0698	1.86
Enthalpy Flow	kcal/hr	-4569039.51	-15420829.78	-18227994.37	804642.70
Mass Flows	tonne/day	60.389	137.5	256.3680996	10
ALGAE	tonne/day	0	0	0	0
H2O	tonne/day	2.3611	62.5	65.9581051	0
METHANOL	tonne/day	29.46	75	69.9520	0
CO2	tonne/day	26.25	0	4.207	0
CH4	tonne/day	2.394409044	0	0.094-	0
STEARICA	tonne/day	1.88E-08	0	19.359-	0
ETHYL-01	tonne/day	1.22E-07	0	19.35929926	0
RICIN-01	tonne/day	2.30E-09	0	19.35929938	0
C18H36O	tonne/day	1.82E-06	0	19.35929756	0
C15H16O2	tonne/day	3.35E-09	0	19.35929937	0
C12H8O	tonne/day	0.000167172	0	19.35913221	0
CARBON	tonne/day	0	0	0	0
CO	tonne/day	0	0	0	0
K	tonne/day	0	0	0	0
KOH	tonne/day	0	0	0	10
HYDROGEN	kg/hr	0	0	0	0

Appendix I: Permission to use

The data used in this thesis were published in Elsevier Journals of Energy, Cleaner Production and Energy Conversion and Management. Based on the Elsevier copy right: as the author of the Elsevier articles, I have got the permission to include them in my thesis.

SPRINGER NATURE

Thank you for your order!

Dear Mrs. Shima Masoumi,

Thank you for placing your order through Copyright Clearance Center's RightsLink® service.

Order Summary

Licensee:	Saskatchewan University
Order Date:	Feb 23, 2021
Order Number:	5015091110475
Publication:	Springer eBook
Title:	Biocrude Oil Production via Hydrothermal Liquefaction of Algae and Upgradation Techniques to Liquid Transportation Fuels
Type of Use:	Thesis/Dissertation
Order Ref:	1
Order Total:	0.00 USD


View or print complete [details](#) of your order and the publisher's terms and conditions.

Sincerely,


Copyright Clearance Center

Tel: [+1-855-239-3415](tel:+1-855-239-3415) / [+1-978-646-2777](tel:+1-978-646-2777)
customer care@copyright.com
<https://myaccount.copyright.com>

 Copyright Clearance Center

 RightsLink®

Journal of Energy:




Biocrude oil and hydrochar production and characterization obtained from hydrothermal liquefaction of microalgae in methanol-water system
Author: Shima Masoumi, Philip E. Boahene, Ajay K. Dalai
Publication: Energy
Publisher: Elsevier
Date: 15 February 2021
© 2020 Elsevier Ltd. All rights reserved.

Please note that, as the author of this Elsevier article, you retain the right to include it in a thesis or dissertation, provided it is not published commercially. Permission is not required, but please ensure that you reference the journal as the original source. For more information on this and on your other retained rights, please visit: <https://www.elsevier.com/about/our-business/policies/copyright#Author-rights>

BACKCLOSE WINDOW

Journal of Cleaner production:




Optimized production and characterization of highly porous activated carbon from algal-derived hydrochar
Author: Shima Masoumi, Ajay K. Dalai
Publication: Journal of Cleaner Production
Publisher: Elsevier
Date: 1 August 2020
© 2020 Published by Elsevier Ltd.

Please note that, as the author of this Elsevier article, you retain the right to include it in a thesis or dissertation, provided it is not published commercially. Permission is not required, but please ensure that you reference the journal as the original source. For more information on this and on your other retained rights, please visit: <https://www.elsevier.com/about/our-business/policies/copyright#Author-rights>

BACKCLOSE WINDOW

Journal of Energy Conversion and Management



NiMo carbide supported on algal derived activated carbon for hydrodeoxygenation of algal biocrude oil
Author: Shima Masoumi, Ajay K. Dalai
Publication: Energy Conversion and Management
Publisher: Elsevier
Date: 1 March 2021
© 2021 Elsevier Ltd. All rights reserved.

Please note that, as the author of this Elsevier article, you retain the right to include it in a thesis or dissertation, provided it is not published commercially. Permission is not required, but please ensure that you reference the journal as the original source. For more information on this and on your other retained rights, please visit: <https://www.elsevier.com/about/our-business/policies/copyright#Author-rights>

BACKCLOSE WINDOW